UNIVERSITÀ DEGLI STUDI DI PADOVA

DEPARTMENT OF CARDIAC, THORACIC, VASCULAR SCIENCES AND PUBLIC HEALTH
Director: Prof. FEDERICO REA

PhD COURSE IN: Translational Specialistic Medicine "G.B. Morgagni"
Coordinator: Prof.ssa Annalisa Angelini

CURRICULUM: Thoracic and Pulmonary Sciences
SERIES XXXV

Clinical, radiological and biological predictors of clinical course in patients with Idiopathic Pulmonary Fibrosis

Supervisor:
Prof. Paolo Spagnolo

Ph.D. Student:
Dott.ssa Elisabetta Cocconcelli

Anno Accademico: 2021 – 2022

CONTENTS

ABSTRACT

Idiopathic pulmonary fibrosis (IPF) is a chronic and progressive lung disease, with an unknown leading cause. The prognosis of IPF is poor and the clinical course of IPF is highly heterogeneous and unpredictable, alternating periods of stability to periods of rapid deterioration.

Staging systems are increasingly considered to estimate prognosis and to guide management decisions in IPF. Nonethelss, to date the mortality rate for IPF is not significantly changed after the recent worldwide diffusion of the two new antifibrotic drugs nintedanib and pirfenidone, emphasizing the need for a more complete understanding in the mechanisms of disease pathogenesis and in predicting IPF clinical behavior.

In this thesis potential clinical, radiological and biological predictors of disease course in IPF were investigated. Specifically, I demonstrated that ground glass opacities at CT scan performed at diagnosis are associated with worse functional decline in IPF patients, and increase over time among progressors. MUC5B polymorphism affects prognosis of the IPF patients on antifibrotic treatment and carrying the mutant T allele is associated to increased ground glass opacities and worst survival. Lymphoid follicles are fundamental structures in IPF natural history and progression of patients with IPF.

In the last three or four years some evidence suggested that almost the forty per cent of non-IPF interstitial lung disease patients, currently treated with specific treatment, may present a clinical course similar to IPF and were named progressive pulmonary fibrosis (PPF). In my research project, I identified the progressive phenotype among the idiopathic inflammatory myopathies (IIMs) of patients followed in our center, and I described patients presenting a progressive phenotype.

Finally, my Coronavirus Disease 19 (COVID-19) research assessed that ultrasound is a useful tool in clinical practice because it correlates with clinical and radiographic parameters. Viral load on nasopharyngeal swab at diagnosis of COVID-19 is similar in asymptomatic and hospitalized patients and is not associated with either worse outcome during hospitalization. A minority of patients with COVID-19 pneumonia showed persisting lung abnormalities at the 6-month follow-up. These patients are predominantly older males with longer hospital stay. The presence of reticulations and consolidation at hospital admission may predict the persistence of radiological abnormalities.

RIASSUNTO

La fibrosi polmonare idiopatica (IPF) è una malattia polmonare cronica e progressiva ad eziologia non nota. La prognosi dei pazienti affetti da IPF è scarsa e il decorso clinico dell'IPF è altamente variabile da paziente a paziente ed imprevedibile nel tempo, alternando periodi di stabilità a periodi di rapido declinico clinico e funzionale.

Alcuni criteri di stadiazione sono stati presi in considerazione per stimare la prognosi e per guidare le decisioni terapeutiche nei pazienti affetti da IPF. Tuttavia, ad oggi il tasso di mortalità per IPF non è cambiato in modo significativo dopo la recente diffusione dei due nuovi farmaci antifibrosanti nintedanib e pirfenidone, sottolineando la necessità di una comprensione più completa dei meccanismi di patogenesi della malattia e nel predire il comportamento clinico della IPF.

In questa tesi sono stati studiati i potenziali indicati clinici, radiologici e biologici di andamento clinico nei pazienti affetti da IPF. In particolare, ho dimostrato che le opacità a vetro smerigliato visibili alla TC eseguita al momento della diagnosi sono associate ad un peggiore declino funzionale e aumentano nel tempo in quei pazienti che progrediscono nonostante la terapia. Il polimorfismo di MUC5B influisce sulla prognosi dei pazienti con IPF in trattamento antifibrosante e, in particolare, il portatore dell'allele T mutante è associato ad un aumento delle opacità del vetro smerigliato e ad una peggiore sopravvivenza. I follicoli linfoidi sono strutture fondamentali nella storia naturale dell'IPF e nella progressione di malattia.

Negli ultimi tre o quattro anni alcuni dati hanno sottolineato che quasi il quaranta per cento dei pazienti con malattia polmonare interstiziale non-IPF, può presentare un decorso clinico simile all'IPF nonostante siano trattati con farmaci specifici per la malattia di base; queste entità cliniche vengono deifinite fibrosi polmonari progressive (PPF). Nel mio progetto di ricerca ho identificato dunque il fenotipo progressivo tra i pazienti affetti da miopatie infiammatorie idiopatiche (IIM) seguiti nel nostro centro, e ho descritto i pazienti che presentavano un fenotipo progressivo.

Infine, la mia ricerca sulla malattia da Coronavirus 19 (COVID-19) ha valutato che l'ecografia toracica è uno strumento utile nella pratica clinica perché correla con i parametri clinici e radiografici. La carica virale sul tampone nasofaringeo alla diagnosi di COVID-19 è simile nei pazienti asintomatici e

ricoverati in ospedale e non è associata a nessun esito peggiore durante il ricovero. Una minoranza di pazienti con polmonite COVID-19 presenta anomalie polmonari al follow-up radiologico di 6 mesi. Questi pazienti sono prevalentemente maschi, più anziani e con una degenza ospedaliera più lunga. La presenza di reticolazioni e consolidamenti al ricovero in ospedale può predire la persistenza di anomalie radiologiche.

Chapter 1

Introduction

Elisabetta Cocconcelli

INTRODUCTION

Idiopathic pulmonary fibrosis (IPF), the most severe among the interstitial lung diseases (ILDs), with a median survival of three to five years from the time of the diagnosis, comparable to that of several malignancies, and with a five-year survival of approximately twenty per cent[1,2]. To date, lung transplant represents the only cure for IPF, although this is a realistic option for only a minority of highly selected patients.

IPF is believed to occur in genetically susceptible individuals as a consequence of an aberrant wound-healing response following repetitive alveolar microinjury, leading to scarring of the lung parenchyma and an irreversible loss of function[3]. As such, IPF is likely to result from a complex interaction between genetic and environmental factors, most of which remain unknown.

From diagnosis, the clinical course of IPF is highly heterogeneous and unpredictable, alternating periods of stability to periods of rapid deterioration. Indeed, while in most cases the inexorable decline in lung function and symptoms occurs over a period of years (*slow decliners*), 10-15% of individuals experience a much faster disease course progressing from mild symptoms to respiratory failure and death over a period of months (*rapid decliners*)[4]. Moreover, in 5% of cases a relatively slow decline is punctuated by episodes of acute worsening - termed acute exacerbations - which are fatal in the majority of cases.

Staging systems are increasingly considered to estimate prognosis and to guide management decisions in chronic and progressive diseases. Several clinical (older age, male sex, smoking history, hospitalizations), physiological (forced vital capacity or gas exchange), radiological and pathological variables have been proposed to assess disease severity and predict survival in IPF. Physiological parameters have historically been considered the major prognosticators in IPF, either alone or integrated in multi-dimensional prediction models. Specifically, longitudinal changes in forced vital capacity (FVC) and diffuse DLCO are more predictive of prognosis than respective baseline values; thus, FVC decline has been used as the primary endpoint in several randomized controlled drug trials, which have led to the approval of nintedanib and pirfenidone for the treatment of IPF. Nonetheless, mortality rate for IPF is not significantly changed after the recent worldwide diffusion of the two new antifibrotic drugs nintedanib and pirfenidone,

emphasizing the need for a more complete understanding in the mechanisms of disease pathogenesis and in predicting IPF clinical behavior.

Despite the vast amount of evidence produced in this field, the perfect marker of prognosis has not been identified yet. Nevertheless, I am reporting here the results of several studies aimed at investigating the potential usefulness of several variables (radiological pattern, genetic polymorphisms and pathological elements), which are promising in the prediction of IPF clinical course.

After evaluating biomarkers potentially useful in the prognostic prediction, some clinical aspects associated with patient disease course were investigated. In particular, three main themes were addressed: the prognostic role of High-Resolution Computed Tomography (HRCT) at baseline and during follow up, the impact of MUC5B rs35705950 genotype on disease behavior and survival, the presence of lymphoid follicles structures in lungs of IPF patients across the disease course from diagnosis to transplant.

The thesis is composed by fifteen chapters, including this chapter. **Chapter 2** and **chapter 3** provide the background, with a brief overview on IPF in **Chapter 2** and an update on a new disease entity, the progressive pulmonary fibrosis (PPF) in **Chapter 3**. Non-IPF interstitial lung diseases have been universally known to have a better disease course and prognosis compared to IPF. Nonetheless, in the last three or four years some evidence suggested that almost the forty per cent of non-IPF ILD patients, currently treated with specific treatment, may present a clinical course similar to IPF[5,6]. In 2019, the efficacy of nintedanib in patients with non-IPF fibrosis was published and, in the current year, the American thoracic society (ATS) and the European Respiratory Society, together with an update in IPF, published the first guidelines on PPF[7,8]. The new recent challenge of respiratory researchers is now to apply their experience in IPF on PPF and to analyze potential predictors in those new clinical entities. With this background, during last year, at the same time as the research on IPF, I am collaborating with our rheumatologists of the University of Padova to define the progressive phenotype among the idiopathic inflammatory myopathies (IIMs) and the first results on our research is described on **chapter 11**.

Aims of the thesis are elucidated in **Chapter 4**. **Chapter** from **5** to **10** cover the studies on clinical, radiological, pathological promising prognostic predictors for IPF disease course. More specifically **chapter 5** contain the description of

radiological pattern in predicting the function decline in IPF patients not yet treated with antifibrotics. **Chapter 6** want to analyze the longitudinal changes of radiological patterns over the 1-st year of follow up in IPF patients on antifibrotic treatment, and how these changes correlate with different functional disease trajectories. These two studies were the real pilot studies of my Ph.D. project and data were published during my first Ph.D. year. **Chapter 7** want to analyze the impact of MUC5B polymorphism on survival of IPF patients on antifibrotic treatment. **Chapter 8** applied previous evidences on radiological patterns and want to observe if our two genotyped populations could be different in radiological abnormalities at treatment initiation and during follow up. **Chapter 9** want to elucidate the presence of adaptive immune cells in the lungs of patients with IPF, from the biopsies obtained at diagnosis to specimens obtained from explanted lung. Specifically, I focused on count and describe the presence of lymphoid follicles in IPF lungs, on the basis of some previous evidences[4, 9, 10]. **Chapter 10** want to investigate the role of serum Carbohydrate Antigen 19-9 (CA 19-9) levels in IPF and other PPF patients with advanced disease referred to our lung transplant center and its relation with different patterns of functional.

During last three years, our clinical and research life has been disrupted by Coronavirus disease 2019 (COVID-19), that has rapidly become a global pandemic with lung disease representing the main cause of morbidity and mortality. As a respiratory clinician, my daily activity for the past two and a half years has included also the care of patients with COVID-19 pneumonia. Consequently, parallel to the research on IPF, during the last years I focused my research activities also on patients with COVID-19. **Chapter 12** to **chapter 14** focused on my research on COVID-19. Specifically, on **Chapter 12** the relationship between Chest X-Ray severity score on admission and the level of medical care was analyzed. **Chapter 13** assessed the viral load in the nasopharyngeal swab and its association with severity score indexes and prognostic parameters. **Chapter 14** want to characterize, among hospitalized patients for COVID-19, those with persisting pulmonary sequelae during follow-up, and clinical and radiological predictors of pulmonary fibrosis were analyzed.

Chapter 15 reports general conclusions of the research.

REFERENCES

1. Raghu G, Collard HR, Egan JJ, et al. An Official ATS/ERS/JRS/ALAT Statement: Idiopathic pulmonary fibrosis: Evidence-based guidelines for diagnosis and management. Am J Respir Crit Care Med 2011;183(6):788–824.
2. Raghu G, Remy-jardin M, Myers JL, et al. AMERICAN THORACIC SOCIETY Diagnosis of Idiopathic Pulmonary Fibrosis. 2018;198(5).
3. Lederer DJ, Martinez FJ. Idiopathic pulmonary fibrosis. NEJM 2018;29(5):283–91.
4. Balestro E, Calabrese F, Turato G, et al. Immune Inflammation and Disease Progression in Idiopathic Pulmonary Fibrosis. PLoS One. 2016 May 9;11(5):e0154516. doi: 10.1371/journal.pone.0154516. PMID: 27159038; PMCID: PMC4861274.
5. Cottin V. Treatment of progressive fibrosing interstitial lung diseases: a milestone in the management of interstitial lung diseases. Eur Respir Rev. 2019 Oct 1;28(153):190109. doi: 10.1183/16000617.0109-2019. PMID: 31578213.
6. Kolb M, Vašáková M. The natural history of progressive fibrosing interstitial lung diseases. Respir Res. 2019 Mar 14;20(1):57. doi: 10.1186/s12931-019-1022-1. PMID: 30871560; PMCID: PMC6417262.
7. Flaherty KR, Wells AU, Cottin V, et al. INBUILD Trial Investigators. Nintedanib in Progressive Fibrosing Interstitial Lung Diseases. N Engl J Med. 2019 Oct 31;381(18):1718-1727. doi: 10.1056/NEJMoa1908681. Epub 2019 Sep 29. PMID: 31566307.
8. Raghu G, Remy-Jardin M, Richeldi L, et al. Idiopathic Pulmonary Fibrosis (an Update) and Progressive Pulmonary Fibrosis in Adults: An Official ATS/ERS/JRS/ALAT Clinical Practice Guideline. Am J Respir Crit Care Med. 2022 May 1;205(9):e18-e47. doi: 10.1164/rccm.202202-0399ST. PMID: 35486072.
9. Marchal-Sommé J, Uzunhan Y, Marchand-Adam S, et al. Cutting edge: nonproliferating mature immune cells form a novel type of organized lymphoid structure in idiopathic pulmonary fibrosis. J Immunol. 2006 May 15;176(10):5735-9. doi: 10.4049/jimmunol.176.10.5735. PMID: 16670278.
10. Todd NW, Scheraga RG, Galvin JR, et al. Lymphocyte aggregates persist and accumulate in the lungs of patients with idiopathic pulmonary fibrosis. J Inflamm Res. 2013;6:63-70. doi: 10.2147/JIR.S40673. Epub 2013 Mar 27. PMID: 23576879; PMCID: PMC3617818.

Chapter 2

Idiopathic Pulmonary Fibrosis (IPF), a general overview

Elisabetta Cocconcelli

INTERSTITIAL LUNG DISEASES

Interstitial Lung Diseases (ILDs) are defined as lung disorders with variable degrees of pulmonary inflammation and fibrosis[1,2]. ILDs include disorders in the context of a clear pathological condition (collagen or vascular disease, environmental exposure or drug related disease) as well as disorders of unknown etiology. The latter group includes idiopathic interstitial pneumonia (IIPs), granulomatous diffuse lung disorders such as sarcoidosis, and other forms of ILDs such as lymphangioleiomyomatosis (LAM), pulmonary Langerhans' cell histiocytosis and eosinophilic pneumonia.

IDIOPATHIC PULMONARY FIBROSIS

IPF is the most common form of IIPs and is characterized by the worst prognosis. In 2011 the American Thoracic Society (ATS), the European Respiratory Society (ERS), the Japanese Respiratory society (JRS), and the Latin American Thoracic Association (ALAT) provided an evidence-based review in order to define guidelines for the diagnosis and the management of this disease. This document addresses issues on disease, definition, epidemiology, risk factors, natural history, diagnosis, staging and prognosis, treatment, monitoring disease course, and future directions. Treatment guidelines and the diagnostic criteria of IPF were then revised in 2015 and 2018, respectively[3–6]. In 2022 the same group of experts, on behalf of ATS, ERS, JRS and ALAT provided a new document where diagnostic criteria were revised[7].

DEFINITION

IPF is defined as a specific form of chronic, progressive fibrosing interstitial pneumonia of unknown cause, inevitably lethal, but limited to the lungs. The elderly male adults are the most frequent type of patients primarily affected by this disease. In the proper clinical context, the diagnosis of IPF requires specific combinations of the radiologic and/or histopathologic pattern of Usual Interstitial Pneumonia (UIP)[5]. Other forms of interstitial pneumonia including other IIPs and interstitial lung disease associated with environmental exposure, medications, or systemic disease have to be excluded. Great importance is the distinction of IPF from other forms of IIPs, since its therapeutic approach and prognosis are different.

CLINICAL PRESENTATION/FEATURES

The disease primarily affects older adults, typically current or former smoking males of over 60 years of age, and specifically is believed to occur in genetically susceptible individuals as a consequence of an aberrant wound-healing response following repetitive alveolar microinjury, leading to scarring of the lung parenchyma and an irreversible loss of function[8]. In patients aged less than 50 years the disease is uncommon and often a family history of ILD is revealed[5].

IPF should be suspected in all adult patients with unexplained chronic exertional dyspnea, chronic dry cough, typical bibasilar dry crackles ('velcro' crackles), and digital clubbing[5]. IPF most commonly presents with an insidious onset of progressive shortness of breath over months to years, and chronic dry cough. The typical nonproductive cough is often refractory to antitussive agents. Patients with interstitial lung disease often initially receive a diagnosis of heart failure or chronic obstructive pulmonary disease, suggesting that clinicians frequently fail to consider interstitial lung disease in patients with dyspnea. At the beginning, dyspnea may only be present on exertion, but it gradually changes to resting shortness of breath. In some case, patients may subsequently manifest overt features of an underlying connective tissue disease that was subclinical at the time IPF was diagnoses. Features of right heart failure, cyanosis and peripheral edema develop only in the last stages.

EPIDEMIOLOGY – INCIDENCE AND PREVALENCE

IPF is still considered a rare disease, even though the prevalence of the disease appears to be increasing (it is unclear whether this reflects increased recognition or a true increase in incidence). The exact values of incidence and prevalence remain very difficult to define for the absence of large-scale epidemiologic studies.

The exact global incidence and prevalence of the disease remain unclear, with incidence estimates ranging from 2 up to 9.6 per 100,000 person-years[9,10]. Among individuals aged 65 years and older, incidence of IPF is approximately 94 per 100,000 per year. Incidence of IPF worldwide is comparable to that of several malignancies, including stomach, liver, testicular and cervical cancers. In the US, between 150,000 and 200,000 people are believed to be affected, and as many as 40,000 people die from IPF each year. Similar numbers have been reported for

Europe[11,12]. The incidence of IPF appears to be higher in North America and Europe (3 to 9 cases per 100,000 person-years) than in South America and East Asia (fewer than 4 cases per 100,000 person-years)[13]. The prevalence of IPF has been reported in United States to range from 10 to 60 cases per 100,000.It has not yet been clarified, whether geographic, ethnic, cultural, or racial factors may influence the incidence and prevalence of IPF.

The prognosis of IPF seems to be very poor with a median survival time of 3 to 5 years from the time of diagnosis and with a 5-year survival of approximately 20 per cent, and these numbers are still not significantly changed after the recent worldwide diffusion of the two new antifibrotic drugs nintedanib and pirfenidone[14,15], emphasizing the need for a more complete understanding in the mechanisms of disease pathogenesis.

RISK FACTORS

As for other type of IIPs, IPF is, by definition, a disease of unknown etiology. Despite uncertainty about the causes, a number of potential risk factors have been analyzed:

- ***cigarette smoking***: it has been noticed that a majority of patients reports a history of cigarette smoking, with significant exposure (more than 20 pack-years). This evidence was observed both in familial as well as in sporadic forms of IPF[16].
- ***environmental exposure***: in addition to smoking, other risk factors from environmental exposure were considered. An important increased risk appears to be attributable to metal and wood dust. Brass, lead and steel are examples of metal dusts, which have been described as potential risk factors involved in the increased incidence of IPF. Among wood dust exposures, pine is often reported. Farming, raising birds, hair dressing, stone cutting/polishing, and exposure to livestock and to vegetable dust/animal dust all seem to be correlated with IPF.
- ***microbial agents***: the attention to the potential role of microbiome in IPF pathogenesis and progression or as a trigger of acute exacerbation has long been postulated[17]. The recent application to IPF of culture-independent techniques for microbiological analysis has revealed previously unappreciated alterations of the lung microbiome, as well as an increased

bacterial burden in the bronchoalveolar lavage (BAL) of IPF patients, although correlation does not necessarily entail causation.

Among all possible microbial agents, most research focused on chronic viral infections. The *human herpes viruses* (HHVs), a large family of DNA viruses that includes herpes simplex virus type 1 (HSV-1), *Epstein-Barr virus* (EBV), *cytomegalovirus* (CMV) and HHV-7 and HHV-8, have received the most attention as causative factors in IPF, mainly because of their ability to cause lifelong latent infection in the alveolar epithelium and to reactivate in older individuals. For example, both *Epstein-Barr virus* (EBV) protein and DNA of EBV have been identified in lung tissue of patients with IPF, specifically in the alveolar epithelial cells. The presence of the virus in replication phase, is demonstrable by searching for EBV genome rearrangement. Some studies have proved, that EBV genome rearrangement is in fact detectable in the majority of DNA-positive IPF biopsies. Tang et al. identified one or more herpes viruses in almost all IPF lung specimens, as compared to one-third of the control lungs. Specifically, the viral DNA detected was referable to EBV, *cytomegalovirus*, *human herpesvirus* (HHV) -*7*, and HHV-*8*[18]. Research has also been focused on *hepatitis C virus* (HCV*)*, although at present it is not yet clear whether hepatitis C plays a role in the etiology of IPF.

Despite the large number of studies, a definite role of infection in pulmonary fibrosis has not been certainly established.

- ***Gastroesophageal reflux***: gastroesophageal reflux (GER) and erosive esophagitis are widely diffused among population. A lot of studies have proved a tight correlation between GER and respiratory affections. Microaspiration of acid and alkaline materials can be extremely damaging to airways and lung parenchyma. Inflammation, edema, aspiration pneumonia, are frequently linked with GER. Abnormal GER is a common finding in patients with IPF. Abnormal acid GER, through microaspiration, seems to be a risk factor for IPF or, on the other hand, it is not clear if it is the consequence of changes in intrathoracic pressure, as a result of poorly compliant lung[19-21]. Nevertheless, GER is clinically silent in the majority of patients. The typical symptoms of heartburn and regurgitation are difficult to distinguish between patients with and without GER. Since abnormal GER

is frequent among IPF patients, alkaline components in the reflux may play an important role in pulmonary fibrosis. However, further studies should to be have to be performed, in order to establish a real role of GER in IPF.

- ***Ageing***: the mechanisms that link ageing with IPF remain unknown. One possible mechanism is related to an accelerated shortening of telomeres (see section 'Genetic Factors'). Ageing is also associated with increased oxidative stress as a result of an imbalance of pro-oxidants (reactive oxygen and nitrogen species) and antioxidants (eg, superoxide dismutases, glutathione). Excessive oxidative stress determines various deleterious effects that might contribute to the pathogenesis of IPF.

GENETIC FACTORS

IPF is likely to result from a complex interaction between environment and genetic factors, most of which remain unknown[22]. Nonetheless, approximately half of IPF patients lack a clear genetic signature. As such, with very few exceptions, genetic testing is not recommended in the routine evaluation of patients with either familial or sporadic IPF[7].

Several lines of evidence suggest the existence of a genetic predisposition to pulmonary fibrosis, including different susceptibility to pulmonary fibrosis among mice challenge with the same amount of bleomycin, and the occurrence of pulmonary fibrosis in the context of rare genetic disorders, such as Hermansky–Pudlak syndrome (HPS) and Dyskeratosis Congenita (DC).

HPS is an autosomal recessive disorder caused by defects in intracellular protein trafficking[23]. Eight human HPS-related genes have been identified (i.e. mutations in AP3B1 gene), each of which can lead to a diverse clinical HPS phenotype. Most commonly, patients with HPS present with oculo-cutaneous albinism and prolonged bleeding, increased predisposition to infection and pulmonary fibrosis. DC, a rare genetic disease secondary to altered telomere biology, is complicated by pulmonary fibrosis in as many as 20% of cases[24]. DC is associated with mutations within dyskerin (dyskeratosis congenita 1, DKC1), a gene involved in telomere biology and maintenance[25]. Patients with DC exhibit a classical triad of abnormal reticular skin pigmentation, leukoplakia, and nail dystrophy[26]. In childhood, bone marrow failure is the most frequent complication, while pulmonary fibrosis is a frequent cause of death in adults.

The identification of a genetic signature however has the potential to provide us with crucial information regarding prediction of disease behavior and, owing to the availability of two effective IPF-specific antifibrotic therapies, response to treatment. In clinical trials of IPF, a major obstacle is the heterogeneity of the patient population enrolled, wherein the rate of disease progression is not uniform. In this scenario, genotype-guided enrolment has the potential to identify compounds that are effective in selected groups of patients.

Familial pulmonary fibrosis (FIP) and sporadic IPF

Most forms of IPF are sporadic, and there are no genetic factors that are consistently associated with sporadic IPF. While genetic studies in familial pulmonary fibrosis have provided useful data for the pathogenesis of IPF, it is not the same for sporadic forms of IPF. Nonetheless, polymorphisms of several genes have been recently associated with increased risk of sporadic IPF. The most likely mode of genetic transmission seems to be autosomal-dominant with variable penetrance. The global incidence of these mutations has been estimated to be up to 15% for familial pulmonary fibrosis (FIP), and 3% for sporadic form of pulmonary fibrosis[27]. Genetics appears to influence also disease progression.

Moreover, current evidence suggests that sporadic and familial cases of IPF may reflect a continuum of genetic risk rather than existing as distinct forms. The term FIP refers to the occurrence of disease in two or more members of the same family. The criteria used to diagnose IPF are the same in familial and sporadic cases. Indeed, familial and sporadic forms of IPF are clinically and histologically indistinguishable, although younger age at diagnosis and different patterns of gene expression appear to distinguish between the two. In addition, recent family-based studies have identified rare genetic variants, which are shared by both familial and sporadic IPF.

Table I. summarizes the main genetic associations with sporadic IPF and familial forms. The occurrence of IPF in twins raised apart along with geographical clustering of cases reinforce the role of genetic factors in the development of the disease[28].

Table I. Summary of the main genetic associations with sporadic and familial idiopathic pulmonary fibrosis.

Familial pulmonary fibrosis		**Sporadic pulmonary fibrosis**	
Gene	**Variant**	**Gene**	**Variant**
SFTPC	Several loss-of-function mutations	*SFTPC*	Several loss-of-function mutations
SFTPA2	G231V and F198S loss-of-function mutations	*IL1RN*	rs408392 rs419598 rs2637988
MUC5B	rs35705950	*TOLLIP*	rs5743890 rs5743894 rs111521887
TERT	Leu55Gln Thr1110Met	*TERT*	Leu55Gln Thr1110Met
TERC	rs6793295	*TERC*	98 G > A 37 A > G
DKC1	Several loss-of-function mutations	*CDKN1A*	rs2395655 rs733590

Specific genetic variants

Genes encoding for cytokines (such as interleukin (IL)-1, tumor necrosis factor (TNF)-α, lymphotoxin α, IL-4, IL-6, IL-8, IL-10, and IL-12), enzymes like α1-antitrypsin and angiotensin-converting enzyme, profibrotic molecules (transforming grow factor (TGF)-β1), coagulation pathway genes (plasminogen activator inhibitors-1 and -2), genes for surfactant protein-A and -B, immunomodulatory genes (complement receptor 1, NOD2/CARD15), and matrix metalloproteinase (MMP)-, are the main polymorphisms detected[29-35]. Despite this evidence, none of these findings has been validated in further studies.

Genome-wide association studies (GWAS) and linkage studies have identified most common genetic variants that appear to contribute the development of IPF[27].

Surfactant protein C (SFTPC) and A2 (SFTPA2) genes

The first genetic variants associated with pulmonary fibrosis were identified after 2000[36]. Nogee and colleagues reported on an infant girl of six weeks of age who was diagnosed with nonspecific interstitial pneumonitis. Her mother had been diagnosed with Desquamative Interstitial Pneumonitis (DIP) at 1 year of age. In both the patient and the mother, the SFTPC mutation was identified on only one allele, indicating an autosomal dominant pattern of inheritance. The baby was treated successfully with corticosteroids and supplemental oxygen, and the respiratory symptoms improved. Since the initial description by Nogee, several mutations in SFPTC and SFTPA2 have been associated with familial pulmonary fibrosis[37]. Mutation in the SFTPC has not been described in patients with the sporadic form of the disease, while SFTPA2, has been recently linked with familial pulmonary fibrosis and lung cancer, in the eventuality of a rare mutation.

Mucin 5B gene (MUC5B)

In 2011, Seibold and colleagues published the most important article on genetics of IPF to date[38]. By applying a genome-wide linkage analysis followed by sequencing, they were able to identify a single nucleotide polymorphism (SNP) (rs35705950) located in the promoter region of MUC5B on chromosome 11p15.5, which was strongly associated both with sporadic IPF and with FIP. For details, see the ‘MUC5B in interstitial lung diseases’ above.

Human telomerase reverse transcriptase (hTERT) or human telomerase rna (hTR)

Telomeres consist of repetitive DNA sequences of TTAGGG at the ends of linear chromosomes, which protect the chromosome ends that progressively shorten with each cell division[39]. Telomerase is a specialized DNA polymerase responsible for telomere elongation onto chromosome ends. Telomerase has two different components that carry out the function of telomere repeat addition: the core telomerase protein TERT, which contains the telomerase reverse transcriptase domain, and an essential RNA component, TR (also known as TERC), which complexes with TERT and provides the template for telomere elongation[26].

Reduced telomerase function leads to accelerated telomere shortening, which, under normal circumstances, occurs with aging. Short telomeres also induce a DNA damage response leading to cell death or permanent cell cycle arrest. As such, telomere shortening has been involved in a number of degenerative age-related diseases. Accelerated telomere shortening may lead to a number of clinical features, referred to as "premature aging syndrome"[26]. Pulmonary fibrosis, similar to bone marrow failure (i.e., bone marrow dysplasia, aplasia or myelodysplastic syndromes) and liver fibrosis/cryptogenic cirrhosis may result from loss of regenerative capacity, and is among the more severe clinical consequences of telomere shortening[40]. Accordingly, compared to age-matched controls, IPF patients display higher frequencies of fibrotic disease outside the lung. Abnormalities of telomere biology and maintenance are believed to represent the "missing" link between ageing and IPF. Several reports have described that mutations within either of the essential components of the telomerase complex, the human telomerase reverse transcriptase (hTERT), or the human telomerase RNA (hTR), are associated with familial IPF[41]. Germline mutations in hTERT and hTR are present in 8-15% of pulmonary fibrosis families. Mutations in hTERT and hTR determine loss of function and decreased telomere activity leading to haploinsufficiency. Interestingly, a small minority (approximately 1-3%) of sporadic cases also carry these same mutations, suggesting the existence of shared pathogenetic mechanisms. Some studies have tested the hypothesis that short telomeres contribute to disease risk also in sporadic IPF by examining telomere length in peripheral blood leukocytes and alveolar cells[42]. Alder and collaborators evaluated patients with sporadic IPF, patients with IPF and known telomerase mutations and healthy lungs. Telomere length was assessed by using quantitative FISH analysis. IPF patients irrespective of carriage of telomerase gene-associated mutations have indistinctly shorter telomeres than controls[42]. Moreover, individuals affected by FIP are clinically indistinguishable from patients with sporadic disease although familial cases have a younger age at presentation and may present some differences in radiological pattern[43].

Genetic variants and survival implications

Genetic variants may also be associated with survival. Noth and colleagues found that variants within Toll interacting protein (TOLLIP) and signal peptide

peptidase like 2C (SPPL2C) influence risk of developing IPF[44]. Specifically, carriers of the minor allele (G) of rs5743890 had both decreased risk of IPF and increased mortality[45], a finding difficult to explain. Similarly, Peljto and colleagues observed that carriers of the MUC5B rs35705950 risk allele had a survival advantage[46]. A functional SNP in Toll-like receptor 3 (TLR3) has also been associated with accelerated disease progression and with increased mortality in patients with IPF[47]. The mechanism for these observed differences in mortality remains unknown, but could be related to underlying differences in disease pathogenesis or in the clinical response to commonly prescribed therapies.

PATHOGENESIS

Collagen deposition is an indispensable and, typically, reversible part of wound healing, even though normal tissue repair can evolve into a progressively irreversible fibrotic response if the tissue injury is severe or if the wound-healing response itself becomes dysregulated.

Fibrosis is defined by the pathological accumulation of excess extracellular matrix (ECM) components, such as collagen and fibronectin, and mainly due to chronic inflammatory diseases. If highly progressive, the fibrotic process finally leads to organ disfunction.

IPF was once thought to be the result of a chronic inflammatory process. The established belief directly relating fibrosis with chronic inflammation has been recently confuted. Current evidence indicates that the fibrotic response arises from multiple repeated damage to alveolar epithelial cells (AECs), followed by an abnormal healing process. AECs cells can produce mediators that induce the accumulation of fibroblasts and myofibroblasts through the proliferation of resident mesenchymal cells, attraction of circulating fibrocytes, and stimulation of the epithelial to mesenchymal transition. The fibroblasts and myofibroblasts secrete excessive amounts of extracellular matrix, mainly collagens, resulting in scarring and destruction of the lung architecture[8]. Many distinct causes can contribute to the development of progressive fibrotic disease. The coagulation response is the first wound-healing mechanism activated after injury. The coagulation cascade is an important pathological process in fibrosis, because has several profibrotic effects. Subsequently, abnormalities in coagulation cascade can substantially contribute to the development of progressive fibrotic disease. TNF-α and IL-1β, in particular,

have been identified as important cytokines involved in a variety of fibrotic diseases. Macrophages belong to the innate inflammatory response and appear early in the wound-healing response. These cells are major producers of TGF-β, which is considered one of the main drivers of fibrosis. Indeed, TGF-β production correlates with the progression of liver, lung, kidney, skin and cardiac fibrosis. On the other hand, inhibition of the TGF-β signaling pathway has been shown to reduce the development of fibrosis.

Fibrocytes are bone marrow derived precursors that can migrate to the sites of injury. As such, they can be detectable in peripheral blood. Fibrocytes may be recruited in response to chemokines generated by infection or injury and may increase fibrogenesis via extracellular matrix production and/or secretion of profibrotic factors. Recent evidence describes that circulating fibrocytes are increased in IPF compared with normal control subjects. Additionally, patients with acute exacerbations of IPF have levels of fibrocytes further elevated[48].

Neovascularization is a fundamental process in tissue repair after injury and it depends on the balance between various factors, mainly chemokines that promote or inhibit angiogenesis. An increased angiogenesis has been described in experimental lung fibrosis; even though, the role of angiogenesis in IPF is unclear.

DIAGNOSTIC CRITERIA

The ideal approach for the diagnosis of fibrosis is an integrated approach and the last guidelines pointed out new aspects in the classical diagnostic algorithm (**Figure 1**)[7].

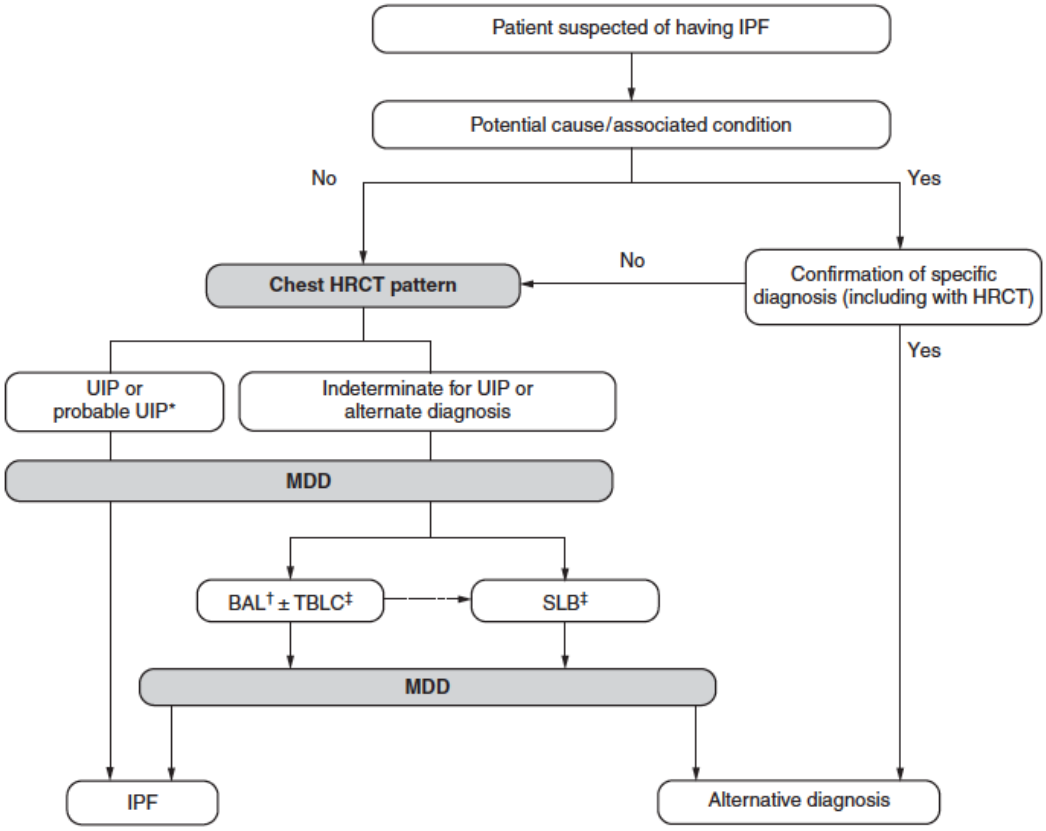

Figure 1: Diagnostic algorithm in suspected IPF[7].

Physicians should use a standardized approach, focusing on several points such as history and physical examination. Diagnosis of IPF requires the following:
1. Exclusion of other known causes of ILD (e.g., domestic and occupational environmental exposures, CTD, drug toxicity), and either:
2. The presence of the HRCT pattern of UIP or UIP probable,
3. Specific combinations of HRCT patterns and histopathology patterns in patients subjected to lung tissue sampling.

When a patient is suspected for IPF, exclusion of other known causes of ILD, such as domestic or occupational environmental exposures, connective tissue disease, drug toxicity, is firstly required. Patients with suspected IPF (i.e., unexplained symptomatic or asymptomatic bilateral pulmonary infiltrates on a chest radiograph or high resolution chest computed tomography (HRCT) scan, bibasilar inspiratory crackles, and age older than 60 years), unexplained dyspnea on exertion, and/or cough with evidence of interstitial lung disease (ILD) should be carefully evaluated for potential and/or identifiable causes of ILD, such as domestic and occupational environmental exposures, connective tissue disease (CTD), or

drug toxicity. If a potential cause for ILD is identified, the patient should undergo a thorough evaluation to confirm or exclude other known causes, such as hypersensitivity pneumonitis, CTD, pneumoconiosis, and iatrogenic causes (e.g., drug toxicity, irradiation). If a specific diagnosis is not made or no potential cause for ILD is identified, further evaluation is influenced by the patterns of HRCT images of the chest and supportive clinical findings surfaced in the course of multidisciplinary discussion to ascertain or exclude the diagnosis of IPF. IPF is diagnosed if the appropriate combination of HRCT patterns and histopathological patterns are present. Surgical lung biopsy may be unnecessary in some familial cases.

As might be expected, in order to perform an accurate diagnosis for ILD, clinical, radiologic, histopathologic evaluations must be considered for the diagnosis of IPF, and analyzed during multidisciplinary discussions (MMD) among experienced clinical experts in the field of ILDs. Proper communication between the various disciplines involved in the diagnosis of IPF (pulmonary, radiology, pathology) has been established to improve inter-observer agreement and diagnostic confidence among experienced clinical experts, in order to the ultimate diagnosis[49]. Some studies have proved that, after a careful exchange between clinical radiographic and histopathologic information, final diagnosis often differs from the initial diagnosis reached by the individual clinician, radiologist, or pathologist working in isolation. This is specifically essential, when the radiologic and the histopathologic patterns are not concordant.

DEFINITION OF UIP PATTERN

HRCT features

Thin-section CT is one of the most important imaging examinations for the evaluation of interstitial pneumonia, and specifically recommendations are stressed in the last guidelines for IPF diagnosis[7,50].

HRCT plays an essential role in the diagnosis of IPF. On HRCT scan of the chest, four possible patterns could be detected: UIP pattern, probable UIP, indeterminate for UIP, CT findings suggestive for an alternative diagnosis.

UIP is the hallmark radiologic pattern of IPF (**Figure 2 A-E**). Honeycombing is a distinguishing feature of ***UIP*** and must be present for a definite

HRCT diagnosis of UIP to be made. It can be seen with or without peripheral traction bronchiectasis or bronchiolectasis. The typical distribution of UIP is subpleural with basal predominance, although some upper lobe involvement is common; in some cases, the craniocaudal distribution of UIP may be relatively uniform. In some case, mediastinal lymph node may be detected, usually with mild enlargement (< 1.5 cm in short axis)[5]. Ground glass opacities are a common finding, but less diffuse than reticulations. If extensive ground glass is found, an alternative diagnosis should be suspected. A definite UIP pattern on HRCT is highly associated to the presence of UIP pattern on surgical lung biopsy. In the absence of honeycombing, the HRCT pattern is defined as probable UIP. Disagreement on the identification of honeycombing may be due to misinterpretation of conditions that may mimic honeycombing, such as traction bronchiectasis and emphysema[51].

An HRCT pattern of ***probable UIP*** with peripheral traction bronchiectasis or bronchiolectasis in the correct clinical setting likely represents histopathologic UIP on biopsy[7]. As with a UIP pattern, ground-glass opacification may be present in probable UIP, but it is not a dominant feature. Many patients with an HRCT pattern of probable UIP will be determined to have IPF once other factors such as histopathology are considered.

It is now recognized that atypical HRCT features frequently (i.e., about 30%) accompany a histopathologic pattern of UIP/IPF. Therefore, the category ***indeterminate for UIP*** pattern should be assigned when HRCT demonstrates features of fibrosis but does not meet UIP or probable UIP criteria and does not explicitly suggest an alternative diagnosis. This category includes a subset of patients with very limited subpleural ground-glass opacification or reticulation without obvious CT features of fibrosis, for whom there is a suspicion that early UIP or probable UIP is present. In such cases, it should be confirmed with prone inspiratory views that the subpleural opacities do not represent dependent atelectasis.

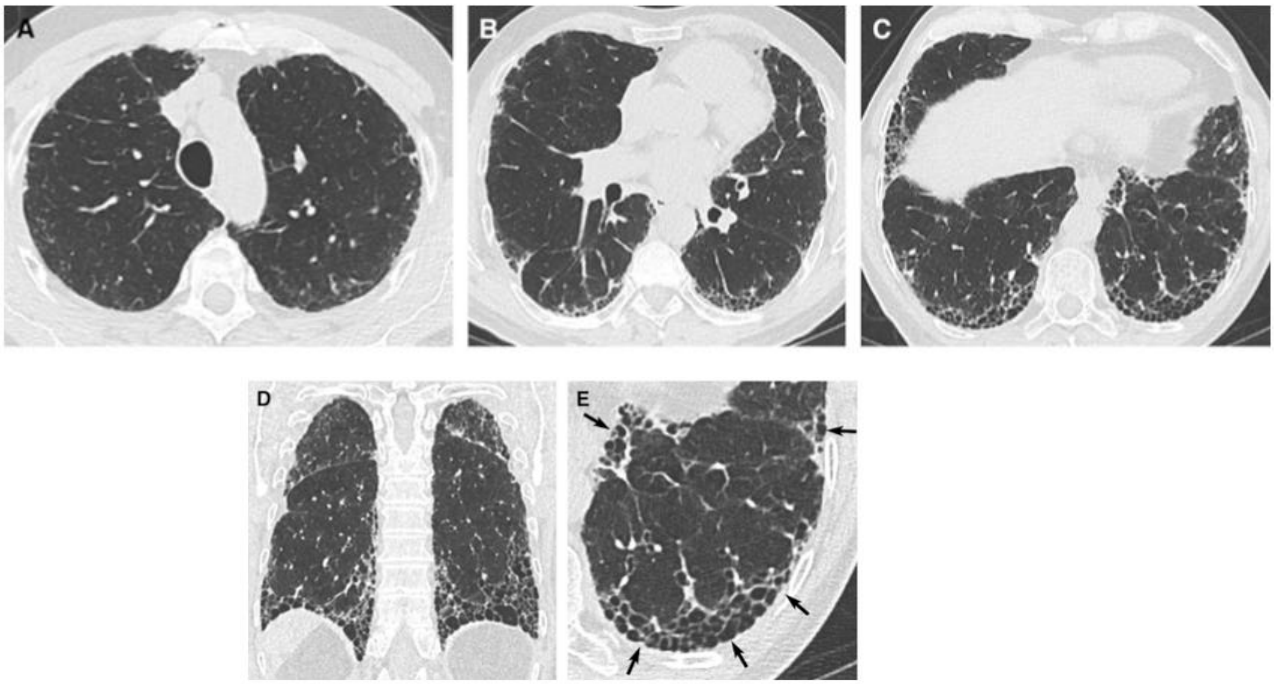

Figure 2A-E: **UIP Pattern on High-resolution computed tomography (HRCT) patchy subpleural reticular opacities and honeycombing with basal predominance, in association with bronchiectasis[6]**. (A–C) Transverse CT section and (D) coronal reconstruction illustrating the presence of honeycombing with subpleural and basal predominance. (E) Magnified view of the left lower lobe showing typical characteristics of honeycombing, consisting of clustered cystic airspaces with well-defined walls and variable diameters, seen in single or multiple layers (arrows).

Histopathology features

Video-assisted thoracoscopic surgery is the preferred approach to surgical lung biopsy (SLB) for patients who can tolerate single-lung ventilation, rather than open thoracotomy. In patients with severe physiologic impairment or substantial comorbidity, the risks of SLB may outweigh the benefits of establishing a secure diagnosis of IPF; therefore, the final decision regarding whether or not to pursue a biopsy must be tailored to the clinical situation of the individual patient. Multiple biopsies should be obtained from two to three lobes, because the histologic patterns on SLB specimens obtained from different segments can be discordant (e.g., coexisting UIP pattern and fibrotic NSIP pattern from different lobes).

The histopathologic hallmark and chief diagnostic criterion of UIP is a low magnification appearance of patchy dense fibrosis that:

- is causing remodeling of lung architecture
- often results in honeycomb change
- alternates with areas of less-affected parenchyma.

These histopathologic changes typically affect the subpleural and paraseptal parenchyma most severely. Inflammation is usually mild and consists of a patchy interstitial infiltrate of lymphocytes and plasma cells associated with hyperplasia of type 2 pneumocytes and bronchiolar epithelium. The fibrotic zones are composed mainly of dense collagen, although scattered convex subepithelial foci of proliferating fibroblasts and myofibroblasts (so-called fibroblast foci) are a consistent finding. Microscopic honeycombing is characterized by cystic fibrotic airspaces that are frequently lined by bronchiolar epithelium and filled with mucus and inflammatory cells. Smooth muscle metaplasia in the interstitium is commonly seen in areas of fibrosis and honeycombing. A definitive pathologic diagnosis of the UIP pattern can be made when all of the above features are present, particularly when honeycombing is present. However, even in the absence of honeycombing, a definite diagnosis of a UIP pattern can still be made if all of the other typical features are present.

We recommend categorizing histopathologic findings of biopsies into ***UIP, probable UIP, indeterminate for UIP,*** and ***alternative diagnosis***[6] (**Figure 3A-D**). Advantages of this approach are that this terminology is consistent with imaging categories (although the specificity of the "alternative diagnosis" categories differs) and it allows us to discuss the patterns in the context of other clinical data during an MDD. This facilitates making the most appropriate overall diagnosis for the patient, regardless of whether the diagnosis is IPF or not IPF. Biopsies designated as indeterminate for UIP demonstrate a pattern of fibrosis that does not meet criteria for UIP or any other histopathologic pattern of fibrotic interstitial pneumonia and, in some cases, may favor an alternative diagnosis while not categorically excluding the possibility of sampling bias in a patient who ultimately proves to have UIP. A subset of patients with previously occult IPF may present with an acute exacerbation, which is commonly characterized by a combination of a UIP pattern complicated by superimposed diffuse alveolar damage with or without associated hyaline membranes.

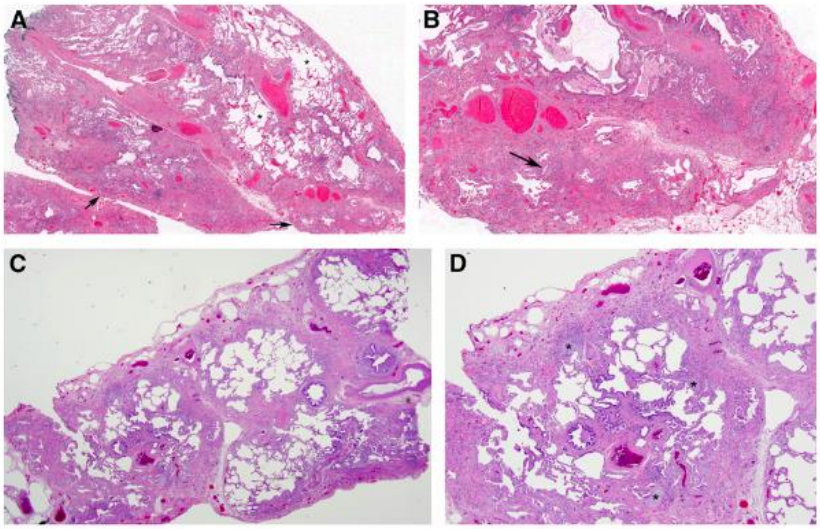

Figure 3A-3D: Histopathology demonstrating UIP[6]. (A) Low-magnification photomicrograph showing classical UIP/idiopathic pulmonary fibrosis (IPF) pattern characterized by dense fibrosis with a predilection for subpleural and paraseptal parenchyma with associated architectural distortion in the form of microscopic honeycomb change (arrow) juxtaposed with relatively unaffected lung parenchyma. Visceral pleura is seen in the upper portion of the figure. (B) Higher-magnification photomicrograph showing subpleural scarring and honeycomb change with associated fibroblast foci (arrow). (C) Low-magnification photomicrograph showing probable UIP/IPF pattern characterized by subpleural and paraseptal predominant patchwork fibrosis that is less well developed and lacks the degree of associated architectural distortion in the form of either destructive scarring or honeycomb change illustrated in A and B. (D) Higher-magnification photomicrograph showing patchy fibrosis and fibroblast foci (*) but without the extent of scarring and honeycomb change illustrated in A and B.

Natural history of IPF

By definition, the natural history of IPF has been described as a progressive, associated with a significant decline in objective and subjective function. Death occurs for respiratory failure or complicating comorbidities (such as coronary artery disease, pulmonary embolism and lung cancer). Risk of death increases with age and older male seem to have a worse prognosis.

There are several possible natural histories for patients with IPF, and the median survival time can only be a rough estimate. Most studies suggest a median survival time of 3 years from the time of diagnosis and a 5 years survival of around 20%. Anyway, for a given patient the natural history is unpredictable at the time of diagnosis. The majority of patients have a slow, gradual progression over many years, some patients remain stable, while other patients have an accelerated decline ('rapid progression')[5,6,51,52] (**Figure 4**). In the course of disease, some patient may present episode of acute respiratory worsening of unknown etiology (named acute exacerbations of IPF), which are almost inevitably fatal. It is unknown if this different natural histories depend on distinct phenotypes of IPF or if the natural history is influenced by geographic, ethnic, cultural, racial or other factors. Other comorbid conditions such as emphysema and pulmonary hypertension may impact the disease progression. The relative frequency of each of these natural histories in unknown.

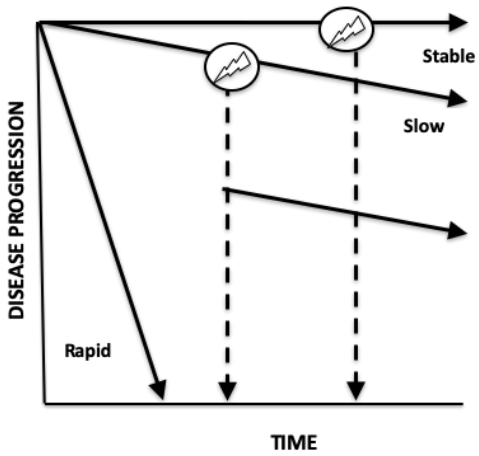

Figure 4: Natural history of IPF.

Disease staging and prognosis

At the time of diagnosis, the clinical evolution of IPF is difficult, almost impossible to define. In other words, clinical impairment is totally variable. For staging IPF, terms such as 'early', 'mild', 'moderate', 'severe' and 'advanced' have been proposed. Suggested stages are commonly based on:

- resting pulmonary function tests[51] and/or
- extent of radiologic abnormalities[53].

In spite of this classification, it is unknown if these staging approaches are relevant to clinical decision making. Recently, some predictors of survivals in IPF

have been described. They may include the following: younger age (<50years), female sex, shorter symptomatic period (<1year) with less dyspnea, relatively preserved lung function.

Some selected features could be involved in increasing mortality. Because of the variability in the natural history of IPF, it is unknown if the number of these mortality predictors could be relevant to identify a subpopulation of patients with 'advanced' or 'end-stage' IPF[5, 54].

- Older male patients seem to have a worse prognosis. It is unknown if smoking could condition the prognosis of the disease. The prognostic value of geographic, ethnic, cultural and racial factors remains unknown.
- Baseline dyspnea is involved in the determination of quality of life and survival. At present, several different metrics for dyspnea have been proposed, including measurement tools with respiratory questionnaires, University of California San Diego shortness of breath questionnaire, clinical-radiological-physiological dyspnea score, and so on. Change in baseline dyspnea over time may predict survival.
- Baseline pulmonary function tests have shown a variable connection with survival in IPF. Baseline forced vital capacity (FVC) is an unsure predictive value. Diffusing capacity for carbon monoxide (DLCO, single breath, hemoglobin corrected) is a more reliable predictive value of survival in patients with IPF. In particular, when DLCO value is a threshold of approximately 40% predicted, it is correlated to an increased risk of mortality.
- Longitudinal factors, connected with progressive changes in physiology over time are important predictor of mortality in IPF. A decline in FVC over 6 or 12 months of 5-10% may be a predictor of decreased survival. A decreasing DLCO value could be connected with a higher risk of mortality, although with less evidence. Decrease in DLCO greater than 15 mmHg change in P (A-a)O2 after 12 months has been shown to be predictive of survival. Finally, six-month change in total lung capacity (TLC) and P(A-a)O2 may also be predictive of survival.

  Several groups have demonstrated that the extent of fibrosis and honeycombing on HRCT are predictor of survival in patients with fibrosis[55]. In 2015, Hansell and co-workers emphasized the role of HRCT in staging IPF, in monitoring clinical conditions over time, and in being considered a primary

endpoint for current and future drug trials[56]. HRCT images seem to be more sensitive than functional measurements and cardiopulmonary exercise test parameters in identifying subjects with asymptomatic pulmonary fibrosis[53,57]. At present, based on the latest guidelines, at least two-thirds of the cases might receive a confident diagnosis of IPF integrating the clinical data of the patient and by recognizing the UIP pattern on the HCRT. Already in 2010, Fell and colleagues have suggested that age combined with a huge amount of fibrosis on HRCT may be considered an accurate diagnostic predictor for diagnosing IPF[58]. A clear correlation between functional changes and CT evolution over time has not yet been established. A composite physiologic index (CPI) has been proposed to combine physiological and radiographic variables in an attempt to provide more accurate prognostic information[59]. CPI takes into account values from FEV1, FVC and DLCO to predict the range of disease on HRCT. The purpose is to provide a stronger predictor of mortality in fibrosis progression, in comparison with individuals measures of lung function such as FEV1, FVC, DLCO, TLC, PaO2 or the single clinical-radiographic-physiological scoring system.

- Some studies have shown that a decline in oxygen saturation to below 88% during 6MWT is a marker of mortality.
- The prognosis for patients with discordant UIP on histopathology, that is pattern of UIP and NSIP within the same patient, seems to be similar to that of patients with a UIP pattern in all lobes analyzed (concordant UIP).
- Pulmonary hypertension is defined as a mean pulmonary artery pressure of > 25mmHg at rest. Pulmonary hypertension has been associated with an increased risk of mortality for patients with IPF.
- The co-existing presence of emphysema in patients with IPF leads to a poor survival rate, in comparison to those without emphysema.
- Only few data try to analyze the predictive value of serum and BAL biomarkers in IPF. The human MUC1 mucin KL-6 is a high-molecular-weight glycoprotein, produced by type 2 pneumocytes, that have been revealed to be increased in patients with IPF. These levels may correlate with increased risk of subsequent mortality. Serum levels of surfactant A and D are also elevated in patients with IPF and are potential predictor of survival. Some studies suggest that matrix metalloproteinase (MMP)-1 and MMP7 in BAL may

correlate with disease progression. In conclusion, more data about the relevance of cellular analysis of bronchoalveolar lavage (BAL) should be provided by further studies. Among all of the mortality predictors mentioned above, biomarkers may represent the main promising parameter to consider, in order to better characterize patients in terms of staging.

- A simple-to-use prognostic staging system for IPF have been recently described[54]. Four variables were included in the final model: gender (G), age (A), and 2 lung physiology variables (P), such as FVC and DLCO. On the base of these parameters, the continuous predictor GAP calculator and the simple point-scoring system GAP index has been proposed to predict mortality in IPF. Consequently, three stages (stages I, II, and III) were identified based on the GAP index with 1-year mortality of 6%, 16%, and 39%, respectively (Table D). In conclusion, the GAP models use commonly measured clinical and physiologic variables to predict mortality in patients with IPF.

TREATMENT

Based on the available evidence, none of the treatments currently available or under investigation has been shown to improve survival or quality of life in patients with IPF.

Recent evidence emphasizes the central role played by aberrant wound healing following repeated lung injury, against the previous idea that IPF is a consequence of chronic inflammation. These new evidences weakened the rationale for the use of corticosteroids in IPF. As consequence corticosteroid and immune-modulator therapy (such as colchicines, cyclosporine A, Interferon-γ 1b, etanercept) are no longer recommended for the treatment of IPF[4].

Recent evidences emphasized a different mechanism based on myofibroblasts and fibroblasts activation, in response to mediators coming from alveolar epithelial cells (AECs). The epithelium might directly determine the expansion of the population of fibroblasts and myofibroblasts through the mesenchimal transition (EMT). In this process, epithelial cells acquire mesenchymal properties through which they increase their capability to move and to synthesize excessive amounts of extracellular matrix, resulting in scarring and

destruction of the lung architecture[8]. As a consequence, new clinical trials about treatment have been focused on an anti-fibrotic targeted approach[15,16,60].

Pirfenidone

Pirfenidone is a pyridine compound with pleiotropic, anti-inflammatory, antifibrotic, and antioxidant properties, in opposition to TGF-β1 effects. The CAPACITY studies (CAPACITY 1 - PIPF 006 and CAPACITY 2 - PIPF 004), two almost identical randomized, double-blind, placebo-controlled, multinational Phase III studies, evaluated the efficacy of oral pirfenidone over 72 weeks[61]. The primary endpoint was change in percentage predicted FVC at week 72, for both the studies. In study 004, mean FVC change at week 72 was -8.0% in the pirfenidone 2,403 mg/day group and -12.4% in the placebo group ($p = 0.001$). Conversely, in the 006 study, the change in FVC at week 72 did not differ significantly between the active and placebo arms ($p = 0.501$). In ASCEND (Assessment of Pirfenidone to Confirm Efficacy and Safety in Idiopathic Pulmonary Fibrosis) study, a randomized, double-blind, placebo-controlled trial, patients were randomized to receiving 1:1 pirfenidone 2,403 mg/die or placebo[62]. The study met his primary outcome of change from baseline to week 52 in the percentage of predicted FVC (−164 mL in the pirfenidone arm versus −280 mL in the placebo arm). In addition, pirfenidone reduced by 47.9% the proportion of patients with a decline of ≥10% in percentage predicted FVC or died and increased of 132.5% the proportion of patients with no decline in FVC ($p<0.001$).

Subsequently pirfenidone approval in October 2014, an open-label extension study (RECAP) evaluating pirfenidone in IPF patients who were previously randomized to the placebo group in the CAPACITY program, have been reported[63]. Patients received oral pirfenidone 2403 mg/day and the primary endpoint was FVC decline at week 60. Results have shown 16.3 % patients experiencing an FVC decline ≥10% at week 60, compared with 16.8 % and 24.8 %, respectively, in the CAPACITY pirfenidone and placebo groups, and a mean decline from baseline to week 60 in % FVC of 5.9 % as compared with 7.0 % and 9.4 % in the CAPACITY pirfenidone and placebo groups.

Nintedanib

The TOMORROW (To Improve Pulmonary Fibrosis With BIBF 1120), a 12-month, randomized, double-blind, placebo-controlled Phase II study, evaluated the safety and efficacy of BIBF 1120 (nintedanib), a tyrosine kinase inhibitor that suppresses pro-angiogenic intracellular signaling by targeting the proliferative growth factor receptors on platelets (PDGFR), vascular endothelium (VEGFR) and fibroblasts (FGFR)[64]. Nintedanib at a dose of 150 mg twice daily showed a trend toward a reduction in the decline in FVC - the primary outcome. Specifically, in the group receiving 150 mg of nintedanib twice a day, FVC declined by 0.06 liters per year, as compared with 0.19 liters per year in the placebo group, an almost 70% reduction in the rate of loss.

The INPULSIS program included INPULSIS-1 and INPULSIS-2, two parallel multinational, randomized, double-blind, placebo-controlled, parallel-group phase 3 studies testing the efficacy and safety of assumption of nintedanib 150 mg twice daily as compared with placebo[15]. The primary end point was the annual rate of decline in FVC over a period of 52 weeks. The annual rate of decline in FVC was 114.7 ml in nintedanib group versus 239.9 ml in placebo group in INPULSIS-1 and 113.6 ml in nintedanib group versus 207.3 ml in placebo group in INPULSIS-2.

Pamrevlumab

CTGF is a secreted glycoprotein produced by various cell types, including fibroblasts, myofibroblasts, and endothelial cells. CTGF is thought to interact with various regulatory modulators, such as TGF-β, vascular endothelial growth factor, and receptors such as integrins. Through these interactions, CTGF modulates cellular responses to their environment, such as secretion or organisation, or both, of extracellular matrix, cell motility, and adhesion— biological activities that are associated with aberrant tissue repair (ie, fibrosis) and tumorigenesis. In patients with IPF, CTGF gene transcription in transbronchial lung biopsy specimens was reported to be approximately four times higher than in patients without idiopathic pulmonary fibrosis[65]. Additionally, CTGF in plasma was reported to be elevated in patients with idiopathic pulmonary fibrosis and the increased concentration correlated with change in FVC[66]. These observations suggest that CTGF might have a role in the pathogenesis of idiopathic pulmonary fibrosis.

Pamrevlumab (FG-3019) is a fully human recombinant monoclonal antibody against connective tissue growth factor (CTGF), which has been shown to act as a central mediator in the process of fibrosis. In the phase 2, randomised, double-blind, placebo-controlled PRAISE trial[60], Pamrevlumab reduced the decline in percentage of predicted FVC by 60% at week 48. The proportion of patients with disease progression was lower in the pamrevlumab group than in the placebo group at week 48. Based on these promising results, phase 3 trial is ongoing in many countries.

Nonpharmacologic therapies

Patients with IPF and clinically significant resting hypoxiemia (SpO2 < 88%) should be treated with long-term oxygen therapy. Selected patients with IPF may undergo lung transplantation. Lung transplantation should be considered for patients with progressive clinical deterioration despite medical treatment[67]. Some studies have shown a reduced risk of death at 5 years in patients undergoing lung transplantation, with a five-years survival rate estimated at 50 to 60%.

Patients with worse baseline functional status can benefit from the effects of pulmonary rehabilitation.

It has been mentioned above the existence of comorbidities associated with IPF. To date, there is no information regarding the usefulness of the treatment of the comorbidities, such as obesity, emphysema and obstructive sleep apnea, in patients with IPF. Treating these comorbidities may influence clinical outcomes. Anyway, it remains a matter to be explored.

MONITORING THE CLINICAL COURSE OF DISEASE

Patients with IPF should be monitored periodically. IPF is a chronic progressive disease and some clinical events may occur during the course of disease. For this reason, monitoring of patients with IPF is necessary to proactively identify patients with progressive disease, to detect worsening of symptoms and oxygenation, and to survey the course of disease or treatment complications.

Increasing respiratory symptoms, worsening in pulmonary function test results, progressive fibrosis in HRCT and acute respiratory decline are the main aspect to consider when a disease progression is suspected. The presence of any of the following changes is consistent with progressive disease:

- progressive dyspnea.
- progressive, sustained decrease from baseline in absolute FVC;
- progressive, sustained decrease from baseline in absolute DLCO;
- progression of fibrosis and ground glass from baseline on HRCT
- acute exacerbation
- death from respiratory failure.

Dyspnea is a relevant symptom, and for patients it represents an important subjective variable of suffering. To date, several different metrics for the objective measurement of dyspnea have been proposed. Measurement tools may be respiratory questionnaires, University of California San Diego shortness of breath questionnaire, clinical-radiological-physiological dyspnea score, and so on. Nevertheless, it remains uncertain which dyspnea metric is most predictive of outcome in patients with IPF. Change in baseline dyspnea over time may predict survival. For this reason, monitoring for progressive dyspnea is an important point to consider.

Pulmonary function test results are other parameters to focus on. Several clinical studies to date emphasize that a change in absolute DLCO of 15% (with or without a concomitant change in FVC) or a change in absolute FVC are critical markers of mortality. In absence of an alternative explanation, they are evidence of disease progression[51,52]. When smaller (5-10%) but progressive changes in FVC occur, this fact may also represent progression of disease. Exact threshold values of this parameters are difficult to explain, but isolated changes of less than 10% FVC and less than 15% in DLCO should be considered critical. A decreasing change in absolute DLCO in absence of an alternative explanation is consistent with progressive disease, although such a decline may be due to changes in pulmonary vasculature and coexistent pulmonary hypertension. Comorbidities such as coexisting emphysema may be a confounding factor on the predictive values in pulmonary function. The presence of a concomitant emphysema impacts FVC measurement, so FVC may be not a reliable indicator of disease progression.

Evidence suggests that longitudinal measurement of other clinical and physiological variables (TLC, P(A-a)O2) and 6MWT variables are not useful for routine monitoring in patients with disease progression, at this time.

Of the parameters listed above, pulmonary function test results provide the most standardize and objective approach to monitoring and to quantification of disease progression.

ROLE OF MUCINS

Respiratory epithelium is lined by mucus, a gel consisting of water, ions, proteins, and macromolecules. Mucus serves a vital role in maintaining health and function of the lungs, is a barrier to prevent water loss and to remove inhaled foreign substances such as microbes, inflammatory cells, and pollutant particles. In the setting of chronic airway inflammation, respiratory mucus contains debris from bacteria or inflammatory cells[68].

The major macromolecular components of mucus, the mucin glycoproteins, are secreted by surface epithelial goblet cells, submucosal gland mucous and serous cells, or are tethered to cell membranes. Cell surface-associated mucins attached to airway epithelial microvilli and cilia generate an osmotic barrier, whereas the secreted, oligomeric mucin proteins retain water and form viscoelastic gels[69].

The coordinated interaction of membrane-associated and secreted mucins in the healthy airway surface liquid (ASL) establishes muco-ciliary clearance. The gel-forming mucins polymerize, this allows the trapped particles in the gel matrix to be cleared by muco-ciliary or cough transport. The innate immune function of mucins goes beyond muco-ciliary clearance to include direct interactions with *dendritic cells* and new assignments for *goblet cells* as primary sensors of environmental threats to the epithelial surface[70].

Mucins are encoded by MUC genes; to date, 21 human MUC genes have been identified of which 14 are expressed in the airway[71]. Seven mucins predominate in airway protein expression: four membrane associated mucins (MUC1, MUC4, MUC16, MUC20); two gel-forming mucins (MUC5AC, MUC5B); and one secreted, non-gel-forming mucin (MUC7). The presence of characteristic repeating sequences of amino acids rich in proline, serine and threonine, where O-linked glycosylation occurs, distinguishes mucins from other glycoproteins[72]. The relatively short O-linked glycans (2-20 monosaccharides per chain) constitute up to 80% of the molecular weight of the mucins, decorating the mucin protein core, whose number of repeated sequences is unique to each mucin. Mucins have a vital

role in airways immunity by capturing infectious agents and expelling them through muco-ciliary or cough clearance.

Mucins in interstitial lung diseases

Due to their essential role in airway protection and inflammatory regulation mucins have been studied in the context of ILDs.

MUC1, also known as KL-6, firstly used as a serum tumor marker, has been dismissed for its high false positive rate in patients with pulmonary fibrosis. This evidence helped understanding the role of this protein in ILD patients[73]. MUC1 additive role in anti-apoptosis and proliferation activities to those of TGFβ in fibroblast has been described by Hirasawa et al.[74]. Also tissue evaluation showed a correlation between MUC1 expression and the presence of ILD; Ohtsuki et al. reported linear and continuous staining for MUC1 on the cell surface of regenerating type II pneumocytes in patients with ILDs of various etiology (CTD-ILD, HP, IPF, NSIP), but only discontinuous staining in normal lung tissues[75].

Secretory mucin **MUC5AC** and **MUC2** concentration in BAL fluid in ILD patients resulted significantly higher than in patients with pleural effusion in a recent study by Wei et al[76]. In the same study MUC5AC resulted connected with the number of lymphocytes in the fluid and negatively associated to ventilation and diffusion capacity of the patients, implying that this glycoprotein has a role in inflammation and function impairment of the lung.

MUC5AC expression was also evaluated on surgical lung biopsies or lower lobes of different ILDs and compared to normal lung tissue in two different studies, with conflicting results: Seibold et al. observed an increased expression of MUC5AC in distal airway of IPF/UIP samples[77]; on the contrary, Conti et al. observed that the MUC5AC expression in honeycomb cyst of IPF/UIP patients were significantly lower than normal lung and comparable only in the distal airways, also they found that in NSIP and CTD-ILD lungs the percentage of MUC5AC positive cells were lower to controls[78].

MUC5B in interstitial lung diseases

MUC5B is one of the pulmonary gel-forming secretive mucins, in normal lungs its expression is localized in submucosal gland mucus cells and forms a mucin layer atop the periciliary layer with MUC5AC.

MUC5B has an important role in airway immunity, such as other mucins, by capturing infectious agents and expelling them through muco-ciliary or cough clearance.

Seibold et al. using a genomic linkage scan in families with familiar interstitial pneumonia detected a linkage between 82 families and a 3.4 Mb region of chromosome 11p15[38]. This region included genes for MUC2, MUC5AC and MUC5B. SNP rs35705950 is sited 3kb upstream the MUC5B transcription starting site, in its promoter region. The wild-type G allele of the rs35705950 SNP is conserved across primate species, it is directly 5′ (or adjacent) to a highly conserved region across vertebrate species. MUC5B minor allele T is common, at least in Caucasian ethnicity, where it is present in approximately 20% of European population. Even sharing the same genetic variant, individuals with this SNP rs35705950 that do not develop to IPF different individuals may not be exposed to other 'risk factors' for fibrosis.

On further investigations, made on 83 subjects with FIP, 492 with IPF and 322 controls, the single-nucleotide polymorphism (SNP) rs35705950 minor allele T demonstrate a strong connection with pulmonary fibrosis. Individuals carrying the mutant allele (T) either in heterozygous (GT) or homozygous form had an odds ratio for disease of 6.8 and 20.8 respectively for familial pulmonary fibrosis (FIP), and 9.0 and 21.8 respectively for IPF. The frequency of the T allele was 34% in familial cases, 38% in sporadic IPF cases, and 9% in control subjects. The association between MUC5B and IPF has been validated in several independent and a meta-analysis confirmed the correlation found in small cohort[44,79,80] (**Figure 5**), so that the MUC5B promoter polymorphism remains the strongest and most replicated genetic risk factor for pulmonary fibrosis to date.

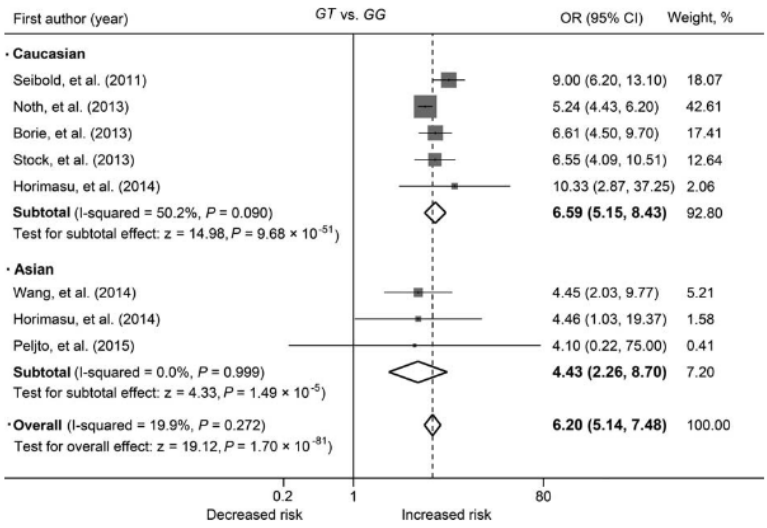

Figure 5.[81] MUC5B rs35705950 GT genotype increased risk of IPF compared with GG genotype. Forest plot of odds ratios (ORs) and 95% confidence intervals (95% CIs) from each study, subgroup and overall analysis were shown. Subgroup analyses were stratified by ethnicity.

Altered MUC5B expression is associated with chronic airway disease and these findings suggest a role in the pathogenesis of pulmonary fibrosis[82]. Mucus overproduction contributes to the morbidity of many airway diseases, among which the most common are chronic obstructive pulmonary disease (COPD), asthma, cystic fibrosis (CF), and diffuse chronic panbronchiolitis. In mice, MUC5B deficiency leads to airway particle accumulation, mucous obstruction of the airways, increased risk of developing infection, and inflammation with impaired macrophage phagocytosis and death. **In addition, many researchers have speculated that the overproduction of MUC5B contributes to the development of IPF resulting from excessive lung injury and aberrant repair,** however, little is known about the influencing factors of gene expression. Two are the mechanisms postulated[83]:

- first, excessive MUC5B compromises the mucosal host defense and reduces lung clearance of inhaled particles, dissolved chemicals, and microorganisms. Over time, reduced clearance may lead to scar tissue formation and persistent fibroproliferation that expands and displaces normal lung tissue. Based on these considerations, as stem cells attempt to regenerate injured bronchiolar and alveolar epithelium, excess expression of MUC5B may disrupt normal

developmental pathways and hijack the normal reparative mechanisms in the distal lung, resulting in chronic fibroproliferation and honeycomb cyst formation **(Figure 6**).

- second, excessive MUC5B in the respiratory bronchioles may interfere with alveolar repair. Too much MUC5B may impair mucociliary function, cause excess retention of inhaled substances (air pollutants, cigarette smoke, microorganisms, etc.), and, over time, the foci of lung injury may lead to scar tissue and persistent fibroproliferation that expands and displaces normal lung tissue (**Figure 7**).

Seibold et al explored the effect of rs35705950 on MUC5B expression in lung tissue from 33 subjects with idiopathic pulmonary fibrosis and 47 control patients. MUC5B expression was 14.1 times higher among the subjects with idiopathic pulmonary fibrosis, the expression of the gene among control patients carrying at least one copy of the variant allele was 37.4 times higher than it was among control patients, who were homozygous for the wild-type allele. The same team found that MUC5B positive distal airways were more frequent in the IPF/UIP lung relative to control subjects, suggesting two processes:

- conversion of MUC5B- distal airways to MUC5B+ airways;
- increased frequency of MUC5B expressing cells in distal airways that were already positive.

Of interest, the same authors reported on the intriguing tightly connection between MUC5B gene variants and honeycomb cysts, one of the pathologic hallmarks of IPF[38]. In subjects with idiopathic pulmonary fibrosis, regions of dense accumulation of MUC5B were observed in areas of microscopical honeycombing and involved patchy staining of the metaplastic epithelia lining the honeycomb cysts[84,85]. Recent evidence showed epithelial cells expressing MUC5B are the dominant mucin-expressing cell type in microscopic honeycomb cysts (**Figure 8**). The microscopic honeycomb cysts are filled with MUC5B protein and chronic inflammation cells and lined by pseudostratified ciliated columnar epithelium similar to those which line the bronchioles. MUC5B immunohistochemical staining has shown a dense accumulation of MUC5B in microscopic honeycomb cysts, in mucous plugs within the cysts as well as pseudostratified bronchial epithelium[84,86].

The observation of over-expression of MUC5B in micro-honeycomb cysts was subsequently confirmed[86].

MUC5B promoter variant, rs35705950, is 32 bp upstream from the FOXA2 binding motif, it's likely that the variant and the binding site function together within a composite regulatory element. There are two probable hypotheses for the interaction:

- MUC5B promoter variant is associated with regional changes in methylation and this could directly affect FOXA2 occupancy. In this case, increased methylation of the surrounding area leads to increased binding of FOXA2;
- MUC5B promoter variant may alter the binding affinity/specificity for other transcription factors that interact with or are recruited by FOXA2 to regulate MUC5B expression.

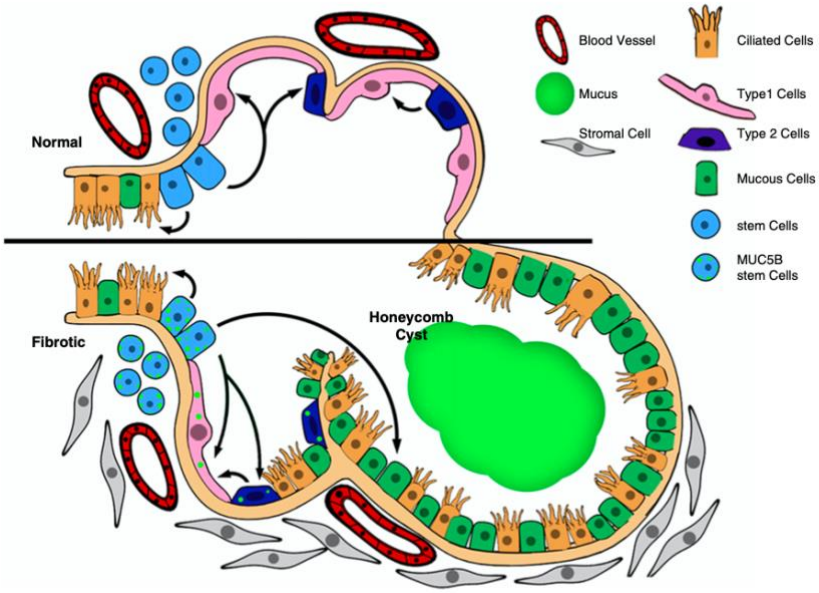

Figure 6[83]. Model of stem cells repopulating bronchioles and alveoli under normal physiologic conditions and when challenged with increased expression of MUC5B. The excessive production of MUC5B by stem cells attempt to regenerate injured bronchiolar and alveolar epithelium disrupt normal developmental pathways and hijack the normal reparative mechanisms in the distal lung, resulting in chronic fibroproliferation and honeycomb cyst formation.

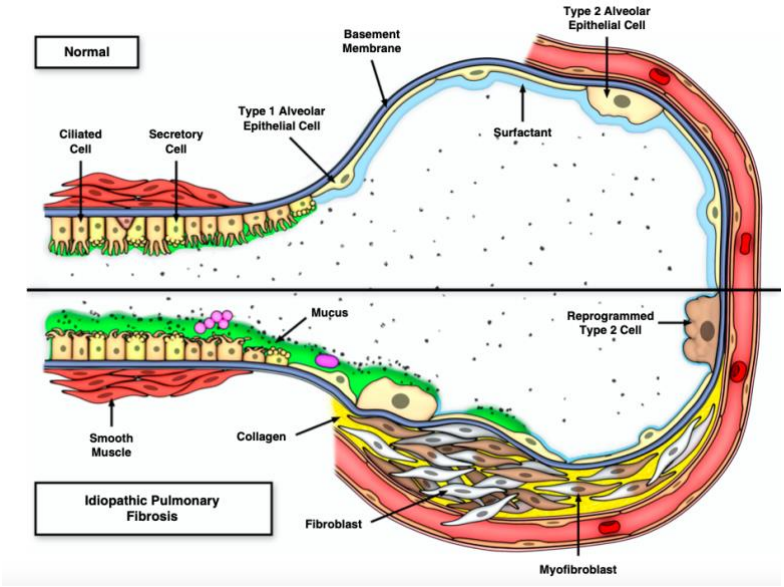

Figure 7[83]. Model of recurrent injury/repair at the bronchoalveolar junction that is initiated and exacerbated by overexpression of MUC5B, retention of inhaled particles, and enhanced lung injury. The upper panel is the normal bronchoalveolar region and the lower panel represents a bronchoalveolar region affected by idiopathic pulmonary fibrosis (IPF). IPF could be a mucociliary disease that is caused by recurrent injury/repair at the bronchoalveolar junction that is initiated and exacerbated by overexpression of MUC5B leading to reduced ciliary function, retention of particles, and enhanced injury.

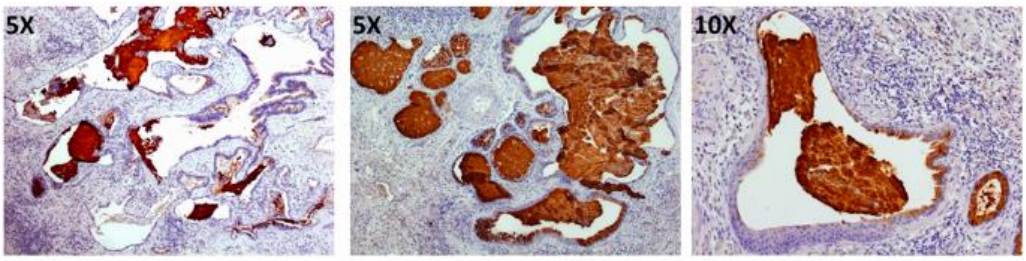

Figure 8[86]. Immunohistochemical staining for MUC5B protein (brown) in cystic structures in idiopathic pulmonary fibrosis (IPF) lung. Left: An area of IPF lung tissue containing histologically normal airway and honeycomb cysts. Middle and right: Honeycomb cysts, exclusively. In all three panels, honeycomb cysts are filled with mucus. Tissue was counterstained with hematoxylin.

In conclusion, besides the promoter variant rs35705950, which definitely causes an overexpression of MUC5B and appears to be predictive of IPF, some transcriptional factors, inflammatory mediators, and associated

signaling pathways may also mediate MUC5B overexpression, leading to fibrogenesis.

Interestingly, the Framingham Heart Study by Hunninghake and colleagues[87] has shown that the odds for radiographic interstitial lung abnormalities (ILA) were 2.8 times greater for each copy of the rs35705950 minor allele. The term ILA refers to the presence on chest CT scans of subtle abnormalities such as subpleural reticular changes, honeycombing, traction bronchiectasis, ground glass, and centrilobular nodules affecting more the 5 % of each lung zone[88]. This study for the first time suggests a link between the polymorphism of MUC5B and ILA, suggesting that MUC5B genotype may potential be useful for early detection of fibrosis in asymptomatic individuals. In a subsequent study, Araki T. and co-workers categorized the Framingham Heart Study population in patients with and without ILA and analyzed the presence of progressive change over time, defined as an increase in lung areas affected with nondependent ground-glass, reticular abnormalities, diffuse centrilobular nodularity, nonemphysematous cysts, honeycombing, or traction bronchiectasis, or a new appearance of at least one such abnormality. They demonstrated that increasing copies of the MUC5B promoter polymorphism were associated with ILA progression, which correlate with functional impairmaint[89].

In IPF, the **prognostic** role of MUC5B had discordant interpretation; Peljito et al. found that the presence of the minor allele was a protective factor for all mortality cause, with a hazard ratio of 0.48 in heterozygous patients and 0.21 in homozygous patients[90]. Otherwise Jiang et al. found that IPF patients with increased presence of T allele tend to have shorter overall survival.

After these findings based on IPF, studies started to focus the interest on understanding a common pathway involving MUC5B SNP rs35705950 with other ILDs:

- Peljto et al. found no significative difference in frequency of the minor allele in systemic sclerosis (SSc) between patients with interstitial pneumonia (IP) and without IP (10.6% and 9.4% frequency respectively), neither between SSc patients and controls (9.0% frequency)[90];

- Stock et al. confirmed the absence of correlation between the minor allele and the patients with SSc and IP, similarly, no difference was found in between patients with sarcoidosis in stage I-III and the ones with stage IV sarcoidosis and fibrotic presentation[79];
- Ley et al. confirmed that also in chronic HP the frequency of minor allele was greater than healthy controls (24/32% vs 10.9%), in the same study was also found that the presence of minor allele correlates more with the presence of moderate/severe fibrosis and traction bronchiectasis than usual HP findings such as air trapping, airway centered fibrosis and granulomas[91];
- Juge et al. in a multicentric study compared the association between rheumatoid arthritis with interstitial lung disease (RA-ILD), rheumatoid arthritis (RA) alone and unaffected controls[92]. MUC5B promoter variant was found as a strong risk factor for RA-ILD, especially among patients with UIP pattern. However, SNP rs35705950 has no role in RA pathogenesis.

REFERENCES

1. Corte TJ, Collard H, Wells AU. Idiopathic interstitial pneumonias in 2015: A new era. Respirology. 2015 Jul;20(5):697-8. doi: 10.1111/resp.12559. Epub 2015 Jun 2. PMID: 26037830.
2. Sverzellati N, Lynch DA, Hansell DM, Johkoh T, King TE, Travis WD. American Thoracic Society– European Respiratory Society Classification of the Idiopathic Interstitial Pneumonias: Advances in Knowledge since 2002. Radiographics 2015;35(2):1849–72.
3. Raghu G, Collard HR, Egan JJ, et al. An Official ATS/ERS/JRS/ALAT Statement: Idiopathic pulmonary fibrosis: Evidence-based guidelines for diagnosis and management. Am J Respir Crit Care Med 2011;183(6):788–824.
4. Raghu G, Rochwerg B, Zhang Y, et al. An official ATS/ERS/JRS/ALAT clinical practice guideline: Treatment of idiopathic pulmonary fibrosis: An update of the 2011 clinical practice guideline. Am J Respir Crit Care Med 2015;192(2):e3–19.
5. Lynch DA, Sverzellati N, Travis WD, et al. Diagnostic criteria for idiopathic pulmonary fibrosis: a Fleischner Society White Paper. Lancet Respir Med. 2018 Feb;6(2):138-153.
6. Raghu G, Remy-Jardin M, Myers JL, et al; American Thoracic Society, European Respiratory Society, Japanese Respiratory Society, and Latin American Thoracic Society. Diagnosis of Idiopathic Pulmonary Fibrosis. An Official ATS/ERS/JRS/ALAT Clinical Practice Guideline. Am J Respir Crit Care Med. 2018 Sep 1;198(5):e44-e68. doi: 10.1164/rccm.201807-1255ST. PMID: 30168753.
7. Raghu G, Remy-Jardin M, Richeldi L, et al. Idiopathic Pulmonary Fibrosis (an Update) and Progressive Pulmonary Fibrosis in Adults: An Official ATS/ERS/JRS/ALAT Clinical Practice Guideline. Am J Respir Crit Care Med. 2022 May 1;205(9):e18-e47.
8. Lederer DJ, Martinez FJ. Idiopathic pulmonary fibrosis. NEJM 2018;29(5):283–91.
9. Spagnolo P, Maher TM, Richeldi L. Idiopathic pulmonary fibrosis: Recent advances on pharmacological therapy. Pharmacol Ther. 2015;152:18–27. doi:10.1016/j.pharmthera.2015.04.005
10. Navaratnam V. et al. Epidemiology, in Idiopathic Pulmonary Fibrosis. ERS Monogr 2016;71(1–15).
11. Hutchinson J, Fogarty A, Hubbard R, McKeever T. Global incidence and mortality of idiopathic pulmonary fibrosis: a systematic review. Eur Respir J. 2015;46(3):795–806. doi:10.1183/09031936.00185114
12. Navaratnam V, Fleming KM, West J, Smith CJ, Jenkins RG, Fogarty A HR. The rising incidence of idiopathic pulmonary fibrosis in the U.K. Thorax 66(6)(6):462–7.
13. Raghu G, Chen SY, Yeh WS, Maroni B, Li Q, Lee YC CH. Idiopathic pulmonary fibrosis in US Medicare beneficiaries aged 65 years and older: incidence, prevalence, and survival, 2001-11. Lancet Respir Med 2014;2((7)):566–72.
14. Lederer DJ, Martinez FJ. Idiopathic Pulmonary Fibrosis. N Engl J Med. 2018;378(19):1811–1823. doi:10.1056/NEJMra1705751

15. Richeldi L, du Bois RM, Raghu G, et al. Efficacy and safety of nintedanib in idiopathic pulmonary fibrosis. N Engl J Med [Internet] 2014;370(22):2071–82. Available from: http://www.ncbi.nlm.nih.gov/pubmed/24836310
16. King TEJ, Bradford WZ, Castro-Bernardini S, et al. A Phase 3 Trial of Pirfenidone in Patients with Idiopathic Pulmonary Fibrosis. N Engl J Med [Internet] 2014;370(22):2083–92. Available from: http://dx.doi.org/10.1056/NEJMoa1402582%5Cnhttp://www.nejm.org/doi/full/10.1056/NEJMoa1402582%5Cnhttp://www.nejm.org/doi/pdf/10.1056/NEJMoa1402582
17. Spagnolo P, Molyneaux PL, Bernardinello N, et al. The role of the lung's microbiome in the pathogenesis and progression of idiopathic pulmonary fibrosis. Int J Mol Sci 2019;20(22).
18. Tang YW, Johnson JE, Browning PJ, et al. Herpesvirus DNA is consistently detected in lungs of patients with idiopathic pulmonary fibrosis. J Clin Microbiol 2003;41(6):2633–40.
19. Kreuter M, Raghu G. Gastro-oesophageal reflux and idiopathic pulmonary fibrosis: The heart burn in patients with IPF can no longer be silent. Eur Respir J [Internet] 2018;51(6):11–3. Available from: http://dx.doi.org/10.1183/13993003.00921-2018
20. Kreuter M, Wuyts W, Renzoni E, et al. Antacid therapy and disease outcomes in idiopathic pulmonary fibrosis: A pooled analysis. Lancet Respir Med [Internet] 2016;4(5):381–9. Available from: http://dx.doi.org/10.1016/S2213-2600(16)00067-9
21. Ghisa M, Marinelli C, Savarino V, Savarino E. Idiopathic pulmonary fibrosis and gerd: Links and risks. Ther Clin Risk Manag 2019;15:1081–93.
22. Sgalla G, Cocconcelli E, Tonelli R, Richeldi L. Novel drug targets for idiopathic pulmonary fibrosis. Expert Rev Respir Med 2016;10(4).
23. Wei ML. Hermansky-Pudlak syndrome: A disease of protein trafficking and organelle function. Pigment Cell Res 2006;19(1):19–42.
24. Zhou W, Wang Y. Candidate genes of idiopathic pulmonary fibrosis: Current evidence and research. Appl Clin Genet 2016;9:5–13.
25. Armanios M, Chen JL, Chang YPC, et al. Haploinsufficiency of telomerase reverse transcriptase leads to anticipation in autosomal dominant dyskeratosis congenita. Proc Natl Acad Sci U S A 2005;102(44):15960–4.
26. Armanios M. Syndromes of Telomere Shortening. Annu Rev Genomics Hum Genet 2009;10(1):45–61.
27. Kropski JA, Blackwell TS, Loyd JE. The genetic basis of IPF. Eur Respir J 2015;45(6):1717–27.
28. Mathai SK, Yang I V., Schwarz MI, Schwartz DA. Incorporating genetics into the identification and treatment of Idiopathic Pulmonary Fibrosis. BMC Med [Internet] 2015;13(1):1–6. Available from: http://dx.doi.org/10.1186/s12916-015-0434-0
29. Zorzetto M, Ferrarotti I, Campo I, Trisolini R, Poletti V, Scabini R, Ceruti M, Mazzola P, Crippa E, Ottaviani S et al. NOD2/CARD15 gene polymorphisms in idiopathic pulmonary fibrosis. Sarcoidosis Vasc Diffus Lung Dis 2005;(22):180–185.

30. Freeburn RW, Kendall H, Dobson L, Egan J, Simler NJ MA. The 39 untranslated region of tumor necrosis factor-alpha is highly conserved in idiopathic pulmonary fibrosis (IPF). Eur Cytokine Netw 2001;(12:):33–38.
31. Pantelidis P, Fanning GC, Wells AU, Welsh KI, Du Bois RM. Analysis of tumor necrosis factor-alpha, lymphotoxin-alpha, tumor necrosis factor receptor II, and interleukin-6 polymorphisms in patients with idiopathic pulmonary fibrosis. Am J Respir Crit Care Med. 2001;163(6):1432–1436. doi:10.1164/ajrccm.163.6.2006064
32. Hutyrova B, Pantelidis P, Drabek J, Zrkova M, Kolek V, Lenhart K, Welsh KI, Du Bois RM PM. Interleukin-1 gene cluster polymorphisms in sarcoidosis and idiopathic pulmonary fibrosis. Am J Respir Crit Care Med 2002;165:148–151.
33. Latsi P, Pantelidis P, Vassilakis D, Sato H, Welsh KI du BR. Analysis of IL-12 p40 subunit gene and IFN-gamma G5644A polymorphisms in Idiopathic Pulmonary Fibrosis. Respir Res 2003;(4:6).
34. Whittington HA, Freeburn RW, Godinho SIH, Egan J, Haider Y MA. Analysis of an IL-10 polymorphism in idiopathic pulmonary fibrosis. Genes Immun 2003;4:258–264.
35. Riha RL, Yang IA, Rabnott GC, Tunnicliffe AM, Fong KM, Zimmerman PV. Cytokine gene polymorphisms in idiopathic pulmonary fibrosis. Intern Med J. 2004;34(3):126–129. doi:10.1111/j.1444-0903.2004.00503.x
36. Nogee LM, Dunbar AE 3rd, Wert SE, Askin F, Hamvas A, Whitsett JA. A mutation in the surfactant protein C gene associated with familial interstitial lung disease. N Engl J Med. 2001;344(8):573–579. doi:10.1056/NEJM200102223440805
37. Lawson WE, Grant SW, Ambrosini V, et al. Genetic mutations in surfactant protein C are a rare cause of sporadic cases of IPF. Thorax 2004;59(11):977–80.
38. Seibold MA, Wise AL, Speer MC, et al. A common MUC5B promoter polymorphism and pulmonary fibrosis. N Engl J Med. 2011;364(16):1503–1512. doi:10.1056/NEJMoa1013660
39. Calado RT, Young NS. Telomere diseases. N Engl J Med. 2009;361(24):2353–2365. doi:10.1056/NEJMra0903373
40. Armanios M. BEH. The Telomere Syndromes. 2013;70(4):646–56.
41. Armanios M. Telomerase and idiopathic pulmonary fibrosis. Mutat Res - Fundam Mol Mech Mutagen 2012;730(1–2):52–8.
42. Steele MP, Speer MC, Loyd JE, et al. Clinical and pathologic features of familial interstitial pneumonia. Am J Respir Crit Care Med 2005;172(9):1146–52.
43. Snetselaar R, van Batenburg AA, Van Oosterhout MFM, et al. Short telomere length in IPF lung associates with fibrotic lesions and predicts survival. PLoS One 2017;12(12).
44. Noth I, Zhang Y, Ma S, et al. Genetic variants associated with idiopathic pulmonary fibrosis susceptibility and mortality: a genome-wide association study. Lancet Respir Med 2014;1(4):309–17.
45. Fingerlin TE, Murphy E, Zhang W, et al. Genome-wide association study identifies multiple susceptibility loci for pulmonary fibrosis. Nat Genet 2013;45(6):613–20.

46. Peljto AL, Zhang Y, Fingerlin TE, et al. Association between the MUC5B promoter polymorphism and survival in patients with idiopathic pulmonary fibrosis. JAMA - J Am Med Assoc 2013;309(21):2232–9.
47. O'Dwyer DN, Armstrong ME, Trujillo G, et al. The toll-like receptor 3 L412F polymorphism and disease progression in idiopathic pulmonary fibrosis. Am J Respir Crit Care Med 2013;188(12):1442–50.
48. Collard HR, Moore BB, Flaherty KR, et al. Acute exacerbations of idiopathic pulmonary fibrosis. Am J Respir Crit Care Med 2007;176(7):636–43.
49. Flaherty KR, King TE, Raghu G, et al. Idiopathic interstitial pneumonia: What is the effect of a multidisciplinary approach to diagnosis? Am J Respir Crit Care Med 2004;170(8):904–10.
50. Watadani T, Sakai F, Johkoh T, et al. Interobserver variability in the CT assessment of honeycombing in the lungs. Radiology 2013;266(3):936–44.
51. Balestro E, Calabrese F, Turato G, et al. Immune inflammation and disease progression in idiopathic pulmonary fibrosis. PLoS One 2016;11(5):1–11.
52. Selman M, Carrillo G, Estrada A, et al. Accelerated variant of idiopathic pulmonary fibrosis: Clinical behavior and gene expression pattern. PLoS One 2007;2(5).
53. Hansell DM, Goldin JG, King TE, Lynch DA, Richeldi L, Wells AU. CT staging and monitoring of fibrotic interstitial lung diseases in clinical practice and treatment trials: A Position Paper from the Fleischner society. Lancet Respir Med [Internet] 2015;3(6):483–96. Available from: http://dx.doi.org/10.1016/S2213-2600(15)00096-X
54. Ley B, Ryerson CJ, Vittinghoff E, et al. A multidimensional index and staging system for idiopathic pulmonary fibrosis. Ann Intern Med. 2012 May 15;156(10):684-91. doi: 10.7326/0003-4819-156-10-201205150-00004. PMID: 22586007.
55. Ley B, Elicker BM, Hartman TE, et al. Idiopathic Pulmonary Fibrosis: CT and Risk of Death. Radiology [Internet] 2014;273(2):570–9. Available from: http://www.ncbi.nlm.nih.gov/pubmed/24927326
56. Rosas IO, Yao J, Avila NA, Chow CK. Automated Quantifi cation of High-Resolution CT Scan Findings in Individuals at Risk for Pulmonary Fibrosis. Chest 2011;140 (6):1590–7.
57. Ley B, Collard HR, King TE. Clinical course and prediction of survival in idiopathic pulmonary fibrosis. Am J Respir Crit Care Med 2011;183(4):431–40.
58. Fell CD, Martinez FJ, Liu LX, et al. Clinical predictors of a diagnosis of idiopathic pulmonary fibrosis. Am J Respir Crit Care Med 2010;181(8):832–7.
59. Wells AU, Desai SR, Rubens MB, et al. Idiopathic pulmonary fibrosis: A composite physiologic index derived from disease extent observed by computed tomography. Am J Respir Crit Care Med 2003;167(7):962–9.
60. Richeldi L, Fernández Pérez ER, Costabel U, et al. Pamrevlumab, an anti-connective tissue growth factor therapy, for idiopathic pulmonary fibrosis (PRAISE): a phase 2, randomised, double-blind, placebo-controlled trial. Lancet Respir Med 2019;2600(19):1–9.
61. Noble PW, Albera C, Bradford WZ, Costabel U, Glassberg MK, Kardatzke D, King TE Jr, Lancaster L, Sahn SA, Szwarcberg J, Valeyre D du BRCSG. Pirfenidone in patients with

idiopathic pulmonary fibrosis (CAPACITY): two randomised trials. Lancet 377(9779):1760-9.

62. King TE Jr, Bradford WZ, Castro-Bernardini S, Fagan EA, Glaspole I, Glassberg MK, Gorina E, Hopkins PM, Kardatzke D, Lancaster L, Lederer DJ, Nathan SD, Pereira CA, Sahn SA, Sussman R, Swigris JJ NP. ASCEND Study Group. A phase 3 trial of pirfenidone in patients with idiopathic pulmonary fibrosis. N Engl J Med 370(22):2083-92.
63. Costabel U, Albera C, Bradford WZ, Hormel P, King TE Jr, Noble PW, Sahn SA, Valeyre D du BR. Analysis of lung function and survival in RECAP: An open-label extension study of pirfenidone in patients with idiopathic pulmonary fibrosis. Sarcoidosis Vasc Diffus Lung Dis 31(3):198-205.
64. Richeldi L, Costabel U, Selman M, Kim DS, Hansell DM, Nicholson AG, Brown KK, Flaherty KR, Noble PW, Raghu G, Brun M, Gupta A, Juhel N, Klüglich M du BR. Efficacy of a tyrosine kinase inhibitor in idiopathic pulmonary fibrosis. N Engl J Med 2011;365(12):1079-87.
65. Ziesche R, Hofbauer E, Wittmann K, Petkov V BL. A preliminary study of long-term treatment with interferon gamma-1b and low-dose prednisolone in patients with idiopathic pulmonary fibrosis. N Engl J Med 1999;341:1264–69.
66. Kono M, Nakamura Y, Suda T et al. Plasma CCN2 (connective tissue growth factor; CTGF) is a potential biomarker in idiopathic pulmonary fibrosis (IPF). Clin Chim Acta 2011;412:2211–15.
67. Balestro E, Cocconcelli E, Tinè M, et al. Idiopathic pulmonary fibrosis and lung transplantation: When it is feasible. Med 2019;55(10).
68. Voynow JA MB. Mucins, mucus, and sputum. Chest 2009;135(2):505–12.
69. Ma J, Rubin BK VJ. Mucins, Mucus, and Goblet Cells. Chest 2018;2018;154(1):169-176.
70. Hill DB, Vasquez PA, Mellnik J et al. A biophysical basis for mucus solids concentration as a candidate biomarker for airways disease. PLoS One 2014;9(2):1-11.
71. D. S. Gene group: Mucins (MUC). https://www.genenames.org/data/genegroup/#!/group/648
72. Rose MC VJ. Respiratory tract mucin genes and mucin glycoproteins in health and disease. Physiol Rev 2006;86(1):245-278.
73. Ishikawa N, Hattori N, Yokoyama A KN. Utility of KL-6/MUC1 in the clinical management of interstitial lung diseases. Respir Investig 2012;50((1)):3-13.
74. Hirasawa Y, Kohno N, Yokoyama A, Inoue Y, Abe M HK. KL-6, a Human MUC1 Mucin, Is Chemotactic for Human Fibroblasts. Am J Respir Cell Mol Biol 1997;17(4):501-507.
75. Ohtsuki Y, Nakanishi N, Fujita J et al. Immunohistochemical distribution of SP-D, compared with that of SP-A and KL-6, in interstitial pneumonias. Med Mol Morphol 2007;40(3):163-167.
76. Wei L, Zhao J, Bao J, Ma Y, Shang Y GZ. The characteristics and clinical significance of mucin levels in bronchoalveolar lavage fluid of patients with interstitial lung disease. J Investig Med 2019;67(4):761-766.

77. Seibold MA, Smith RW, Urbanek C et al. e Idiopathic Pulmonary Fibrosis Honeycomb Cyst Contains A Mucocilary Pseudostratified Epithelium. PLoS One 2013;8(3).
78. Conti C, Montero-Fernandez A, Borg E et al. Mucins MUC5B and MUC5AC in Distal Airways and Honeycomb Spaces: Comparison among Idiopathic Pulmonary Fibrosis/Usual Interstitial Pneumonia, Fibrotic Nonspecific Interstitial Pneumonitis, and Control Lungs. Am J Respir Crit Care Med 2016;193(4):462-464.
79. Stock CJ, Sato H, Fonseca C, et al. Mucin 5B promoter polymorphism is associated with idiopathic pulmonary fibrosis but not with development of lung fibrosis in systemic sclerosis or sarcoidosis. Thorax 2013;68(5):436–41.
80. Borie R, Crestani B, Dieude P, et al. The MUC5B Variant Is Associated with Idiopathic Pulmonary Fibrosis but Not with Systemic Sclerosis Interstitial Lung Disease in the European Caucasian Population. PLoS One 2013;8(8):1–6.
81. Zhu QQ, Zhang XL, Zhang SM, et al. Association between the MUC5B promoter polymorphism rs35705950 and idiopathic pulmonary fibrosis: A meta-analysis and trial sequential analysis in Caucasian and asian populations. Med (United States) 2015;94(43):1–8.
82. Zhang Q, Wang Y, Qu D, Yu J, Yang J. The Possible Pathogenesis of Idiopathic Pulmonary Fibrosis considering MUC5B. Biomed Res Int 2019;2019:12–9.
83. Schwartz DA. Idiopathic pulmonary fibrosis is a genetic disease involving mucus and the peripheral airways. Ann Am Thorac Soc 2018;15(November):S192–7.
84. Seibold MA, Wise AL, Speer MC et al. A Common MUC5B Promoter Polymorphism and Pulmonary Fibrosis. N Engl J Med 2011;364(16):1503–12.
85. Seibold MA, Smith RW, Urbanek C, et al. The Idiopathic Pulmonary Fibrosis Honeycomb Cyst Contains A Mucocilary Pseudostratified Epithelium. PLoS One 2013;8(3).
86. Yang I V., Fingerlin TE, Evans CM, Schwarz MI, Schwartz DA. MUC5B and idiopathic pulmonary fibrosis. Ann Am Thorac Soc 2015;12:S193–9.
87. Hunninghake GM, Hatabu H, Okajima Y et al. MUC5B Promoter Polymorphism and Interstitial Lung Abnormalities. N Engl J Med 2011;23(1):1–7.
88. Putman RK, Rosas IO, Hunninghake GM. Genetics and early detection in idiopathic pulmonary fibrosis. Am J Respir Crit Care Med 2014;189(7):770–8.
89. Araki T, Putman RK, Hatabu H, et al. Development and progression of interstitial lung abnormalities in the Framingham Heart Study. Am J Respir Crit Care Med 2016;194(12):1517–22.
90. Peljto AL, Steele MP, Fingerlin TE et al. The pulmonary fibrosis-associated MUC5B promoter polymorphism does not influence the development of interstitial pneumonia in systemic sclerosis. Chest 2012;142(6):1584-1588.
91. Ley B, Newton CA, Arnould I et al. The MUC5B promoter polymorphism and telomere length in patients with chronic hypersensitivity pneumonitis: an observational cohort-control study. Lancet Respir Med 2017;5(8):639–47.
92. Juge PA, Lee JS, Ebstein E et al. MUC5B promoter variant and rheumatoid arthritis with interstitial lung disease. N Engl J Med 2018 379(23):2209–19.

Chapter 3

Progressive pulmonary fibrosis (PPF), a new clinical entity

Elisabetta Cocconcelli

PROGRESSIVE PULMONARY FIBROSIS

Together with the update on IPF diagnostic algorithm, the ATS/ERS/JRS/ALAT defined the new clinical entity of progressive pulmonary fibrosis (PPF).

In recent almost four years, clinicians have pointed out the existence of some patients with ILD other than IPF, presenting a clinical course similar to IPF despite a good adherence to specific treatments (including corticosteroids and/or immunosuppressive therapy).

We have previously discussed ILDs are defined as lung disorders with variable degrees of pulmonary inflammation and fibrosis, including disorders occurring in the context of a clear pathological condition (connective tissue diseases (CTD), environmental exposure or drug related disease) as well as disorders of unknown etiology[1]. IPF is the most common among the idiopathic interstitial pneumonia and presents a clinical/functional/radiological decline irrespective of the current antifibrotic treatments[2-4].

ILDs other than IPF were worldwide known to present a better prognosis compared to IPF[5,6]. Nonetheless, in addition to IPF, clinicians observed that a number of fibrosing ILDs can develop a progressive phenotype characterized histologically by self-sustaining fibrosis, a process common to a variety of conditions, and which leads to worsening quality of life, decline in lung function and, eventually, early mortality despite common treatments[7,8]. The real occurrence of PPF is unknown, but some studies postulated that up to 40% of ILD different from IPF may present a clinical course similar to IPF[7].

Certain types of chronic fibrosing ILD are more at risk of developing a progressive phenotype[3,7], and mostly include idiopathic nonspecific interstitial pneumonia, unclassifiable ILD, autoimmune ILDs especially rheumatoid arthritis-associated ILD, chronic hypersensitivity pneumonitis, genetic pulmonary fibrosis, and exposure-related diseases. On the contrary, ILDs like sarcoidosis (even stage IV), cryptogenic organizing pneumonia, desquamative interstitial pneumonia and respiratory bronchitis-ILD rarely have a relentless, progressive course with worsening fibrosis despite appropriate therapy.

Some evidences suggested that PPFs share similarities to IPF regarding pathogenesis and clinical behavior[9]. Several mechanisms are known to be involved in the pathogenesis and progression of all PPF. ILDs are believed to be triggered

by repetitive chronic epithelial or vascular injuries, or by granulomatous inflammation, which lead to cell destruction and, in the case of fibrotic disease, to unregulated repair. Fibroblasts, are drawn from blood and other different sources and migrate to the site of injury. Resident interstitial fibroblasts proliferate and migrate, and finally all these fibroblasts are activated to become myofibroblasts, which secrete excessive amounts of extracellular matrix, resulting in increased tissue stiffness and loss of function of the alveolar tissue.

Defining PPF was vary challenge, but the main guide was the experience of the last decades on IPF. In IPF, most studies have defined disease progression in terms of a decline in forced vital capacity (FVC), measured as the change from baseline or as a categorical change (typically ⩾10% predicted in patients without antifibrotic treatment and ⩾5% in treated patients), or more recently as a composite of categorical change and mortality[10]. Decline in FVC and diffusing capacity of the lungs for carbon monoxide (DLCO) and, less frequently, worsening of fibrotic features at serial high-resolution computed tomography (HRCT) are other important parameters considered in clinical practice for progression. Our first PPF guidelines published on May 2022 pointed out the criteria in order to worldwide define the progressive entity [3]. Specifically, progression is considered when, over the last year of treatment at least two of three criteria occurred: (a) worsening respiratory symptoms; (b) physiological evidence of disease progression (defined below as FVC% pred. decline of ⩾5% or DLCO% pred. decline ⩾10%; (c) radiological evidence of disease progression.

Finally, the direct implication of these new evidences was to apply our knowledge on IPF treatment on PPFs. It has been postulated that the efficacy and tolerability of the antifibrotic drugs pirfenidone and nintedanib could be evaluated in PPFs[11]. The cornerstone of this implications is the publication of the results of the phase III trial on the efficacy of nintedanib in progressive fibrosing interstitial lung diseases. To date, the Food and Drug Administration (FDA), the European Medicine Agency (EMA) and also the Agenzia Italiana del Farmaco (AIFA) approved nintedanib for the treatment of PPFs.

REFERENCES

1. Travis WD, Costabel U, Hansell DM, et al. ATS/ERS Committee on Idiopathic Interstitial Pneumonias. An official American Thoracic Society/European Respiratory Society statement: Update of the international multidisciplinary classification of the idiopathic interstitial pneumonias. Am J Respir Crit Care Med. 2013 Sep 15;188(6):733-48.
2. Lynch DA, Sverzellati N, Travis WD, et al. Diagnostic criteria for idiopathic pulmonary fibrosis: a Fleischner Society White Paper. Lancet Respir Med. 2018 Feb;6(2):138-153.
3. Raghu G, Remy-Jardin M, Richeldi L, et al. Idiopathic Pulmonary Fibrosis (an Update) and Progressive Pulmonary Fibrosis in Adults: An Official ATS/ERS/JRS/ALAT Clinical Practice Guideline. Am J Respir Crit Care Med. 2022 May 1;205(9):e18-e47.
4. Raghu G, Rochwerg B, Zhang Y, et al. An official ATS/ERS/JRS/ALAT clinical practice guideline: Treatment of idiopathic pulmonary fibrosis: An update of the 2011 clinical practice guideline. Am J Respir Crit Care Med 2015;192(2):e3–19.
5. Park JH, Kim DS, Park IN, et al. Prognosis of fibrotic interstitial pneumonia: idiopathic versus collagen vascular disease-related subtypes. Am J Respir Crit Care Med. 2007 Apr 1;175(7):705-11.
6. Nicholson AG, Fulford LG, Colby TV, et al. The relationship between individual histologic features and disease progression in idiopathic pulmonary fibrosis. Am J Respir Crit Care Med. 2002 Jul 15;166(2):173-7.
7. Cottin V. Treatment of progressive fibrosing interstitial lung diseases: a milestone in the management of interstitial lung diseases. Eur Respir Rev. 2019 Oct 1;28(153):190109.
8. Wells AU, Brown KK, Flaherty KR, Kolb M, Thannickal VJ; IPF Consensus Working Group. What's in a name? That which we call IPF, by any other name would act the same. Eur Respir J. 2018 May 17;51(5):1800692.
9. Wollin L, Distler JHW, Redente EF, et al. Potential of nintedanib in treatment of progressive fibrosing interstitial lung diseases. Eur Respir J. 2019 Sep 19;54(3):1900161.
10. Spagnolo P, Cocconcelli E, Cottin V. Clinical trials in IPF: what are the best endpoints? In: Meyer KC, Nathan SD, eds. Idiopathic Pulmonary Fibrosis. 2nd Edn. Switzerland, Springer Nature, 2019; pp. 433–453.
11. Flaherty KR, Wells AU, Cottin V, et al.; INBUILD Trial Investigators. Nintedanib in Progressive Fibrosing Interstitial Lung Diseases. N Engl J Med. 2019 Oct 31;381(18):1718-1727.

Chapter 4

Aims of the Thesis

AIMS OF THE TESIS

Idiopathic pulmonary fibrosis (IPF) is a chronic disorder, of unknown origin. The actual antifibrotic drugs (nintedanib and pirfenidone) aim to slow down its inevitably progressive course through respiratory failure and death, even though the mortality rate for IPF does not significantly change in last years, emphasizing the need for a more complete understanding in the mechanisms of disease pathogenesis and in predicting IPF clinical behavior.

With this background, the aim of my project during the three-year PhD course was to investigate which variables may be used to predict the clinical course of patients with IPF. Specifically, I developed three main research topics:

1. To investigate the role of High-Resolution Computed Tomography (HRCT) at baseline and during follow up in predicting the clinical course of IPF patients on antifibrotic treatment.
2. To investigate the role of MUC5B rs35705950 genotype on disease behavior and survival of IPF patients on antifibrotic treatment and to analyze how this polymorphism may impact radiological patterns at CT scan.
3. To identify, quantify, and describe lymphoid follicles structures in lungs of patients with IPF across the disease course, and to compare them with those in control smokers.

In the meantime, I applied my research on the analysis of prognostic predictors also on the new clinical entity of progressive pulmonary fibrosis (PPF). First, I was involved, with my research group, in the analysis of the role of serum Carbohydrate Antigen 19-9 (CA 19-9) levels in IPF and other PPF patients with advanced disease referred to our lung transplant center and its relation with different patterns of functional. Second, together with the rheumatologist of our center of Padova, I want to assess clinical and serological predictors of pulmonary fibrosis among idiopathic inflammatory myopathies (IIMs), the potential association between different HRCT features and the clinical presentation in IIM-ILD patients and which parameters could be predictive features associated to progressive fibrosis despite treatment.

Finally, in the meantime of the pandemic burden, my research activities on Coronavirus disease 2019 (COVID-19) wanted:

- to analyze the relationship between Chest X-Ray severity score of patients hospitalized for COVID-19 and the level of medical care;

- to analyze the association between the viral load in the nasopharyngeal swab and its association with severity score indexes and prognostic parameters;
- to characterize, among hospitalized patients for COVID-19, those with persisting pulmonary sequelae during follow-up, and which clinical and radiological parameters may be considered predictors of pulmonary fibrosis.

Chapter 5

High-Resolution Computed Tomography (HRCT) Reflects Disease Progression in Patients with Idiopathic Pulmonary Fibrosis (IPF): Relationship with Lung Pathology

Elisabetta Cocconcelli, Elisabetta Balestro, Davide Biondini, Giulio Barbiero, Roberta Polverosi, Fiorella Calabrese, Federica Pezzuto, Donato Lacedonia, Federico Rea, Marco Schiavon, Erica Bazzan, Maria Pia Foschino Barbaro, Graziella Turato, Paolo Spagnolo , Manuel G. Cosio, and Marina Saetta

J Clin Med. 2019 Mar 22;8(3):399. Doi: 10.3390/jcm8030399. PMID: 30909411; PMCID: PMC6463252.

ABSTRACT

High-Resolution Computed Tomography (HRCT) plays a central role in diagnosing Idiopathic Pulmonary Fibrosis (IPF) while its role in monitoring disease progression is not clearly defined. Given the variable clinical course of the disease, we evaluated whether HRCT abnormalities predict disease behavior and correlate with functional decline in untreated IPF patients. Forty-nine patients (with HRCT1) were functionally categorized as rapid or slow progressors. Twenty-one had a second HRCT2. Thirteen patients underwent lung transplantation and pathology was quantified. HRCT Alveolar (AS) and Interstitial Scores (IS) were assessed and correlated with Forced Vital Capacity (FVC) decline between HRCT1 and HRCT2. At baseline, AS was greater in rapids than in slows, while IS was similar in the two groups. In the 21 subjects with HRCT2, IS increased over time in both slows and rapids, while AS increased only in rapids. The IS change from HRCT1 to HRCT2 normalized per month correlated with FVC decline/month in the whole population, but the change in AS did not. In the 13 patients with pathology, the number of total lymphocytes was higher in rapids than in slows and correlated with AS. Quantitative estimation of HRCTs AS and IS reflects the distinct clinical and pathological behavior of slow and rapid decliners. Furthermore, AS, which reflects the immune/inflammatory infiltrate in lung tissue, could be a useful tool to differentiate rapid from slow progressors at presentation.

INTRODUCTION

Idiopathic pulmonary fibrosis (IPF) is a chronic and progressive lung disease of unknown origin with a highly heterogeneous and unpredictable clinical course[1,2]. While in most cases the inexorable decline in lung function and symptoms occur over a period of years (slow progressors), 10–15% of individuals experience a much faster course, progressing from mild symptoms to respiratory failure and death over a period of months (rapid progressors)[1,3,4]. The identification of Usual Interstitial Pneumonia (UIP) pattern by High Resolution Computed Tomography (HRCT) plays a central role in the diagnosis of IPF, avoiding the need of lung biopsies in a high proportion of cases[2,5]. Furthermore, HRCT-derived scores for fibrosis extent have been widely shown to correlate with degree of physiological impairment and may be more sensitive to subtle changes in disease status than physiological metrics[6-11].

Although the crucial role of HRCT in staging and monitoring IPF over time has been emphasized[12], the big challenge for clinicians remains the possibility to forecast the disease course (slow or rapid) at the time of diagnosis[13-15]. To predict the variable and poorly defined natural history of IPF, composite scoring systems are increasingly being developed[6,7,16]. The Gender, Age, Physiology (GAP) index, which is based only on clinical and functional variables, was able to predict one-year mortality in a cohort of patients with IPF[16]. Moreover, integrating CT scores to the GAP model increased the accuracy of mortality prediction[7], indicating a potential role for the HRCT in the prediction schemes. However, these scoring systems, even if useful, are still neither able to foresee prospectively the highly heterogeneous and unpredictable disease behavior, nor able to guide treatment response.

We thought that a careful evaluation of the different HRCT patterns, including not only fibrotic changes but also ground glass opacities, might help to predict the future rate of functional decline in patients with IPF not conditioned by antifibrotic treatment. Taking advantage of our unique population of IPF patients not yet treated with antifibrotics, in this study, we assessed if HRCT pattern at diagnosis may: (a) predict disease behavior (slow or rapid progressors); (b) have a pathological basis; and (c) if changes of the HRCT pattern over time are linked to functional decline, without the confounding factor of treatment.

METHODS

Study Population

In this longitudinal study, we analyzed a well-characterized cohort of Idiopathic Pulmonary Fibrosis (IPF) patients, with a long clinical functional and radiological follow up, referred between 2011 and 2014, naïve of antifibrotics. All patients in our study, whether from our center or referred to our center, were offered antifibrotic therapy as soon as it became available, provided they met the Forced Vital Capacity (FVC), DLCO and age criteria for treatment and they had no clear contraindications to it. However, given that the aim of our study was to look at a population of patients off treatment, we considered only radiological and functional data before antifibrotic therapy was instituted. In addition, a minority of our patients belonged to an historical cohort from the pre-antifibrotic therapy era (before 2014) and they had no access to antifibrotic therapy. Forty-nine patients from two Interstitial Lung Disease Centres in Italy (University of Padova, Italy, n = 43 and University of Foggia, Italy n = 6) were included. The diagnosis of IPF was made in accordance with the latest guidelines[1,2] (Supplementary Materials). Clinical and functional data were collected at the time of diagnosis (**Table 1**).

Table 1. Demographics and clinical characteristics of the entire population (n=49), of which 30 *slow* and 19 *rapid progressors*.

	Entire population (n=49)	*Slow progressors* (n=30)	*Rapid progressors* (n=19)	p value
Male – *n (%)*	42 (86)	24 (80)	18 (94)	0.22
Age at diagnosis – *years*	58 (33-74)	58 (46-74)	60 (33-69)	0.75
Smoking history – *pack years*	20 (0-93)	15 (0-60)	21 (0-93)	0.24
• **Current – *n (%)***	2 (4)	1 (3)	1 (5)	1
• **Former – *n (%)***	40 (82)	23 (77)	17 (89)	0.45
• **Non smokers – *n (%)***	7 (14)	6 (20)	1 (5)	0.22
Symptoms duration at diagnosis – *months*	20 (0-240)	20 (0-240)	18 (0-120)	0.58
Radiological diagnosis – *n (%)*	28 (57)	20 (67)	8 (42)	0.13
FVC at diagnosis – *L*	2.34 (1.19-4.06)	2.18 (1.19-4.06)	2.51 (1.75-4)	0.38
FVC at diagnosis – *%pred.*	67 (36-109)	66 (36-109)	76 (46-107)	0.52
DL_{CO} at diagnosis – *%pred.*	47 (10-97)	45 (25-97)	50 (10-82)	0.73
FVC decline per year – *ml*	275 (-330-1498)	130 (-330-380)	689 (331-1498)	**< 0.0001**
FVC decline per year – *%pred.*	9 (-30-35)	4 (-30-9)	16 (11-35)	**< 0.0001**
Patients undergoing transplant – *n (%)*	13 (27)	6 (20)	7 (37)	0.31
Patients who died – *n (%)*	28 (57)	15 (50)	13 (68)	0.2

Based on their annual rate of decline in forced vital capacity percent (FVC%) predicted, patients were categorized as slow (<10%) or rapid progressors (⩾10%). The study was performed in accordance with the Declaration of Helsinki and approved by the Ethics Committee of the University Hospital of Padova (4280/AO/17). Informed consent was obtained for all study participants.

Study Design and Radiological Analysis

A HRCT was obtained at diagnosis (HRCT1) in all patients. Twenty-one patients had a second HRCT (HRCT2), after a median of 17 months of follow-up. The clinical and functional data of this subgroup are shown in Table S1. HRCT1 and HRCT2 were scored blindly and independently by two expert thoracic radiologists by using a quantitative scale, as previously described[8]. Briefly, this score consists of the assessment of ground glass opacities (GGO) (alveolar score, AS%) and fibrotic extent (interstitial score, IS%) for each lung lobe. After each individual lobe was scored for both IS and AS, the final result was expressed as mean value of the five lobes for the whole lung and in different lung regions (upper and lower). The inter-observer agreement between the two radiologists was good

(Cohen's kappa 0.7), a value similar to that reported in previous studies[11]. In the twenty-one IPF patients in whom a second HRCT was available, we studied the correlation between radiological changes and FVC% decline by calculating the change of Alveolar Score (△AS/month), the change of Interstitial Score (△IS/month) and the change in FVC (△FVC mL/month) in the period from HRCT1 to HRCT2. We expressed the radiological changes per month to normalize the differences in timing between HRCT1 and HRCT2 in the slow and rapid progressors.

Pathological Analysis

Thirteen of the 49 patients underwent lung transplantation during the follow up (for clinical-functional data, see Table S2). In all cases, the presence of UIP pattern was histologically confirmed by our expert pathologist (FC)[1]. The native lungs were fixed in formalin by airway perfusion and samples from upper and lower lobes were obtained and embedded in paraffin. Sections with a thickness of 5 um were cut and stained for histological and immunohistochemical analysis, as previously described[5]. Fibroblastic foci were counted in sections stained with hematoxylin–eosin and expressed as number of fibroblastic foci/mm2 of area examined (Figure 1). Cellular infiltrate including total leukocytes (CD45+), neutrophils, macrophages (CD68+), and total lymphocytes calculated as sum of CD4+, CD8+ T lymphocytes as well as B lymphocytes (CD20+) was identified by immunohistochemistry as previously described[3,17-19] (**Figure 1**). Each inflammatory cell type was quantified in 20 non-overlapping high-power fields per slide and expressed as cells/mm2 of area examined.

In the thirteen IPF patients in whom the histological tissue and a HRCT performed at time close to the transplantation were available, we studied the correlation between the radiological changes and the cellular inflammatory infiltrate and between the radiological changes and the fibroblastic foci count.

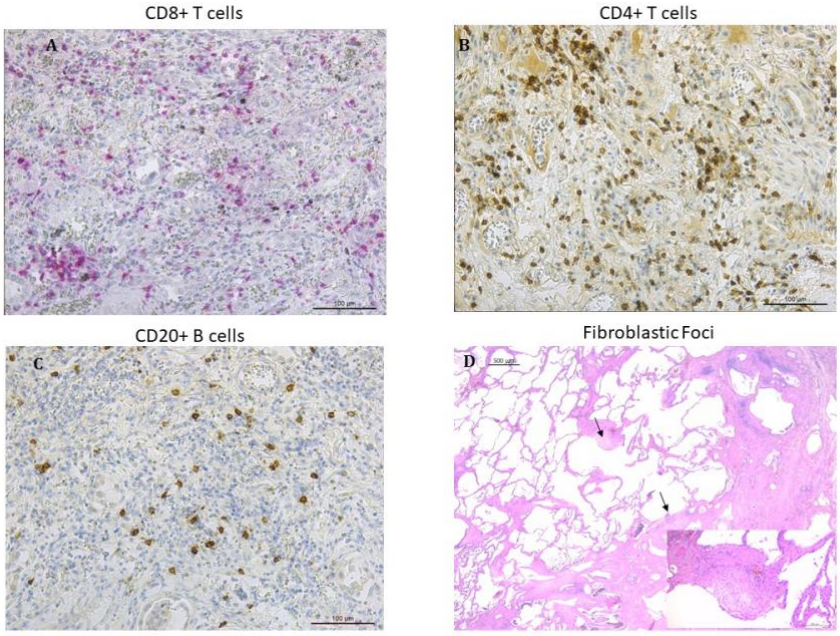

Figure 1. Microphotographs showing lymphocytes infiltrating the lung tissue in patients with IPF. Panel A: CD8+ T lymphocytes stained in red. Panel B: CD4+ T lymphocytes stained in brown. Panel C: CD20+ B lymphocytes stained in brown. Immunostaining with monoclonal antibodies anti-human CD8, anti-human CD4 and anti-human CD20. Panel D: fibroblastic foci (arrows) in the transition zone between the normal lung (on the left) and the dense remodelled parenchyma with microhoneycombing (on the right) (hematoxylin and eosin staining). Insert at higher magnification: detail showing a fibroblastic focus composed of spindle cells with overlying hyperplastic pneumocytes (hematoxylin and eosin staining)

Statistical Analysis

Statistical analyses were performed as previously described[20] (Supplementary Materials). To compare clinical and pathological data between rapids and slows, Chi square test or Fisher's exact test and Mann–Whitney U test were used when appropriate. To evaluate the difference between HRCT1 and HRCT2, Wilcoxon analysis was performed. Correlation coefficients between radiological, functional and pathological findings were calculated using the nonparametric Spearman's rank method. Adjusted p-values for multiple comparisons were calculated using the Holm method. The inter-observer agreement between the two radiologists was evaluated by kappa statistic measure[21]. All data were analyzed using SPSS Software version 25.0 (New York, NY, US: IBM Corp. USA) p-values < 0.05 were considered statistically significant.

RESULTS

Clinical and Radiological Characteristics at Baseline

The clinical characteristics at baseline are shown in **Table 1**. Most patients were males and former smokers. Thirty patients were slow and 19 rapid progressors (median annual FVC decline: 130 mL and 689 mL respectively). None of the patients was treated with antifibrotics and 60% % (equally distributed between the two groups) were treated with low dose prednisone with or without azathioprine according to previous guidelines[22]. In HRCT1, AS was significantly greater in rapid than in slow progressors (p=0.008), while IS was similar in the two groups, either in the entire lung (**Figure 2**) or in different lung regions, upper and lower zones (Table S3).

To corroborate the findings observed in previous analyses, we obtained a ROC curve on Alveolar Score data in rapid and slow progressors. We found that the area under the curve was 0.72, (95% Confidence Interval 0.57–0.87; p = 0.008). On the other hand, in ROC curve for Interstitial Score, we did not observe any statistically significant results (95% Confidence Interval 0.35–0.67; p = 0.88).

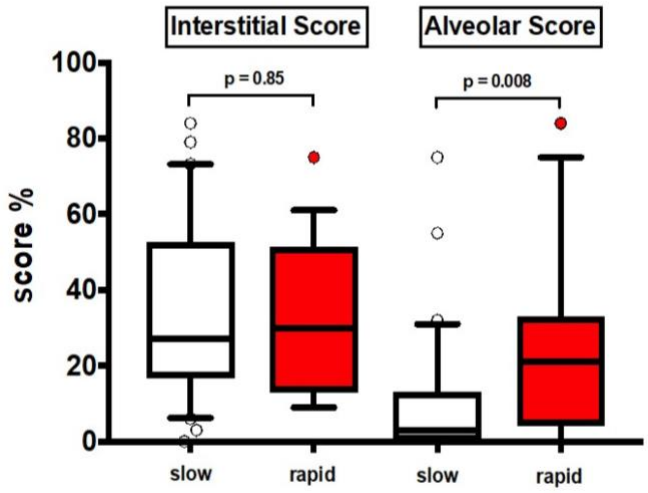

Figure 2. Values of HRCT1 Interstitial Score and Alveolar Score at baseline in slow progressors (slow) and rapid progressors (rapid). Horizontal bars represent median values; bottom and top of each box plot 25th and 75th, brackets 10th and 90th percentiles, while circles represent outliers. White boxes indicate slow progressors and red boxes rapid progressors.

Pathological Analysis

In the 13 patients who were transplanted (Table S2), we quantified the lung pathology (**Figure 1A–C**). The number of CD20+ B lymphocytes, CD4+ and CD8+ T lymphocytes (considered both individually or all together as total lymphocytes) was significantly increased in rapids than in slows (**Table 2**). No significant difference in the number of CD45+, neutrophils, macrophages and fibroblastic foci was found between rapid and slow progressors.

Table 2. Inflammatory cells numbers of the entire population with lung pathology (n=13), of which 6 slow and 7 rapid progressors.

	Entire population (n=13)	***Slow progressors* (n=6)**	***Rapid progressors* (n=7)**	**p value**
Total leukocytes $CD45^+$ - *cells/mm²*	352 (149-732)	284 (149-383)	379 (333-732)	0.7
Macrophages- *cells/mm²*	136 (63-308)	132 (63-308)	136 (71-303)	0.9
Neutrophils- *cells/mm²*	51 (2-138)	6 (2-62)	51 (4-138)	0.1
Total lymphocytes - *cells/mm²*	273 (74-414)	152 (74-273)	353 (256-414)	**0.002**
• **CD 20^+ B lymphocytes**	42 (25-115)	36 (27-115)	62 (25-115)	**0.008**
• **CD 4^+ T lymphocytes**	138 (20-284)	87 (20-138)	194 (115-284)	**0.002**
• **CD 8^+ T lymphocytes**	44 (12-120)	33 (12-45)	66 (26-120)	**0.001**
Fibroblastic foci- *n/mm²*	2.7 (1-7)	2.8 (2-7)	2 (1-4.6)	0.09

Values are expressed as median and ranges. P values refers to comparison between slow and rapid progressors.

Pathological-radiological correlations

The total number of lymphocytes/mm2 was positively correlated with the HRCT AS in the whole population (**Figure 3**).

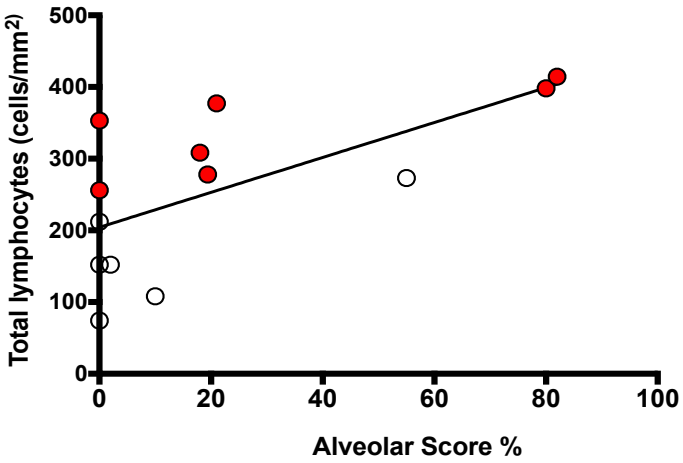

Figure 3. Relationship between the number of total lymphocytes infiltrating the lung tissue and the HRCT Alveolar Score. The black line represents the correlation in the entire population. White circles indicate slow progressors and red circles rapid progressors. Spearman's rank correlation: r=0.67, p=0.01 in the entire population; r=0.33, p=0.48 in slow progressors alone; r=0.81, p=0.03 in rapid progressors alone.

Functional and Radiological Characteristics at Follow Up

In the 21 patients who had a follow up HRCT2 (Table S1), we found that both AS and IS increased significantly over time in both groups together (Table S4). When the patients were divided by rate of decline, IS increased over time in both slows and rapids, while AS increased significantly only in rapids (**Figure 4**) (Table S4).

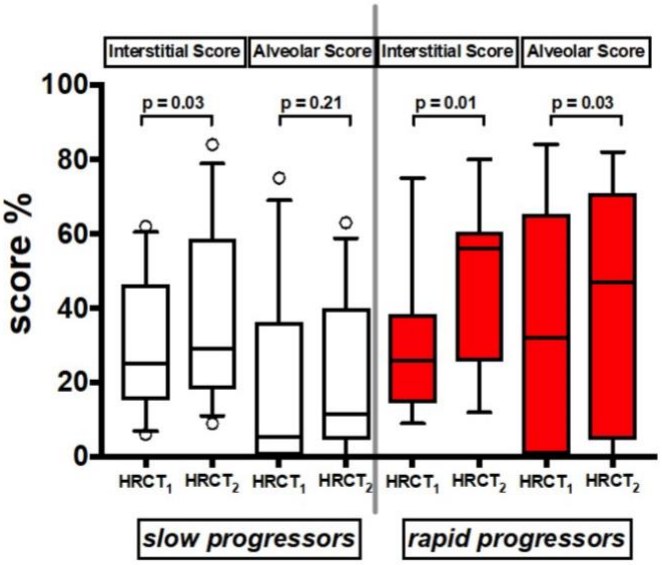

Figure 4. Values of Interstitial Score and Alveolar Score of the two serial HRCT scans (HRCT1 at baseline and HRCT2 at follow up). Horizontal bars represent median values; bottom and top of each box plot 25th and 75th, brackets 10th and 90th percentiles, while circles represent outliers. White boxes indicate slow progressors and red boxes rapid progressors.

Functional-radiological correlations

There was a significant correlation between the functional decline, defined as ΔFVC ml/month, and the radiological changes in IS, defined as ΔIS/month, but not with ΔAS/month. However, when stratified by the rate of decline, the correlation between ΔFVC ml/month and ΔIS/month was no longer significant in the rapid and slow decliners (**Figure 5**). When the delta IS was normalized by IS at the beginning, the correlation with the delta FVC was maintained in the patient population as a whole (p = 0.01, r = 0.57) but not in the slow and rapid subgroups.

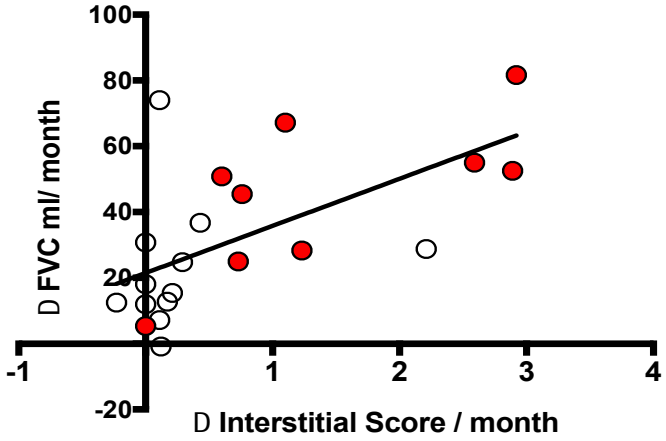

Figure 5. Relationship between the change over time in FVC ml (ΔFVC ml/month) and the change over time in Interstitial Score (ΔInterstitial Score/month). The black line represents the correlation in the entire population. White circles indicate *slow progressors* and red circles represent *rapid progressors*. Spearman's rank correlation: r=0.66, p=0.002in the entire population; r=0.31, p=0.6 in *slow progressors* alone; r=0.73, p=0.06 in *rapid progressors* alone.

DISCUSSION

High-Resolution Computed Tomography (HRCT) plays a central role in diagnosing and staging the severity of IPF[2,5,7,8,10,12].The HRCT relevance in IPF underlines its potential usefulness as a tool to predict future disease behavior at the time of diagnosis and to design future clinical trials[12].

In this study, we investigated in a group of IPF patients, followed long term (prior to available anti-fibrotic treatment), whether radiological quantification of fibrotic abnormalities and ground glass opacities in HRCT at diagnosis may predict disease behavior over time. Our results showed that, in the HRCT performed at diagnosis, patients who had experienced a rapid functional decline, rapid progressors, had a higher alveolar score (AS) than slow progressors, while the extent of fibrosis (Interstitial Score, IS) was similar in the two groups. Furthermore, in a second HRCT at follow up, changes in IS over time was correlated with functional decline. Idiopathic Pulmonary Fibrosis is a heterogeneous disease, the outcome of which is determined by the rapidity of the longitudinal loss of forced vital capacity, a major prognostic predictor linked to an increase in mortality risk[16, 23-25]. The diagnosis of IPF can be done in most cases by HRCT, considered a good reflection of UIP, the pathological counterpart of IPF. Based on its diagnostic accuracy, the scoring of the different abnormalities seen in HRCT has been used in an attempt to improve the prediction of IPF outcomes[7,10]. In general, these studies show an important variability in individual disease progression and an association between mortality and increased fibrosis score over time, especially when combined with changes in FVC[7,8,10-12,26].

According to the annual FVC decline greater or lower than 10%pred, two clinical IPF phenotypes have been repeatedly reported in the literature, the rapid and the slow progressors[3-5,27]. These phenotypes have been shown to have a distinct gene expression profile, including the activation of important pro-inflammatory pathways that may potentially play a role in disease progression of rapid

decliners[4,27]. Previous studies assessing the value of HRCT in the prediction of IPF behavior did not differentiate their patients by the predetermined rate of progression, rapid or slow, a factor of crucial significance for the understanding of disease prognosis. In the present study, we analyzed a group of patients naïve to antifibrotics classified as slow or rapid progressors, based on FVC decay over time, with the aim to identify HRCT features that could possibly differentiate at presentation rapid from slow decliners, a major prognostic predictor in IPF. Differently from previous studies[6,7], we evaluated not only the degree of interstitial score (IS) but also the degree of ground glass opacities, alveolar score (AS). Although pure ground glass opacity is not usually a feature of UIP, many patients with fibrotic lung disease have ground glass opacity admixed with reticular abnormality and/or traction bronchiectasis. In this context, the ground glass opacity should be regarded as part of the fibrotic process, as indicated by the recent Fleischner Society white paper[5] and, as such, we believe it needed to be assessed[2]. The HRCT findings in our study, showing that at baseline rapid progressors had an AS significantly greater (almost double) than slow progressors, is of high interest since it might help to identify, early in the course of the disease, the more aggressive phenotype with worse prognosis.

The significance of ground glass opacities in IPF is not clear, but it might be related to parenchymal inflammatory/exudative infiltrates, probably more evident in cases with more aggressive disease and rapid progression. In support of this possibility are our recently published findings that the different clinical course (rapid or slow) of an IPF population undergoing lung transplantation was associated with distinct underlying pathology in the explanted lungs[3]. Rapid progressors showed an extensive cellular immune infiltrate, both innate and adaptive, more prominent than slow progressors[3]. The possibility that AS might represent an alveolar inflammatory/exudative infiltrate is supported by the correlation observed in the present study between AS and the total number of lymphocytes in the 13 explanted lungs. Because the timing to the second HRCT was different in the 21 patients with two consecutive HRCTs, to compare the results, we calculated the changes over time in IS, AS, and FVC and expressed them as change/per month. As suggested by others[26], the change in FVC/month in the whole group (rapids and slows together) correlated significantly with IS change/month. Of interest and fitting with our previous findings, the AS, plausibly representing a

cellular/exudative inflammatory response, increased significantly at follow up in rapid progressors while it remained stable in slow progressors. The exact explanation of this feature needs to be elucidated, however we can speculate that the AS signals a more exudative and thus unstable disease, rich in fibroblast foci, and more likely to rapidly progress towards fibrotic changes and consequently rapid functional worsening. These findings seem in line with our previous evidence on lung pathology that showed the presence of an intense lung immune infiltrate in the rapid progressors, but not in the slow progressors[3]. These results would support a role of inflammation and of adaptive immune response in determining disease behavior[28] and might account, at least in part, for the different responses to anti-fibrotic drugs among IPF patients. In favor of this possibility is our recent report showing that pirfenidone reduces FVC decline in IPF patients with a more pronounced beneficial effect in rapid than in slow progressors[29]. A strength of our study is the unique opportunity to investigate a population of IPF patients naïve of anti-fibrotic treatment, followed for at least one year, in which the disease decline phenotype, rapid or slow, could be determined by changes in FVC. Knowing the rate of decline allowed us to investigate if patterns of HRCT abnormalities could separate the rapid from slow phenotype, since the rate of FVC decay signals the worse prognosis of the disease and the response to treatment. Another important and unique feature of the study is that both AS and IS, radiological parameters which correlated with FVC decay, had a pathological confirmation. Due to the availability of effective anti-fibrotic drugs[30,31], studies on IPF patients naïve of antifibrotics will become progressively less common, if at all possible (and ethical). Thus, the HRCT patterns described could help to predict the long-term disease behavior and prognosis and be the bases for further studies in treated patients.

A limitation of our study is the relative low number of cases and the fact that the time interval between HRCT1 and HRCT2 was not the same in all patients. We corrected for this difference in timing by expressing AS and IS as changes per month. Since the pulmonary function tests were performed at the same time of HRCT, we could correlate the radiological changes with the functional changes. The quantitative estimation of HRCTs disease extent was independently evaluated by two

expert radiologists with a good inter-observer agreement. It may appear a limitation not having used the automated quantitative imaging analysis[32-34], however visual

lung scores are and have been used as “gold standard” to validate software analyses[11,35] that, in any case, have themselves some limitations and disadvantages such as the applicability to retrospective CT dataset[34,36].

Conclusion

In conclusion, quantitative estimation of High-Resolution Computed Tomography alveolar (AS) and interstitial (IS) scores reflects the distinct clinical and pathological behavior of Idiopathic Pulmonary Fibrosis slow and rapid decliners. Furthermore, the alveolar score, which reflects the immune/inflammatory infiltrate found in lung tissue, could be a useful tool to differentiate rapid from slow progressors at presentation.

SUPPLEMENTARY MATERIAL

METHODS

Study population and radiological analysis

This is a longitudinal study in which we analysed a well characterized cohort of IPF patient with a long clinical, functional and radiological follow up, referred in our transplant centre between 2011 and 2014 and before starting antifibrotic treatment.

For each patient the diagnosis of IPF was made in accordance with the last ATS/ERS/JRS/ALAT guidelines[1,2], either by clinical-radiological diagnosis (28 patients) or clinical-radiological-histological diagnosis (21 patients). Patients with a clear history of environmental or occupational exposure, and with clinical or serological data suggestive for a connective tissue disease were excluded.

For each patient the annual rate of decline in FVC% pred. was used to categorize the disease progression as *slow* (decline in FVC% pred. <10% per year) or *rapid* (decline in FVC% pred. ≥ 10% per year). Negative values of annual FVC% pred. and FVC ml decline during the follow-up indicated improvement.

A HRCT was available at diagnosis ($HRCT_1$) for all patients. Twenty-one patients (43%) had a second HRCT ($HRCT_2$), after a median of 17 (range 5-87) months of follow-up, and the clinical and functional data of this subgroup are shown in Table S1.

Table S1. Demographics and clinical characteristics of the 21 subjects with available follow up $HRCT_2$ (of which 12 *slow* and 9 *rapid progressors*)

	All population (n=21)	Slow progressors (n=12)	Rapid progressors (n=9)	p value
Male – *n (%)*	16 (76)	8 (67)	8 (89)	0.33
Age at diagnosis – *years*	58 (40-73)	58 (42-73)	58 (40-64)	0.88
Smoking history – *pack years*	13 (0-57)	13 (0-57)	17 (0-30)	0.96
• **Current – *n (%)***	1 (5)	1 (8)	0 (0)	1
• **Former – *n (%)***	17 (82)	9 (75)	8 (89)	0.6
• **Non smokers – *n (%)***	3 (14)	2 (17)	1 (11)	1
Symptoms duration at diagnosis – *months*	24 (1-240)	23 (1-240)	24 (2-29)	0.43
Radiological diagnosis – *n (%)*	9 (43)	5 (42)	4 (44)	1
FVC at diagnosis – *L*	2.03 (1.75-4.06)	2.06 (1.84-4.06)	1.99 (1.75-3.49)	0.59
FVC at diagnosis – *%pred.*	69 (46-109)	73 (49-109)	59 (46-86)	0.24
DL_{CO} at diagnosis – *%pred.*	51 (13-106)	43 (37-106)	53 (13-97)	0.90
FVC decline per year – *ml*	210 (-330-1440)	95 (-330-380)	660 (331-1440)	**0.0004**
FVC decline per year – *%pred.*	9 (-30-29)	3 (-30-9)	16 (11-29)	**0.0002**
Time between $HRCT_1$ and $HRCT_2$ – *months*	17 (5-87)	24 (6-87)	11 (5-40)	**0.03**
Patients undergoing transplant – *n (%)*	6 (29)	4 (33)	2 (22)	0.55
Patients who died – *n (%)*	13 (62)	6 (50)	7 (78)	0.19

Values are expressed as numbers and (%) or medians and ranges. P values refers to comparison between *slow* and *rapid progressors*.

At diagnosis, sex, age, smoking history and respiratory function (FVC both % predicted and millilitres-ml) were similar in *slow* and *rapid progressors*. The radiological follow-up period was longer in *slow* than in *rapid progressors* (median; range: 24; 6-87 months *vs* 11; 5-40 months; p=0.03).

$HRCT_1$ and $HRCT_2$ were scored blindly and independently by two expert thoracic radiologists by using a quantitative scale, as previously described [8]. This score is made up by the assessment of ground glass opacities (alveolar score, AS%) and fibrotic extent (interstitial score, IS%) for each lung lobe, analyzing each series with axial slice thickness ≤ 2.5 mm and a limited slice spacing ≤ 10 mm. After each individual lobe was scored, the final result of AS% and IS% for the whole lung was expressed as mean value of the five lobes (AS and IS, respectively).

In the twenty-one IPF patient in whom a second HRCT and lung function assessment were available, we studied the correlation between the radiological changes and FVC decline by calculating the change per month of Alveolar Score (ΔAS/month) and Interstitial Score (ΔIS/month), and the change per month in FVC (ΔFVC% pred./month and ΔFVC ml/month) in the period from $HRCT_1$ to $HRCT_2$. We express the radiological changes per month to normalise the differences in timing between $HRCT_1$ and $HRCT_2$ in the *slow* and *rapid progressors*.

Pathological analysis

Thirteen of the forty-nine patients underwent lung transplantation during the follow up. Clinical and functional data of this subgroup are shown in Table S2.

Table S2. Demographics and clinical features of the 13 subjects undergoing lung transplantation (of which 6 *slow* and 7 *rapid progressors*)

	Entire population (n=13)	Slow progressors (n=6)	Rapid progressors (n=7)	p value
Male – *n (%)*	13 (100)	6 (100)	7 (100)	1
Age at diagnosis – *years*	54 (33-64)	59 (56-80)	52 (33-64)	0.56
Smoking history – *pack years*	22 (0-92)	26 (0-57)	19 (0-92)	0.59
• **Current – *n (%)***	0 (0)	0 (0)	0 (0)	1
• **Former – *n (%)***	11 (85)	5 (84)	6 (86)	1
• **Non smokers – *n (%)***	2 (15)	1 (16)	1 (14)	1
Symptoms duration at diagnosis – *months*	10 (1-48)	12 (1-48)	10 (1-44)	0.83
Radiological diagnosis – *n (%)*	7 (54)	5 (83)	2 (29)	0.1
FVC at diagnosis – *L*	2 (1.28-3.17)	2.17 (1.28-3.17)	2.09 (1.75-2.51)	0.9
FVC at diagnosis – *%pred.*	59 (36-86)	50 (36-74)	62 (52-86)	**0.045**
DL_{CO} at diagnosis – *%pred.*	40 (10-97)	40 (28-97)	36 (10-54)	0.2
FVC decline per year – *ml*	444 (0-1498)	140 (0-320)	783 (588-1498)	**0.0039**
FVC decline per year – *%pred.*	11 (1-27)	4 (1-9)	16.3 (11-27)	**0.0082**
Time between HRCT and transplantation – *months*	1 (0-20)	3 (0-14)	4 (0-20)	0.9
Patients who died – *n (%)*	10 (77)	5 (83)	5 (71)	1

Values are expressed as numbers and (%) or median and ranges. P values refers to comparison between *slow* and *rapid progressors*.

At diagnosis, sex, age, smoking history and FVC values (both % predicted and millilitres-ml) were similar in *slow* and *rapid progressors*. Time between the last HRCT performed and lung transplantation were similar in *slow* and *rapid progressors*.

The native lungs were fixed in formalin by airway perfusion and samples were obtained and embedded in paraffin. Sections 5 μm thick were cut and stained for histological and immunohistochemical analysis, as previously described [3]. Fibroblastic foci were counted in sections stained with hematoxylin–eosin and expressed as number of fibroblastic foci/mm^2 of area examined. Cellular infiltrate including total leukocytes ($CD45^+$), neutrophils, macrophages ($CD68^+$), and total lymphocytes calculated as sum of $CD4^+$, $CD8^+$ T lymphocytes and $CD20^+$ B lymphocytes was identified by immunohistochemistry as previously described [17,18]. Each inflammatory cell type was quantified in 20 non-overlapping high-power fields per slide and expressed as cells/mm^2 of area examined.

Statistical analysis

Categorical variables were described as absolute (n) and relative values (%) and continuous variables were described as median and range. To compare demographic and pathological data between *rapid* and *slow progressors* Chi square test and Fisher's exact test ($n < 5$) for categorical variables and Mann-Whitney U test for continuous variables were used. To evaluate the difference between $HRCT_1$ and $HRCT_2$, we performed a Wilcoxon (paired test) analysis.

The relationship between ΔAS/month, ΔIS/month and ΔFVC ml/month and the relationship between AS and IS scores with inflammatory infiltrates and FF were evaluated using Spearman's rank correlation. The inter-observed agreement between the two radiologists in the scoring of the abnormality was evaluated by kappa statistic measure. All data were analyzed using SPSS Software version 22.0 (IBM USA). p-values < 0.05 were considered statistically significant.

RESULTS

Radiologic analyses for different regions (upper and lower lobes) and for total lung are shown in Table S3. In $HRCT_1$, Alveolar Score, considered both separated for lung regions or all together in total lung, was significantly greater in rapid than slow progressors. In $HRCT_1$, Interstitial Score, considered both separated

for lung regions or all together in total lung, was similar between rapid and slow progressors.

Table S3. Alveolar Score (AS) and Interstitial Score (IS) of $HRCT_1$ in the entire population (n=49), of which 30 *slow* and 19 *rapid progressors*.

	Entire population (n=49)	Slow progressors (n=30)	Rapid progressors (n=19)	p value
$HRCT_1$ Total lung AS - %	10 (0-84)	3 (0-75)	21 (0-4)	**0.008**
• **Upper region AS - %**	5 (0-82)	2 (0-70)	17 (0-82)	**0.02**
• **Lower region AS - %**	10 (0-100)	5 (0-100)	23 (0-88)	**0.006**
$HRCT_1$ Total lung IS - %	28 (1-84)	27 (1-84)	30 (9-75)	0.85
• **Upper region IS - %**	18 (0-82)	19 (0-82)	17 (0-70)	0.63
• **Lower region IS - %**	38 (1-100)	38 (1-100)	38 (5-88)	0.74

Values are expressed as medians and range. P values refers to comparison between *slow* and *rapid progressors*.

Table S4. Alveolar Score (AS) and Interstitial Score (IS) of both h HRCT scans ($HRCT_1$ and $HRCT_2$) in the entire population (n=49), of which 30 *slow* and 19 *rapid progressors*.

	Entire population (n=21)		p	Slow progressors (n=12)		p	Rapid progressors (n=9)		p
	$HRCT_1$	$HRCT_2$		$HRCT_1$	$HRCT_2$		$HRCT_1$	$HRCT_2$	
AS	7 (0-84)	13 (0-82)	**0.02**	6 (0-75)	12 (0-63)	0.21	32 (0-84)	47 (0-82)	**0.03**
IS	26 (6-75)	40 (9-84)	**0.0009**	25 (6-62)	29 (9-84)	**0.03**	26 (9-75)	56 (12-80)	**0.01**

Values are expressed as medians and ranges. P values refers to comparison between $HRCT_1$ and $HRCT_2$.

Functional-radiological correlations

The positive correlation between ΔFVC and ΔIS was confirmed when the change in FVC was expressed as ΔFVC% predicted (r=0.55, p=0.01). When stratified in *slow* and *rapid progressors*, the correlation was equally confirmed in the *rapid* group (r=0.87, p=0.01), but not in the *slow* group (r=0.27, p=0.38). Again, the correlation between ΔFVC% pred./month and ΔAS/month was not significant (r= 0.11; p=0.64).

REFERENCES

1. Raghu G, Collard HR et al. An Official ATS/ERS/JRS/ALAT Statement: Idiopathic pulmonary fibrosis: Evidence-based guidelines for diagnosis and management. Am J Respir Crit Care Med. 2011;183(6):788-824.
2. Raghu G, Remy-Jardin M et al. Diagnosis of Idiopathic Pulmonary Fibrosis. An Official ATS/ERS/JRS/ALAT Clinical Practice Guideline. Am J Respir Crit Care Med. 2018 Sep 1;198(5):e44-e68.
3. Balestro E, Calabrese F et al. Immune inflammation and disease progression in idiopathic pulmonary fibrosis. PLoS One. 2016;11(5):1-11.
4. Selman M, Carrillo G et al. Accelerated variant of idiopathic pulmonary fibrosis: Clinical behavior and gene expression pattern. PLoS One. 2007;2(5).
5. Lynch DA, Sverzellati N et al. Diagnostic criteria for idiopathic pulmonary fibrosis: a Fleischner Society White Paper. Lancet Respir Med. 2018;6(2):138-153.
6. Wells AU, Desai SR et al. Idiopathic pulmonary fibrosis: a composite physiologic index derived from disease extent observed by computed tomography. Am J Respir Crit Care Med. 2003;167(7):962-969.
7. Ley B, Elicker BM et al. Idiopathic Pulmonary Fibrosis: CT and Risk of Death. Radiology. 2014;273(2):570-579.
8. Fell CD, Martinez FJ et al. Clinical predictors of a diagnosis of idiopathic pulmonary fibrosis. Am J Respir Crit Care Med. 2010;181(8):832-837.
9. Lynch DA, Godwin JD et al. High-resolution computed tomography in idiopathic pulmonary fibrosis: Diagnosis and prognosis. Am J Respir Crit Care Med. 2005;172(4):488-493.
10. Best AC, Meng J et al. Idiopathic pulmonary fibrosis: physiologic tests, quantitative CT indexes, and CT visual scores as predictors of mortality. Radiology. 2008;246(3):935-940.
11. Salisbury ML, Lynch DA et al. Idiopathic Pulmonary Fibrosis : The Association between the Adaptive Multiple Features Method and Fibrosis Outcomes. Am J Respir Crit Care Med. 2017;195(7):921-929.
12. Hansell DM, Goldin JG et al. CT staging and monitoring of fibrotic interstitial lung diseases in clinical practice and treatment trials: A Position Paper from the Fleischner society. Lancet Respir Med. 2015;3(6):483-496.
13. Ley B, Bradford W, et al. Predictors of Mortality Poorly Predict Common Measures of Disease Progression in Idiopathic Pulmonary Fibrosis. Am J Respir Crit Care Med. 2016;194 (6):711-718.
14. Schmidt SL, Nabihah Tayob M et al. Predicting Pulmonary Fibrosis Disease Course From Past Trends in Pulmonary Function. Chest. 2014; 145(3):579-585.

15. Salisbury ML, Xia M, Zhou Y et al. Idiopathic Pulmonary Fibrosis: Gender-Age-Physiology Index Stage for Predicting Future Lung Function Decline. Chest. 2016 Feb;149(2):491-498.

16. Ley B, Ryerson CJ et al. A multidimensional index and staging system for idiopathic pulmonary fibrosis. Ann Intern Med. 2012 May 15;156(10):684-91.

17. Ballarin A, Bazzan E et al. Mast cell infiltration discriminates between histopathological phenotypes of chronic obstructive pulmonary disease. Am J Respir Crit Care Med. 2012;186(3):233-239.

18. Bazzan E, Saetta M et al. Expression of the atypical chemokine receptor D6 in human alveolar macrophages in COPD. Chest. 2013;143(1):98-106.

19. Saetta M, Baraldo S et al. CD8+ve cells in the lungs of smokers with chronic obstructive pulmonary disease. Am J Respir Crit Care Med. 1999 Aug;160(2):711-7.

20. Bonato M, Bazzan E et al. Clinical and Pathologic Factors Predicting Future Asthma in Wheezing Children. A Longitudinal Study. Am J Respir Cell Mol Biol. 2018 Oct;59(4):458-466.

21. Altman DG., Practical statistics for medical research. Chapman and Hall, London, 1991. 10:1635-1636.

22. American Thoracic Society. Idiopathic pulmonary fibrosis: diagnosis and treatment. International consensus statement. American Thoracic Society (ATS), and the European Respiratory Society (ERS). Am J Respir Crit Care Med. 2000 Feb;161(2 Pt 1):646-64.

23. Zappala CJ, Latsi PI et al. Marginal decline in forced vital capacity is associated with a poor outcome in idiopathic pulmonary fibrosis. Eur Respir J. 2010;35(4):830-835.

24. Du Bois RM, Weycker D et al. Forced vital capacity in patients with idiopathic pulmonary fibrosis: test properties and minimal clinically important difference. Am J Respir Crit Care Med. 2011;184(12):1382-1389.

25. Ley B, Collard HR et al. Clinical course and prediction of survival in idiopathic pulmonary fibrosis. Am J Respir Crit Care Med. 2011;183(4):431-440.

26. Oda K, Ishimoto H et al. High-resolution CT scoring system-based grading scale predicts the clinical outcomes in patients with idiopathic pulmonary fibrosis. Respir Res. 2014;15(1):1-9.

27. Boon K, Bailey NW et al. Molecular phenotypes distinguish patients with relatively stable from progressive idiopathic pulmonary fibrosis (IPF). PLoS One. 2009;4(4).

28. Kwapiszewska G, Gungl A et al. Transcriptome profiling reveals the complexityof pirfenidone effects in idiopathic pulmonary fibrosis. Eur Respir J 2018 52:1800564.

29. Biondini D, Balestro E et al. Pretreatment rate of decay in forced vital capacity predicts long-term response to pirfenidone in patients with idiopathic pulmonary fibrosis. Sci Rep. 2018;8(1):5961.

30. Richeldi L, du Bois RM et al. Efficacy and safety of nintedanib in idiopathic pulmonary fibrosis. N Engl J Med. 2014;370(22):2071-2082.

31. King TEJ, Bradford WZ et al. A Phase 3 Trial of Pirfenidone in Patients with Idiopathic Pulmonary Fibrosis. N Engl J Med. 2014;370(22):2083-2092.

32. Humphries SM, Swigris JJ et al. Quantitative high-resolution computed tomography fibrosis score : performance characteristics in idiopathic pulmonary fibrosis. Eur Respir J. 2018;52(3).

33. Maldonado F, Moua T et al. Automated quantification of radiological patterns predicts survival in idiopathic pulmonary fibrosis. Eur Respir J. 2014 Jan;43(1):204-12

34. Jacob J, Bartholmai BJ et al. Predicting Outcomes in Idiopathic Pulmonary Fibrosis Using Automated Computed Tomographic Analysis. Am J Respir Crit Care Med. 2018 Sep 15;198(6):767-776.

35. Humphries SM, Schroeder JD et al. Idiopathic Pulmonary Fibrosis : Data-driven Textural Analysis of Extent of Fibrosis at Baseline and 15-Month Follow-up. Radiology. 2017 Oct;285(1):270-278.

36. Wu X, Kim GH et al. Computed Tomographic Biomarkers in Idiopathic Pulmonary Fibrosis: The Future of Quantitative Analysis. Am J Respir Crit Care Med. 2018 Jul 9.

Chapter 6

High-Resolution CT Change over Time in Patients with Idiopathic Pulmonary Fibrosis on Antifibrotic Treatment

Elisabetta Balestro† , Elisabetta Cocconcelli†, Chiara Giraudo , Roberta Polverosi, Davide Biondini, Donato Lacedonia, Erica Bazzan, Linda Mazzai, Giulia Rizzon, Sara Lococo, Graziella Turato, Mariaenrica Tinè, Manuel G. Cosio, Marina Saetta and Paolo Spagnolo

J Clin Med. 2019 Sep 15;8(9):1469. doi: 10.3390/jcm8091469. PMID: 31540181; PMCID: PMC6780456.

ABSTRACT

Antifibrotic treatment slows down functional decline and disease progression in idiopathic pulmonary fibrosis (IPF). High-resolution computed tomography (HRCT) is useful to diagnose IPF; however, little is known about whether and to what extent HRCT changes reflect functional changes during antifibrotic therapy. The aim of this study was, therefore, to assess HRCT change over time after 1 year of treatment and to evaluate whether these changes correlate with functional decline over the same period of time. Sixty-eight IPF patients on antifibrotic treatment (i.e., pirfenidone or nintedanib) were functionally categorized as stable or progressors based on whether (or not) they had a decline in forced vital capacity (FVC) >5% predicted/year, and their HRCT were scored blindly and independently by two expert thoracic radiologists at treatment initiation (HRCT1) and after 1 year of treatment (HRCT2). Ground glass opacities (Alveolar Score, AS), reticulations (Interstitial Score, IS) and honeycombing (HC) were quantified and correlated with FVC decline between HRCT1 and HRCT2. At treatment initiation, HRCT scores were similar in both stable patients and progressors. After one year of treatment, in the entire population, AS and HC increased significantly, while IS did not. However, when stratified by the rate of functional decline, in stable patients, HC increased significantly while AS and IS did not. On the other hand, among progressors AS and HC increased significantly whereas IS did not. In the entire population, the combined score of fibrosis (IS + HC) correlated significantly with FVC decline. In conclusion, IPF patients on antifibrotic treatment exhibit different patterns of HRCT change over time based on their rate of functional decline. HRCT data should be integrated to lung function data when assessing response to antifibrotic treatment in patients with IPF.

INTRODUCTION

Idiopathic pulmonary fibrosis (IPF) is a chronic progressive interstitial lung disease (ILD) of unknown etiology that leads to respiratory failure and death within 3-5 years from diagnosis if untreated[1]. In addition, the clinical course of IPF patients is highly heterogeneous and largely unpredictable with the majority of individuals experiencing a slow but inexorable decline and a minority succumbing to an acute worsening[2,3]. The 2015 ATS/ERS/JRS/ALAT guidelines conditionally recommend nintedanib and pirfenidone for the treatment of patients with IPF owing to their ability to slow down functional decline and disease progression with an acceptable safety and tolerability profile[4]. However, neither drug is a real cure for IPF, and neither drug is able to stabilize the disease or reverse fibrosis[4]. Assessment of disease severity over time and prediction of disease behavior are critically important for optimal patient management. Historically, lung function tests have been used for monitoring IPF and forced vital capacity (FVC) decline is widely accepted as a surrogate of disease progression, and possibly mortality, in IPF[5,6]. High Resolution Computed Tomography (HRCT) is an essential component of the diagnostic work-up of IPF[3]. Indeed, the identification of a usual interstitial pneumonia (UIP) pattern on HRCT along with the exclusion of known causes of ILD allows a confident diagnosis of IPF to be made thus avoiding the need for histological confirmation and invasive procedures[3]. In addition, disease extent on HRCT (i.e., extent of reticular and honeycombing change) correlates with disease severity and prognosis in untreated patients with IPF[7-9]. However, what represents an ideal radiological scoring method to evaluate disease extension and predict progression remains highly controversial. Several semiquantitative methods of CT scoring based on visual assessment have been developed, some of which may help predict prognosis[10,11]. Yet, a number of methodological issues remain to be addressed including the time interval needed to detect clinically meaningful changes, the correlation between radiological and functional changes and the variable (and often suboptimal) level of agreement between observers on the presence and extent of disease patterns. Inter-observer variation for the visual estimation of the extent of disease pattern is unavoidable, but can be mitigated with a continuous learning method to reach a consensus[12,13]. With this background, we aimed to evaluate whether and to what extent HRCT abnormalities - as assessed by

semiquantitative visual score - change after 1 year of antifibrotic treatment and how these changes correlate with different functional disease trajectories (i.e., stable patients vs. progressors) in patients with IPF.

METHODS

Study population and study design

In this restrospective longitudinal study, we analyzed a cohort of phenotypically well characterized patients with IPF referred to our center between April 2014 and April 2018 and followed clinically, functionally (FVC, forced vital capacity in one second (FEV1) and diffusing capacity of the lung for carbon monoxide (DLCO) and radiologically for at least one year after initiation of anti-fibrotic treatment (either pirfenidone or nintedanib).

Sixty-eight patients were included from two ILD centers in Italy (University Hospital of Padova, n= 59 and University Hospital of Foggia, n=9). For all patients the diagnosis of IPF was made in accordance with the ATS/ERS/JRS/ALAT guidelines[2,3]. Thirty-three cases required a histological confirmation of the diagnosis of IPF whereas in the remaining cases (n=35) the diagnosis was made based on clinical and radiological data only. Patients with a clear history of environmental or occupational exposure and those with clinical features or serological data suggestive of an underlying connective tissue disease were excluded.

For all patients clinical and lung function data were collected at the time of treatment initiation and at regular time intervals (every three months) for up to 12 months while HRCT was performed at treatment initiation and after 12 months (**Table 1**). Based on their annual rate of decline in absolute FVC% pred., patients were classified as progressors (absolute FVC% pred. decline/year > 5%, n=20) or stable (absolute FVC% pred. decline/yr ≤ 5%, n=48). Improvement of FVC (%pred. and mL) was expressed as negative value.

The study was performed in accordance with the Declaration of Helsinki and was approved by the Ethics Committee of the University Hospital of Padova (4280/AO/17). Informed consent was obtained for all study participants.

Table 1. Patients demographics and clinical characteristics.

	Entire Population (n =68)	Stables (n =48)	Progressors (n =20)	*p* Value
Male – *n (%)*	55 (81)	37 (77)	18 (90)	0.31
Female – *n (%)*	13 (19)	11 (23)	2 (10)	0.31
Age at diagnosis – *years*	66 (44–78)	68 (46–78)	61 (44–78)	0.07
Smoking history – *pack years*	15 (0–80)	15 (0–80)	15 (0–55)	0.31
• **Current – *n (%)***	9 (13)	7 (15)	2 (10)	1.00
• **Former – *n (%)***	40 (59)	29 (60)	11 (55)	1.00
• **Nonsmokers – *n (%)***	19 (28)	12 (25)	7 (35)	0.55
Clinical-radiological diagnosis – *n (%)*	35 (51)	27 (56)	8 (40)	0.29
Histological diagnosis – *n (%)*	33 (49)	21 (44)	12 (60)	0.29
FVC at diagnosis – *L*	2.76 (1.19–5.68)	2.6 (1.19–5.29)	2.97 (1.68–5.68)	**0.04**
FVC at diagnosis – *%pred.*	78 (44–120)	78 (44–120)	78 (50–107)	0.40
FEV1 at diagnosis – *L*	2.21 (1.02-4.45)	2.19 (1.02-4.45)	2.50 (1.40-3.70)	0.06
FEV1 at diagnosis - *% pred.*	83 (40-127)	83 (40-127)	86 (49-122)	0.27
DL_{CO} at diagnosis – *%pred.*	57 (34–114)	53 (34–114)	65 (37–97)	**0.02**
6MWT at diagnosis - mt	400 (125-600)	400 (125-600)	408 (250-540)	0.50
FVC decline per year – *mL*	86 (-1381–1155)	37 (-1381–371)	413 (135–1155)	**< 0.0001**
FVC decline per year – *%pred.*	2 (-25-29)	0 (-25-4.7)	9 (5-29)	**< 0.0001**
Deaths – *n (%)*	16 (23)	8 (17)	8 (40)	0.05
Alveolar score in HRCT1 - *%*	21 (0-90)	21 (0-90)	22 (0-44)	0.68
Honeycombing in HRCT1 - *%*	7 (0-70)	6 (0-70)	9 (0-50)	0.32
Interstitial score in HRCT1 - *%*	26 (0-100)	26 (0-100)	28 (0-52)	0.92
Pooled interstitial score and honeycombing - %	40 (8-100)	38 (17-100)	43 (8-70)	0.52

Values are expressed as numbers and (%) or median and ranges as appropriate. Negative values mean improvement of FVC. To compare demographic data and baseline clinical characteristics between stable and progressors, Chi square test and Fisher t test ($n < 5$) for categorical variables and Mann-Whitney t test for continuous variables were used.

Radiological and functional analysis

For each patient, an HRCT was available at treatment (either pirfenidone or nintedanib) initiation (HRCT1) and at the 12-month follow-up (HRCT2). The HRCTs were performed by a 64 slice Siemens Somatom Sensation (Siemens Healthcare, Erlangen, Germany) applying a slice thickness ≤ 1.5 mm.

Two expert thoracic radiologists, who were blind to clinical and functional data and timing of HRCT, scored HRCT1 and HRCT2 images independently using a semi-quantitative scale. This represented a modification of the previously reported scoring systems [14,15] that allowed to evaluation “reticulation” more precisely. Specifically, the radiologic features considered in this study were ground glass opacities (GGO) (alveolar score, AS), reticulation (interstitial score, IS) and honeycombing (HC) (honeycombing score, HC). For each lung lobe, the two radiologists assessed the extent of AS, IS and HC using a scale from 0-100 and estimated extent to the nearest 5%. After each individual lobe was scored, the result was expressed as mean value of the five lobes in AS, IS and HC. Finally, the IS and

HC were pooled (IS+HC) to analyze the amount of fibrotic abnormalities. The level of interobserver agreement was obtained for each patient as a mean of 5 lobes and for each radiologic abnormality (i.e., IS, AS and HC) and expressed as Cohen's k value. Disagreement between radiologists was resolved by consensus. The correlation between radiological change and FVC decline was calculated as the change in AS (ΔAS/month), IS (ΔIS/month), HC (ΔHC/month), pooled IS and HC (ΔIS+HC/month) and the change in FVC milliliters (ml) per month (ΔFVC ml/month) and FVC% pred. per month (ΔFVC% pred./month) between HRCT1 and HRCT2[15].

Statistical analysis

Categorical variables are described as absolute (n) and relative values (%) whereas continuous variables are described as median and range. To compare demographic data and baseline clinical characteristics between stable patients and progressors, Chi square test and Fisher's exact test for categorical variables and Mann-Whitney U test for continuous variables were used as appropriate.

Wilcoxon signed rank test was performed to compare HRCT1 and HRCT2 for the grading scores of different variables (AS, IS, HC and IS+HC) in the entire population, in stable patients and progressors. Correlation coefficients between radiological and functional data were calculated using the nonparametric Spearman's rank method. The level of interobserver agreement between the two radiologists was evaluated by kappa statistic measure[16].

The overall survival was calculated from diagnosis to death or lung transplantation with data censured at June 1st, 2019. The cumulative survival rate was calculated using Kaplan-Meier method and clinical characteristics and radiological scores were evaluated to determine their relationship with disease progression in a univariate and multivariate analysis of Cox proportional hazards regression testing (Supplementary Materials).

All data were analyzed using SPSS Software version 25.0 (New York, NY, US: IBM Corp. USA). P-values < 0.05 were considered statistically significant.

RESULTS

Clinical, functional and radiological evaluation at baseline.

Sixty-eight patients with IPF were included in the study (**Table 1**). Most patients were males (81%) and former smokers (59%) with a median age at diagnosis of 66 years (range 44-78). Based on the annual FVC% pred. decline during treatment over the study period, 48 patients were classified as stable (stable FVC or FVC% pred. decline/yr ≤ 5%) and 20 as progressors (FVC% pred. decline/year > 5%) (**Table 1, Figure 1**).

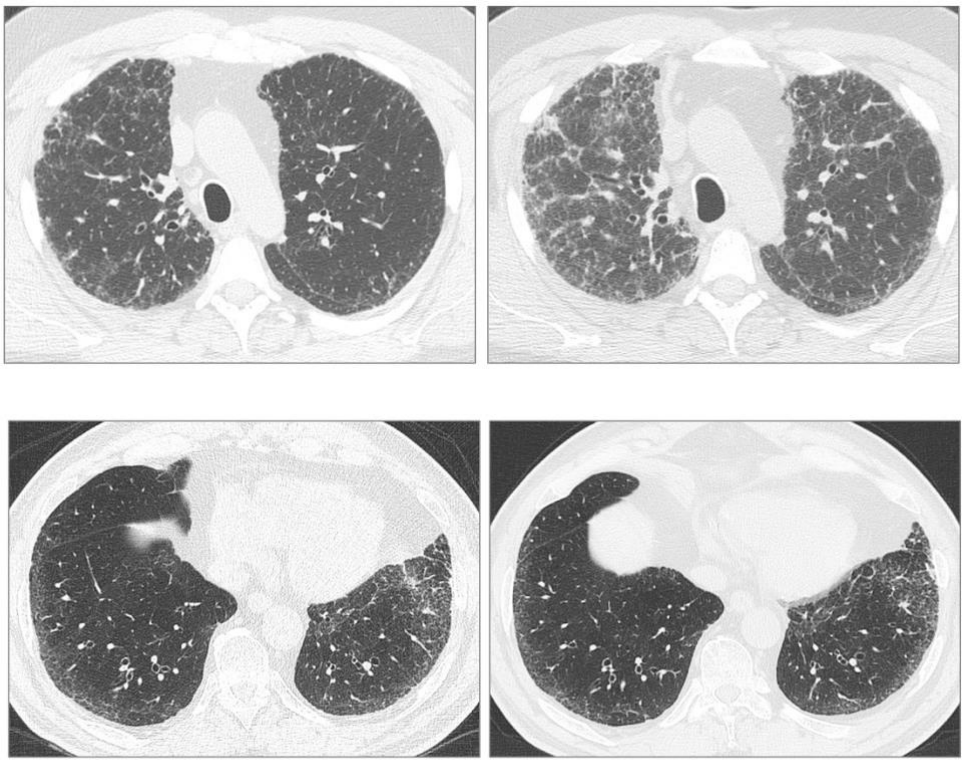

Figure 1. Axial HRCT images of two patients: a 53 year-old male with a progression of disease (patient 1) (a, b) and a 63 year-old male with stable disease (patient 2) (c, d). Patient 1: HRCT at treatment start (a) and after one year of treatment (b) demonstrating a significant progression of ground glass opacities and reticulation. Patient 2: HRCT at treatment start (c) and after one year of treatment (d) demonstrating stability of ground glass opacities and reticulation.

At treatment initiation, sex, smoking history and % of radiological diagnosis did not differ between stable patients and progressors, while progressors tended to be younger and with significantly more preserved FVC and DLCO as compared to stable patients. At treatment initiation there were no between-group differences in HRCT score (Table 1). Forty-seven patients were treated with pirfenidone and

twenty-one with nintedanib and none of them discontinued treatment due to adverse effects during the study period.

Functional and Radiological evaluation

Overall, the inter-observer agreement between the two radiologists with regard to change in AS, IS and HC was good (Cohen's kappa = 0.71 for IS, k=0.76 for AS, k=0.80 for HC). In the entire study population, AS and HC increased significantly between HRCT1 and HRCT2 from 22 ± 17 % to 26 ± 21 % (p=0.008) and from 13 ± 16 % to 19 ± 22 % (p < 0.0001), respectively (**Table 2**). When the study population was stratified by rate of functional decline, in stable patients HC increased significantly between HRCT1 and HRCT2 from 12 ± 17 % to 17 ± 21 % (p < 0.0001) (**Figure 3, Panel B**), whereas AS and IS did not (**Figure 3, Panel A-C).** Conversely, among progressors both AS and HC increased significantly from 23 ± 12 % to 29 ± 23 % (p=0.04) and from 15 ± 16 % to 23 ± 23 % (p = 0.0004), respectively (**Figure 3, Panel A-B**), whereas IS did not (**Figure 3, Panel C**).

When IS and HC were pooled together, the IS+HC score increased significantly both in stable patients (from 41 ± 17 % to 47 ± 21 %, p = 0.0005) and progressors (from 42 ± 16 % to 52 ± 25 %,; p = 0.001), respectively (**Figure 3, Panel D**). Finally, when radiologic scores were analyzed for the nintedanib and pirfenidone group separately, after 1 year of treatment AS increased significantly in the pirfenidone but not in the nintedanib group (p=0.013 and p=0.36, respectively). On the other hand, HC increased significantly in both nintedanib and pirfenidone group (0.007 and p < 0.0001, respectively), whereas IS did not.

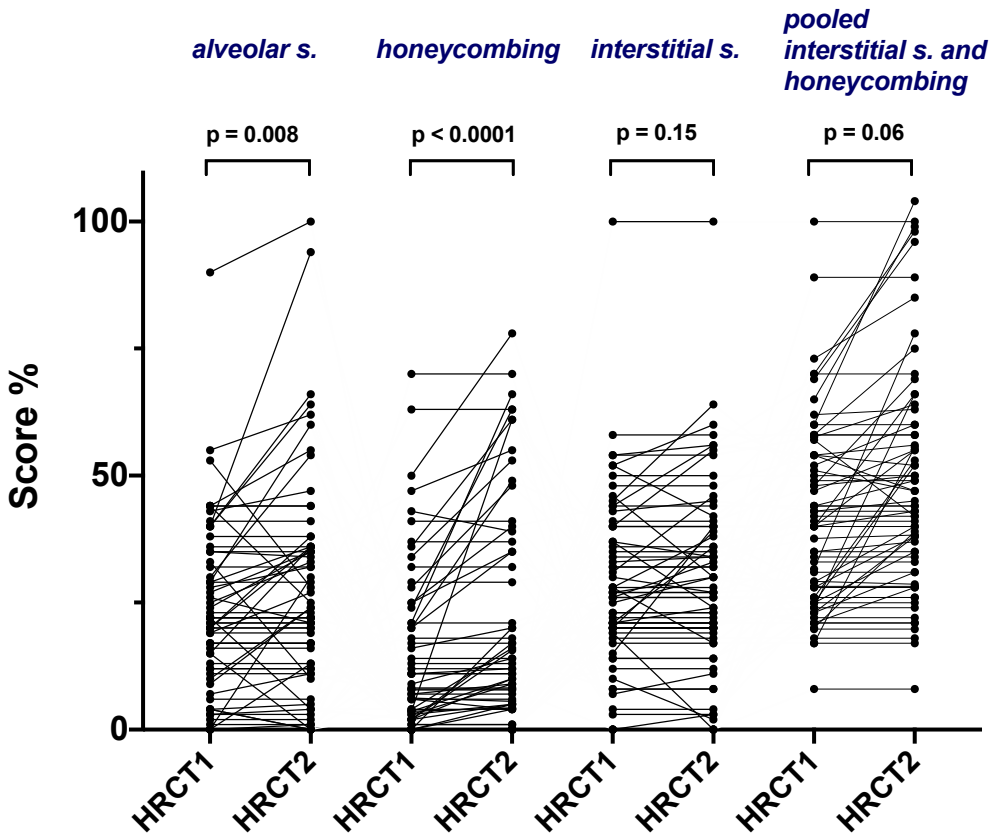

	$HRCT_1$	$HRCT_2$	*p value*		$HRCT_1$	$HRCT_2$	*p value*
AS	22 ± 17	26 ± 21	**0.008**	**HC**	13 ± 16	19 ± 22	**< 0.0001**
IS	28 ± 17	29 ± 18	0.15	**IS+HC**	41 ± 18	48 ± 22	0.06

Figure 2. Alveolar score, interstitial score, honeycombing and pooled interstitial score and honeycombing at treatment initiation (HRCT1) and after one year of treatment (HRCT2) in the entire study population. Values in the table below are expressed as mean and standard deviations. P values refer to comparisons between HRCT1 and HRCT2.

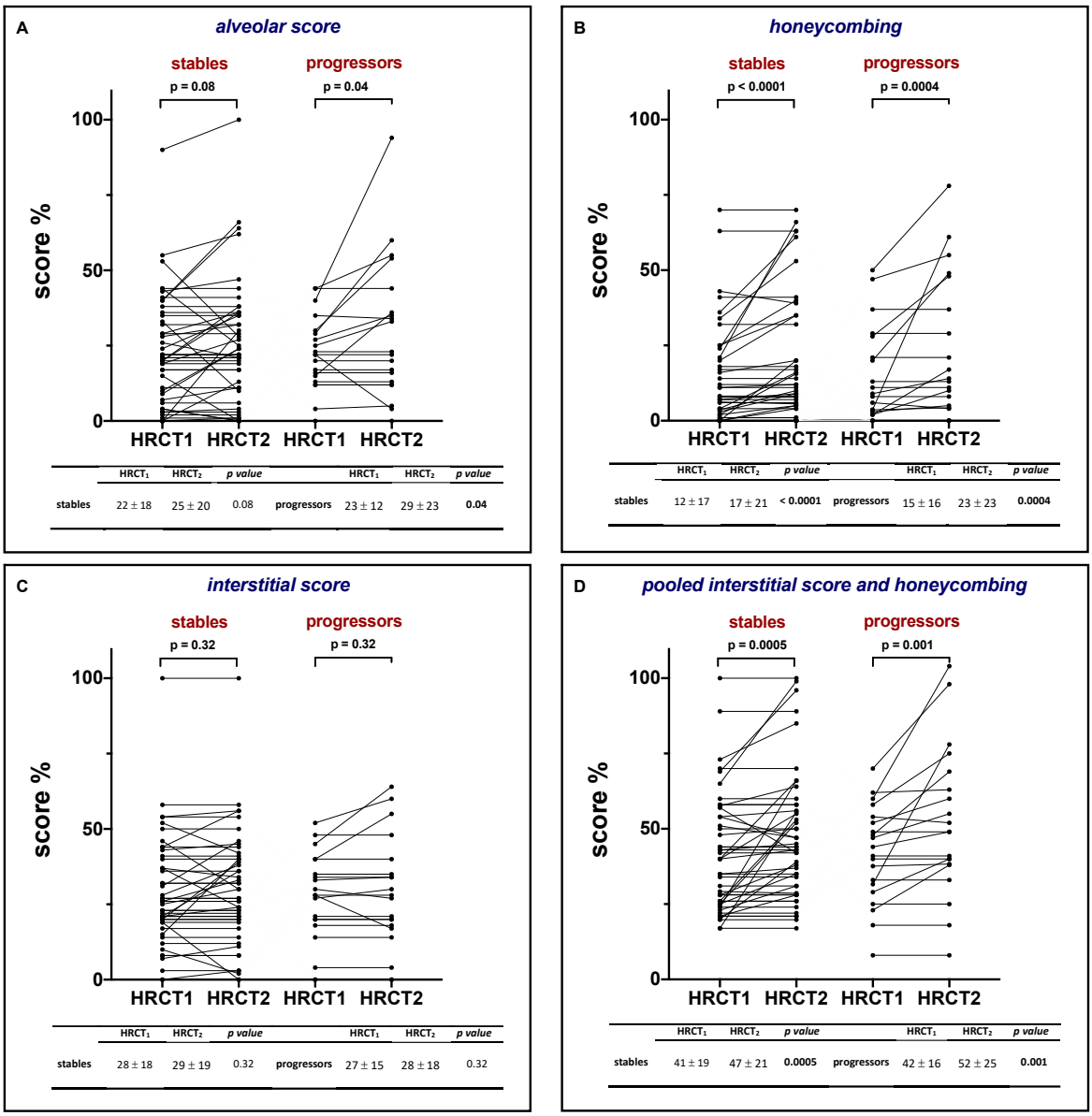

Figure 3. Change in alveolar score, honeycombing, interstitial score and pooled interstitial score and honeycombing between HRCT1 (at treatment initiation) and HRCT2 (after one year of treatment) in stable patients (n=48) and progressors (n=20). Values in the table below are expressed as mean and standard deviations. P values refer to comparisons between HRCT1 and HRCT2.

Functional and radiological correlations

In the entire study population, we observed a positive correlation between ΔFVC ml/month and ΔIS+HC/month (r=0.24, p=0.04) (**Figure 4**), while none of the correlations between ΔFVC ml/month and ΔAS, ΔIS and ΔHC was significant (r=0.10, p=0.40; r= -0.04, p= 0.60 and r= -0.07, p=0.50, respectively). When stratified by FVC decline (stable patients vs. progressors), the correlation between

ΔFVC ml/month and ΔIS+HC/month was not confirmed in either group (r=0.14, p=0.32; r=0.40, p=0.07, respectively).

The previously observed correlation between ΔFVC and ΔIS+HC/month was confirmed when the change in FVC was expressed as ΔFVC% predicted (r=0.25, p=0.04), whereas the correlations between ΔFVC% pred./month and ΔAS, ΔIS and ΔHC were not significant (r=0.01, p=0.90; r= 0.19, p= 0.15 and r= 0.04, p=0.7, respectively). Similarly, there was no significant correlation between ΔFVC% pred./month and ΔIS+HC/month neither in patients functionally stable nor in progressors (r= 0.40, p= 0.07 and r=0.15, p=0.29, respectively).

For survival analysis and univariate and multivariate analysis of Cox proportional hazards regression testing, see Supplementary Materials.

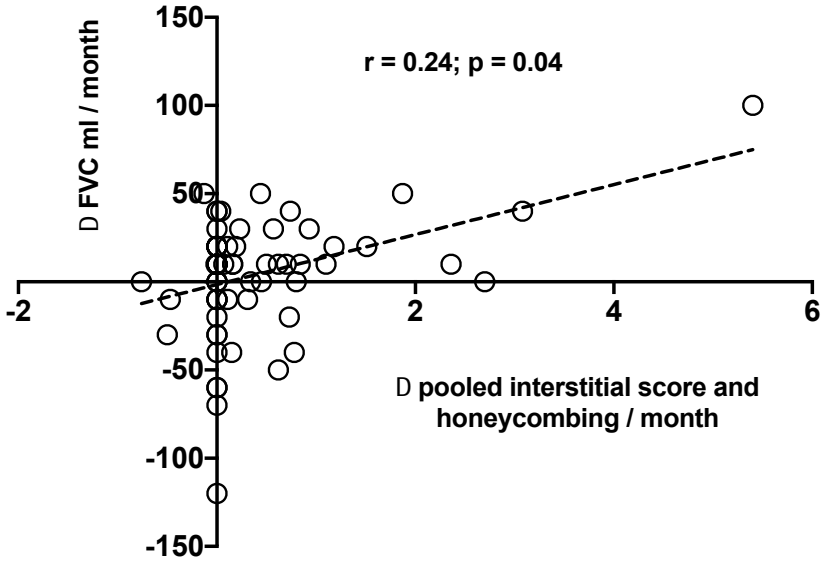

Figure 4. Correlation between change over time in FVC ml (ΔFVC ml/month) and change over time in the pooled Interstitial Score and Honeycombing (Δ pooled Interstitial Score and Honeycombing) in the entire study population. Negative values mean improvement of FVC.

DISCUSSION

The present study aimed to assess whether and to what extent radiologic abnormalities evolve after 1 year of antifibrotic treatment and whether these changes correlate with different trajectories of disease course - as assessed by lung function - in patients with IPF stratified by their rate of functional decline (stable vs. progressors). In our study population, antifibrotic therapy slowed down the rate of FVC decline; indeed, IPF patients under treatment lost on average approximately

100mL/year of FVC, which mirrors what has been observed both in clinical trials[17,18] and in a number of real-world studies[19,21]. However, despite this clear treatment effect on lung function after 1 year of treatment, we also observed an increased extension of HRCT abnormalities both in terms of alveolar opacity and honeycombing [**Figure 2, table 2**]. In addition, the observed correlation between the combined score of fibrosis (IS+HC) and FVC decline is in keeping with previous studies[22,23] and supports the concept that patients with IPF experience an inexorable disease progression – both functional and radiological.

IPF patients display a heterogeneous (and unpredictable) disease course, namely slow or rapid progression[24-26]. In a cohort of IPF patients stratified in slow and rapid progressors based on their pretreatment rate of FVC decay, we have recently shown that the beneficial effect of antifibrotic treatment (pirfenidone) differed significantly between the two phenotypes, being significantly more pronounced in the rapidly progressive group[27]. Given this clear between-group difference in treatment response, in this study we investigated whether and to what extent the assessment and quantification of HRCT patterns of disease may identify disease progression, including different responses to antifibrotic treatment. Similar to previous studies, we stratified our IPF patients under treatment in stable and progressors based on an FVC loss $\leq$ and $>$ 5%[21,28] and analyzed longitudinally the type and extent of HRCT changes in these two patient subgroups. At treatment start, HRCT scores were similar in both stable and progressors. Among progressors, both AS and HC increased significantly after 1 year of treatment, whereas IS did not [**Figure 3-5, table 2**]. On the other hand, in stable patients, HC increased significantly, while AS and IS did not [**Figure 3-5, table 2**]. The observation that HC tends to progress in both stable patients and progressors confirms previous findings in untreated patients and demonstrates that overall extent of lung fibrosis on CT (combination of reticulation and honeycombing) is a proxy of disease severity as well as representing a strong independent predictor of mortality in patients with IPF[23]. Notably, the extent of honeycombing at baseline and its progression over time are important determinants of mortality also in patients with fibrosing ILD other than IPF[29].

Our study shows that progressors displayed a significant increase of AS over time despite treatment whereas stable patients did not. This is an interesting finding, although the significance of alveolar opacity or ground glass attenuation remains

debated. The term "ground-glass attenuation" refers to the presence of a hazy and diffuse homogeneous increase in lung density and, when located akin dense fibrotic areas, may represent mild/initial fibrosis[30]. However, ground glass attenuation may also be associated with the presence of inflammatory cells in the alveolar or interstitial space (i.e., alveolitis)[31-33], which is often more evident in cases with more aggressive disease. In support of this possibility is our recent observation that the different clinical course (rapid or slow) of untreated IPF patients undergoing lung transplantation is associated with distinct underlying pathology in the explanted lungs[26]. In particular, as compared to slow progressors, rapid progressors showed an extensive cellular immune/inflammatory infiltrate[26]. Moreover, we have also demonstrated that the alveolar score on HRCT may reflect the extent of the alveolar infiltrate as suggested by its correlation with the total number of lymphocytes in the explanted lungs[15]. Notably, untreated patients experiencing a rapid functional decline have at baseline a higher alveolar score than slow progressors[15]. This finding coupled with the observation that rapid progressors despite treatment also exhibit an increased extension in alveolar score suggests that the alveolar score may help to identify, even early in the disease course, the more aggressive IPF phenotype and supports the routine use of CT and its visual characterization in clinical practice both in treated and untreated patients with IPF. When we analyzed radiologic scores in nintedanib and pirfenidone group separately, we found that after 1 year of treatment AS increased significantly in the pirfenidone ($p=0.013$) but not in the nintedanib group ($p=0.36$). Whether this difference is real or is simply due to the smaller number of patients in the nintedanib group ($n=21$ vs. 46 in the pirfenidone group) is difficult to ascertain. Answering this question would need a larger dataset that currently is not available.

Currently, longitudinal HRCT is used predominantly in clinical practice to identify complications of IPF, such as lung cancer or indirect sign of pulmonary hypertension. To the best of our knowledge, this is the first study that explores the role of change over time in CT scores and its correlation with functional decline in IPF patients on antifibrotic therapy. Our findings, we believe, are of particular interest as they may potentially help in early detection of disease progression by identifying subtle abnormalities that are not captured by lung function test.

Only Iwasawa et al. have investigated longitudinal radiologic abnormalities during treatment in patients with IPF[34]. The authors reported the utility of

quantitative CT analysis for predicting the efficacy of pirfenidone. They compared treated and untreated IPF patients and found that the change in fibrotic lesions was significantly smaller among pirfenidone treated patients compared to controls and that the decline in vital capacity (VC) correlated significantly with the increase in fibrotic lesions[34].

The findings of our study should be interpreted in the light of some limitations, such as the relatively small number of patients. Nevertheless, our study population was larger than that evaluated in previous studies of IPF patients on antifibrotic treatment and, of note, our patients were followed-up longitudinally with serial lung function test and HRCT, which were scored by two expert thoracic radiologists with good interobserver agreement. Secondly, we did not perform automated quantitative imaging analysis[35] as this tool is not available at our Institution. However, the good agreement of the readers demonstrates that the proposed score is robust and guarantees reliable results. Furthermore, visual analysis continues to play a key role in diagnosing, monitoring and assessing disease severity in IPF[13]. In this regard, Robbie and colleagues have recently reviewed pros and cons of automated and manual CT measurements of lung volume[36] and concluded that lung volume (i.e., volume loss) and extent of fibrosis on CT correlate significantly with pulmonary function test parameters of lung volume irrespective of whether visual or automated techniques are used, and may therefore be complementary measures for disease monitoring in IPF[36]. Moreover, as elegantly pointed out by Wu X and colleagues, these software analyses have themselves, in any case, some limitations and disadvantages such as the applicability to retrospective CT dataset[37]. Finally, the follow-up time was relatively short (i.e., 12 months), and we are currently in the process of collecting functional and radiological data over a longer period of time.

In conclusion, in patients with IPF on antifibrotic treatment, the extent of honeycombing increases over time both in patients experiencing functional decline and in those who remain functionally stable over 12 months, suggesting that CT is able to capture subtle subclinical disease progression. Longitudinal HRCT evaluation may therefore provide important information that integrate those provided by lung function and clinical evaluation.

SUPPLEMENTARY MATERIAL

METHODS

Statistical analysis

The overall survival was calculated from diagnosis to death or lung transplantation with data censured at June 1st, 2019. The cumulative survival rate was calculated using Kaplan-Meier method and the difference in the survival time between the two groups (stable and progressors) was assessed with log-rank test. Clinical characteristics and radiological scores were evaluated to determine their relationship with disease progression in a univariate analysis of Cox proportional hazards regression testing. Variables with an association statistically significant or almost significant ($0.05 < p < 0.09$) with overall survival at univariate analysis were included in a multivariate Cox proportional hazard regression test to find the factors independently associated with disease progression.

RESULTS

Survival analysis and association between clinical – radiological parameters and survival

Survival of stable patients was not statistically different from survival of progressors (HR 1.93, 95% CI 0.85 - 4.41; p= 0.11) (**Figure 1**).

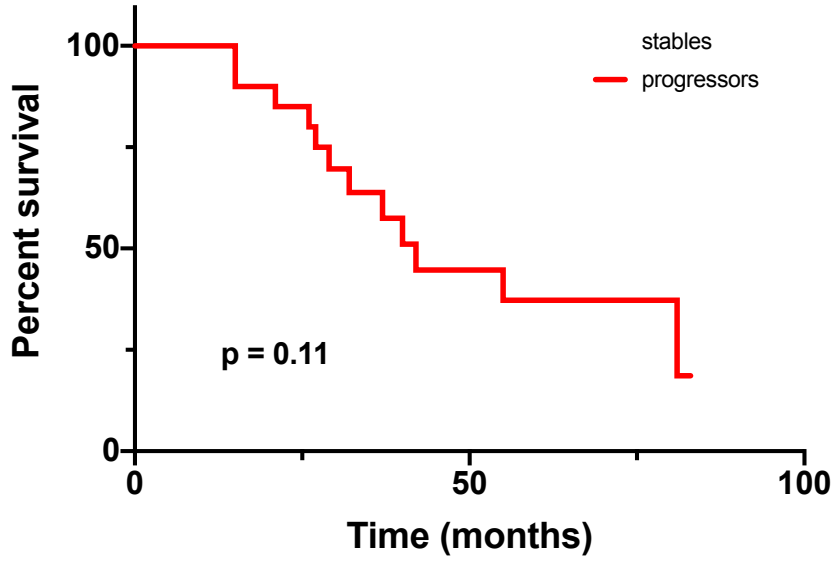

Figure 1. Survival analysis of stables and progressor patients. The gray line represents the survival in the stables and the red line represents the survival in the progressors. Kaplan Meier analysis was used with a log-rank test (HR 1.93, 95% CI 0.85 - 4.41; p=0.11).

To detect factors predictive of disease progression in the entire IPF population, we used Cox proportional hazards regression analysis. Univariate analysis of factors associated with survival revealed that FVC (liters (L)) at diagnosis, FEV1 (L) at diagnosis, DLCO after one year of antifibrotic drug, FVC (L) and FVC % pred. after one year of antifibrotic drug, 6-minute walking test (6MWT) after one year of antifibrotic drug and IS+HC in HRCT1 had significant positive association with disease progression in the entire IPF population (**Table 1**). Of interest, univariate analysis of factors associated with survival showed that 6MWT at diagnosis, 6MWT change over one year of treatment, △HC, IS+HC in HRCT2 had an almost significant positive association with disease progression. Multivariate analysis performed using variables having statistical significance or almost significant in univariate analysis, revealed that only 6MWT at diagnosis (HR: 3.64; 95%CI: 1.16 – 11.42; p = 0.03) and 6MWT change over one year of treatment (HR: 0.32; 95%CI: 0.11 – 0.91; p = 0.03) are independent predictors of disease progression in IPF patients.

Table 1. Predictive factors of overall survival in the entire population of IPF patients treated with antifibrotics

	Univariate analysis		Multivariate analysis	
	HR (95% CI)	***p* Value**	**HR (95% CI)**	***p* Value**
Disease progression (*stables* vs. *progressors*)	0.55 (0.26 – 1.17)	0.12	-	-
Sex (*male* vs. *female*)	0.90 (0.36 – 2.24)	0.82	-	-
Age at diagnosis (*years ≥ 66* vs. *< 66*)	1.02 (0.48 – 2.20)	0.94	-	-
Smoking history (*pack years≥ 15* vs. <15)	1.67 (0.75 – 3.70)	0.20	-	-
Smoking status (*no* vs *current* vs. *former*)	1.40 (0.90 – 2.18)	0.13	-	-
FVC at diagnosis (≥ *2.76 L* vs. *< 2.76*)	0.34 (0.15 – 0.76)	**0.009**	2.63 (0.63 – 10.87)	0.18
FVC at diagnosis (≥*78%* vs. *< 78%*)	0.66 (0.31 – 1.40)	0.28	-	-
FEV_1 at diagnosis (≥*83%* vs. *< 83%*)	0.7 (0.33 – 1.47)	0.34	-	-
FEV_1 at diagnosis (≥*2.21 L* vs. *< 2.21 L*)	0.43 (0.20 – 0.95)	**0.037**	0.58 (0.13 – 2.51)	0.46
DL_{CO} at diagnosis (≥*57%* vs. *< 57%*)	0.84 (0.40 – 1.76)	0.64	-	-
DL_{CO} after 1-yr of antifibrotic drug (≥*48%* vs. *< 48%*)	0.40 (0.18 – 0.90)	**0.03**	1.01 (0.31 – 3.27)	0.98
DL_{CO} change (Δ) (≥*4.5%* vs. *< 4.5%*)	1.36 (0.64 – 2.90)	0.42	-	-
FVC after 1-yr of antifibrotic drug (≥*75%* vs. *< 75%*)	2.28 (1.03 – 5.06)	**0.04**	0.85 (0.25 – 2.86)	0.80
FVC after 1-yr of antifibrotic drug (≥*2.6L* vs. *< 2.6L*)	2.66 (1.17 – 6.07)	**0.02**	1.83 (0.52 – 6.39)	0.34
FVC decline after 1-yr of antifibrotic drug (≥ *86ml* vs. *< 86ml*)	1.03 (0.45 – 2.37)	0.93	-	-
6MWT at diagnosis (≥*400 mt* vs. *< 400 mt*)	0.51 (0.23 – 1.11)	0.09	3.64 (1.16 – 11.42)	**0.03**
6MWT after 1-yr of antifibrotic drug (≥*400 mt* vs. *< 400 mt*)	0.40 (0.18 – 0.88)	**0.02**	0.81 (0.26 – 2.55)	0.72
6MWT change (Δ) (≥*20 mt* vs. *< 20 mt*)	2.24 (0.97 – 5.17)	0.05	0.32 (0.11 – 0.91)	**0.03**
Alveolar score in HRCT1 (≥*21%* vs *< 21%*)	1.54 (0.72 – 3.29)	0.26	-	-
Alveolar score in HRCT2 (≥*22%* vs *< 22%*)	1.17 (0.55 – 2.48)	0.68	-	-
Alveolar score change (Δ) (> *0%* vs ≤*0%*)	1.28 (0.60 – 2.71)	0.51	-	-
Honeycombing in HRCT1 (≥*7%* vs *< 7%*)	0.96 (0.45 – 2.03)	0.91	-	-
Honeycombing in HRCT2 (≥*7%* vs *< 7%*)	1.13 (0.53 – 2.39)	0.75	-	-
Honeycombing change (Δ) (> *0%* vs ≤*0%*)	2.10 (0.99 – 4.46)	0.05	0.52 (0.22 – 1.23)	0.14
Interstitial score in HRCT1 (≥*26%* vs *< 26%*)	1.73 (0.79 – 3.74)	0.16	-	-
Interstitial score in HRCT2 (≥*27%* vs *< 27%*)	1.29 (0.60 – 2.76)	0.51	-	-
Interstitial score change (Δ) (> *0%* vs ≤*0%*)	0.61 (0.24 – 1.52)	0.29	-	-
Interstitial s. and honeycombing in HRCT1 (≥*26%* vs *< 26%*)	0.27 (0.10 – 0.67)	**0.005**	0.32 (0.08- 1.16)	0.08
Interstitial s. and honeycombing in HRCT2 (≥*26%* vs *< 26%*)	0.47 (0.21 – 1.04)	0.06	1.39 (0.46 – 4.22)	0.55
Interstitial s. and honeycombing change (Δ) (> *0%* vs ≤*0%*)	0.80 (0.37 – 1.69)	0.56	-	-

Values are expressed as HR (95%CI). Univariate and multivariate Cox proportional hazard regression tests were used to determine the relationship of clinical, functional and radiological characteristics with disease progression.

REFERENCES

1. Lederer, D. J. ; Martinez, F.J. Idiopathic Pulmonary Fibrosis. N Engl J Med. 2018 May 10;378(19):1811-1823.

2. Raghu, G.; Collard, H.R.; Egan, J.J.; Martinez, F.J.; Behr, J.; Brown, K.K.; Colby, T.V.; Cordier, J.F.; Flaherty, K.R.; Lasky, J.A.; et al. An Official ATS/ERS/JRS/ALAT Statement: Idiopathic pulmonary fibrosis: Evidence-based guidelines for diagnosis and management. Am. J. Respir. Crit. Care Med. 2011, 183, 788–824.

3. Raghu, G.; Remy-Jardin, M.; Myers, J.L.; Richeldi, L.; Ryerson, C.J.; Lederer, D.J.; Behr, J.; Cottin, V.; Danoff, S.K.; Morelli, F.; et al. Diagnosis of Idiopathic Pulmonary Fibrosis. An Official ATS/ERS/JRS/ALAT Clinical Practice Guideline. Am. J. Respir. Crit. Care Med. 2018, 198, e44–e68.

4. Raghu, G.; Rochwerg, B.; Zhang Y. Garcia, C.A. ; Azuma, A.; Behr J.; Brozek, J.L.; Collard, H.R. ; Cunningham, W. ; Homma S.; Johkoh, T.; et al.; American Thoracic Society; European Respiratory society; Japanese Respiratory Society; Latin American Thoracic Association. An Official ATS/ERS/JRS/ALAT Clinical Practice Guideline: Treatment of Idiopathic Pulmonary Fibrosis. An Update of the 2011 Clinical Practice Guideline. Am J Respir Crit Care Med. 2015 Jul 15;192(2):e3-19.

5. du Bois, R.M., Weycker, D., Albera, C., Bradford, W.Z., Costabel, U., Kartashov, A., King, T.E. Jr, Lancaster, L., Noble, P.W., Sahn, S.A., et al. Forced vital capacity in patients with idiopathic pulmonary fibrosis: test properties and minimal clinically important difference. Am J Respir Crit Care Med. 2011 Dec 15;184(12):1382-9.

6. du Bois, R.M. ; Weycker. D. ; Albera, C. ; Bradford, W.Z. ; Costabel, U. ; Kartashov, A. ; Lancaster, L. ; Noble, P.W. ; Raghu, G. ; Sahn, S.A. ; Szwarcberg, J. ; et al. Ascertainment of individual risk of mortality for patients with idiopathic pulmonary fibrosis. Am J Respir Crit Care Med. 2011 Aug 15;184(4):459-66.

7. Wells, A.U.; Desai, S.R.; Rubens, M.B.; Goh, N.S.; Cramer, D.; Nicholson, A.G.; Colby, T.V.; du Bois, R.M.; Hansell, D.M. Idiopathic pulmonary fibrosis: A composite physiologic index derived from disease extent observed by computed tomography. Am. J. Respir. Crit. Care Med. 2003, 167, 962–969.

8. Ley, B.; Elicker, B.M.; Hartman, T.E.; Ryerson, C.J.; Vittinghoff, E.; Ryu, J.H.; Lee, J.S.; Jones, K.D.; Richeldi, L.; King, T.E., Jr.; Collard, H.R. Idiopathic Pulmonary Fibrosis: CT and Risk of Death. Radiology 2014, 273, 570–579.

9. Salisbury, M.L.; Lynch, D.A.; van Beek, E.J.; Kazerooni, E.A.; Guo, J.; Xia, M.; Murray, S.; Anstrom, K.J.; Yow, E.; Martinez, F.J.; et al. Idiopathic Pulmonary Fibrosis: The Association between the Adaptive Multiple Features Method and Fibrosis Outcomes. Am. J. Respir. Crit. Care Med. 2017, 195, 921–929.

10. Lynch, D.A.; Godwin, J.D.; Safrin, S.; Starko, K.M.; Hormel, P.; Brown, K.K.; Raghu, G.; King, T.E., Jr.; Bradford, W.Z.; et al. High-resolution computed tomography in idiopathic pulmonary fibrosis: Diagnosis and prognosis. Am. J. Respir. Crit. Care Med. 2005, 172, 488–493.

11. Sumikawa, H. ; Johkoh, T. ; Colby, T.V. ; Ichikado, K. ; Suga, M. ; Taniguchi, H. ; Kondoh, Y. ; Ogura, T. ; Arakawa, H. ; Fujimoto, K. ; et al. Computed tomography findings in pathological

usual interstitial pneumonia: relationship to survival. Am J Respir Crit Care Med. 2008 Feb 15;177(4):433-9.

12. Sverzellati, N. ; Devaraj, A. ; Desai, S.R. ; Quigley, M. ; Wells, A.U. ; Hansell, D.M. Method for minimizing observer variation for the quantitation of high-resolution computed tomographic signs of lung disease. J Comput Assist Tomogr. 2011 Sep-Oct;35(5):596-601.

13. Hansell, D.M.; Goldin, J.G.; King, T.E., Jr.; Lynch, D.A.; Richeldi, L.; Wells, A.U. CT staging and monitoring of fibrotic interstitial lung diseases in clinical practice and treatment trials: A Position Paper from the Fleischner society. Lancet Respir. Med. 2015, 3, 483–496.

14. Fell, C.D.; Martinez, F.J.; Liu, L.X.; Murray, S.; Han, M.K.; Kazerooni, E.A.; Gross, B.H.; Myers, J.; Travis, W.D.; Colby, T.V. Clinical predictors of a diagnosis of idiopathic pulmonary fibrosis. Am. J. Respir. Crit. Care Med. 2010, 181, 832–837.

15. Cocconcelli, E. ; Balestro, E. ; Biondini, D. ; Barbiero, G. ; Polverosi, R. ; Calabrese, F. ; Pezzuto, F. ; Lacedonia, D. ; Rea, F. ; Schiavon, M. ; et al. High-Resolution Computed Tomography (HRCT) Reflects Disease Progression in Patients with Idiopathic Pulmonary Fibrosis (IPF): Relationship with Lung Pathology. J Clin Med. 2019 Mar 22;8(3).

16. Altman, D.G. Practical Statistics for Medical Research; Chapman and Hall: London, UK, 1991; Volume 10, pp. 1635–1636.

17. King, T.E.J.; Bradford, W.Z.; Castro-Bernardini, S.; Fagan, E.A.; Glaspole, I.; Glassberg, M.K.; Gorina, E.; Hopkins, P.M.; Kardatzke, D.; Lancaster, L.; et al. A Phase 3 Trial of Pirfenidone in Patients with Idiopathic Pulmonary Fibrosis. N. Engl. J. Med. 2014, 370, 2083–2092.

18. Richeldi, L.; du Bois, R.M.; Raghu, G.; Azuma, A.; Brown, K.K.; Costabel, U.; Cottin, V.; Flaherty, K.R.; Hansell, D.M.; Inoue, Y.; et al. Efficacy and safety of nintedanib in idiopathic pulmonary fibrosis. N. Engl. J. Med. 2014, 370, 2071–2082.

19. Okuda, R. ; Hagiwara, E. ; Baba, T. ; Kitamura, H. ; Kato, T. ; Ogura, T. Safety and efficacy of pirfenidone in idiopathic pulmonary fibrosis in clinical practice. Respir Med. 2013 Sep;107(9):1431-7.

20. Bando, M. ; Pirfenidone: Clinical trials and clinical practice in patients with idiopathic pulmonary fibrosis. Respir Investig. 2016 Sep;54(5):298-304.

21. Brunnemer, E. ; Wälscher, J. ; Tenenbaum, S. ; Hausmanns, J. ; Schulze, K. ; Seiter, M. ; Heussel, C.P. ; Warth, A. ; Herth, F.J.F. ; Kreuter M. Real-World Experience with Nintedanib in Patients with Idiopathic Pulmonary Fibrosis. Respiration. 2018;95(5):301-309.

22. Best, A.C. ; Lynch, A.M. ; Bozic, C.M. ; Miller, D. ; Grunwald, G.K. ; Lynch, D.A. Quantitative CT indexes in idiopathic pulmonary fibrosis: relationship with physiologic impairment. Radiology. 2003 Aug;228(2):407-14.

23. Best, A.C.; Meng, J.; Lynch, A.M.; Bozic, C.M.; Miller, D.; Grunwald, G.K.; Lynch, D.A. Idiopathic pulmonary fibrosis: Physiologic tests, quantitative CT indexes, and CT visual scores as predictors of mortality. Radiology 2008, 246, 935–940.

24. Boon, K.; Bailey, N.W.; Yang, J.; Steel, M.P.; Groshong, S.; Kervitsky, D.; Brown, K.K.; Schwarz, M.I.; Schwartz, D.A. Molecular phenotypes distinguish patients with relatively stable from progressive idiopathic pulmonary fibrosis (IPF). PLoS ONE 2009, 4, e5134.

25. Selman, M.; Carrillo, G.; Estrada, A.; Mejia, M.; Becerril, C.; Cisneros, J.; Gaxiola, M.; Pérez-Padilla, R.; Navarro, C.; Richards, T.; et al. Accelerated variant of idiopathic pulmonary fibrosis: Clinical behavior and gene expression pattern. PLoS ONE 2007, 2, e482.

26. Balestro, E.; Calabrese, F.; Turato, G.; Lunardi, F.; Bazzan, E.; Marulli, G.; Biondini, D.; Rossi, E.; Sanduzzi, A.; Rea, F.; et al. Immune inflammation and disease progression in idiopathic pulmonary fibrosis. PLoS ONE 2016, 11, e0154516.

27. Biondini, D.; Balestro, E.; Lacedonia, D.; Cerri, S.; Milaneschi, R.; Luppi, F.; Cocconcelli, E.; Bazzan, E.; Clini, E.; Foschino Barbaro, M.P.; et al. Pretreatment rate of decay in forced vital capacity predicts long-term response to pirfenidone in patients with idiopathic pulmonary fibrosis. Sci. Rep. 2018, 8, 5961.

28. Kreuter, M. ; Costabel, U. ; Richeldi, L. ; Cottin, V. ; Wijsenbeek, M. ; Bonella, F. ; Bendstrup, E. ; Maher, T.M. ; Wachtlin, D. ; Stowasser, S. ; et al. Statin Therapy and Outcomes in Trials of Nintedanib in Idiopathic Pulmonary Fibrosis. Respiration. 2018;95(5):317-326

29. Lee, H.Y. ; Lee, K.S. ; Jeong, Y.J. ; Hwang, J.H. ; Kim, H.J. ; Chung, M.P. ; Han, J. High-resolution CT findings in fibrotic idiopathic interstitial pneumonias with little honeycombing: serial changes and prognostic implications. AJR Am J Roentgenol. 2012 Nov;199(5):982-9.

30. Chung, J.H. ; Goldin, J.G. Interpretation of HRCT Scans in the Diagnosis of IPF: Improving Communication Between Pulmonologists and Radiologists. Lung. 2018 Oct;196(5):561-567.

31. Launay, D. ; Remy-Jardin, M. ; Michon-Pasturel, U. ; Mastora, I. ; Hachulla, E. ; Lambert, M. ; Delannoy, V. ; Queyrel, V. ; Duhamel, A. ; Matran, R. ; et al High resolution computed tomography in fibrosing alveolitis associated with systemic sclerosis. J Rheumatol. 2006 Sep;33(9):1789-801.

32. Remy-Jardin, M. ; Giraud, F. ; Remy, J. ; Copin, M.C. ; Gosselin, B. ; Duhamel, A. Importance of ground-glass attenuation in chronic diffuse infiltrative lung disease: pathologic-CT correlation. Radiology. 1993 Dec;189(3):693-8.

33. Bouros, D. ; Wells, A.U. ; Nicholson, A.G. ; Colby, T.V. ; Polychronopoulos, V. ; Pantelidis, P. ; Haslam, P.L. ; Vassilakis, D.A. ; Black, C.M. ; du Bois, R.M. Histopathologic subsets of fibrosing alveolitis in patients with systemic sclerosis and their relationship to outcome. Am J Respir Crit Care Med. 2002 Jun 15;165(12):1581-6.

34. Iwasawa, T. ; Ogura, T. ; Sakai, F. ; Kanauchi, T. ; Komagata, T. ; Baba, T. ; Gotoh, T. ; Morita, S. ; Yazawa, T. ; Inoue, T. CT analysis of the effect of pirfenidone in patients with idiopathic pulmonary fibrosis. Eur J Radiol. 2014 Jan;83(1):32-8.

35. Jacob, J.; Bartholmai, B.J.; Rajagopalan, S.; van Moorsel, C.H.M.; van Es, H.W.; van Beek, F.T.; Struik, M.H.L.; Kokosi, M.; Egashira, R.; Brun, A.L.; Nair, A.; Walsh, S.L.F.; et al. Predicting Outcomes in Idiopathic Pulmonary Fibrosis Using Automated Computed Tomographic Analysis. Am. J. Respir. Crit. Care Med. 2018, 198, 767–776

36. Robbie, H. ; Wells, A.U. ; Jacob, J. ; Walsh, S.L.F. ; Nair, A. ; Srikanthan, A. ; Tazoniero, P. ; Devaraj, A. Visual and Automated CT Measurements of Lung Volume Loss in Idiopathic Pulmonary Fibrosis. AJR Am J Roentgenol. 2019 May 7:1-7.

37. Wu X, Kim GH et al. Computed Tomographic Biomarkers in Idiopathic Pulmonary Fibrosis: The Future of Quantitative Analysis. Am J Respir Crit Care Med. 2018 Jul 9.

Chapter 7

Prognostic role of MUC5B rs35705950 genotype in patients with Idiopathic Pulmonary Fibrosis (IPF) on antifibrotic treatment

Davide Biondini #, Elisabetta Cocconcelli #, Nicol Bernardinello, Giulia Lorenzoni, Chiara Rigobello, Sara Lococo, Gioele Castelli, Simonetta Baraldo, Manuel G Cosio, Dario Gregori, Marina Saetta, Elisabetta Balestro, Paolo Spagnolo

Respir Res. 2021 Apr 1;22(1):98. doi: 10.1186/s12931-021-01694-z. PMID: 33794872; PMCID: PMC8017848.

ABSTRACT

Background. A common variant located in the promoter region of MUC5B (rs35705950) is the strongest risk factor for sporadic and familiar IPF, as well as a predictor of outcome. However, there are no data on the effect of MUC5B rs35705950 genotype on the prognosis of IPF patients on antifibrotic treatment. The aim of this study is to determine, in a phenotypically well-characterized population of patients with IPF treated with antifibrotics, the impact of MUC5B rs35705950 genotype on disease progression and survival.

Methods. 88 IPF patients on antifibrotic treatment were followed-up from 2014 until transplantation, death or end of follow-up (December 2019). Disease progression was defined as a forced vital capacity (FVC) loss ≥5% per year. All patients were genotyped for MUC5B rs35705950 by PCR amplification and Sanger sequencing.

Results. Out of 88 patients, 61 (69%) carried the mutant T allele (TT or TG) and 27 (31%) did not (GG). Carriage of the MUC5B rs35705950 T allele was not associated with a faster decline in FVC. Conversely, at the end of the follow-up, overall survival in carriers of the TT/TG genotype was longer compared to that of the GG genotype carriers. FVC (L) at baseline and time to respiratory failure at rest were independent predictors of worse prognosis.

Conclusions. In IPF patients on antifibrotic treatment, carriage of the MUC5B rs35705950 T allele is associated with longer survival, highlighting the usefulness of MUC5B genetic data in clinical decision making.

BACKGROUND

Idiopathic pulmonary fibrosis (IPF) is a chronic progressive fibrosing interstitial lung disease of unknown origin, characterized by relentless respiratory failure leading to death within 3-5 years from diagnosis[1]. IPF is believed to occur in genetically susceptible individuals because of an aberrant wound-healing response following repetitive alveolar microinjury, resulting in scarring of the lung parenchyma and irreversible loss of function. IPF is likely to result from a complex interaction between environmental and genetic factors; for instance, as many as 20% of affected individuals report to have a family member with pulmonary fibrosis[2].

In 2011, Seibold and colleagues, using a genome-wide linkage analysis, demonstrated that the minor allele (T) of a single nucleotide polymorphism (SNP) located 3kb upstream of the MUC5B gene transcription start site on 11p15 (rs35705950) was present in 38% of subjects with sporadic IPF and in 34% of subjects with familial interstitial pneumonia[3]. Notably, the risk of disease development increased in a dose-dependent manner, from an odds ratio of 9 for heterozygous carriers of the T allele (i.e., GT) up to 21.8 for the homozygous carriers3. The association of MUC5B rs35705950 with IPF has been replicated in several independent cohorts[4-8] and represents the strongest genetic risk factor for sporadic and familial IPF described thus far.

MUC5B encodes a mucin 5B precursor protein that contributes to airway mucus production and homeostasis[9]. Although the precise mechanisms through which MUC5B dysregulation contributes to IPF development are currently unknown, MUC5B overexpression may cause mucociliary dysfunction, retention of particles and disruption of the normal reparative mechanisms in the distal lung, leading to chronic fibroproliferation and regenerative process that results in honeycomb cyst formation[10-14].

MUC5B rs35705950 T allele not only predisposes to IPF but has also been associated with improved survival, although this latter association remains debated and somehow controversial.

With this background, the aim of our study was to evaluate the influence of MUC5B rs35705950 genotype on disease behavior and survival of IPF patients on antifibrotic treatment. To the best of our knowledge, this has never been investigated before.

METHODS

Study population and study design

In this longitudinal retrospective study, we analyzed a consecutively collected cohort of well-characterized Caucasian adult patients with sporadic IPF referred to our center between April 2014 and September 2018. Patients were followed-up until transplantation, death or end of follow-up (December 2019), and those who permanently discontinued treatment were excluded from the study. Eighty-eight patients were included in the study (**Table 1**). The diagnosis of IPF was re-evaluated according to the ATS/ERS/JRS/ALAT guidelines1. Occupational or environmental exposure and connective tissue disease were excluded, and only sporadic IPF were considered for the analysis.

Patients were followed clinically and functionally for at least one year after initiation of antifibrotic. Patients were treated with pirfenidone or nintedanib according to eligibility criteria and the risk of associated adverse events.

Based on their annual rate of decline in absolute FVC% pred. during the first year of treatment, patients were defined as progressors (≥5%pred.) or stable (<5%pred.), as previously reported[15,16]. Improvement of FVC was expressed as negative value.

The progression-free survival (PFS) was calculated from the time of treatment initiation until functional progression, which was defined as absolute FVC% pred. loss ≥5% compared to the basal FVC% pred.

Based on the level of oxygen in the blood (PaO2), we defined respiratory failure when this value was <60 mmHg (8.0 kPa).

The time to development of respiratory failure (RF) on exercise and at rest was defined as the time from treatment initiation and development of RF.

The occurrence of acute exacerbation of IPF, defined as an acute worsening of dyspnea with bilateral ground glass opacities superimposed on the UIP pattern not fully explained by fluid overload[17], has been collected.

Blood sample was taken for each patient included in the study for DNA extraction and MUC5B rs35705950 genotyping. Based on their MUC5B genotype, patients were then divided in two groups (TT/TG or GG genotype).

The study was performed in accordance with the Declaration of Helsinki and was approved by the Ethics Committee of the University Hospital of Padova (4280/AO/17). Informed consent was obtained for all study participants.

Sample processing were described in the Additional file 1.

Table 1. Clinical and functional characteristics of the entire IPF population, IPF patients with TT/TG genotype and with GG genotype.

	Entire Population (n =88)	TT/TG genotype (n =61)	GG genotype (n =27)	*p* Value
Male – *n (%)*	71 (81)	49 (80)	22 (81)	0.99
Age at diagnosis – *years*	70 (44 – 84)	69 (44 – 84)	71(50 – 82)	0.30
Body mass index – *kg/m²*	26 (19 – 37)	26 (19 – 33)	27 (22 – 37)	0.49
Smoking history – *pack years*	10 (0 – 240)	10 (0 – 50)	30 (0 – 240)	**0.0001**
• **Current – *n (%)***	7 (8)	5 (8)	2 (7)	
• **Former – *n (%)***	59 (67)	38 (62)	21 (78)	0.31
• **Nonsmokers – *n (%)***	22 (25)	18 (30)	4 (15)	
Radiological diagnosis – *n (%)*	49 (56)	29 (48)	20 (74)	**0.03**
UIP	49	29	20	
Probable UIP	31	24	7	**0.03**
Indeterminate UIP	8	8	0	
FVC at baseline – *L*	2.60	2.68	2.32	**0.02**
	(1.20 – 4.61)	(1.56 – 4.36)	(1.20 – 4.61)	
FVC at baseline – *%pred.*	77 (47 – 126)	78 (52 – 126)	68 (47 – 118)	**0.05**
TLC at baseline – *%pred.*	73 (40 – 96)	73 (45 – 96)	73 (40 – 93)	0.37
DL_{CO} at baseline – *%pred.*	56 (7 – 93)	56 (7 – 89)	56 (28 – 93)	0.67
Gastroesophageal reflux – *n (%)*	32 (36)	23 (38)	9 (33)	0.69
Cardiovascular diseases – *n (%)*	63 (72)	44 (72)	19 (70)	0.86
Metabolic syndrome – *n (%)*	37 (42)	25 (41)	12 (44)	0.76
Pirfenidone treatment – *n (%)*	51 (58)	37 (61)	14 (52)	0.48
Nintedanib treatment – n *(%)*	37 (42)	24 (39)	13 (48)	0.48
FVC decline in the 1st year– *mL*	50	84	34	0.54
	(-573 – 657)	(-573 – 657)	(-559 – 461)	
FVC decline in the 1st year – *%pred.*	1 (-29 – 21)	1 (-29 – 21)	0 (-12 – 16)	0.80
Stable in the 1st year – *n (%)*	63 (72)	45 (74)	18 (67)	0.60
Progressors in the 1st year – *n (%)*	25 (28)	16 (26)	9 (33)	
RF on exercise – (months)	19 (0 – 89)	21 (0 – 89)	16 (0 – 44)	0.13
RF at rest – (months)	27 (0 – 110)	31 (5 – 110)	24 (0 – 59)	**0.04**
Nausea or vomiting – n (%)	15 (17)	13 (21)	2 (7)	0.10
Diarrhea – n (%)	16 (18)	12 (20)	4 (15)	0.58
Weight loss – n (%)	25 (28)	19 (31)	6 (22)	0.39
Increase in AST, ALT – n (%)	2 (2)	2 (3)	0 (0)	0.34
Acute exacerbations	5 (6)	3 (5)	2 (7)	0.56
Lung transplant – n (%)	5 (6)	4 (6)	1 (4)	0.17
Death – *n (%)*	27 (31)	15 (25)	12 (44)	0.06

FVC=forced vital capacity, TLC=total lung capacity, DLCO=lung diffusion carbon oxide, RF=respiratory failure, AST=aspartate aminotransferase, ALT=alanine aminostransferase. Values are expressed as numbers and (%) or median and ranges as appropriate. Negative values mean improvement of FVC. To compare demographic data and baseline clinical characteristics between TT/GT genotype and GG genotype, Chi square test and Fisher t test (n<5) for categorical variables and Mann-Whitney U test for continuous variables were used.

Statistical analysis

Categorical variables are described as absolute (n) and relative values (%) whereas continuous variables are described as median and interquartile range. To compare demographic data and baseline clinical characteristics between TT/TG and GG genotypes, Chi square test and Fisher's exact test for categorical variables and Mann-Whitney U test for continuous variables were used, as appropriate. Due to the low number of events, in survival analysis, death and death/lung transplantation were combined. Survival was estimated using the Kaplan-Meier method and the p-value of the log-rank test was reported. Analysis on progression was conducted using the Cumulative Incidence Functions (CIF) to account for competing risks.

Clinical characteristics were evaluated to determine their relationship with survival in a univariate analysis of Cox proportional hazards regression testing. The time dependency was evaluated via visual examination of Schoenfeld residuals plot. Variables with a statistically significant association with overall survival on univariate analysis were included in a multivariate Cox proportional hazard regression test to find factors independently associated with disease progression.
All data were analyzed using SPSS Software version 25.0 (New York, NY, US: IBM Corp. USA) and R software. P-values <0.05 were considered statistically significant.

RESULTS

Clinical and functional characteristics

Clinical and functional characteristics at baseline for the entire study population are shown in **Table 1**. Most patients were males and former smokers with a median age at diagnosis of 70 years. Almost half of the patients (56%) had a radiological diagnosis, while the remaining required histological confirmation. Mean FVC was 77%, reflecting a mild functional defect, and cardiovascular disease represented the most frequent comorbidity (72%). During their first year of

treatment, 63 patients (72%) remained functionally stable while 25 (28%) progressed. Over the entire study period (2014-2019) 27 patients (31%) died 5 (6%) were transplanted and 5 (6%) experienced an acute exacerbation.

The allele frequency of the MUC5B rs35705950 T was 42% (74/176), while the frequency of the wild type G allele was 58% (102/176). The MUC5B rs35705950 genotype frequencies met the Hardy-Weinberg equilibrium (Additional file 2: Table S1).

Based on the absence or presence of the minor allele (T) either in homozygosity or in heterozygosity, the population was categorized in two groups: patients with TT/TG genotype (n=61, 69%) and with GG genotype (n=27, 31%) (Table 1). The two groups did not differ regarding age, sex, body mass index, comorbidities and antifibrotic treatment. Patients carrying the GG genotype had consistently higher smoking history (30 vs. 10 PY; p<0.001), lower FVC at treatment start (2.32 vs. 2.86L, p=0.02; 68 vs. 78%, p=0.05) and more radiological diagnosis (74 vs. 48%, p=0.03) compared to TT/TG genotype. However, FVC decline (at the first year) and the percentage of patients with stable disease were similar between the two groups. Respiratory failure (RF) at rest occurred later in patients with the TT/TG genotype (31 vs. 24 months, p=0.04) (**Table 1**).

Progression-free survival and survival analysis

The progression-free survival was similar between patients with the TT/TG and GG genotypes, with a median of 19 months and 20 months, respectively (p=0.21) (**Figure 1**). On univariate analysis earlier occurrence of RF at rest and on exercise and higher levels of neutrophils were associated with disease progression. However, on multivariate analysis, only earlier occurrence of RF at rest (HR 2.36, 95%CI 1.12–4.97; p=0.02) was independently associated with disease progression in the entire population (Additional file 3: Table S2). Conversely, survival analysis revealed that patients carrying the GG genotype had a significantly worse survival than patients carrying the TT/TG genotypes (42 vs. 74 months, respectively; HR 2.59, 95%CI 1.24–5.40, p=0.0082) (**Figure 2**).

On multivariate analysis, earlier occurrence of RF at rest (HR 36.7, 95%CI 2.83–47.78; p=0.006) and lower FVC (L) at treatment initiation (HR 77.2, 95%CI 2.99–199.0; p=0.009) were significantly associated with mortality (**Table 2**).

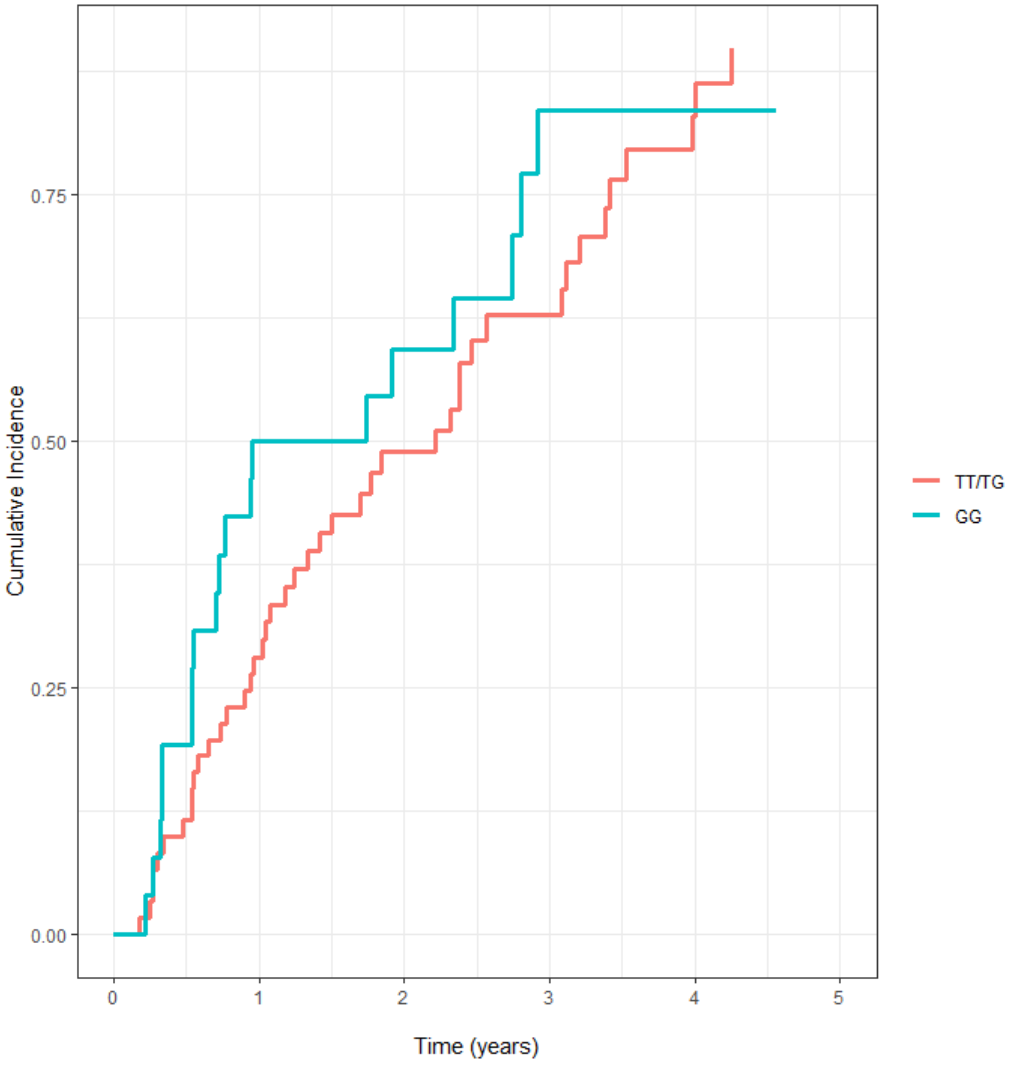

Figure 1: Progression-free survival of TT/TG and GG genotype patients. The red line represents the progression-free survival in the TT/TG group and the green line represents the progression-free survival in the GG group. Kaplan Meier analysis was used with a log-rank test (HR 1.41, 95% CI 0.81-2.44; p=0.21).

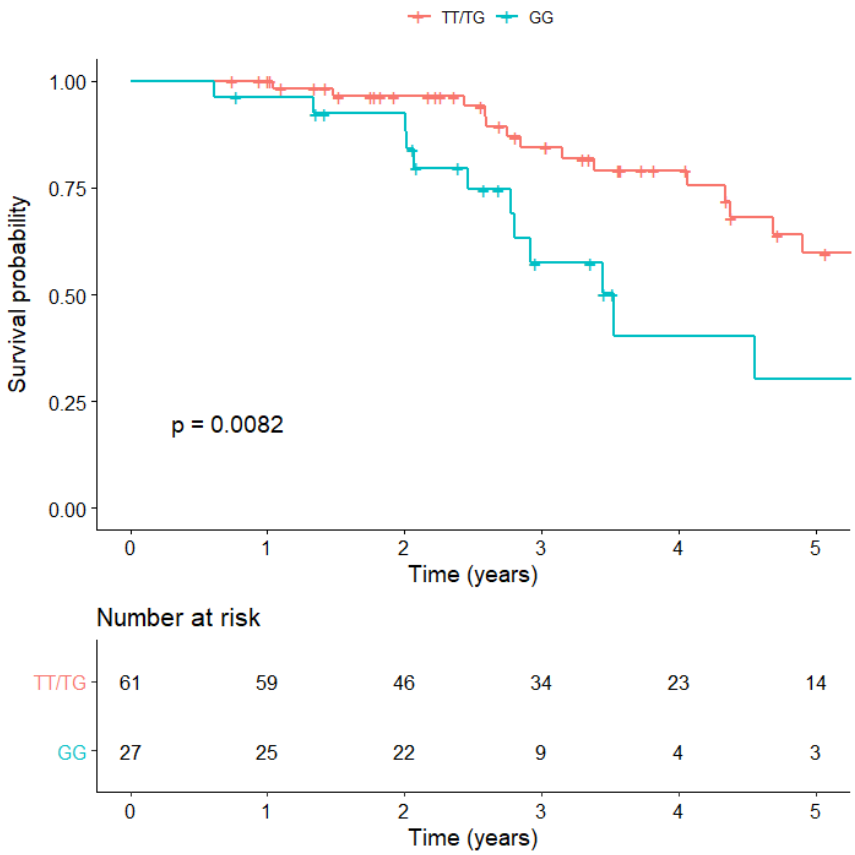

Figure 2: Survival analysis of TT/TG and GG genotype patients. The red line represents the survival in the TT/TG group and the green line represents the survival in the GG group. Kaplan Meier analysis was used with a log-rank test (HR 2.59, 95% CI 1.24-5.40; p=0.0082).

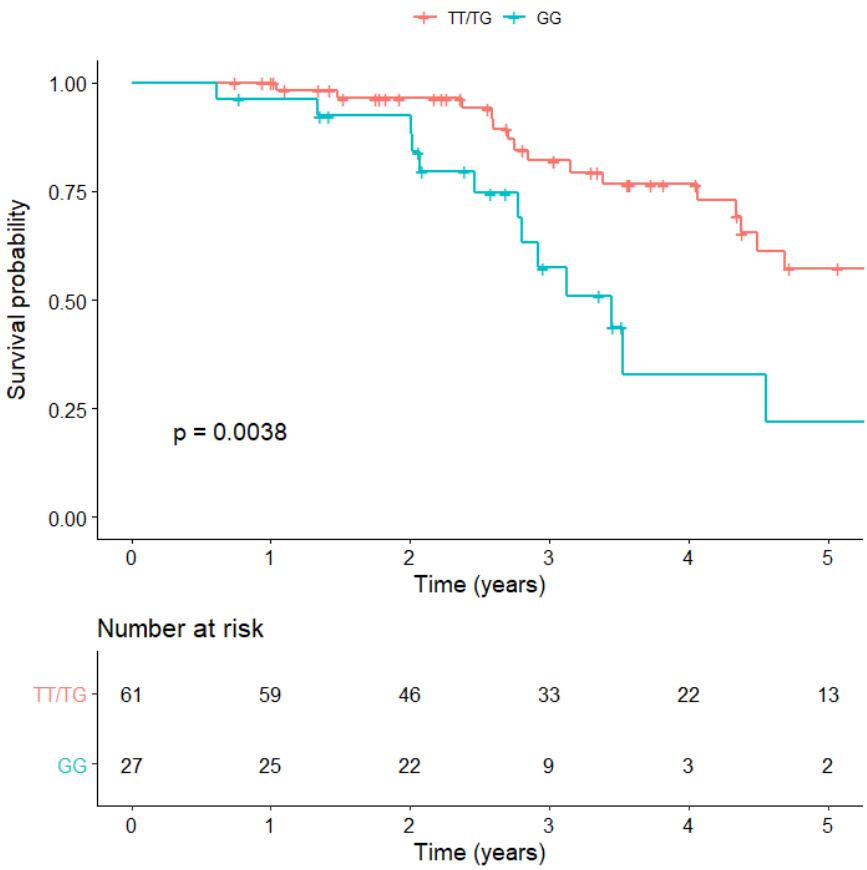

Figure 3: Combined survival and transplantation analysis of TT/TG and GG genotype patients. The red line represents the analysis in the TT/TG group and the green line represents the analysis in the GG group. Kaplan Meier analysis was used with a log-rank test (HR 2.73, 95% CI 1.34-5.54; p=0.0038).

When death is considered together with transplantation, we confirmed that patients carrying the GG genotype had a significantly worse survival than patients carrying the TT/TG genotypes (41 vs. 71 months, respectively; HR 2.73, 95%CI 1.34–5.54, p=0.0038) (**Figure 3**).

In further analysis, stratifying patients with the TT/TG and GG genotypes by the median time to RF at rest (26 months) and FVC at treatment start (2.6L), a significantly higher percentage of GG genotype carriers had a FVC lower than the median value (67 vs. 41%, p=0.02), whereas no differences were observed with regard to development of RF at rest (Additional file 4: Table S3).

Table 2. **Predictive factors of overall mortality in the entire population of IPF patients treated with antifibrotics**

		Univariate analysis HR (95% CI)	*p*	Multivariate analysis HR (95% CI)	*p*
Sex	***female***	-	-	-	-
	male	1.33 (0.51 – 3.49)	0.55	-	-
Age at diagnosis (*years)*	***< 70***	-	-	-	-
	≥ 70	1.26 (0.61 – 2.58)	0.52	-	-
BMI (*kg/m²)*	***< 26***	-	-	-	-
	≥ 26	0.85 (0.41 – 1.73)	0.66	-	-
Smoking history (*packyears)*	**< 10**	-	-	-	-
	≥ 10	1.72 (0.83 – 3.59)	0.14	-	-
Smoking status	***no***	-	-	-	-
	current	1.91 (0.36 – 10.01)	0.44	-	-
	former	1.93 (0.76 – 4.88)	0.16	-	-
Gastroesophageal reflux	***no***	-	-	-	-
	yes	0.26 (0.11 – 0.64)	**0.003**	0.11 (0.09 – 1.6)	0.10
Cardiovascular diseases	***no***	-	-	-	-
	yes	1.57 (0.69 – 3.56)	0.27	-	-
Metabolic syndrome	***no***	-	-	-	-
	yes	0.90 (0.42 – 1.92)	0.79	-	-
Treatment type	***nintedanib***	-		-	-
	pirfenidone	2.27 (0.78 – 6.60)	0.13	-	-
MUC5B rs35705950	***TT/TG***	-	-	-	-
	GG	2.39 (1.12 – 5.06)	**0.02**	1.75 (0.09 – 31.8)	0.70
Respiratory failure at rest (*months)*	***≥ 26***	-	-	-	-
	< 26	9.44 (4.10 – 21.77)	**< 0.0001**	36.7 (2.83 – 47.7)	**0.006**
Respiratory failure on effort (*months*)	***≥ 19***	-	-	-	-
	< 19	4.54 (2.06 – 10.00)	**< 0.0001**	4.96 (0.45 – 53.8)	0.18
Nausea and vomiting during treatment	***no***	-	-	-	-
	yes	0.64 (0.24 – 1.68)	0.37	-	-
Weight loss during treatment (*Kg*)	***no***	-	-	-	-
	yes	0.96 (0.39 – 2.34)	0.93	-	-
Diarrhea during treatment	***no***	-	-	-	-
	yes	0.17 (0.04 – 0.74)	**0.02**	0.45 (0.04 – 4.73)	0.50
Increase in AST and ALT	***no***	-	-	-	-
	yes	6.42 (0.78 – 52.41)	0.08	-	-
FVC at treatment initiation (L)	***≥ 2.60***	-	-	-	-
	< 2.60	3.03 (1.42 – 6.48)	**0.004**	77.2 (2.99 – 199.0)	**0.009**
FVC at treatment initiation (%)	***≥ 77***	-	-	-	-
	< 77	1.80 (0.87 – 3.71)	0.11	-	-

TLC at treatment initiation (%)	***≥ 73***	-	-	-	-
	< 73	1.89 (0.90 – 3.74)	0.09	-	-
DL_{CO} at treatment initiation (%)	***≥ 56***	-	-	-	-
	< 56	1.30 (0.64 – 2.65)	0.45	-	-
FVC after 1-yr of antifibrotic drug (L)	***≥ 2.56***	-	**-**	-	-
	< 2.56	2.25 (1.08 – 4.94)	**0.04**	0.16 (0.01 – 2.21)	0.17
FVC decline in 1-yr of antifibrotic drug (ml)	***< 50***	-	-	-	-
	≥ 50)	1.13 (0.52 – 2.47)	0.74	-	-
FVC after 1-yr of antifibrotic drug (%)	***≥ 78***	-	**-**	-	-
	< 78)	2.61 (1.10 – 6.19)	**0.03**	0.68 (0.10 – 4.23)	0.68
FVC decline in 1-yr of antifibrotic drug (%)	***< 1.02***	-	-	-	-
	≥ 1.02	1.44 (0.67 – 3.12)	0.34	-	-
Disease progression	***stables***	-	-	-	-
	progressors	2.12 (0.90 – 4.98)	0.08	-	-
TLC after 1-yr of antifibrotic drug (%)	***≥ 69***	-	**-**	-	-
	< 69	2.30 (1.04 – 5.08)	**0.04**	7.07 (0.95 – 52.66)	0.56
TLC decline in 1-yr of antifibrotic drug (%)	***< 3.02***	-	-	-	-
	≥ 3.02	1.96 (0.85 – 4.49)	0.11	-	-
DLCO after 1-yr of antifibrotic drug *(%)*	***≥ 54***	-	-	-	-
	< 54	1.47 (0.67 – 3.21)	0.33	-	-
DLCO decline in 1-yr of antifibrotic drug *(%)*	**< 0**	-	-	-	-
	≥ 0	1.52 (0.69 – 3.35)	0.30	-	-

FVC=forced vital capacity, TLC=total lung capacity, DLCO=lung diffusion carbon oxide, RF=respiratory failure, AST = aspartate aminotransferase; ALT = alanine aminostransferase. Values are expressed as HR (95%CI). Univariate and multivariate Cox proportional hazard regression tests were used to determine the relationship of clinical, functional and radiological characteristics with progression.

DISCUSSION

This study shows for the first time that in IPF patients on antifibrotic treatment, survival may be affected by carriage of MUC5B rs35705950 T allele, whether in homozygous or heterozygous form.

MUC5B encodes a major gel-forming mucin that is secreted by proximal submucosal glands and distal airway secretory cells, and plays a key role in mucociliary clearance and host defense[10-14]. A common variant in the promoter region of MUC5B gene has been identified as the strongest genetic risk factor for sporadic and familiar pulmonary fibrosis, although its role in disease development remains speculative. Moreover, mutant T allele has also been associated with pulmonary fibrosis in asbestosis[18], chronic HP[19] and rheumatoid arthritis-ILD[20].

Whether carriage of the mutant rs35705950 T allele has prognostic implications in patients with IPF is also debated, and conflicting results have been reported. However, these studies were performed before antifibrotics became the standard of care for patients with IPF and the effect of MUC5B rs35705950T on treatment response could not be assessed.

The finding of our study is in line with previous work by Peljto et al.[6], who described the protective effect of the MUC5B rs35705950 T allele in two IPF independent cohorts, one enrolled in the INSPIRE trial and the other recruited at the University of Chicago between 2007 and 2010. Moreover, rs35705950 T was also reported to be independently associated with lower bacterial burden in the bronchoalveolar lavage ($p=0.01$), lower lung function decline and mortality[21].

Conversely, Jiang and colleagues showed that T allele was associated to increased mortality in a Chinese population[22]; specifically, T allele carriers had a more severe disease, as assessed by lower FVC and DLCO. One bias that makes it difficult to compare these studies was the T allele frequency of 20%, consistently lower to that reported in previous studies[3,6,7] (almost 40%) and replicated in our cohort. Indeed, as with many other genes, the frequency of MUC5B polymorphisms depends on the individual's ethnic background, with a lower prevalence reported among Asians compared to white non-Hispanics[23].

Nonetheless, the prognostic role of MUC5B polymorphism is under debate, and conflicting results have been recently published as abstracts by two study groups, where no effect of MUC5B variant on survival in IPF patients has been

shown[24,25]. In both cases, it was not clarified whether IPF patients were on antifibrotic treatment or not.

The reason why the T allele may increase the risk of developing IPF in the general population, but confers a survival advantage within the IPF population, can only be speculated upon.

The genetic peculiarity of the MUC5B rs35705950 polymorphism resides in being a common variant with a high effect. Indeed, variants that are common in the general population (i.e., polymorphisms) rarely determine significant clinical or biological effects, except for conferring increased disease susceptibility. Conversely, rare variants (i.e., mutations) tend to be highly penetrant with substantial phenotypic effect. The wild type (G) and mutant (T) allele may interact with distinct environmental factor to determine opposite effect on disease susceptibility and prognosis, but this needs to be explored further. Intuitively, carriers of the T allele may have a better survival than noncarriers as a result of a slower disease progression, but this does not seem to be the case. Indeed, evidence of an association of less severe pathological changes and MUC5B polymorphism is reported, but it is not clear how these changes were defined[26]. Moreover, in a study by Stock[7], it was described only a trend towards a longer time to decline in FVC (HR 0.59, p=0.052) in those carrying the T allele when multivariate stepwise regression was used.

IPF population in our cohort had a relatively stable disease under antifibrotics, with FVC decline of approximately 50mL/year, similar in TT/TG and GG carriers. Moreover, the survival rate was very high, up to 70% at 5 years with only 5 cases of acute exacerbations leading the patient to death, confirming the efficacy of antifibrotic treatment in reducing mortality and also acute exacerbations. This rate is higher to that reported in literature; indeed, a recent study described survival rate of the INSIGHT-IPF registry[27] of nearly 60% at 2 years in the treated group, but the disease was more severe compared to our cohort.

Similarly to FVC decline, no between-group difference was observed in progression-free survival, that was nearly two years, supporting the beneficial effect of antifibrotic treatment in IPF, irrespective of MUC5B genotype[28-30].

However, at treatment initiation the two groups differed in terms of FVC, which was an independent predictor of mortality. Functional differences between TT and GG genotypes were described also by Peljto and coworkers6, but authors

did not clarify whether the difference was significant; however, in multivariate analysis, MUC5B genotype was associated with survival independently from FVC. Given the prognostic role of FVC in IPF, it is not surprising that patients with a lower FVC at baseline had a worse survival, and that patients with more preserved lung function at diagnosis live longer[31,32]. What remains difficult to explain, and somehow counterintuitive, is why patients with more preserved lung function are diagnosed earlier. Answering to this question requires larger prospective studies.

MUC5B has an important role in airway immunity, similar to other mucins, by capturing and removing infectious agents through mucociliary clearance[33]. MUC5B rs35705950 T allele is associated with overproduction and accumulation of mucin in distal airspaces and this could lead to an impaired mucociliary activity, that may trigger cough[3]. Interestingly, the mutant MUC5B allele has also been associated with cough severity[34]. Therefore, patients with early cough may seek medical attention when their lung function is still preserved, which may confer a survival benefit.

Another potential consequence of mucociliary dysfunction is the retention of inhaled substances (air pollutants, cigarette smoke, microorganisms, etc.) and endogenous inflammatory debris that over time may result in temporally and spatially distinct areas of microscopic scaring and progressive fibroproliferation in the lung. In this regard, Seibold[3] reported an association between MUC5B gene polymorphism and honeycomb cysts, one of the pathologic hallmarks of IPF. In subjects with IPF, regions of dense accumulation of MUC5B were observed in areas of microscopic honeycombing and involved patchy staining of the metaplastic epithelia lining the honeycomb cysts[35].

These pathological changes are reflected in the radiological abnormalities, characteristic of IPF. Indeed, MUC5B polymorphism is associated with a more typical subpleural distribution of fibrosis and with a greater proportion of confident radiological diagnosis (probable UIP and UIP)[36]. In our cohort, the presence of T allele MUC5B polymorphism was associated with a lower percentage of radiological diagnosis, which implies that carriers of the T allele did not have a CT pattern of UIP and required a histological diagnostic confirmation. In the study by Chung and coworkers[36], no information about functional parameters were given, age was lower compared to our cohort, suggesting a possible more advanced disease.

Our study has some limitation. Firstly, the study population is relatively small and there is no independent validation cohort. Secondly, the retrospective nature of the study might have introduced unintentional biases. However, the study population was carefully characterized and enrolled consecutively, which may have mitigated the selection bias. Finally, although we selected only sporadic cases, three patients were younger than 50 years, which makes one wonder about familiar disease. To the best of our knowledge they are all sporadic cases, although telomere gene mutations screening and monitoring extended to their family members would be needed to detect family aggregation.

CONCLUSIONS

In conclusion, we have shown for the first time that MUC5B rs35705950 genotype does not seem to affect response to antifibrotic treatment in patients with IPF. In addition, carriage of the mutant T allele is associated with longer survival in IPF patients on antifibrotic treatment. Larger studies and genotyping of additional genes involved in disease pathogenesis are needed to assess the role of genotype stratification in clinical trial design and in clinical decision making.

ADDITIONAL FILE 1

Sample processing

All patients were genotyped for SNP rs35705950 in the promoter region of MUC5B gene by PCR amplification and Sanger sequencing. Briefly, volumes of 5 mL of blood were collected from each patient in EDTA tubes. For plasma separation samples were centrifuged at 1,800 g for 15 min within 8 h from collection. Samples of plasma and blood cell pellet were transferred to 2 mL sterile tubes, which were stored at-80°C until subsequent analyses. DNA was isolated from 300 uL of all cell pellet using the QIAamp® DNA FFPE tissue kit (Quiagen, Netherlands) in accordance with the manufacturer's operational manual. DNA extracted from the cell pellet was used as the template for the polymerase chain reaction (PCR). PCR was performed with this primer sequence 5'-3': forward GGTTCTGTGTGGTCTAGG, reverse: TGTTTGCTCAGCGTGTTTG. The PCR reaction phase was performed as follows:

- initial denaturation at 94°C for 5 minutes;
- three step-cycle repeated for 40 cycles: denaturation at 94°C for 15 seconds,at annealing at 56°C for 20 seconds and elongation 72°C for 20 s;
- final step maintainging the samples at 72°C for 5 min.

The amplified DNA was evaluated by agarose gel electrophoresis and its size was estimated with GeneRuler 1 kb DNA Ladder (#SM0311 -ThermoFisher scientifics, Italy). The amplified DNA was purified with PureLink® PCR Purification Kit (#K310001 - ThermoFisher scientifics, Italy) and the concentration evaluated with NanoDrop 1000 Spectrophotometer V3.8 (ThermoFisher scientifics, Italy). The purified DNA was desiccated with the forward primer and sequenced using Sanger's technique with BigDyeTM Terminator v3.1 (ThermoFisher scientifics, Italy) on the instrument AB3730XL (ThermoFisher scientifics, Italy).

The minor allele was defined as T, and three possible combination of patient genotype could be obtained: wild type (GG), heterozygosis (TG) or variant homozygosis (TT).

Given that no genotyping method is 100% accurate and that genotype mistakes can lead to increased random error and bias in gene-disease associations, test of Hardy-

Weinberg equilibrium (HWE) is widely used for a prompt check of genotype information and to detect genotyping error. This latter method is based on the assumption that in a large, randomly mating population, in the absence of disturbing forces, genotype frequencies should correspond to the HWE proportions. Deviation from these proportions can be caused by many factors, one of which is genotyping error. To validate the genotype distribution of our population, we tested our genotype frequencies for HWE.

ADDITIONAL FILE 2

Table S1. MUC5B rs35705950 genotype frequency.

		Observed	Expected	*p* Value
T allele: 74/176 (42%)	**TT genotype – n (%)**	13 (14)	16 (17)	
	TG genotype – n (%)	48 (55)	43 (49)	0.69
G allele: 102/176 (58%)	**GG genotype – n (%)**	27 (31)	30 (34)	

Chi square test for categorical variables was used.

ADDITIONAL FILE 3

Table S2. Predictive factors of progression in the entire population of IPF patients treated with antifibrotics

		Univariate analysis		Multivariate analysis	
		HR (95% CI)	*p* Value	HR (95% CI)	*p* Value
Sex	***female***	-	-	-	-
	male	1.39 (0.77 – 2.67)	0.32	-	-
Age at diagnosis (*years*)	***< 70***	-	-	-	-
	≥ 70	0.97 (0.58 – 1.61)	0.91	-	-
BMI (*kg/m²*)	***< 26***	-	-	-	-
	***≥ 26*)**	0.96 (0.58 – 1.59)	0.90	-	-
Smoking history (*packyears*)	**< 10**	-	-	-	-
	≥ 10	0.94 (0.56 – 1.56)	0.81	-	-
Smoking status	***no***	-	-	-	-
	current	0.67 (0.22 – 2.04)	0.49	-	-
	former	1.14 (0.63 – 2.07)	0.64	-	-
Gastroesophageal reflux	***no***	-	-	-	-
	yes	0.85 (0.50 – 1.43)	0.54	-	-
Cardiovascular diseases	***no***	-	-	-	-
	yes	0.99 (0.57 – 1.72)	0.99	-	-
Metabolic syndrome	***no***	-	-	-	-
	yes	1.04 (0.62 – 1.75)	0.86	-	-
MUC5B rs35705950	***TT/TG***	-	-	-	-
	GG	0.96 (0.56 – 1.64)	0.88	-	-
Respiratory failure at rest (*months*)	***≥ 26***	-	-	-	-
	< 26	1.92 (1.12 – 3.29)	**0.02**	2.36 (1.12 – 4.97)	**0.02**
Respiratory failure on effort (*months*)	***≥ 19***	-	-	-	-
	< 19	1.67 (1.00 – 2.78)	**0.04**	1.15 (0.59 – 2.23)	0.66
Nausea and vomiting during treatment	***no***	-	-	-	-
	yes	0.48 (0.22 – 1.02)	0.05	-	-
Weight loss during treatment (*Kg*)	***no***	-	-	-	-
	yes	0.78 (0.43 – 1.40)	0.41	-	-
Diarrhea during treatment	***no***	-	-	-	-
	yes	0.92 (0.51 – 1.65)	0.78	-	-
Increase in AST and ALT	***no***	-	-	-	-
	yes	2.64 (0.35 – 19.65)	0.34	-	-
FVC at treatment initiation (L)	***≥ 2.60***	-	-	-	-
	< 2.60	1.49 (0.90 – 2.48)	0.12	-	-
FVC at treatment initiation (%)	***≥ 77***	-	-	-	-
	< 77	1.29 (0.78 – 2.14)	0.32	-	-
TLC at treatment initiation (%)	***≥ 73***	-	-	-	-
	< 73	1.15 (0.69 – 1.91)	0.57	-	-
DL_{CO} at treatment initiation (%)	***≥ 56***	-	-	-	-
	< 56	1.42 (0.86 – 2.36)	0.16	-	-
White blood cells (n*10^9/L)	***< 7.47***	-	-	-	-
	≥ 7.47	1.45 (0.82 – 2.54)	0.19	-	-
Neutrophils (n*10^9/L)	***< 4.18***	-	-	-	-
	≥ 4.18	1.67 (0.95 – 2.94)	0.07	-	-
Neutrophils (%)	***< 58***	-	-	-	-
	≥ 58	1.78 (1.00 – 3.17)	**0.04**	1.79 (0.95 – 3.03)	0.07
Lymphocytes (n*10^9/L)	***< 2.3***	-	-	-	-
	≥ 2.3	0.90 (0.51 – 1.57)	0.71	-	-
Lymphocytes (%)	***< 30***	-	-	-	-
	≥ 30	0.59 (0.33 – 1.05)	0.07	-	-
Monocytes (n*10^9/L)	***< 0.69***	-	-	-	-
	≥ 0.69	1.23 (0.70 – 2.14)	0.46	-	-
Monocytes (%)	***< 8.5***	-	-	-	-
	≥ 8.5	0.97(0.53 – 1.77)	0.93	-	-

FVC=forced vital capacity, TLC=total lung capacity, DLCO=lung diffusion carbon oxide, RF=respiratory failure, AST = aspartate aminotransferase; ALT = alanine aminostransferase. Values are expressed as HR (95%CI). Univariate and multivariate Cox proportional hazard regression tests were used to determine the relationship of clinical, functional and radiological characteristics with progression.

ADDITIONAL FILE 4

Table S4. Occurrence of respiratory failure (RF) at rest and FVC (L) at treatment initiation according to MUC5B genotype (TT/TG vs. GG patients).

	TT/TG genotype (n = 61)	**GG genotype (n =27)**	***p* Value**
RF at rest ≥ 26 moths – *n (%)*	34 (56)	11 (41)	0.19
RF at rest < 26 months – *n (%)*	27 (44)	16 (59)	
FVC (L) T0 ≥ 2.60 L – n (%)	36 (59)	9 (33)	**0.02**
FVC (L) < 2.60 L – n (%)	25 (41)	18 (67)	

Chi square test for categorical variables was used.

REFERENCES

1. Raghu G, Remy-Jardin M, Myers JL, Richeldi L, Ryerson CJ, Lederer DJ, et al. Diagnosis of Idiopathic Pulmonary Fibrosis. An Official ATS/ERS/JRS/ALAT Clinical Practice Guideline. Am J Respir Crit Care Med. 2018; 198: e44-e68.
2. Loyd JE. Pulmonary fibrosis in families. Am J Respir Cell Mol Biol. 2003; 29: S47-50.
3. Seibold MA, Wise AL, Speer MC, Steele MP, Brown KK, Loyd JE, et al. A common MUC5B promoter polymorphism and pulmonary fibrosis. N Engl J Med. 2012; 364: 1503–12. doi:10.1056/NEJMoa1013660.
4. Fingerlin TE, Murphy E, Zhang W, Peljto AL, Brown KK, Steele MP, et al. Genome-wide association study identifies multiple susceptibility loci for pulmonary fibrosis. Nat Genet. 2013; 45: 613–20. doi:10.1038/ng.2609.
5. Noth I, Zhang Y, Ma SF, Flores C, Barber M, Huang Y, et al. Genetic variants associated with idiopathic pulmonary fibrosis susceptibility and mortality: a genome-wide association study. Lancet Respir Med. 2013; 1: 309–17. doi:10.1016/S2213-2600(13)70045-6.
6. Peljto AL, Zhang Y, Fingerlin TE, Ma SF, Garcia JG, Richards TJ, et al. Association between the MUC5B promoter polymorphism and survival in patients with idiopathic pulmonary fibrosis. JAMA 2013; 309: 2232–9. doi:10.1001/jama.2013.5827.
7. Stock CJ, Sato H, Fonseca C, Banya WAS, Molyneaux PL, Adamali H, et al. Mucin 5B promoter polymorphism is associated with idiopathic pulmonary fibrosis but not with development of lung fibrosis in systemic sclerosis or sarcoidosis. Thorax 2013. 68: 436–41. doi:10.1136/thoraxjnl-2012-201786.
8. Moore C, Blumhagen RZ, Yang IV, Walts A, Powers J, Walker T, et al. Resequencing Study Confirms That Host Defense and Cell Senescence Gene Variants Contribute to the Risk of Idiopathic Pulmonary Fibrosis. Am J Respir Crit Care Med. 2019; 200: 199-208.
9. Roy MG, Livraghi-Butrico A, Fletcher AA, McElwee MM, Evans SE, Boerner RM, et al. Muc5b Is Required for Airway Defence. Nature. 2014; 505: 412-6.
10. Seibold MA, Smith RW, Urbanek C, Groshong SD, Cosgrove GP, Brown KK, et al. The idiopathic pulmonary fibrosis honeycomb cyst contains a mucociliary pseudostratified epithelium. PLoS ONE 2013; 8: e58658.
11. Helling BA, Gerber AN, Kadiyala V, Sasse SK, Pedersen BS, Sparks L, et al. Regulation of MUC5B expression in idiopathic pulmonary fibrosis. Am J Respir Cell Mol Biol. 2017; 57: 91–99.
12. Evans CM, Fingerlin TE, Schwarz MI, Lynch D, Kurche J, Warg L, et al. Idiopathic pulmonary fibrosis: a genetic disease that involves mucociliary dysfunction of the peripheral airways. Physiol Rev. 2016; 96: 1567–1591.
13. Hancock LA, Hennessy CE, Solomon GM, Dobrinskikh E, Estrella A, Hara N, et al. Muc5b overexpression causes mucociliary dysfunction and enhances lung fibrosis in mice. Nat Commun. 2018; 9: 5363.

14. Nakano Y, Yang IV, Walts AD, Watson AM, Helling BA, Fletcher AA, et al. MUC5B promoter variant rs35705950 affects MUC5B expression in the distal airways in idiopathic pulmonary fibrosis. Am J Respir Crit Care Med. 2016; 193: 464–466.
15. Kreuter M, Costabel U, Richeldi L, Cottin V, Wijsenbeek M, Bonella F, et al. Statin Therapy and Outcomes in Trials of Nintedanib in Idiopathic Pulmonary Fibrosis. Respiration 2018; 95, 317–326.
16. Balestro E, Cocconcelli E, Giraudo C, Polverosi R, Biondini D, Lacedonia D, et al. High-Resolution CT Change over Time in Patients with Idiopathic Pulmonary Fibrosis on Antifibrotic Treatment. J Clin Med. 2019 Sep 15;8(9):1469.
17. Collard HR, Ryerson CJ, Corte TJ, Jenkins G, Kondoh Y, Lederer DJ, et al. Acute Exacerbation of Idiopathic Pulmonary Fibrosis. An International Working Group Report. Am J Respir Crit Care Med. 2016 Aug 1;194(3):265-75.
18. Platenburg MGJP, Wiertz IA, van der Vis JJ, Crestani B, Borie R, Dieude P, et al. The MUC5B promoter risk allele for idiopathic pulmonary fibrosis predisposes to asbestosis. Eur Respir J. 2020 Apr 30;55(4):1902361.
19. Ley B, Newton CA, Arnould I, Elicker BM, Henry TS, Vittinghoff E, et al. The MUC5B promoter polymorphism and telomere length in patients with chronic hypersensitivity pneumonitis: an observational cohort-control study. Lancet Respir Med. 2017 Aug;5(8):639-647.
20. Juge PA, Lee JS, Ebstein E, Furukawa H, Dobrinskikh E, Gazal S, et al. MUC5B Promoter Variant and Rheumatoid Arthritis with Interstitial Lung Disease. N Engl J Med. 2018 Dec 6;379(23):2209-2219.
21. Molyneaux PL, Cox MJ, Willis-Owen SA, Mallia P, Russell KE, Russell AM, et al. The Role of Bacteria in the Pathogenesis and Progression of Idiopathic Pulmonary Fibrosis. Am J Respir Crit Care Med. 2014; 190: 906-13.
22. Jiang H, Hu Y, Shang L, Li Y, Yang L, Chen Y. Association between MUC5B polymorphism and susceptibility and severity of idiopathic pulmonary fibrosis. Int J Clin Exp Pathol. 2015; 8: 14953-14958.
23. Wang C, Zhuang Y, Guo W, Cao L, Zhang H, Xu L, et al. Mucin 5B promoter polymorphism is associated with susceptibility to interstitial lung diseases in Chinese males. PLoS One 2014; 9: e104919.
24. Stock C, Molyneaux P, Saunders P, Kokosi M, George P, Kouranos V, et al. MUC2MUC5B and TOLLIP variants: no association with disease progression and survival in an IPF cohort [abstract]. Eur Respir J 2020; 56: 736.
25. Bonella F, Campo I, Boerner E, Theegarten D, Guzman J, Costabel U., et al. Potential clinical utility of MUC5B and TOLLIP single nucleotide polymorphisms (SNP) in in the management of patients with IPF [abstract]. Eur Respir J 2019; 54: PA5370.
26. Cosgrove GP, Groshong SD, Peljto AL, Talbert J, McKean D, Markin C, et al. The MUC5B promoter polymorphism is associated with a less severe pathological form of familial interstitial pneumonia (FIP) [abstract]. Am J Respir Crit Care Med. 2012; 185: A6865.

27. Behr J, Prasse A, Wirtz H, Koschel D, Pittrow D, Held M, et al. Survival and course of lung function in the presence or absence of antifibrotic treatment in patients with idiopathic pulmonary fibrosis: long-term results of the INSIGHTSIPF registry. Eur Respir J. 2020; 56: 1902279.
28. King TE Jr, Bradford WZ, Castro-Bernardini S, Fagan EA, Glaspole I, Glassberg MK, et al. A phase 3 trial of pirfenidone in patients with idiopathic pulmonary fibrosis. N Engl J Med. 2014; 370: 2083–2092.
29. Richeldi L, du Bois RM, Raghu G, Azuma A, Brown KK, Costabel U, et al. Efficacy and Safety of Nintedanib in Idiopathic Pulmonary Fibrosis. N Engl J Med. 2014; 370: 2071-2082.
30. Biondini D, Balestro E, Lacedonia D, Cerri S, Milaneschi R, Luppi F, et al. Pretreatment rate of decay in forced vital capacity predicts long-term response to pirfenidone in patients with idiopathic pulmonary fibrosis. Sci Rep. 2018; 8: 5961. doi: 10.1038/s41598-018-24303-4.
31. Ley B, Collard HR & King TE Jr. Clinical course and prediction of survival in idiopathic pulmonary fibrosis. Am J Respir Crit Care Med. 2011; 183: 431–440.
32. Erbes R, Schaberg T, Loddenkemper R. Lung function tests in patients with idiopathic pulmonary fibrosis. Are they helpful for predicting outcome? Chest 1997; 111: 51–57.
33. Schwartz DA. Idiopathic pulmonary fibrosis is a genetic disease involving mucus and the peripheral airways. Ann. Am. Thorac. Soc. 2018; 15: S192–7.
34. Scholand MB, Wolff R, Crossno PF, Sundar K, Winegar M, Whipple S, et al. Severity of cough in idiopathic pulmonary fibrosis is associated with MUC5 B genotype. Cough 2014; 10: 3.
35. Yang IV, Fingerlin TE, Evans CM, Schwarz MI, Schwartz DA. MUC5B and idiopathic pulmonary fibrosis. Ann Am Thorac Soc. 2015; 12: S193–9.
36. Chung JH, Peljto AL, Chawla A, Talbert JL, McKean DF, Rho BH, et al. CT Imaging Phenotypes of Pulmonary Fibrosis in the MUC5B Promoter Site Polymorphism. Chest 2016; 149: 1215-22.

Chapter 8

Radiological scores in Idiopathic pulmonary fibrosis (IPF) patients according to MUC5B polymorphism

Original data not yet published

ABSTRACT

Background. The MUC5B rs35705950 mutant T allele is the strongest genetic risk factor for familiar and sporadic IPF. In addition, carriage of the T allele has been associated with better outcomes. We sought to determine whether MUC5B rs35705950 genotype affects radiological patterns of IPF patients and how they may change during the first year of antifibrotic therapy.

Methods. 78 IPF patients on antifibrotic treatment and on regular follow-up were genotyped for MUC5B rs35705950 by PCR amplification and Sanger sequencing and classified according to the carriage of the mutant T allele. HRCT patterns were quantified at treatment initiation (HRCT0) and after 1 year (HRCT1) as: ground glass opacities (Alveolar Score,AS), reticulations (Interstitial Score,IS) and honeycombing (HC).

Results. 54/78 patients (69%) carried at least one copy of the T allele. At HRCT0, radiological scores were similar across the TT/TG/GG subgroups. Carriers of the T allele displayed similar FVC loss in the 1-year of treatment as GG carriers, but overall survival was longer in the TT/TG group compared to the GG group (69vs.41months, HR 0.52, 95% CI 0.28 – 0.98; p= 0.04). In the TT/TG group, HC increased significantly [from 2(0-41) % to 5(0-50)%;p=0.001], whereas in the GG group both AS [from 16(0-44)% to 18(1-86)%;p=0.05] and HC [from 3(0-70)% to 7(0-83)%;p=0.007] increased significantly at HRCT1.

Conclusions. In IPF patients carrying the MUC5B rs35705950 T allele, HC increases over time, whereas in noncarriers both HC and AS increase despite a similar FVC loss in the 1-year of treatment. Longitudinal HRCT may help in clarifying the prognostic role of MUC5B rs35705950.

BACKGROUND

Idiopathic pulmonary fibrosis (IPF) is a chronic disorder of unknown origin and the overall survival of affected patients is very poor and unpredictable. The actual antifibrotic drugs aim to slow down the inevitably progressive course until respiratory failure and death, remaining a disease still orphan of curative treatment. Despite uncertainty about its leading cause, a number of potential risk factors have been suggested. IPF is believed to occur in genetically susceptible individuals as a consequence of an aberrant wound-healing response following repetitive alveolar microinjury, resulting in scarring of the lung parenchyma and irreversible loss of function. Familial clustering of cases and the occurrence of pulmonary fibrosis in the context of rare genetic disorders (such as Hermansky–Pudlak syndrome or dyskeratosis congenita) indicate that genetic predisposition contributes significantly to the pathogenesis of IPF.

The single nucleotide polymorphism (SNP) rs35705950 located in the promoter region of the gene mucin 5B (MUC5B) on 11p15.5 is well known to be strongly associated with both sporadic IPF and familial forms of pulmonary fibrosis, and this association has been validated in several independent cohorts[1-4]. The increased risk in developing pulmonary fibrosis is maintained when individuals carry the mutant allele (T) either in heterozygous (GT) or in homozygous form (TT). The prognostic role of the SNP rs35705950 in IPF patients is still debated, with some studies suggesting a protective effect on mortality for patients carrying the minor allele T in heterozygous or homozygous form[5]. In our recent work, for the first time we demonstrated the impact of MUC5B polymorphism on prognosis of IPF patients on antifibrotic treatment[6]. More specifically, in our IPF cohort we demonstrated that carriers of the mutant T allele, either in heterozygous or homozygous form, present a significantly prolonged survival compared to the wild type population.

On this basis, the aim of our present study was to determine whether MUC5B rs35705950 genotype affects radiological patterns of IPF patients at diagnosis and its association with radiologic changes during the first year of treatment.

METHODS

Study population and study design

In this longitudinal retrospective study, we consecutively collected and analyzed a cohort of well characterized patients with IPF referred to our center between April 2014 and June 2022. Those patients were followed clinically, functionally (measuring periodically forced vital capacity (FVC), total lung capacity (TLC) and diffusing capacity of the lung for carbon monoxide (DLCO)) and radiologically for at least one year after initiation of anti-fibrotic treatment (either pirfenidone or nintedanib).

Seventy-eight patients were included (**Table 1**) due to the inclusion criteria of having two HRCT available, at diagnosis and after 1-year treatment. Each patient received a diagnosis of IPF according to the ATS/ERS/JRS/ALAT guidelines published in 2011 and revised according to the last guidelines of 2022[7,8]. Thirty-eight cases required a histological confirmation of the diagnosis of IPF whereas in the majority of cases (n=40) the diagnosis was reached on the basis of a clinical and radiological consensus. Patients with a clear history of environmental or occupational exposure and those with clinical features or serological data suggestive of an underlying connective tissue disease were excluded.

Clinical and functional data were collected in every patient at the time of treatment initiation and at regular time intervals (every four months) for almost twelve months, while HRCT was regularly performed at treatment initiation and after 12 months. All patients were genotyped for MUC5B promoter's SNP rs35705950 by PCR amplification and Sanger sequencing and finally categorized in two groups: the TT/TG genotype (n=54) and the GG genotype (n=24), respectively (**Table 1**). Each patient provided a blood sample for DNA extraction and morphometric analysis before starting antifibrotic treatment.

Patients were treated with pirfenidone or nintedanib, and the choice between these two drugs was made according to eligibility criteria and the risk of associated adverse events. Adverse events occurring during treatment were periodically collected (every four months).

Based on their annual rate of decline (≥ 5 or $< 5\%$ pred.) in absolute FVC% pred. during the first year of treatment, patients were defined as progressors or stable, respectively. Improvement of FVC (%pred. and mL) was expressed as negative value. The overall survival (OS) was calculated from the beginning of the treatment to death, transplant or loss to follow-up; survival data were censored at the end of the study (June 2022).

The study was performed in accordance with the Declaration of Helsinki and was approved by the Ethics Committee of the University Hospital of Padova (4280/AO/17). Informed consent was obtained for all study participants.

Table 1. Patient's demographics and clinical characteristics of the entire study population, and cathegorized in TT/TG genotype or GG gentotype.

	Entire Population (n =78)	**TT/TG genotype (n =54)**	**GG genotype (n =24)**	**p Value**
Male – n (%) **Female – n (%)**	64 (82) 14 (18)	44 (82) 10 (18)	20 (83) 4 (17)	0.84
Age at diagnosis – years	69 (44–82)	68 (44-82)	72 (50-82)	0.16
Body mass index (BMI) – kg/m²	27 (19-37)	26 (19-33)	27 (23-37)	0.83
Smoking history – pack years	10 (0–240)	10 (0-50)	30 (0 - 240)	**0.0006**
• **Current – n (%)**	7 (9)	5 (9)	2 (8)	0.36
• **Former – n (%)**	50 (64)	32 (59)	18 (75)	
• **Nonsmokers – n (%)**	21 (27)	17 (32)	4 (17)	
Radiological diagnosis – n (%) **Histological diagnosis – n (%)**	40 (51) 38 (49)	23 (43) 31 (57)	17 (71) 7 (29)	**0.02**
FVC at diagnosis – L	2.66 (1.53–4.61)	2.79 (1.67-4.36)	2.40 (1.53-4.61)	**0.03**
FVC at diagnosis – %pred.	77 (47–126)	79 (56–126)	72 (47–118)	0.08
TLC at diagnosis - %pred.	73 (40-96)	73 (45-96)	73 (40-93)	0.32
DL_{CO} at diagnosis – %pred.	56 (7–93)	56 (7-89)	56 (28-93)	0.60
Gastroesophageal reflux – n (%)	31 (40)	22 (41)	9 (38)	0.78
Cardiovascular diseases – n (%)	53 (68)	37 (69)	16 (67)	0.87
Metabolic syndrome – n (%)	33 (42)	22 (41)	11 (46)	0.67
Pirfenidone– n (%)	42 (54)	31 (57)	11 (46)	0.34
Nintedanib – n (%)	36 (46)	23 (43)	13 (54)	
FVC decline in the 1st year– mL	46 (-573–657)	59 (-573-657)	34 (-559-461)	0.70
FVC decline in the 1st year – %pred.	0 (-29-21)	1 (-29-21)	0 (-12-16)	0.80
Stable – n (%)	62 (79)	43 (80)	19 (79)	0.96
Progressors – n (%)	16 (21)	11 (20)	5 (21)	

Nausea and vomiting - n (%)	11 (14)	10 (19)	1 (4)	0.09
Diarrhea – n (%)	25 (18)	19 (20)	7 (29)	0.60
Weight loss - n (%)	14 (32)	10 (35)	5 (21)	0.81
Increase in AST, ALT – n (%)	2 (3)	2 (4)	0 (0)	0.33
Transplanted – n (%)	4 (5)	3 (6)	1 (4)	0.79
Deaths – n (%)	27 (35)	9 (17)	8 (33)	0.09

Values are expressed as numbers and (%) or median and ranges as appropriate. Negative values mean improvement of FVC. To compare demographic data and baseline clinical characteristics between TT / GT genotype and GG genotype, Chi square test and Fisher t test (n < 5) for categorical variables and Mann-Whitney U test for continuous variables were used. AST = aspartate aminotransferase; ALT = alanine aminostransferase. Values are expressed as numbers and (%) or median and ranges as appropriate. Negative values mean improvement of FVC. To compare demographic data and baseline clinical characteristics between TT / GT genotype and GG genotype, Chi square test and Fisher t test (n < 5) for categorical variables and Mann-Whitney U test for continuous variables were used.

Sample processing, DNA extraction and Sanger sequencing

Volumes of 5-10 mL of blood were collected from each patient, placed in EDTA tubes and stored at 4°C before plasma separation and centrifuged at 1,600 g for 10 min at 4°C within 8 h from collection. Plasma samples were transferred to 2 mL sterile tubes, which were shipped in a dry ice container. DNA was isolated from 300 uL of plasma using the QIAamp® DNA FFPE tissue kit (Quiagen, Netherlands) in accordance with the manufacturer's operational manual. DNA extracted from plasma was used as the template for the polymerase chain reaction (PCR). PCR was performed with this primer sequence 5'-3': forward GGTTCTGTGTGGTCTAGG, reverse: TGTTTGCTCAGCGTGTTTG The PCR reaction phase was performed as follows: (step 1) initial denaturation at 94°C for 5 minutes; (step 2) three step-cycle repeated for 40 cycles: denaturation at 94°C for 15 seconds, annealing at 56°C for 20 seconds and elongation at 72°C for 20 s; (step 3) final step maintaining the samples at 72°C for 5 min.

The amplified DNA was evaluated by agarose gel electrophoresis and its size was estimated with GeneRuler 1 kb DNA Ladder (#SM0311 -ThermoFisher scientifics, Italy). The amplified DNA was purified with PureLink® PCR Purification Kit (#K310001 - ThermoFisher scientifics, Italy) and the concentration evaluated with NanoDrop 1000 Spectrophotometer V3.8 (ThermoFisher scientifics, Italy). The purified DNA was desiccated with the forward primer and sequenced using Sanger's technique with BigDyeTM Terminator v3.1 (ThermoFisher scientifics, Italy) on the instrument AB3730XL (ThermoFisher scientifics, Italy).

Three possible results could be obtained: wild type (GG); heterozygosis (TG) or variant homozygous (TT).

Radiological scoring

The HRCTs available at treatment initiation (either pirfenidone or nintedanib) (HRCT1) and at 12-month follow-up (HRCT2) were scored by two expert thoracic radiologists (C.G.; R.P.). The HRCTs were performed by a 64 slice Siemens Somatom Sensation (Siemens Healthcare, Erlangen, Germany) applying a slice thickness ≤ 1.5 mm.

The two thoracic radiologists were blind to clinical and functional data and timing of HRCT, and scored HRCT1 and HRCT2 images independently using a semi-quantitative scale as previously described[9]. This represented a modification of the previously reported scoring systems[10,11], that allowed us to evaluate the interstitial "reticulations" more precisely. Specifically, the radiologic features considered in this study were ground glass opacities (GGO) (alveolar score, AS), reticulations (interstitial score, IS) and honeycombing (HC) (honeycombing score, HC). For each lung lobe, the two radiologists assessed the extent of AS, IS and HC using a scale from 0-100 and estimated extent to the nearest 5%. After each individual lobe was scored, the result was expressed as the mean value of the five lobes in AS, IS and HC. Finally, the IS and HC were pooled (IS+HC) to analyze the amount of fibrotic abnormalities. The level of interobserver agreement was obtained for each patient as a mean of 5 lobes and for each radiological abnormality (i.e., IS, AS and HC) and expressed as Cohen's k value. Disagreement between radiologists was resolved by consensus. The association between radiological change and FVC decline was calculated as the change in AS (ΔAS/month), IS (ΔIS/month), HC (ΔHC/month), pooled IS and HC (ΔIS+HC/month) and the change in FVC milliliters (ml) per month (ΔFVC ml/month) and FVC% pred. per month (ΔFVC% pred./month) between HRCT1 and HRCT2.

Statistical analysis

Categorical variables are described as absolute (n) and relative values (percentage, %) whereas continuous variables are described as median and range. To compare demographic data and baseline clinical characteristics between stable TT/TG and GG genotypes, Chi square test and Fisher's exact test for categorical

variables and Mann-Whitney U test for continuous variables were used as appropriate.

Wilcoxon signed rank test was performed to compare HRCT1 and HRCT2 for the grading scores of different variables (AS, IS, HC and IS+HC) in the entire population, in TT/TG patients and GG patients. Correlation coefficients between radiological and functional data were calculated using the nonparametric Spearman's rank method. The level of interobserver agreement between the two radiologists was evaluated by kappa statistic measure[12].

The overall survival was calculated from treatment initiation to death or lung transplantation with data censured at June 2022. The cumulative survival rate was calculated using Kaplan-Meier method and the difference in the survival time between the two groups (TT/GT and GG genotype) was assessed with a log-rank test. Radiological scores were evaluated to determine their relationship with survival in a univariate analysis of Cox proportional hazards regression testing. Variables with an association statistically significant with overall survival at univariate analysis were included in a multivariate Cox proportional hazard regression test to find the factors independently associated with mortality.

All data were analyzed using SPSS Software version 25.0 (New York, NY, US: IBM Corp. USA) and figures were created with GraphPad Prism (version 8.3.1, GraphPad Software, La Jolla, CA, USA). P-values < 0.05 were considered statistically significant.

RESULTS

Clinical and functional evaluation at baseline and during the 1-st year follow up.

Clinical and functional characteristics at baseline of the patients included in study are shown in **Table 1**. Most patients were males (82%) and former smokers (64%) with a median age at diagnosis of 69 years (range 44–82). Based on the MUC5B rs35705950 genotyping, 54 patients were classified as having a TT/TG genotype and 24 patients having a GG genotype (**Table 1**).

At treatment initiation, the TT/GT and GG genotype groups were homogeneous for sex, age and body mass index (BMI) and main comorbidities (gastroesophageal reflux, cardiovascular diseases and metabolic syndrome), while GG genotype patients have a heavier smoking history of 30 pack years (0 - 240) vs.

10 pack years (0 – 50; p = 0.0006). GG genotype patients have a significantly less preserved FVC (% pred. and L) at treatment initiation and a higher % of patients receiving a clinical - radiological diagnosis [17 (71%) vs. 23 (43%), p = 0.02], as compared to TT/TG genotype patients.

Forty-two patients were treated with pirfenidone and thirty-six with nintedanib, with similar proportion between the two genotype groups (57% in TT/TG and 47% in GG genotype treated with pirfenidone, 43% in TT/TG and 54% in GG genotype treated with nintedanib).

Based on the annual FVC% pred. decline during treatment (≥ 5 or < 5% pred.), most patients were classified as stables [62 stable patients (79%) vs. 16 progressors (21%)], with equal proportion between the two groups (80% in TT/TG and 79% in GG genotype stable patients, and 20% progressors in TT/TG group and 21% in GG group, respectively).

27 (35%) patients died during the follow up period, with equal proportion between the two genotyped groups.

The allele frequency of the MUC5B rs35705950 T allele was 66/156 (42%), while the frequency of the wild type G allele was 90/156 (58%). The MUC5B rs35705950 genotype frequencies met the Hardy–Weinberg equilibrium (**Table 2**).

Table 2. MUC5B rs35705950 genotype frequency.

		Observed	Expected	p Value
T allele: 66/156 (42%)	**TT genotype – n (%)**	12 (15)	16 (17)	
G allele: 90/156 (58%)	**TG genotype – n (%)**	42 (54)	43 (49)	0.82
	GG genotype – n (%)	24 (31)	30 (34)	

Chi square test for categorical variables was used.

Radiological scoring at baseline

Alveolar, honeycombing, interstitial and pooled honeycombing and interstitial score in the HRCT performed at diagnosis (HRCT1) were similar between the two genotype groups (**Table 3**). In particular, at baseline AS was 22% (0 - 62) in TT/TG and 16% (0 - 44) in GG (p=0.52), HC was 2% (0 - 41) in TT/TG and 3% (0 - 70) in GG (p=0.54), IS was 22% (0 - 52) in TT/TG and 25% (0 - 45) in GG (p = 0.91), HC+IS was 28% (9 - 73) % in TT/TG and 30% (8 - 89) in GG (p = 0.76) (**Figure 1 Panel A-D**). The inter-observer agreement between the two radiologists with regard to change in AS, IS and HC was good (Cohen's kappa = 0.71 for IS, k=0.76 for AS, k=0.80 for HC), as previously described[9].

Table 3. Radiological scores at treatment initiation (HRCT1) of the entire study population, and cathegorized in TT/TG genotype or GG gentotype.

	Entire Population (n =78)	TT/TG genotype (n =54)	GG genotype (n = 24)	p Value
Alveolar score - %	20 (0-62)	22 (0-62)	16 (0-44)	0.53
Honeycombing score - %	2 (0-70)	2 (0-41)	3 (0-70)	0.54
Interstitial score - %	23 (0-52)	22 (0-52)	25 (0-45)	0.91
Pooled interstitial score and honeycombing - %	28 (8-89)	28 (9-73)	30 (8-89)	0.76

Values are expressed as median and ranges. To compare the radiological scores in HRCT1 between TT / GT and GG genotype groups, and Mann-Whitney U test for continuous variables was used.

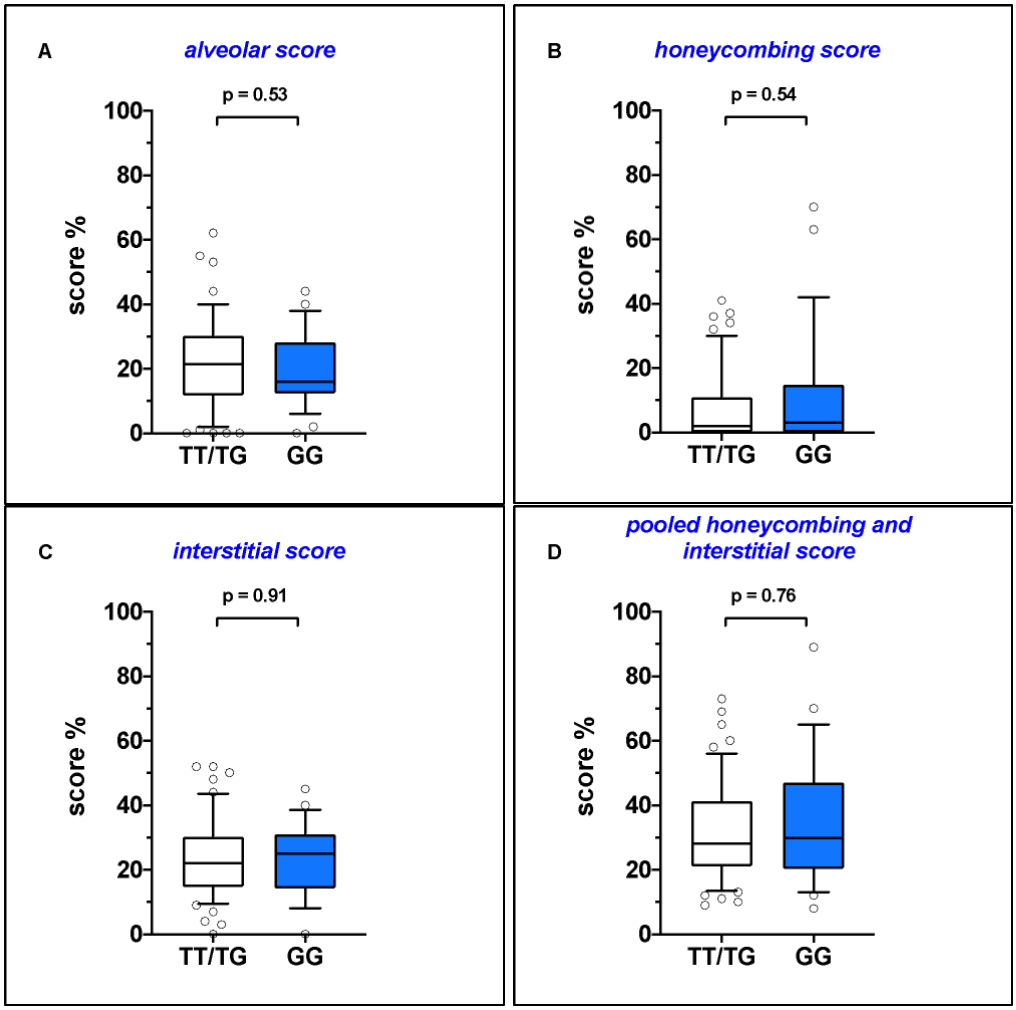

Figure 1. Radiological scores at treatment initiation (HRCT1) of the study population cathegorized in TT/TG genotype or GG gentotype. Values of alveolar score (Panel A), honeycombing score (panel B), interstitial score (panel C) and pooled honeycombing and interstitial score (Panel D) at treatment initiation (HRCT1) in TT/TG genotype patients (TT/TG) and GG genotype patients (GG). Horizontal bars represent median values; bottom and top of each box plot 25th and 75th, brackets 10th and 90th percentiles, while circles represent outliers. White boxes indicate TT/TG genotype patients and blue boxes GG genotype patients.

Radiological scoring during 1-st year follow up

In the entire study population, HC and HC+IS increased significantly between HRCT1 and HRCT2 from 2% (0 - 70) to 6% (0 – 70, $p < 0.0001$) and from 28% (8 - 89) to 33% (8 – 98, $p < 0.0001$), respectively (**Figure 2, Table 4**). AS and IS remain similar between HRCT1 and HRCT2 from 20% (0 - 62) to 20% (0 – 64, $p = 0.16$) and from 22% (0 - 52) to 23% (0 - 59, $p = 0.12$), respectively (**Figure 2, Table 4).**

When the study population was stratified by MUC5B rs35705950 genotype, in TT/TG patients HC increased significantly between HRCT1 and HRCT2 from 2% (0 - 41) to 5% (0 – 63, $p = 0.001$) (**Figure 3, Panel B**), whereas AS and IS did not, from 22% (0 - 62) to 21% (0 – 64, $p = 0.81$) and from 22% (0 - 52) to 23% (0 – 59, $p = 0.47$) respectively (**Figure 3, Panel A, C**). Conversely, among GG patients both AS and HC increase significantly from 16% (0 - 44) to 18% (1 – 86, $p = 0.05$) and from 3% (0 - 70) to 7% (0-83, $p = 0.007$), whereas IS remain similar between HRCT1 and HRCT2: from 26% (0 – 45) to 26% (0 – 53, $p = 0.15$), respectively (**Figure 3, Panel A-C**).

When HC and IS were pooled together, the HC+IN score increased significantly in TT/TG patients (from 28% (9 - 73) to 30% (9 - 93), $p = 0.001$), and in GG patients (from 28% (8 - 89) to 42% (8 – 89, $p = 0.002$), respectively (**Figure 3, Panel D**).

Table 4. Radiological scores at treatment initiation (HRCT1) and after one year of treatment (HRCT2) in the entire study population.

	$HRCT_1$	**$HRCT_2$**	**p value**		**$HRCT_1$**	**$HRCT_2$**	**p value**
AS	20 (0-62)	20 (0-64)	0.16	**IS**	22 (0-52)	23 (0-59)	0.12
HC	2 (0-70)	6 (0-83)	**< 0.0001**	**HC+IS**	28 (8-89)	33 (8-98)	**< 0.0001**

AS = alveolar score; IS = interstitial score; HC = honeycombing; HC+IS = pooled interstitial score and honeycombing. Values are expressed as median and range. P values refer to comparisons between HRCT1 and HRCT2, and Wilcoxon signed rank test for pared non parametric data was used.

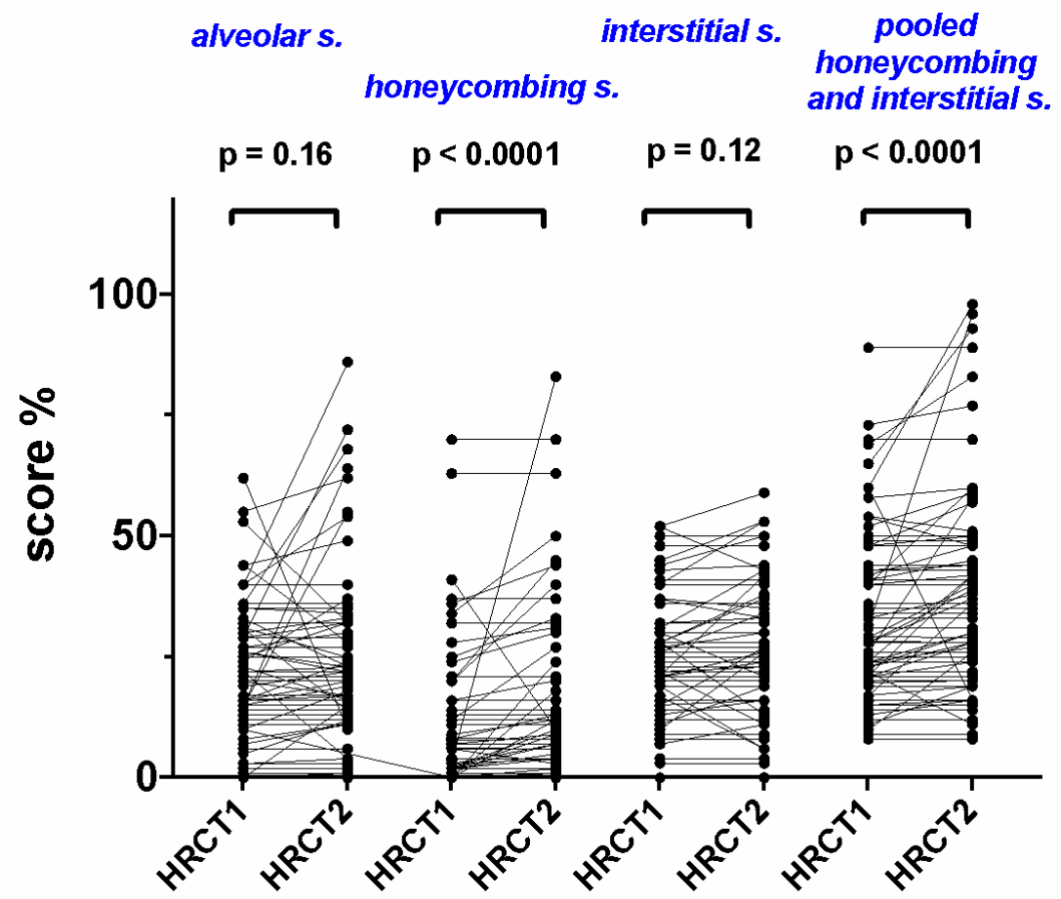

Figure 2. Radiological scores at treatment initiation (HRCT1) and after one year of treatment (HRCT2) in the entire study population. Change in alveolar score, interstitial score, honeycombing and pooled interstitial score and honeycombing at treatment initiation (HRCT1) and after one year of treatment (HRCT2) in the entire study population. P values refer to comparisons between HRCT1 and HRCT2 and Wilcoxon signed rank test for pared non parametric data was used.

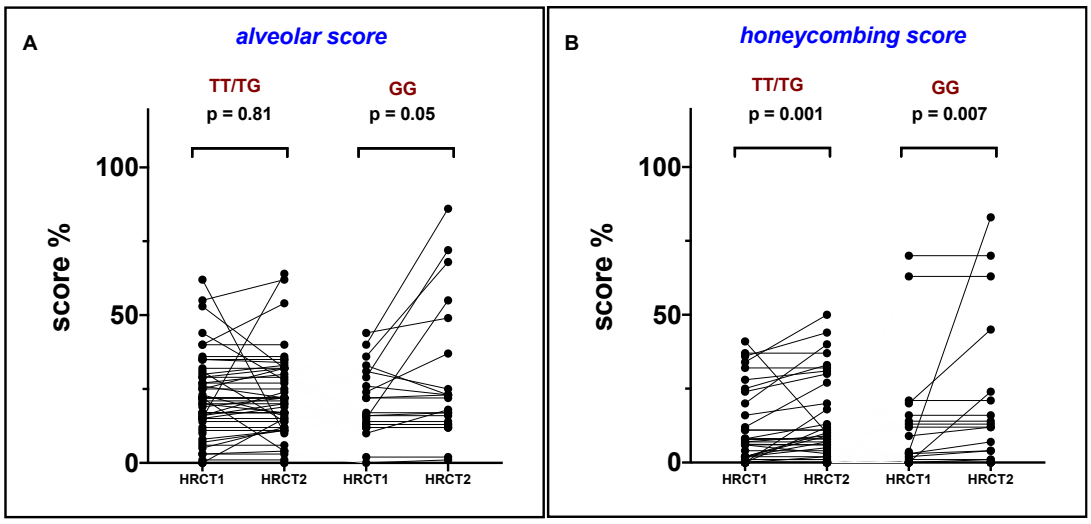

	$HRCT_1$	$HRCT_2$		$HRCT_1$	HRC
TT/TG	22 (0-62)	21 (0-64)	GG	16 (0-44)	18 (1

	$HRCT_1$	$HRCT_2$		$HRCT_1$	$HRCT_2$
TT/TG	2 (0-41)	5 (0-50)*	GG	3 (0-70)	7 (0-83)*

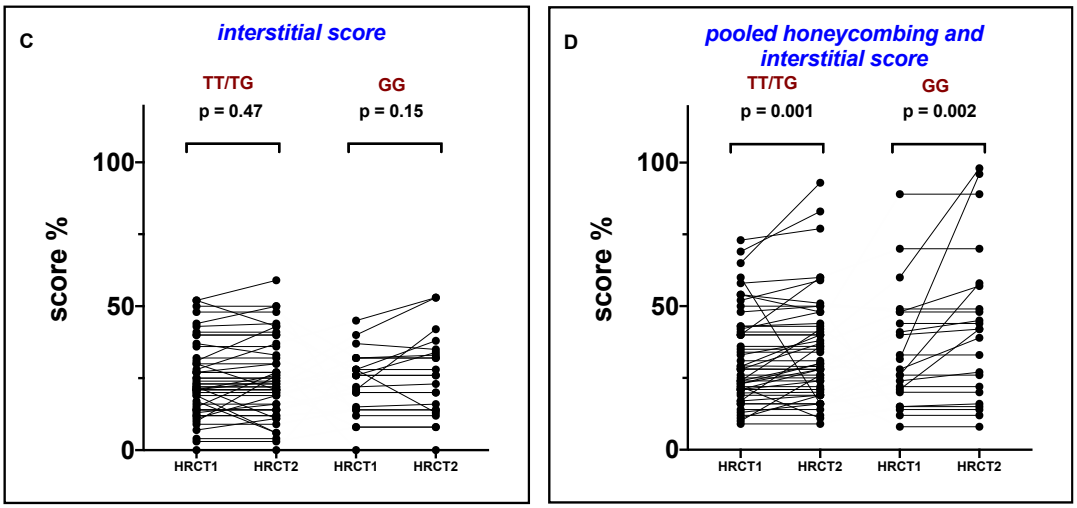

	$HRCT_1$	$HRCT_2$		$HRCT_1$	$HRCT_2$
TT/TG	22 (0-52)	23 (0-59)	**GG**	26 (0-45)	26 (0-53)

	$HRCT_1$	$HRCT_2$		$HRCT_1$	$HRCT_2$
TT/TG	28 (9-73)	30 (9-93)*	**GG**	28 (8-89)	42 (8-98)*

Figure 3. Change in alveolar score (Panel A), honeycombing (Panel B), interstitial score (Panel C) and pooled interstitial score and honeycombing (Panel D) at treatment initiation (HRCT1) and after one year of treatment (HRCT2) in TT/TG and GG genotype patients. P values and * refer to comparisons between HRCT1 and HRCT2 and Wilcoxon signed rank test for pared non parametric data was used.

Survival analysis and multivariate analysis

In the current cohort study we had the chance to analyze a longer observational period as compared with our previous study[6] and we were able to confirm that the overall survival of TT/TG genotype patients was higher than overall survival of GG genotype patients. Indeed, the proper median survival was 69 months for TT/TG genotype patients and 41 months for GG genotype patients (HR 0.52, 95% CI 0.28 – 0.98; p= 0.04) **(Figure 4).**

To detect if radiological scores may be considered factors predictive of survival in the entire IPF population, we used Cox proportional hazards regression analysis. Univariate analysis of radiological factors associated with survival revealed that IS, HC+IS on HRCT1, AS, IS, HC+IS on HRCT2, the absolute increase in honeycombing and in HC had a significant positive association with survival in the entire IPF population (**Table 6**). Multivariate analysis performed including variables having statistical significance in univariate analysis, revealed that only HC+IS on HRCT2 (HR: 1.02; 95%CI: 1.00 – 1.03; p = 0.01) are independent predictors of mortality in IPF patients **(Table 6).**

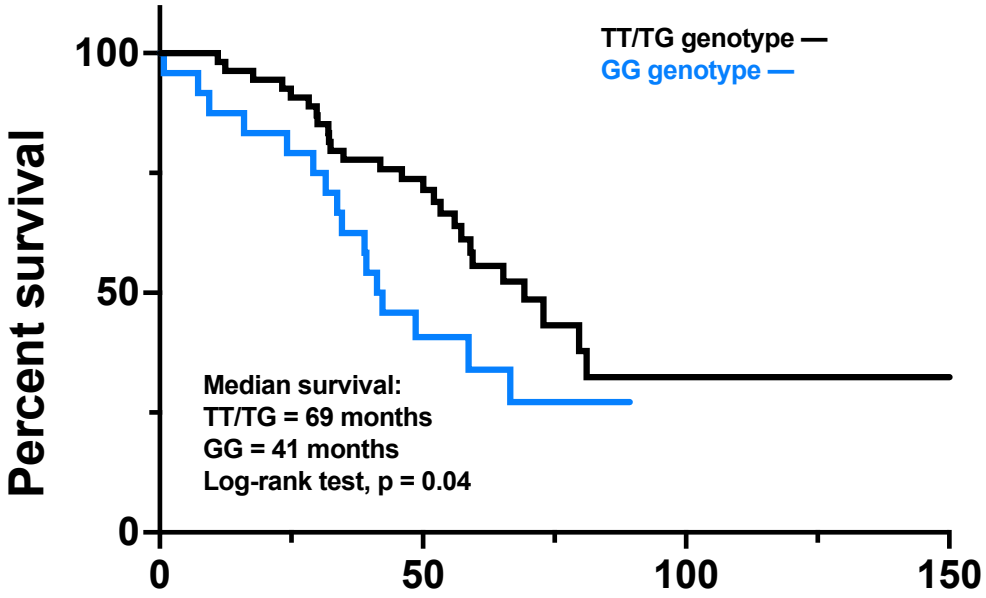

Figure 4. Survival of the study population categorized in TT/TG genotype or GG genotype. Survival analysis of TT/TG and GG genotype patients. The black line represents the survival in the TT/TG group and the blue line represents the survival in the GG group. Kaplan Meier analysis was used with a log-rank test (HR 0.52, 95% CI 0.26 – 0.96; p= 0.04).

Table 6. Predictive factors of overall mortality in the entire population of IPF patients treated with antifibrotics.

	Univariate analysis		**Multivariate analysis**	
	HR (95% IC)	**p**	**HR (95% IC)**	**p**
Alveolar score in HRCT1 (%)	1.01 (0.99 – 1.03)	0.11	-	-
Honeycombing in HRCT1 (%)	1.00 (0.98 – 1.02)	0.52	-	-
Interstitial score in HRCT1 (%)	1.03 (1.00 – 1.05)	**0.01**	1.08 (0.99 – 1.17)	0.07
Interstitial s. and honeycombing in HRCT1 (%)	1.01 (1.00 – 1.03)	**0.02**	0.97 (0.93 – 1.01)	0.15
Alveolar score in HRCT2 (%)	1.02 (1.00 – 1.04)	**0.008**	1.01 (0.99 – 1.04)	0.15
Honeycombing in HRCT2 (%)	1.01 (0.99 – 1.03)	0.16	-	-
Interstitial score in HRCT2 (%)	1.03 (1.00 – 1.05)	**0.009**	0.94 (0.88 – 1.01)	0.14
Interstitial s. and honeycombing in HRCT2 (%)	1.02 (1.00 – 1.03)	**0.003**	1.02 (1.00 – 1.03)	**0.01**
Change in Alveolar score (%)	1.00 (0.99 – 1.05)	0.98	-	-
Change in Interstitial score (%)	1.02 (0.94 – 1.10)	0.44	-	-
Change in Honeycombing (%)	1.03 (1.01 – 1.06)	**0.03**	1.05 (0.97 – 1.13)	0.18

Change in Interstitial s. and honeycombing (%)	1.02 (0.99 – 1.05)	0.058	-	-

Values are expressed as HR (95%CI). Univariate and multivariate Cox proportional hazard regression tests were used to determine the relationship of radiological scores with survival.

CONCLUSIONS

This study investigated for the first time the association between MUC5B rs35705950 polymorphisms and radiological features in the IPF cohort, both at baseline and after treatment. Indeed the current study showed that carriers of the mutant rs35705950 T allele presented a better survival than the wild type group, regardless of the extension of HRCT changes at baseline which was similar in the two groups.

Regarding radiologic features we observed that alveolar score was significantly increased after treatment in the GG genotype patients but not in the TT/TG group.

These evidences confirmed the protective role of MUC5B polymorphism on prognosis of patients with IPF. Moreover, the association of ground opacities on CT scan with the genotype with worse prognosis confirm our previous data[9,11]. Ground glass opacities associated to fibrotic extent on HRCT may help identifying the more aggressive IPF phenotype and genotype.

REFERENCES

1. Seibold MA, Wise AL, Speer MC, et al. A common MUC5B promoter polymorphism and pulmonary fibrosis. N Engl J Med. 2011 Apr 21;364(16):1503-12.
2. Stock CJ, Sato H, Fonseca C, et al. Mucin 5B promoter polymorphism is associated with idiopathic pulmonary fibrosis but not with development of lung fibrosis in systemic sclerosis or sarcoidosis. Thorax. 2013 May;68(5):436-41.
3. Noth I, Zhang Y, Ma SF, et al. Genetic variants associated with idiopathic pulmonary fibrosis susceptibility and mortality: a genome-wide association study. Lancet Respir Med. 2013 Jun;1(4):309-317.
4. Borie R, Crestani B, Dieude P, et al. The MUC5B variant is associated with idiopathic pulmonary fibrosis but not with systemic sclerosis interstitial lung disease in the European Caucasian population. PLoS One. 2013 Aug 5;8(8):e70621.
5. Peljto AL, Zhang Y, Fingerlin TE, Ma SF, et al. Association between the MUC5B promoter polymorphism and survival in patients with idiopathic pulmonary fibrosis. JAMA. 2013 Jun 5;309(21):2232-9. doi: 10.1001/jama.2013.5827. PMID: 23695349; PMCID: PMC4545271.
6. Biondini D, Cocconcelli E, Bernardinello N, et al. Prognostic role of MUC5B rs35705950 genotype in patients with idiopathic pulmonary fibrosis (IPF) on antifibrotic treatment. Respir Res. 2021 Apr 1;22(1):98.
7. Raghu G, Remy-Jardin M, Myers JL, et al; American Thoracic Society, European Respiratory Society, Japanese Respiratory Society, and Latin American Thoracic Society. Diagnosis of Idiopathic Pulmonary Fibrosis. An Official ATS/ERS/JRS/ALAT Clinical Practice Guideline. Am J Respir Crit Care Med. 2018 Sep 1;198(5):e44-e68. doi: 10.1164/rccm.201807-1255ST. PMID: 30168753.
8. Raghu G, Remy-Jardin M, Richeldi L, et al. Idiopathic Pulmonary Fibrosis (an Update) and Progressive Pulmonary Fibrosis in Adults: An Official ATS/ERS/JRS/ALAT Clinical Practice Guideline. Am J Respir Crit Care Med. 2022 May 1;205(9):e18-e47.
9. Balestro E, Cocconcelli E, Giraudo C, et al. High-Resolution CT Change over Time in Patients with Idiopathic Pulmonary Fibrosis on Antifibrotic Treatment. J Clin Med. 2019 Sep 15;8(9):1469. doi: 10.3390/jcm8091469. PMID: 31540181; PMCID: PMC6780456.
10. Fell CD, Martinez FJ, Liu LX, et al. Clinical predictors of a diagnosis of idiopathic pulmonary fibrosis. Am J Respir Crit Care Med. 2010 Apr 15;181(8):832-7.
11. Cocconcelli E, Balestro E, Biondini D, et al. High-Resolution Computed Tomography (HRCT) Reflects Disease Progression in Patients with Idiopathic Pulmonary Fibrosis (IPF): Relationship with Lung Pathology. J Clin Med. 2019 Mar 22;8(3):399.
12. Altman, D.G. Practical Statistics for Medical Research; Chapman and Hall: London, UK, 1991; Volume 10, pp. 1635–1636.].

Chapter 9

Role of activated lymphoid follicles in disease progression of patients with idiopathic pulmonary fibrosis

Original data not yet published

ABSTRACT

Background. Increasing evidence suggests that an immune dysregulation may be involved in the progression of IPF. The presence of lymphoid follicles (LF) (sites where the immune response is triggered) in earlyIPF and their evolution with the progression of the disease, have never been caracterized as part of the natural history of IPF.

Aim. 1) To investigate the presence of LF in earlyIPF and end-stage late IPF 2) To quantify LF numbers, dimensions and state of activation and their evolution from EIPF to LIPF.

Methods. LF immunostained for B-lymphocytes were counted and measured in 18 early IPF (surgical biopsies), 42 end stage IPG (explanted lungs) and 12 smoking controls (SC) (surgical resection). Immunostaining for CD40, a costimulatory molecule expressed by B lymphocytes, was used to study the degree of LF activation in early IPF and end stage IPF.

Results. LF were present in 100% of EIPF and LIPF and in 7/12 of SC. LF number was higher in early IPF than in end stage IPF [9 (3-36) vs 6 (1–16)/cm^2; p=0.01] and SC [0.7 (0-9) cm^2; p < 0.0001], while LF area was increased in end stage IPF compared to early IPF [27,97 (12,59-58,09) vs 13,32 (4,72-48,41) μm2; p<0.0001) and similar to SC [21,18(6,01 - 37,32) μm^2; p = 0.58]. LF in end stage IPF are more activate than LF in early IPF (CD40+) (73%vs33%;p=0.005) and compared to smoking controls (25%, 0 = 0.002).

Conclusions. The large number of Lymphoid Follicles found in EIPF and the increase in LF volume and degree of immune activation as the disease progresses, suggest that an immune response has an important role in driving the progressive damage characteristic of the IPF course.

INTRODUCTION

Idiopathic pulmonary fibrosis (IPF) is the most common form of idiopathic interstitial pneumonia (IIP), a chronic, progressive and fibrotic interstitial lung disease of unknown cause, with radiological and histological aspects identified by the presence of the *usual interstitial pneumonia* (UIP) pattern and leading the

patients to respiratory failure and death within tree or five years from diagnosis[1]. As the other forms of interstitial lung diseases, IPF is characterized by cell proliferation, interstitial inflammation, fibrosis deposition and an irreversible scarring of the lung[2].

In the last decades, the ineffectiveness of traditional anti-inflammatory therapies in the treatment of IPF has caused the shift of researcher attention away from inflammation[3]. A part from the accredited hypothesis of excessive scar response to alveolar damage, the role of the immune system in promoting and maintaining the pro-fibrotic process remains controversial. Subclinical and continuous alveolar epithelium lesions induced by oxidative stress, mitochondrial dysfunction, environmental exposures and an accelerated cellular aging lead to an aberrant repair of the alveolus with excessive cicatricial response promoted by stromal cells such as activated fibroblasts and myofibroblasts[4]. In this context, the adaptive immune response seems to play a crucial role in maintaining and progressing the damage after initiation[5]. In 2006, new types of lymphocyte aggregates have been identified for the first time in the parenchyma of patients with IPF[6]. These types of structures named lymphoid follicles (LF) show organization of T and B lymphocytes in aggregates, with the presence of reticular fibroblasts and dendritic cells, immunohistochemical positivity for CD40, CD40L and other markers expressed by the lymphoid organizing tissue. To date, the main role of LF in IPF diseases progression has never been elucidated. CD40 and CD40L are important markers, expressed respectively by B and T lymphocytes. Their presence is relevant because their interaction is considered one of the first reactions which then lead to the formation of germinal centers. LF follicles were found to be present in greater numbers in advanced disease (explanted tissue) than in early disease, supporting the concept that active cellular inflammation continues in IPF even in severe end-stage disease[7,8].

Some evidences suggest that lymphoid follicles may be present in IPF patients, even though their role across the disease course from early onset up to organ failure remains to be established. For this reason, the rationale of the present study focused on quantifying and characterize the lymphoid follicle structure across the disease course of IPF (early and end stage phase), to quantify their degree of activation and to compare them with smoking controls.

METHODS

Study population

In this retrospective study, we consecutively enrolled one cohort of patients undergoing a video-assisted thoracic surgery (VATS) biopsy to achieve a definite diagnosis of IPF (*early IPF*) and one cohort of IPF patients in the terminal phase of the natural history of their disease undergoing lung transplant (*end stage IPF*).

Eighteen patients from two Interstitial Lung Disease Centers in Italy (University of Padova, Italy, n = 7 and University of Naples, Italy n = 11) referred between 2014 and 2018, and with a definite diagnosis of IPF according with the current ATS/ERS/JRS/ALAT guidelines[1], were included in the *early IPF* cohort of patients. Forty-two IPF patients referred to our center for transplantation between 2011 and 2014 were included in the *end stage IPF* cohort of patients. *End stage IPF* patients belonged to an historical group of individuals referring to our center of Padova in the pre-antifibrotic therapy era (before 2014), having therefore no access to antifibrotic therapy. Patients with a clear history of environmental or occupational exposure, and with clinical or serological data suggestive for a connective tissue disease were excluded.

Twelve smokers with normal lung function, undergoing lung resection for nodules, were included as control group (*smoking controls*, SC).

Clinical and functional data for the three study population were retrospectively collected and reviewed.

The study was performed in accordance with the Declaration of Helsinki and approved by the Ethics Committee of the University Hospital of Padova (4280/AO/17). Informed consent was obtained for all study participants before surgery.

Pathological Analysis

Formalin fixed and paraffin embedded lung tissue blocks were obtained from early IPF, end stage IPF and smoking controls (avoiding areas affected by tumor in patients who underwent lung resection for nodules). Five-μm thickened sections were cut and stained for immunohistochemical identification and

characterization of lymphoid follicles (LFs). B lymphocytes (CD20+), T lymphocytes (CD4+ and CD8+), activated B-lymphocytes (CD40+), as well as total leukocytes (CD45+), were identified by immunohistochemistry as previously described[5]. For each biopsied and transplanted patient the presence of UIP pattern was histologically confirmed by our expert pathologist (F.C.) by the presence of a usual interstitial pneumonia (UIP) pattern on lung specimens.

LFs were defined as aggregates containing more than 40 mononuclear cells that exhibit the typical topographical arrangement with a germinal center of CD20+ B cells surrounded by CD4+ and CD8+ T cells[9]. (**Figure 1**).

LFs were identified on sections stained for B lymphocytes, and expressed as number per square cm of lung tissue examined. LFs area was also measured and expressed in square micrometer (um^2).

To investigate the activation state of LFs, the expression of the co-stimulatory and activation marker CD40 was analyzed inside the LF using a semiquantitative score ranging from 0 to 4 as follows: 0 = absence of CD40 expression; 1 = CD40 expression involving <= 25% of the LF area; 2 = CD40 expression between 26 and 50% of LF area; 3 = CD40 expression between 51 and 75% of LF area; 4 = CD40 expression up to the 100% of LF area (**Figure 2**). The CD40 expression/activation scores of all LFs of each patient were summed and expressed as percentage of the maximum computable score for that patient[10].

To better characterize LFs, CD4+ and CD8+ T Lymphocytes were quantified inside the LFs and expressed as number per mm^2 of LF area and as ratio CD4/CD8. CD4+ and CD8+ T Lymphocytes as well as CD45+ cell were quantified also in the lung tissue as previously described[5], and results were expressed as number per mm^2 of tissue area.

Point counting was used to estimate the fraction of total lung volume occupied by parenchyma excluding non-parenchyma zones, according with the ATS/ERS guidelines[11]. Briefly, 15 non-overlapping microscopic fields for each lung specimens at magnification 20x were overlaid by a grid of 10 x 10 rows and the mean number of points falling on lung tissue with respect to the total 100 points corresponded to the percentage (%) of tissue per lung section. The % of tissue per lung section was finally multiplied by the total area of the section, obtaining therefore the exact area occupied by lung tissue (in mm^2).

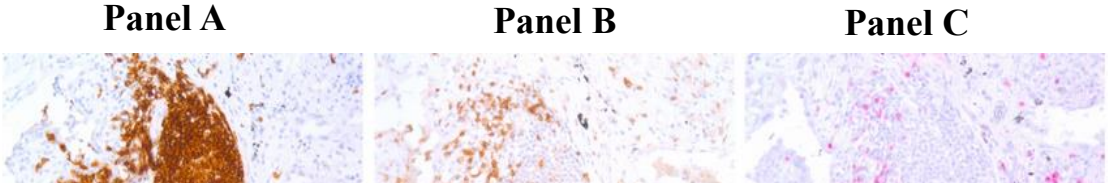

Figure 1. Lymphoid follicles in one patient with *end stage IPF* immunostained for CD20 (panel A), CD4 (panel B) and CD8 (panel C).

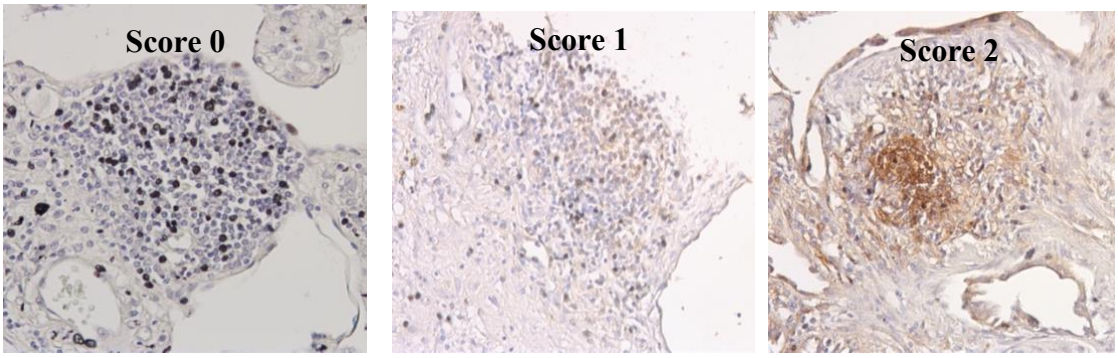

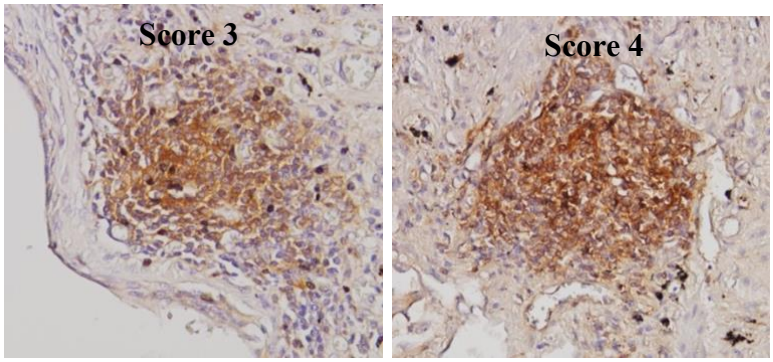

Figure 2. Lymphoid follicles immunostained for CD40 with increasing activation scores.

Statistical analysis

Categorical variables are expressed as absolute (n) and relative values (%) whereas continuous variables as median and 5th and 95th percentiles. To compare demographic, functional and morphometric data between *early*, *end stage IPF* patients and SC Chi square test and Fisher's exact test for categorical variables and one-way ANOVA non-parametric test (Kruskal-Wallis test) for continuous variables was used. To compare two groups, Mann-Whitney U test for continuous variables and Chi square test and Fisher's exact test for categorical variables were used, as appropriate.

To compare the number of CD4 + cells in lung tissue with the number of CD4+ cells in LF Wilcoxon signed rank test was performed. To compare the number of CD8 + cells in lung tissue with the number of CD8+ cells in LF Wilcoxon signed rank test was performed.

All data were analyzed using SPSS Software version 25.0 (New York, NY, US: IBM Corp. USA). P-values < 0.05 were considered statistically significant. The statistical package GraphPad Prism 7.0 (GraphPad Software, Inc. La Jolla, CA, USA) was used for graphs.

RESULTS

Clinical and functional evaluation at baseline.

Eighteen patients were included in the *early IPF* cohort, forty-two patients in the *end stage IPF* cohort and twelve smoking patients were enrolled as smoking controls (SC). The clinical and functional data at baseline of the three cohorts of patients are shown in **Table 1**. Most subjects were males (78%, 76% and 92%, respectively). Compared to SC, both *early IPF* and *end stage IPF* are younger at diagnosis [median 66 years (range 56 - 82) vs. 58 years (54 - 61), p = 0.005 and vs. 53 (33 - 64), p < 0.0001; respectively]. 61%, 69% and 100% of patients have a current or former history of smoking in the three groups respectively, with SC having a heavier smoking history compared to *early* [49 pack/years (15 - 102) vs. 4 (0 – 30; p = 0.002)] and end *stage IPF* [15 (0 - 90); p = 0.003].

SC have a more preserved baseline functional data than *early* and *end stage IPF* in terms of FVC % pred. [123% (90 - 142) vs. 75% (40 - 109), p < 0.0001, and vs. 61% (23 - 86), p <0.0001, respectively] flow expiratory volume in one second (FEV_1) % pred. [98% (74 - 116) vs. 81% (51 - 118), p = 0.03 and vs. 62% (26 - 86), p <0.0001, respectively] and DLCO % pred. [81% pred. (75 - 91) vs. 39% (16 - 74), p = 0.001 and vs. 36% (10 - 81), p = 0.0007].

None of the patients was treated with antifibrotics and 70% (equally distributed between the two groups) were treated with low dose prednisone with or without azathioprine according to previous guidelines[12].

Table 1. Clinical and functional data at baseline of smoking controls, the *early IPF* and *end stage IPF*.

	Early IPF **(n=18)**	***End stage IPF*** **(n=42)**	**Smoking controls (n=12)**	***P*** **early vs. end**	***P*** **early vs. SC**	***P*** **end vs. SC**
Male – *n (%)*	14 (78)	32 (76)	11 (92)	n.s.	n.s.	n.s.
Age at diagnois - *yr*	58 (54 - 61)	53 (33 - 64)	66 (56 - 82)	n.s.	**0.005**	**<0.0001**
Smoking history - ***n (%)*** - ***p/y***	11 (61) 4 (0 - 30)	29 (69) 15 (0 - 90)	12 (100) 49 (15 - 102)	n.s. n.s.	n.s. **0.002**	n.s. **0.003**
FEV_1 at diagnosis - *L*	3.06 (1.87 – 3.58)	2.46 (1.09 – 3.68)	2.39 (1.54 – 3.54)	n.s.	n.s.	n.s.
FEV_1 at diagnosis - % pred.	81 (51 - 118)	62 (26 - 85)	98 (74 - 116)	**0.0006**	**0.03**	**<0.0001**
FVC at diagnosis - *L*	2.96 (1.45 - 4.06)	2.47 (0.7 – 3.75)	3.02 (1.75 – 4.60)	n.s.	n.s.	**0.01**
FVC at diagnosis - *% pred.*	75 (40-109)	61 (23 - 86)	123 (90 - 142)	**0.009**	**<0.0001**	**<0.0001**

FEV_1/FVC at diagnosis	98 (75 - 131)	102 (80 - 125)	80 (74 - 91)	n.s.	**0.0004**	**<0.0001**
DLCO at diagnosis – *%pred.*	39 (16 - 74)	36 (10 - 81)	81 (75 - 91)	n.s.	**0.001**	**0.0007**

Values are expressed as numbers and (%) or median and 5th and 95th percentiles, as appropriate. To compare demographic data and baseline clinical characteristics, Mann-Whitney U test for continuous variables was used and Chi square, Fisher t test for categorial variables were used as appropriate.

Pathological analysis

Morphometric analysis of the lung biopsies and of the explanted lungs showed a relevant cellular inflammatory infiltrate in IPF populations. In particular, the number of total leukocytes (CD45+) cells in lung tissue was similarly high between *early* and *end stage* IPF patients [633 cells (277 – 1,290) / mm^2 vs. 536 (277 – 1,201) / mm^2; p = 0.18], but both higher compared to SC [243 cells (116 - 503) / mm^2; p <0.0001 in both cases] (**Figure 3**).

LF were present in all IPF patients, at both diagnosis and transplantation, but only in 7/12 SC.

The number of LF was increased in *early* IPF compared both to *end stage* IPFs [9 (3-36) LF / cm^2 in *early* IPF compared to 6 LF (0.5-16) / cm^2 in *end stage* IPF; p = 0.01] and SC [0.7 LF (0 - 9) / cm^2 (p < 0.0001) (**Figure 4**).

When the LF dimension was analyzed, we observed that the LF size was higher in *end stage* IPFs compared to *early* IPF [27,974 um^2 (12,595 – 58,098) vs. 13,329 um^2 (4,724 - 48,418), p<0.0001)] and SC [21,184 um^2 (6,012 – 37,323), p = 0.04] (**Figure 5**). The analysis of the activation score for LF revealed that *end stage IPF* patients presented a higher level of CD40 positive activity compared to both *early IPF* [73% (9 - 92) vs 33 % (0 - 90); p = 0.005] and smoking controls [23% (0 - 75); p = 0.002] (**Figure 6**).

Immunochemistry was used to further characterize the composition of LF, as shown in figure 1 from an explanted lung. The number of CD4+ T cells in lymphoid follicle area was higher than the number of CD8+ T cells both in *early IPF* [4,736 / mm^2 (815 – 12,784) vs. 739 / mm^2 (182 – 2,137), p < 0.0001], in *end stage IPF* [5,539 / mm^2 (2,061 – 11,098) vs. 1,009 / mm^2 (387 – 4,541), p < 0.0001], and in smoking controls [5,159 / mm^2 (2,738 – 27,023) vs. 753 / mm^2 (595 – 10,525), p = 0.07] (**Figure 7**). When then number of CD4+ T and CD8+ T cells inside lymphoid follicles is compared between the three groups, no difference can be detected between early, end stage and smoking controls (**Figure 8**).

The number of CD4+ T cells in lung tissue was higher than the number of CD8+ T cells both in *early IPF* [310 / mm^2 (84 – 839) vs. 117 / mm^2 (18 – 248), $p < 0.0001$], in *end stage IPF* [214 / mm^2 (47 – 729) vs. 59 / mm^2 (17 – 248), $p < 0.0001$], and in smoking controls [261 / mm^2 (131 – 531) vs. 108 / mm^2 (14 – 238), $p = 0.0001$] (**Figure 9**). When then number of CD4+ T inside lung tissue is compared between the three groups, end stage IPF presented the lower number compared to *early IPF* ($p = 0.02$) and smoking controls (**Figure 10**). No differences between groups is observed when the number of CD8+ in lung tissue is considered.

The CD4/CD8 ratio both in lymphoid follicles and in lung tissue is similar among *early IPF*, *end stage IPF* and smoking controls (**Figure 11**).

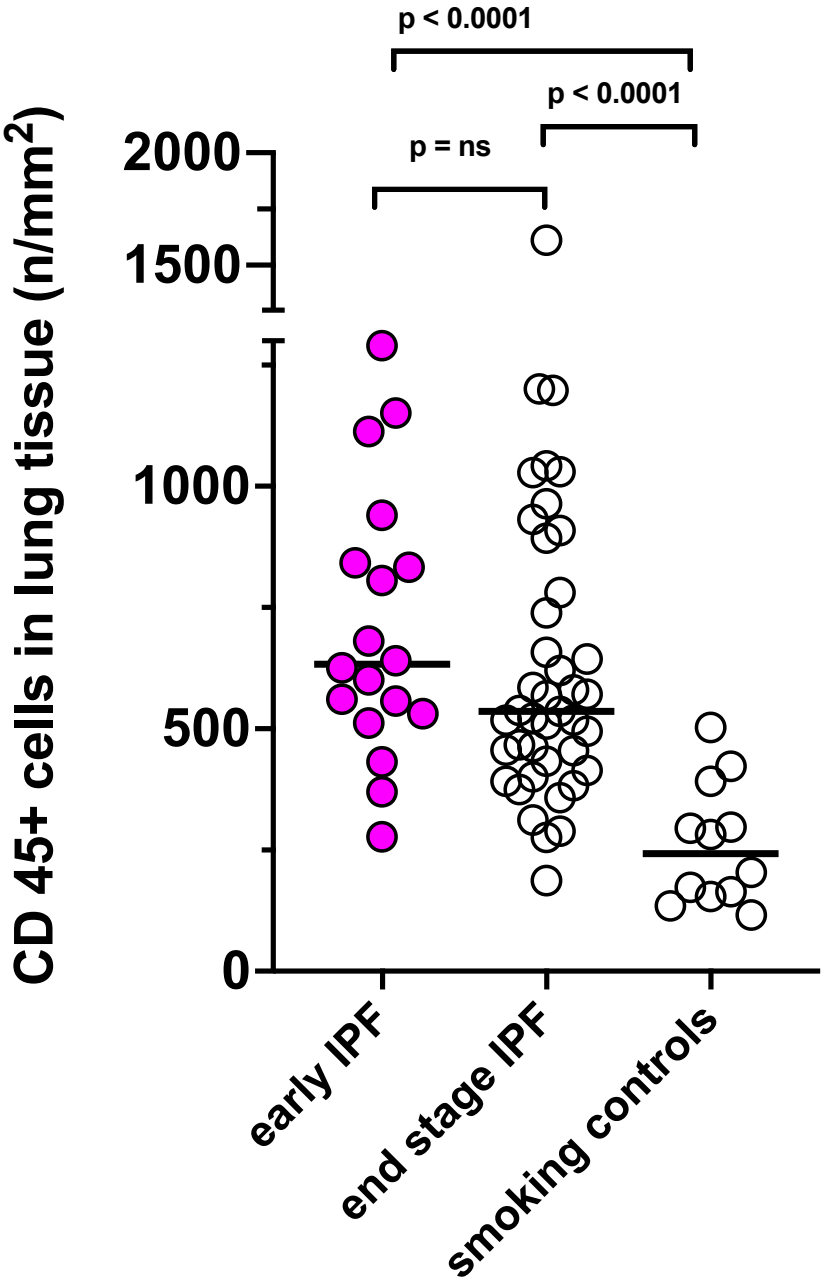

Figure 3. Number of total leukocytes (CD45+ cells) per mm^2 of lung tissue in *earlyIPF*, *end stage* IPF and smoking controls.
P values refer to comparisons with Mann-Whitney U test (Kruskal-Wallis test p value < 0.0001)

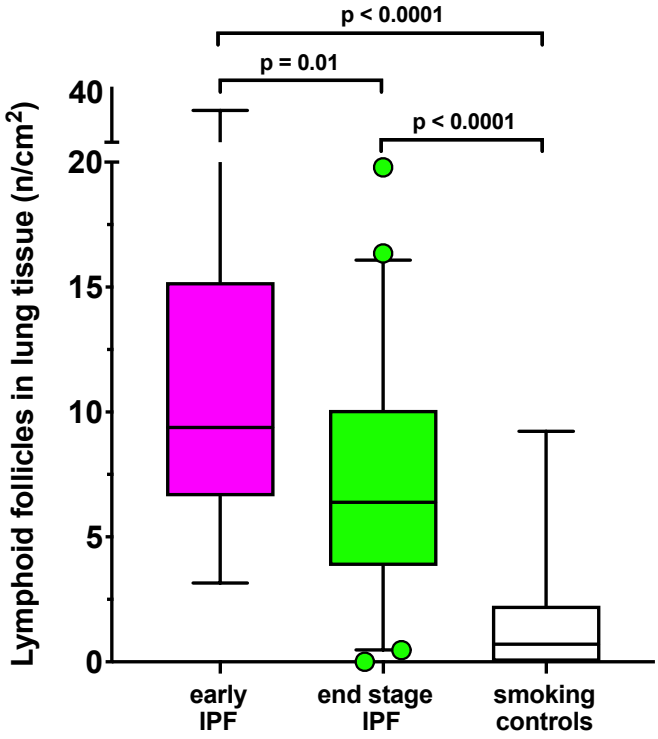

Figure 4. Number of LF per cm^2 of lung tissue in *early* IPF, *end stage* IPF and smoking controls. Horizontal bars represent median values; bottom and top of each box plot 25th and 75th; brackets show 5^{th} and 95^{th} percentiles; and circles represent outliers. P values refer to comparisons with Mann-Whitney U test (Kruskal-Wallis test p value = 0.0001)

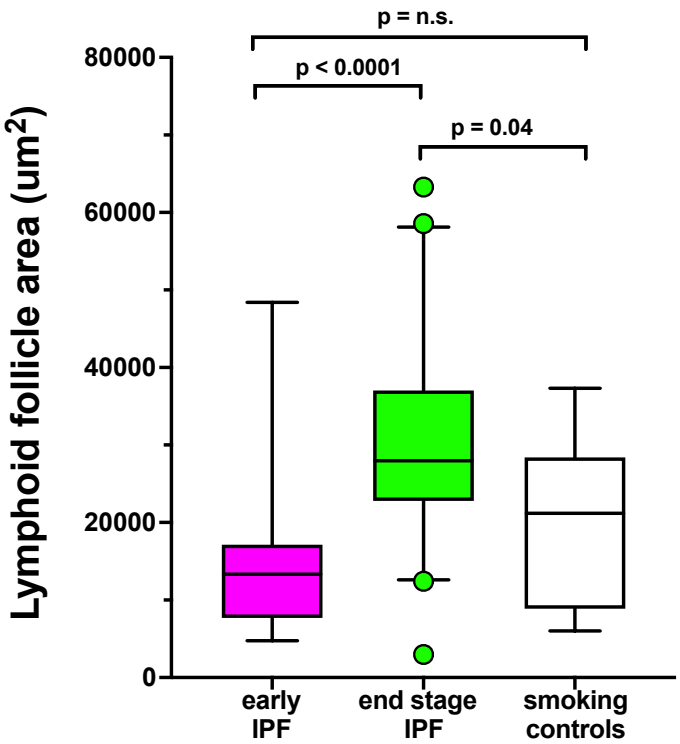

Figure 5. LF area (um^2) in *early* IPF, *end stage* IPF and smoking controls . Horizontal bars represent median values; bottom and top of each box plot 25th and 75th; brackets show 5^{th} and 95^{th} percentiles; and circles represent outliers. P values refer to comparisons with Mann-Whitney U test; Kruskal-Wallis p value: $p<0.0001$

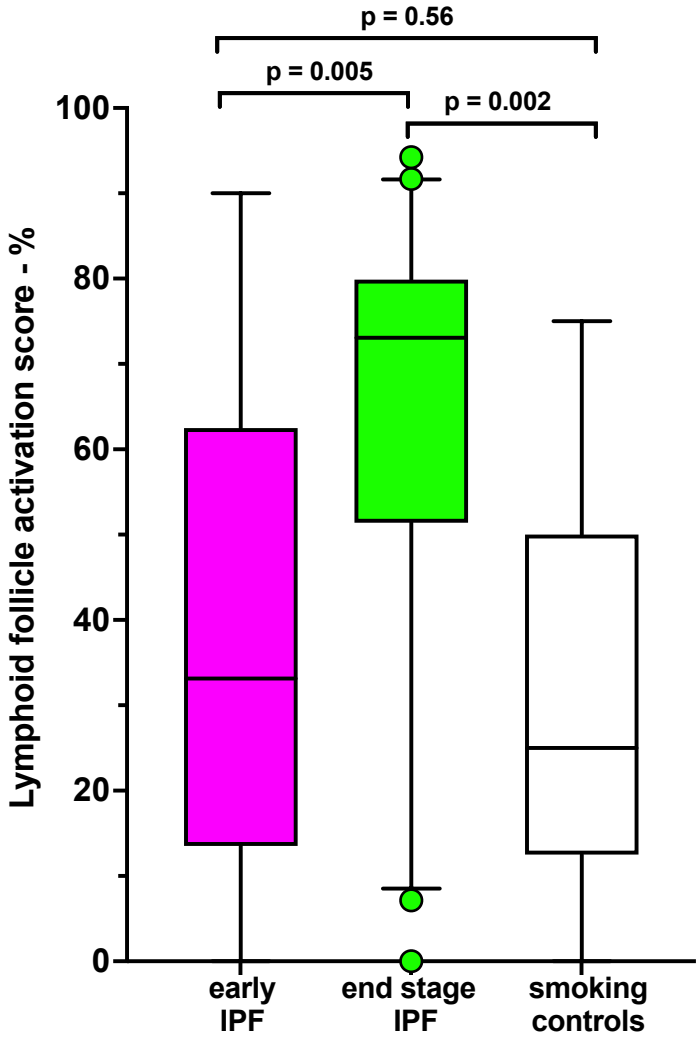

Figure 6. Lymphoid follicles activation score (%) based on the degree of CD40 expression in *early* IPF, *end stage* IPF and smoking controls. Horizontal bars represent median values; bottom and top of each box plot 25th and 75th; brackets show 5th and 95th percentiles; and circles represent outliers. P values refer to Mann-Whitney U test; Kruskal-Wallis p value: $p<0.001$

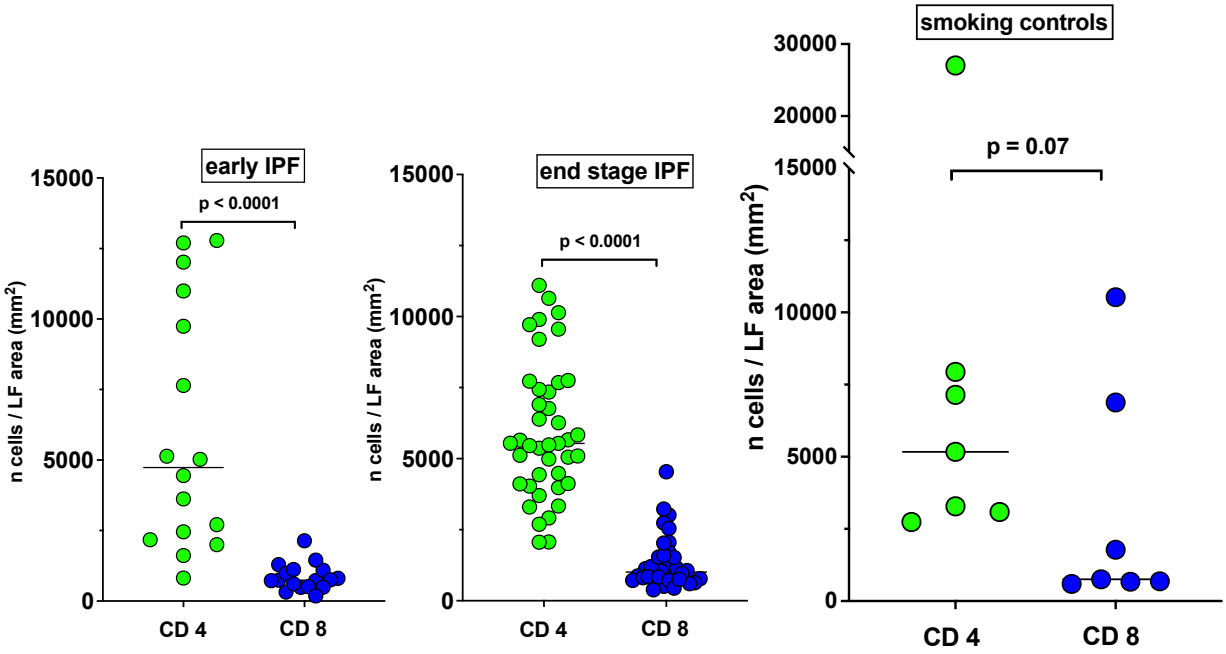

Figure 7. Number of CD4+ and CD8+ T lymphocytes in lymphoid follicles in *early* IPF, *end stage* IPF and smoking controls patients, respectively. Bars indicate the median values.

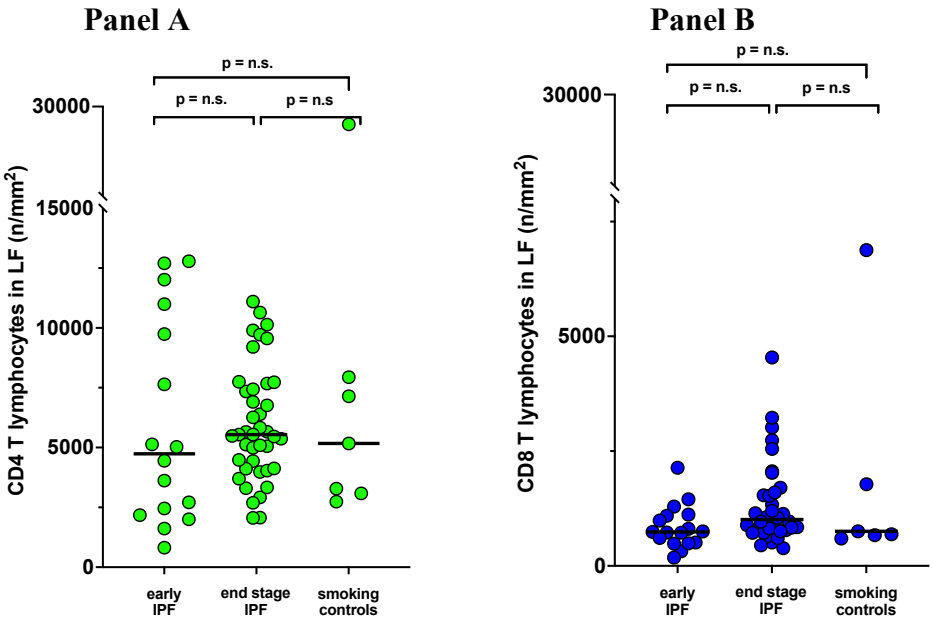

Figure 8. CD4+ T lymphocytes (**Panel A**) and CD8+ T lymphocytes (**panel B**) in lymphoid follicles in *early* IPF, *end stage* IPF and smoking controls . Bar indicates the median value.

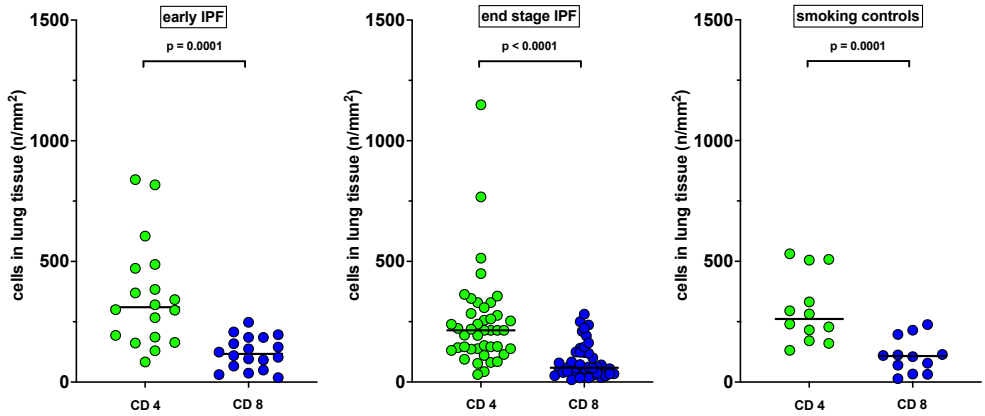

Figure 9. Number of CD4+ and CD8+ T lymphocytes in lung tissue in *early* IPF, *end stage* IPF and smoking controls patients, respectively. Bar indicates the median value.

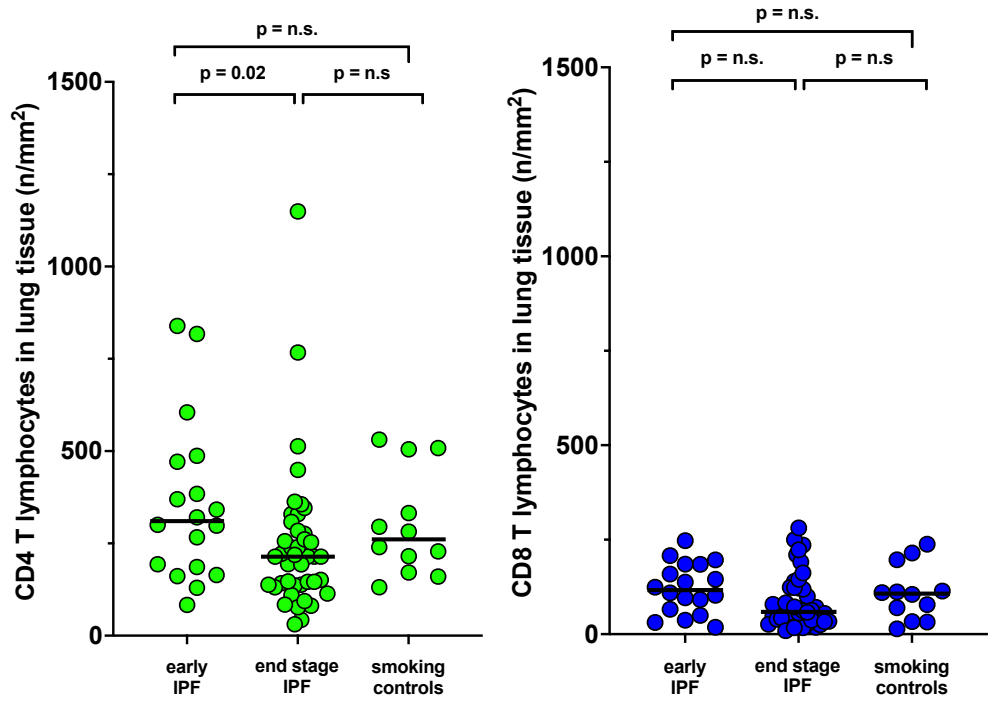

Figure 10. CD4+ T lymphocytes (**Panel A**) and CD8+ T lymphocytes (**panel B**) in lung tissue in *early* IPF, *end stage* IPF and smoking controls . Bar indicates the median value.

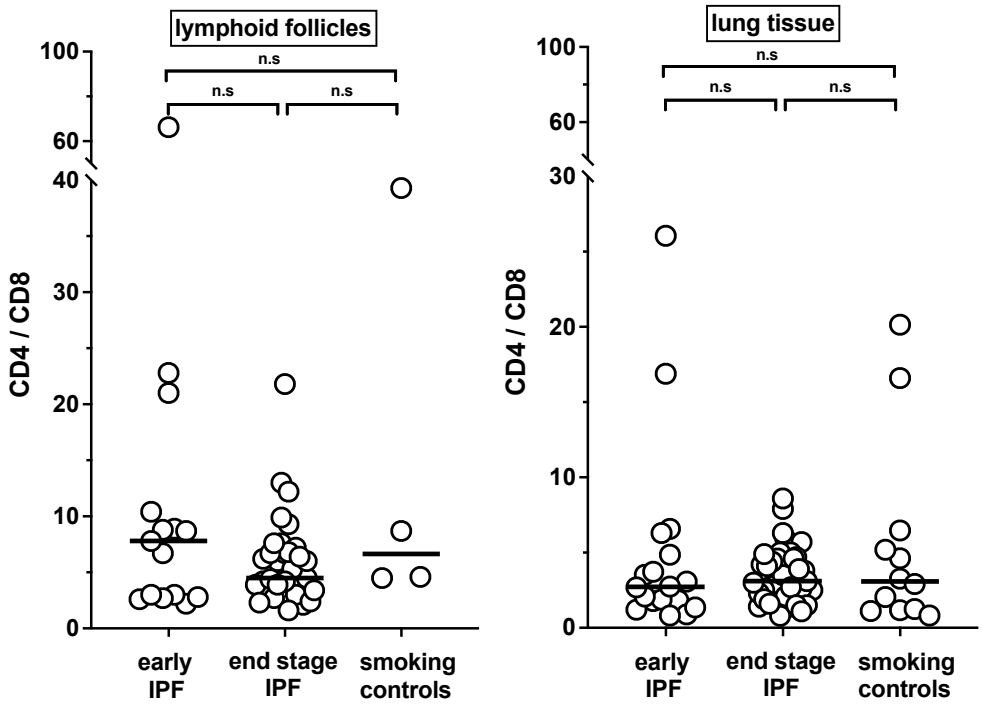

Figure 11. CD4+/CD8+ T lymphocytes ratio in lymphoid follicles and in lung tissue in *early* IPF, *end stage* IPF and smoking controls. Bars indicates the median value.

DISCUSSION

In the present study, we demonstrate the presence of lymphoid aggregates in the lungs of subjects with idiopathic pulmonary fibrosis both at diagnosis and to the terminal phase of the lung disease. We found that, despite to smoking history, lymphoid follicles are present in each patient with IPF and specifically are more numerous at the beginning of the disease history but become wider and more activated in the end phase of the disease. These results are not confirmed in subjects with heavier smoking history without pulmonary fibrosis and enrolled as controls.

To date, the main challenge for pulmonary researcher remains to better understand the pathogenesis of IPF, in order to detect more useful target point for new potential drugs blocking the irreversible course of this fatal disease. Mortality rate for IPF is not significantly changed after the recent worldwide diffusion of the two antifibrotic drugs *nintedanib* and *pirfenidone*, emphasizing the need for a more complete understanding in the mechanisms of disease pathogenesis and in predicting IPF clinical behavior.

IPF was originally thought to be a process of chronic repair resulting from persistent inflammation, but in the last decade, the relative role of inflammation in the fibrotic process has been overshadowed in favor of alveolar damage that directly

induces activation of fibroblasts and myofibroblast[2]. This change of perspective was leaded also by the fact that the traditional anti-inflammatory therapies resulted ineffective or even harmful in IPF patients[3]. This finding was even stronger in patients with short telomere, a marker of lymphocyte senescence[13]. Nonetheless, some interesting studies observed and pointed out the presence of innate and adaptive immune cells in the lungs of patients with IPF[5,6].

For the first time we enrolled a multicentric cohort of patients undergoing surgical lung biopsy confirming the presence of a histological pattern of UIP in an IPF context, a wide cohort of patients undergoing lung transplant and compared to patients undergoing single nodule resection, with positive smoking history and without pulmonary fibrosis. In our study population, we confirmed our previous evidence that a huge amount of inflammation (total CD45+ leukocytes) is present in IPF populations and that overcomes the inflammation detectable in smoking controls.

Lymphoid follicles are aggregates of lymphocytes B organized in germinal centers and surrounded by CD4+ and CD8+ T lymphocytes and are typically described in chronic diseases like chronic obstructive pulmonary disease (COPD)[14] or connective pulmonary fibrosis[15].

More specifically, in 2006 Marchal-Sommé J and colleagues described for the first-time new types of lymphocyte aggregates in the parenchyma of some patients diagnosed and transplanted for IPF[6]. Lymphoid follicles were detected and cytokine expression analyzed. Their data suggested that lymphoid neogenesis could occur in IPF lung, but lymphoid follicles observed in IPF have never been characterized.

IPF patients at the early phase of disease present a higher number of lymphoid follicles per square centimeter of lung tissue, compared to IPF patients in the end stage of the disease and compared to controls. Our data confirmed the analysis of Todd NW and colleagues, who counted the number of lymphoid follicles in two time-point of some IPF patients[7]. The added value of our study is the precious availability of lung biopsies for IPF diagnosis. Last guidelines suggest not performing histological samples when a radiological UIP definite or UIP probable on high resolution CT scan and in the clinical context of a IPF is present. Moreover, for the first time we compare our data with controls with a heavy smoking history. Of interest, not all smoking controls present lymphoid follicles.

Moreover, for the first time we measured the dimension of lymphoid follicles and we found that in the end phase of disease these aggregates become larger and express a higher positivity for CD40, a B-cell costimulatory molecule. Interaction between CD40 and CD40 ligand on T lymphocytes is considered one of the first reactions which then lead to the formation of germinal centers. First evidence on the expression of CD40 in IPF was always suggested by Marchal-Sommé J and colleagues[6].

Of interest, we further characterize lymphoid follicles and observed a huge amount of CD4+ T cells inside the germinal center compared to CD8+ T cells both in early IPF, in end stage IPF and in smoking controls. These numbers are also higher when the number of CD4+ and CD8+ T cells in lymphoid follicles are compare to the same type cells in the lung parenchyma. We can speculate that adaptive immune cells may migrate and concentrate inside lymphoid aggregates and drive the pathogenesis of the disease.

We are aware of some limitations for our study. It could be interesting to compare the same patient at the beginning of the disease with his last phase of fibrosis. This is a retrospective study, and there may be some selection bias.

In conclusion, in our study, for the first time we confirmed that the adaptive immune response plays a crucial role in maintaining and progressing the damage after initiation. Lymphoid follicles are constantly present in IPF patients, are more numerous at the early phase of the disease, become larger at the end and are more activated. These findings may provide a basis for future investigation on personalized treatment in this lethal and unpredictable diseases.

REFERENCES

1. Raghu G, Remy-Jardin M, Myers JL, et al. Diagnosis of idiopathic pulmonary fibrosis An Official ATS/ERS/JRS/ALAT Clinical practice guideline. *Am J Respir Crit Care Med*. 2018;198(5):e44-e68. doi:10.1164/rccm.201807-1255ST
2. Lederer DJ, Martinez FJ. Idiopathic pulmonary fibrosis. *N Engl J Med*. 2018;379(19):1811-1823. doi:10.6314/JIMT.201810-29(5).02
3. Network IPFCR. Prednisone, Azathioprine, and N -Acetylcysteine for Pulmonary Fibrosis. *N Engl J Med*. 2012;366(21):1968-1977. doi:10.1056/NEJMoa1113354
4. Selman M, Pardo A. Revealing the pathogenic and aging-related mechanisms of the enigmatic idiopathic pulmonary fibrosis: An integral model. *Am J Respir Crit Care Med*. 2014;189(10):1161-1172. doi:10.1164/rccm.201312-2221PP
5. Balestro E, Calabrese F, Turato G, et al. Immune Inflammation and Disease Progression in Idiopathic Pulmonary Fibrosis. Eickelberg O, ed. *PLoS One*. 2016;11(5):e0154516. doi:10.1371/journal.pone.0154516
6. Marchal-Sommé J, Uzunhan Y, Marchand-Adam S, et al. Cutting Edge: Nonproliferating Mature Immune Cells Form a Novel Type of Organized Lymphoid Structure in Idiopathic Pulmonary Fibrosis. *J Immunol*. 2006;176(10):5735-5739. doi:10.4049/jimmunol.176.10.5735
7. Todd NW, Scheraga RG, Galvin JR, et al. Lymphocyte aggregates persist and accumulate in the lungs of patients with idiopathic pulmonary fibrosis. *J Inflamm Res*. 2013;6(1):63-70. doi:10.2147/JIR.S40673
8. Verleden SE, Tanabe N, McDonough JE, et al. Small airways pathology in idiopathic pulmonary fibrosis: a retrospective cohort study. *Lancet Respir Med*. 2020;8(6):573-584. doi:10.1016/S2213-2600(19)30356-X
9. Polverino F, Baraldo S, Bazzan E, et al. A novel insight into adaptive immunity in chronic obstructive pulmonary disease: B cell activating factor belonging to the tumor necrosis factor family. *Am J Respir Crit Care Med*. 2010;182(8):1011-1019. doi:10.1164/rccm.200911-1700OC
10. Cosio M, Ghezzo H, Hogg JC, et al. The Relations between Structural Changes in Small Airways and Pulmonary-Function Tests. *N Engl J Med*. 1978;298(23):1277-1281. doi:10.1056/nejm197806082982303
11. Hsia CCW, Hyde DM, Ochs M, Weibel ER. An official research policy statement of the American Thoracic Society/European Respiratory Society: Standards for quantitative assessment of lung structure. *Am J Respir Crit Care Med*. 2010;181(4):394-418. doi:10.1164/rccm.200809-1522ST
12. Idiopathic Pulmonary Fibrosis: Diagnosis and Treatment. *Am J Respir Crit Care Med*. 2000;161(2):646-664. doi:10.1164/ajrccm.161.2.ats3-00
13. Newton CA, Zhang D, Oldham JM, et al. Telomere length and use of immunosuppressive medications in idiopathic pulmonary fibrosis. *Am J Respir Crit Care Med*. 2019;200(3):336-347. doi:10.1164/rccm.201809-1646OC

14. Baraldo S, Turato G, Lunardi F, et al. Immune activation in α1-antitrypsin-deficiency emphysema: Beyond the protease-antiprotease paradigm. *Am J Respir Crit Care Med*. 2015;191(4):402-409. doi:10.1164/rccm.201403-0529OC

15. Peng M, Wang W, Qin L, et al. Association between nonspecific interstitial pneumonia and presence of CD20+ B lymphocytes within pulmonary lymphoid follicles. *Sci Rep*. 2017;7(1):1-10. doi:10.1038/s41598-017-17208-1

Chapter 10

CA 19-9 serum levels in patients with end-stage idiopathic pulmonary fibrosis (IPF) and other interstitial lung diseases (ILDs):

Correlation with functional decline

Elisabetta Balestro, Gioele Castelli, Nicol Bernardinello, Elisabetta Cocconcelli, Davide Biondini, Federico Fracasso, Federico Rea, Marina Saetta, Simonetta Baraldo and Paolo Spagnolo

Chron Respir Dis. 2020 Jan-Dec;17:1479973120958428. doi: 10.1177/1479973120958428. PMID: 32969271; PMCID: PMC7521048.

ABSTRACT

Idiopathic pulmonary fibrosis presents a progressive and heterogeneous functional decline. CA 19-9 has been proposed as biomarker to predict disease course, but its role remains unclear. We assessed CA 19-9 levels and clinical data in end-stage ILD patients (48 IPF and 20 non-IPF ILD) evaluated for lung transplant, to correlate these levels with functional decline. Patients were categorized based on their rate of functional decline as slow (n = 20; △FVC%pred ≦ 10%/year) or rapid progressors (n = 28; △ FVC%pred > 10%/year). Nearly half of the entire patients (n ¼ 32; 47%) had CA 19-9 levels ≧ 37kU/L. CA 19-9 levels in IPF were not different from non- IPF ILD populations, however, the latter group had a median CA 19-9 level above the normal cut-off value of 37 KU/l (60 [17–247] kU/L). Among IPF patients, CA 19-9 was higher in slow than in rapid progressors with a trend toward significance (33vs17kU/L; p = 0.055). In the whole population, CA19-9 levels were inversely related with DFVC/year (r = 0.261; p = 0.03), this correlation remained in IPF patients, particularly in rapid progressors (r = 0.51; p = 0.005), but not in non. Moreover, IPF rapid progressors with normal CA 19-9 levels showed the greater △FVC/year compared to those with abnormal CA 19-9 (0.95 vs. 0.65 L/year; p = 0.03). In patients with end-stage ILD, CA 19-9 may represent a marker of disease severity, whereas its level is inversely correlated with functional decline, particularly among IPF rapid progressors.

INTRODUCTION

Idiopathic pulmonary fibrosis (IPF) is a specific form of chronic, progressive fibrosing interstitial pneumonia of unknown etiology associated with significant morbidity and mortality.1 The clinical course of IPF is highly heterogeneous and unpredictable with some patients progressing rapidly (rapid progressors), others declining slowly (slow progressors), and others experiencing episodes of sudden worsening following periods of relative stability[1-3]. Such variable disease course makes it challenging to predict the trajectory of IPF in individual patients and several studies have tried to identify tools to predict both disease progression and risk of mortality. A number of risk models have been developed that incorporate demographic, clinical and physiological variables, including the du Bois' model and the Gender, Age, Physiology (GAP) index[4,5]. Though undoubtedly valuable, these scoring systems are not able to predict disease behavior. Change in forced vital capacity (FVC) is a reliable, valid and reproducible measure of disease progression as well as an independent predictor of mortality and treatment response[6-8]. However, considerable interand intra-individual variability exists in the rate of FVC decline over time in patients with IPF[9,10]. These issues highlight the need for additional and more reliable non-invasive tools to improve risk stratification and prediction of outcome in IPF.

Significant advances in the pathogenesis of IPF over the last two decades have led to the identification of several potential predictors of disease behavior, such as KL-6, CCL18 and MMP-7[11,12]. However, they are neither able to predict disease progression nor are they routinely available in clinical practice[13].

Recently, Maher and colleagues have conducted a large prospective study of patients with IPF to investigate the predictive power of selected biomarkers and to identify individuals with IPF at risk of progression or death. Among all biomarkers examined, including cytokines, chemokines, growth factors, extracellular matrix proteins and markers of epithelial injury, the authors found that serum levels of Carbohydrate Antigen 19-9 (CA 19-9), a marker of epithelial damage, was significantly associated to disease progression in the first year of follow-up[14]. However, it is unclear whether CA 19-9 will maintain the same prognostic power throughout the natural history of the disease. With this

background, the aim of our study was to investigate the role of serum CA 19-9 levels in IPF patients with advanced disease referred to our lung transplant center and its relation with different patterns of functional decline (rapid vs. slow progression as assessed by the rate of FVC decline). In addition, we evaluated the significance of CA 19-9 levels in patients with interstitial lung disease (ILD) other than IPF who also displayed a progressive fibrosing phenotype.

MATERIAL AND METHODS

Study population

The study population included a well-characterized cohort of patients with end-stage IPF and non-IPF ILD referred to our center and evaluated for lung transplantation. Clinical, laboratory and lung function data were retrospectively collected at the time of listing for transplant. In all patients, the diagnosis of IPF or non-IPF ILD was made following multidisciplinary discussion and in accordance with the ATS/ERS/JRS/ ALAT guidelines on IPF[1].

CA 19-9 levels were determined by the solidphase, two-site chemiluminescent enzyme immunometric assay with levels above 37 kU/L considered abnormal[15]. Measurements were performed by an experienced technician blinded to clinical information.

All causes of increased CA 19-9 levels, such as gastrointestinal cancers and concomitant nonmalignant diseases (i.e. extra-hepatic cholestasis, hepatic cirrhosis or gallbladder disease) were carefully investigated by the examinations routinely performed during the lung transplant evaluation and excluded. FVC changes in the year before referral (median follow-up value 13 months) were used to phenotype patients as either “rapid” (n = 39, decline in % predicted FVC >10% per year) or “slow” (n = 29, decline in % predicted FVC $\leqq$10% per year) progressors, as previously reported[3]. The absolute fall in FVC in mL normalized per year was also calculated. Additional functional parameters such as diffusing capacity of the lung for carbon monoxide (DLCO) and 6-minute walking test were available for only a minority of patients and were therefore excluded from the analysis.

Statistical analysis

All continuous variables were tested for normality. To compare clinical and functional data between IPF and non-IPF ILD patients, and between rapid and slow progressors, Mann–Whitney U test was used when normality assumptions were not met. In IPF patients, analyses were also performed after treatment stratification (treated versus untreated). Correlation coefficients between functional and laboratory data were calculated using the nonparametric Spearman's rank method. ROC curves for CA 19-9 were performed using Youden J test. All data were analyzed using SPSS Software version 25.0 (New York, NY, US: IBM Corp. USA). p-values <0.05 were considered statistically significant.

RESULTS

The study population included 68 patients referred to our center for potential listing for lung transplantation. Forty-eight (n = 48) patients had IPF (age 60 [54–62] years) and 20 (n = 20) patients had ILD other than IPF (age 57 [55–60] years), including idiopathic Non-Specific Interstitial Pneumonia (n = 9), chronic Hypersensitivity Pneumonitis (n = 6), pulmonary Sarcoidosis (n = 3) and Pleuroparenchymal Fibroelastosis (n = 2). Nearly half of IPF patients (n = 23, 48%) were on antifibrotic therapy. Clinical, functional characteristics and CA 19-9 levels of the entire study population and of different subgroups are shown in **Table 1**.

Values are expressed as numbers and (%) or median and interquartile range as appropriate. As expected, most patients were males and former smokers, with a similar smoking history between IPF and non-IPF ILD patients (p = 0.44). Patients with IPF and non-IPF ILD differed in terms of age at diagnosis (55 vs. 51 years), but did not differ significantly with regard to time from diagnosis to referral (36 vs. 35 months). Patients with IPF and non-IPF ILD were comparable with regard to degree of lung function decline; indeed, although patients with non-IPF ILD had slightly lower values of FVC at referral (37% vs. 48% pred), the two groups had a similar FVC loss per year (400 vs. 460 mL).

In the entire study population, 32 patients (47%) presented CA 19-9 levels above the cut-off value (37 kU/L). Levels of CA 19-9 were not significantly different in IPF patients than in non-IPF ILD patients (26 [7–106] vs. 60 [17–247], p = 0.14) (**Figure 1A**); however, the latter group had a median CA 19-9 level above

the normal cut-off value of 37 KU/l (60 [17– 247] kU/L). The established cut-off of 37 KU/l is derived from studies in malignancies, though it has also been applied to IPF. We then applied a ROC curve analysis to our data, which resulted in best threshold value at 24.6 kU/L, with a modest accuracy. An analysis of the cohort in relation to this threshold is presented in Table S1 (supplementary material). Given the heterogeneous clinical course of IPF patients, in further analyses we evaluated CA 19-9 levels in patients stratified by the rate of their functional decline (i.e., slow [S, n = 20] or rapid [R, n = 28] progressors).

The median FVC decline %pred/year before referral was 17% in rapid progressors (absolute FVC decline 0.72 L) and 2% in slow progressors (absolute FVC decline 0.13 L). Slow and rapid progressors were similar with regard to age at diagnosis (55 vs. 56 years), age at listing (59 vs. 60 years) as well as time from diagnosis to referral (36 vs. 36 months). Similarly, there were no between group differences with regard to number of patients on antifibrotic therapy (9 [45%] vs. 14 [50%]). Conversely, FVC both as absolute value (L) and %predicted at referral was significantly lower in rapid progressors than in slow progressors (1.70 L vs. 2.11 L, p = 0.02; 43% vs. 55% %pred., p = 0.005 respectively).

Interestingly, rapid progressors displayed lower serum levels of CA 19-9 compared to slow progressors, although this difference did not reach statistical significance (17 [3–70] kU/L vs. 33 [16–415] kU/L, p = 0.055 respectively) (**Figure 1B**).

We then analyzed the correlation between CA 19-9 values and loss of FVC L/year before referral in the entire patient population, in the IPF and non-IPF ILD subgroups as well as in rapid and slow progressors. We observed an inverse correlation between CA 19-9 Levels and FVC L/year in the entire study population (r = 0.261, p = 0.031) (**Figure 2**). This negative correlation remained significant in patients with IPF (r = 0.335, p = 0.020), but not in those with non- IPF ILD (r = 0.100, p = 0.67) (**Figure 3**).

Noteworthy, CA 19-9 serum levels were inversely correlated with FVC L/year among rapid (r = 0.515, p = 0.005), but not slow progressors (r = 0.239, p = 0.31) (**Figure 4**).

Finally, when rapid progressors were considered, we observed that patients with CA 19-9 levels below 37 kU/L (n = 17) experienced a significantly more

rapid FVC decline L/year compared to patients with CA 19-9 >37 kU/L (n = 11) (0.95 vs. 0.65 L/year; p = 0.03) (**Figure 5**).

When we compared clinical and functional characteristics between IPF patients with and without antifibrotic treatment, we did not observe any statistical significance with the exception of age at diagnosis, which was lower in untreated patients. In particular CA 19-9 levels were similar between treated and untreated patients (supplementary material, Table S2).

Table 1. Demographics and clinical characteristics of the entire population

	Entire population (n=68)	**IPF (n=48)**	**Non-IPF (n=20)**	**p value**
Male – n (%)	54 (80)	42 (88)	12 (60)	0.01
Age at diagnosis – years	54 (49-59)	55 (51-59)	51 (48-54)	0.01
Smoking history – pack years **• Former – n (%)** **• Nonsmokers– n (%)**	6 (0-25) 40 (59) 28 (41)	6 (0-24) 31 (65) 18 (35)	0 (0- 25) 9 (45) 11 (55)	0.44 0.13
Age at listing - years	59 (55-61)	60 (54-62)	57 (55-60)	0.28
Ca 19-9 listing – kU/L **• >37 kU/L – n (%)** **• <37 kU/L –n (%)**	32 (11-180) 32 (47) 36 (53)	26 (7-106) 20 (42) 28 (58)	60 (17-247) 12 (60) 8 (40)	0.14 0.17
FVC at listing – L	1.70 (1.24-.2.18)	1.84 (1.38-2.27)	1.34 (0.95-1.69)	0.003
FVC at listing – %pred.	46 (35-57)	48 (36-58)	37 (34-55)	0.09
FVC decline per year – L	0.43 (0,20-0,89)	0.46 (0,18-0,93)	0,40 (0,20-0,72)	0.76
FVC decline per year – %pred.	12 (5-19)	11 (5-19)	11 (3-14)	0.73
Time from diagnosis to listing - months	35 (23-65)	36 (26-59)	35 (18-151)	0.72

Values are expressed as numbers and (%) or median and Q1-Q3 as appropriate. Negative values mean improvement of FVC.

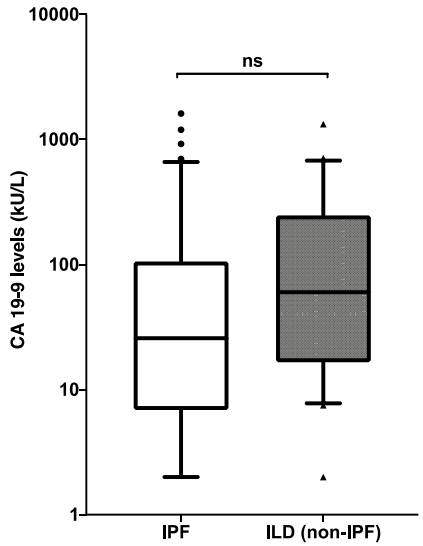

Figure 1. CA 19.9 levels (logarithmic expression of kU/L) in patients with IPF and patients with ILD (non-IPF). Horizontal bars represent median values; bottom and top of each box plot 25th and 75th; brackets show 10th and 90th percentiles; points and triangles indicate outliners. White indicate IPF and grey boxes ILD (non-IPF).

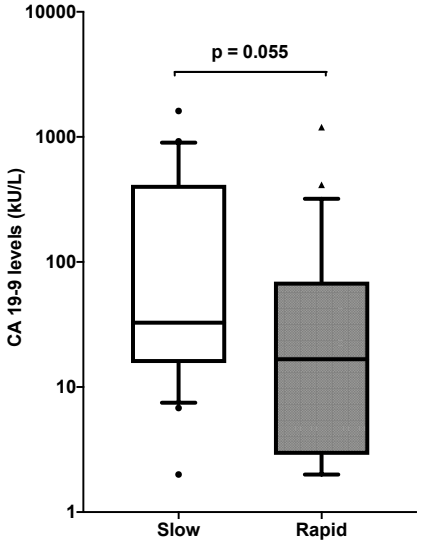

Figure 2. CA 19.9 levels (logarithmic expression of kU/L) in patients with slow progression and rapid progression of IPF. Horizontal bars represent median values; bottom and top of each box plot 25th and 75th; brackets show 10th and 90th percentiles; points and triangles indicate outliners. White indicate slow progressors and grey boxes rapid progressors.

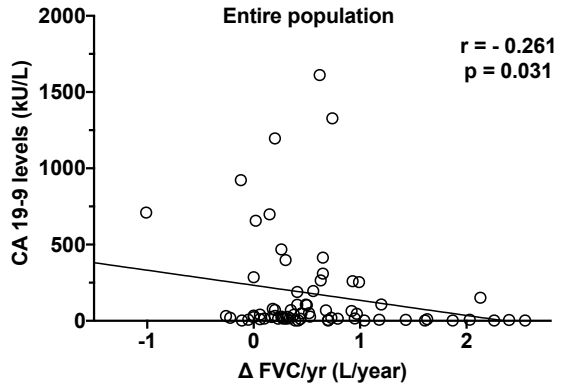

Figure 3. Correlation between CA 19-9 levels (kU/L) and ΔFVC L/year in the entire population (IPF and ILD non-IPF). The black line represents the correlation in the entire population. Spearman's rank correlation: r = -0.261, p=0.03 in the entire population.

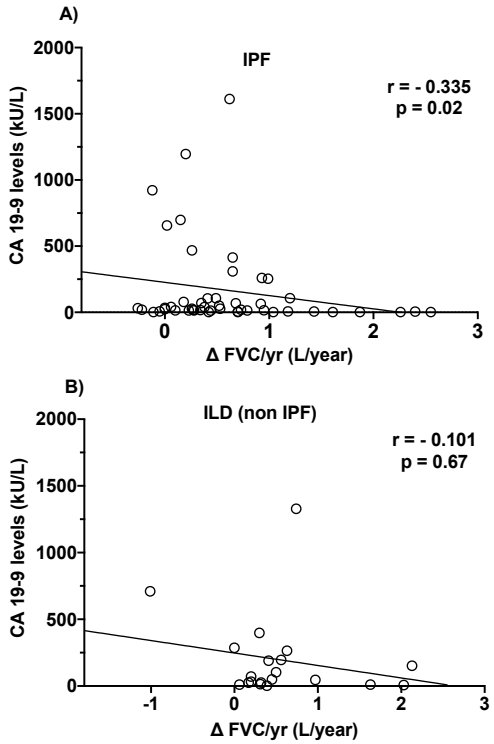

Figure 4. Correlation between CA 19-9 levels (kU/L) and ΔFVC L/year in IPF and non-IPF ILD patients. The black line represents the correlation. a) Correlation in IPF patients. Spearman's rank correlation: r=-0.335, p=0.02. b) Correlation in non-IPF ILD patients. Spearman's rank correlation: r=-0.101, p=0.67.

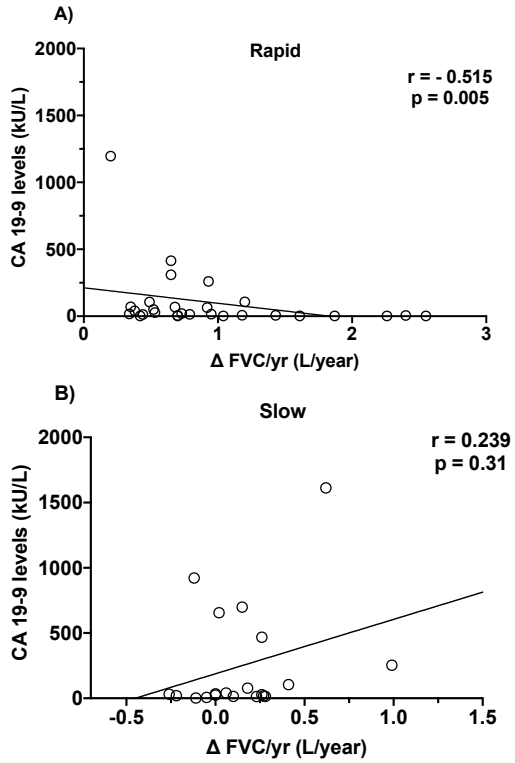

Figure 5. Correlation between CA 19-9 levels (kU/L) and ΔFVC L/year in IPF patients with rapid and slow progression. The black line represents the correlation. a) Correlation in rapid progressors. Spearman's rank correlation: r=-0.515, p=0.005. b) Correlation in slow progressors. Spearman's rank correlation: r=0.239, p=0.31.

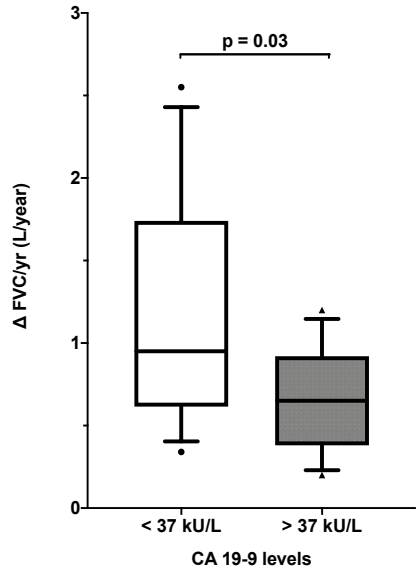

Figure 6. ΔFVC (L/year) in rapid progressors with CA 19-9 above or below normal cut-off (≤37 kU/L). Horizontal bars represent median values; bottom and top of each box plot 25th and 75th; brackets show 10th and 90th percentiles; points and triangles indicate outliners. White indicate patients below cut-off and grey boxes patients above.

DISCUSSION

In this study, we assessed CA 19-9 serum levels in patients with end-stage IPF and compared them with those of patients with end-stage non-IPF ILD undergoing evaluation for lung transplantation. In addition, we stratified data analysis based on the rate of FVC decline over the 12-month period (slow vs. rapid progressors) preceding listing for transplantation. Nearly half (n = 32, 47%) of our entire study population had CA19-9 levels higher than the cut-off value of 37 kU/ L. Somewhat unexpectedly, CA 19-9 levels correlated inversely with the rate of FVC decline; this correlation remained intact among the IPF population and, further subgrouping these patients, only in the group of rapid progressors. In addition, among rapid progressors, those with CA 19-9 levels below the cut-off of 37 kU/L had statistically more rapid FVC decline in the year before referral than rapid progressors with high CA19-9 levels (0.95 vs. 0.65 L/year, p = 0.03).

In a large prospective, longitudinal cohort of treatment-naive patients with IPF, Maher and coworkers assessed an array of biomarkers, with the aim to identifying potential predictors of clinical outcome. Specifically, by using a multiplex immunoassay, they quantified a panel of 123 possible biomarkers with putative pathogenic roles in IPF. The protein that most clearly distinguished progressive from stable disease was CA 19-9 and this was the only biomarker that remained significant after multivariate correction for the others 123 variables. Notably, in the Maher's study, CA19-9 was significantly increased in patients with progressive disease (mean value: 53 U/mL) than in those with stable disease whose CA 19-9 levels remained within normal limits (22 U/mL)[14]. In a different study, Rusanov and coworkers collected samples from patients with progressive IPF referred for lung transplantation and observed increased CA 19-9 levels (121+28 kU/L)[16]. Taken together, these observations suggest that CA 19-9 levels tend to progressively increase over the disease course.

CA 19-9 has been primarily evaluated as a tumor marker, especially in gastro-enteric tumors[17]; however, increased serum levels of CA 19-9 have been shown in a number of non-malignant diseases such as extra-hepatic cholestasis, hepatic cirrhosis or gallbladder disease[18]. With regard to respiratory diseases, increased CA19-9 levels have been observed in idiopathic non-specific interstitial pneumonia, hypersensitivity pneumonitis and sarcoidosis[19]. Totani and colleagues measured CA 19-9 levels in the serum, bronchoalveolar lavage fluid (BALF) and epithelial lining fluid (ELF) of 31 patients with IPF[20]. Serum CA19-9 levels

correlated positively with disease extent on chest X-ray, number of BALF neutrophils as well as ELF CA 19-9 levels. Notably, serum CA 19-9 did not correlate with markers of disease activity such as serum LDH, KL-6, SP-A, and SP-D, suggesting that serum CA 19-9 levels may reflect progression rather than activity of pulmonary fibrosis. In a Japanese study, Kodama and coworkers analyzed CA 19-9 in 554 patients diagnosed with either lung cancer (n = 323) or nonmalignant pulmonary disease (n = 231), including, among others, idiopathic interstitial pneumonia and connective tissue disease-associated ILD[21]. 30.7% of patients with lung cancer and 38.9% of patients with nonmalignant lung disease displayed CA 19-9 higher than the cut-off level of 37 U/mL. Several studies have shown that patients with IPF have a significantly higher risk to develop lung cancer compared with the general population, with incidence rates ranging between 3% and 22%[22] and prevalence rates exceeding 50%[23].

Therefore, in the presence of elevated levels of tumor markers, it is imperative to carefully screen IPF patients with advanced disease (before listing for lung transplant, as was the case in our entire study population) for an occult neoplasm. The mechanisms leading to elevation of CA 19-9 level in ILDs are unknown. One hypothesis is that excessive CA 19-9 is released by regenerating epithelial cells in damaged lungs[24,25]. Low levels of CA 19-9 have also been reported for severely damaged lungs but this could be due to the loss of the ability to regenerate the alveolar epithelium in some patients[21]. At present, the determinants of the elevated CA 19-9 levels in ILD and its correlation with poor prognosis remain speculative.

In our study, pre-transplant serum levels of CA 19-9 between rapid and slow progressors trended toward significance ($p = 0.055$). Interestingly, CA 19-9 levels inversely correlated with FVC loss among rapid, but not slow progressors. In addition, among rapid progressors, patients with CA 19-9 levels below the cut-off displayed the greater FVC loss in the year before referral (0.95 vs. 0.65 L/year; $p = 0.03$). This seems apparently in contrast from previous literature, were rapid progressors, in the first year after diagnosis, presented higher CA 19-9 serum levels[14]. However, our study captures the end-stage disease scenario, searching if this prognostic value remains along the disease course. In fact, analyses were conducted in the end stage of the natural history of the disease that was never investigated in relation to disease progression. Differently, Maher and coauthors

investigated patients with IPF at diagnosis and followed them for 1 year to determine disease progression. In our investigation we wanted to capture the later phase of the disease when marked fibrosis with architectural distortion of the lung has already happened.

The inverse correlation between CA 19-9 levels and functional decline, particularly among IPF rapid progressors raised an interesting hypothesis. We can speculate that rapid progressors, especially those with the greater functional loss, may experience a very rapid evolution toward epithelial to-mesenchymal transition. As CA 19-9 is a marker of bronchial epithelial proliferation, exhausted cells from rapid progressors in severely damaged lungs may not be able to regenerate and produce sufficient amount of CA 19-9. Conversely, in Maher's study, the positive correlation between CA 19-9 levels and progression may reflect the active phase of the disease (initial phase) with extensive regeneration of epithelial cells. Our observation highlights the potential utility of measuring CA 19-9 at different time points during the disease course to evaluate its role as a prognostic biomarker. However, the contribution retrospective cohort study, therefore data were collected from medical records, which may introduce inaccuracies. However, every effort was made to reduce this risk. Antifibrotic treatment (i.e., pirfenidone and nintedanib) slow down functional decline and disease progression of patients with IPF[7,8].

In our study, nearly half of patients (48%) were on antifibrotic therapy as they were part of an historical cohort from the pre-antifibrotics era. However, the percentage of patients on antifibrotic therapy was equally distributed between slow and rapid progressors, and no statistical difference were found in any of the subgroups. The study included a relatively small number of patients. However, it should be noticed that only a small minority of the IPF population is referred to and evaluated for lung transplantation. On the other hand, our study cohort is phenotypically very well defined and includes deliberately patients for whom lung function data were fully available. We measured CA 19-9 levels at a single time point (i.e. referral for transplant); however, Maher and colleagues observed similar CA 19-9 levels at baseline and after 3 months later suggesting that there may not be a progressive increase of CA 19-9 levels over a short period of time[14]. Whether this is the case in the longer term remains to be elucidated. Finally, our study included a highly selected subgroup of patients; therefore, our findings may not be

generalizable to the entire IPF patient population due to the great variability of natural history and disease phenotypes.

Notwithstanding these limitations, our study suggest that CA 19-9 levels may be variable during the course of IPF, with increased levels in the end-stage disease. However, there could be a possible decline in secretion in those lungs, which reached a loss of epithelial regeneration. Further prospective studies are needed to validate these findings about CA 19-9 role in IPF prognosis and assess whether they hold true outside the setting of end-stage IPF patients undergoing evaluation for lung transplantation.

SUPPLEMENTARY MATERIALS

METHODS

The study population included a well-characterized cohort of patients with end-stage IPF referred to our center and evaluated for lung transplantation. Clinical, laboratory and lung function data were retrospectively collected at the time of listing for transplant. CA 19-9 levels were determined by the solid-phase, two-site chemiluminescent enzyme immunometric assay. Measurements were performed by an experienced technician blinded to clinical information. Causes of increased CA 19-9 levels, such as gastrointestinal cancers, were carefully investigated and excluded. The absolute fall in FVC in ml normalized per year was also calculated. All continuous variables were tested for normality. To compare clinical and functional data between IPF with and without antifibrotic treatment, Mann-Whitney U test was used, when normality assumptions were not met. Finally, a ROC curve for CA 19-9 was performed considering the whole population (IPF patients versus other ILD patients) to establish prognostic cut-off of the CA 19-9 marker, taking as threshold value the one with maximal sensitivity and specificity (Youden J test). Whereas a ROC curve method was applied in patients with IPF (treated and untreated) considering slow and rapid progressors to obtain the area under the curve.

RESULTS

Considering the whole population (IPF and other ILD non IPF), a ROC curve method was used to try to find the optimal cut-off of CA 19-9 in a non malignant disease and obtaining a threshold value of 24.6 kU/L the one with maximal sensitivity and specificity (AUC= 0,61, Std. Error 0,07, 95% confidence interval 0,4722 to 0,7559, p value = 0,14). We then changed our results in relation to this new threshold value obtained (24.6 kU/L). Clinical, functional and serological data are summarized in the table below.

Table S2. Clinical, functional and serological data of the entire population and of each subgroups: Idiopathic Pulmonary Fibrosis (IPF), non-IPF Interstitial Lung Disease, IPF patients with slow progression and rapid progression.

	Entire population (n=68)	*IPF (n=48)*	*Non-IPF ILD (n=20)*	*p value*	*IPF - Slow progressor (n=20)*	*IPF - Rapid progressor (n=28)*	*p value*
Male – n (%)	*54 (80)*	*42 (88)*	*12 (60)*	*0,01*	*18 (90)*	*24 (86)*	*0,66*
Age at diagnosis – years	*54 (49-59)*	*55 (51-59)*	*51 (48-54)*	*0,01*	*55 (51-59)*	*56 (47-59)*	*0,85*
Smoking history – pack years	*6 (0-25)*	*6 (0-24)*	*0 (0- 25)*	*0,44*	*17 (1-28)*	*5 (0-18)*	*0,17*
• Former – n (%)	*40 (59)*	*31 (65)*	*9 (45)*	*0,13*	*15 (75)*	*16 (57)*	*0,20*
• Nonsmokers– n (%)	*28 (41)*	*18 (35)*	*11 (55)*		*5 (25)*	*12 (43)*	
Age at referral - years	*59 (55-61)*	*60 (54-62)*	*57 (55-60)*	*0,28*	*59 (56-61)*	*60 (49-62)*	*0,95*
CA 19-9 referral – kU/L	*32 (11-180)*	*26 (7-106)*	*60 (17-247)*	*0,14*	*33 (16-415)*	*17 (3-70)*	*0,05*
• >24.6 kU/L – n (%)	39 *(57)*	*24 (50)*	*15 (75)*	*0,05*	12 *(60)*	12 *(43)*	*0,24*
• <24.6 kU/L –n (%)	28 *(41)*	*24 (50)*	*5 (25)*		8 *(40)*	*16 (57)*	
FVC at referral – L	*1,70 (1,24-2,18)*	*1,84 (1,38-2,27)*	*1,34 (0,95-1,69)*	*0,003*	*2,11 (1,77-2,46)*	*1,70 (1,25-2,06)*	*0,02*
FVC at referral – %pred.	*46 (35-57)*	*48 (36-58)*	*37 (34-55)*	*0,09*	*55 (49-62)*	*43 (34-52)*	*0,005*
FVC decline per year – L	*0,43 (0,20-0,89)*	*0,46 (0,18-0,93)*	*0,40 (0,20-0,72)*	*0,76*	*0,13 (0,03-0,26)*	*0,72 (0,50-1,20)*	*<0,0001*
FVC decline per year – %pred.	*12 (5-19)*	*11 (5-19)*	*11 (3-14)*	*0,73*	*2 (3-7)*	*17 (13-24)*	*<0,0001*
Time from diagnosis to referral - months	*35 (23-65)*	*36 (26-59)*	*35 (18-151)*	*0,72*	*36 (23-57)*	*36 (25-67)*	*0,74*

Values are expressed as numbers and (%) or median and interquartile as appropriate.

Considering only patients with IPF, when we compared clinical and functional characteristics between patients with antifibrotics and untreated we did not observe any statistical significance with the exception of age at diagnosis which was lower in untreated patients. In particular CA 19-9 levels were similar between treated and

untreated patients (Table S2). When we performed a ROC curve for CA 19-9 levels both subgroups (untreated and treated IPF patients) we obtained the following results.

For untreated patients (slow progressors, n=11; rapid progressors, n=14) AUC was 0,6; Std. Error 0,1199, 95% confidence interval 0,3495 to 0,8193, p value= 0,5. Whereas for treated patients (slow progressors, n=9; rapid progressors, n=14) the AUC was 0,7; Std. Error 0,1134 95% confidence interval 0,5000 to 0,9445, p value = 0,08.

Table S2. Demographics and clinical characteristics of the IPF population sorted for antifibrotic treatment.

	IPF (n=48)	***IPF with antifibrotic treatment (n=23)***	***IPF without antifibrotic treatment (n=25)***	***p value***
Male – n (%)	*42 (88)*	*20 (87)*	*22 (88)*	*0,91*
Age at diagnosis – years	*55 (51-59)*	*58 (54-60)*	*54 (46-58)*	***0,01***
Smoking history – pack years ***• Former – n (%)*** ***• Nonsmokers– n (%)***	*6 (0-24)* *31 (65)* *18 (35)*	*4 (0-21)* *10 (43)* *13 (57)*	*10 (0- 29)* *18 (72)* *7 (28)*	*0,20* *0,26*
Age at listing - years	*60 (54-62)*	*61 (57-62)*	*58 (47-61)*	*0,06*
Ca 19-9 listing – kU/L ***• >37 kU/L – n (%)*** ***• <37 kU/L –n (%)***	*26 (7-106)* *20 (42)* *28 (58)*	*18 (6-68)* *8 (35)* *15 (65)*	*34 (7-183)* *12 (48)* *13 (52)*	*0,21* *0,35*
FVC at listing – L	*1,84 (1,38-2,27)*	*1,79 (1,30-2,21)*	*2,05 (1,62-2,31)*	*0,22*
FVC at listing – %pred.	*48 (36-58)*	*49 (36-57)*	*48 (40-58)*	*0,80*
FVC decline per year – L	*0,46 (0,18-0,93)*	*0,53 (0,26-0,95)*	*0,42 (0,09-0,93)*	*0,43*
FVC decline per year – %pred.	*11 (5-19)*	*11 (5-19)*	*12 (2-19)*	*0,94*
Time from diagnosis to listing - months	*36 (26-59)*	*29 (24-61)*	*40 (30-60)*	*0,56*

Values are expressed as numbers and (%) or median and interquartile as appropriate.

REFERENCES

1. Raghu G, Remy-Jardin M, Myers JL, et al. Diagnosis of idiopathic pulmonary fibrosis: an Official ATS/ ERS/JRS/ALAT Clinical practice guideline. Am J Respir Crit Care Med 2018; 198: e44–e68.
2. Selman M, Carrillo G, Estrada A, et al. Accelerated variant of idiopathic pulmonary fibrosis: clinical behavior and gene expression pattern. PLoS One 2007; 2: e482.
3. Balestro E, Calabrese F, Turato G, et al. Immune inflammation and disease progression in idiopathic pulmonary fibrosis. PLoS One 2016; 11: e0154516.
4. Ley B, Ryerson CJ, Vittinghoff E, et al. A multidimensional index and staging system for idiopathic pulmonary fibrosis. Ann Intern Med 2012; 156: 684–691.
5. du Bois RM, Weycker D, Albera C, et al. Ascertainment of individual risk of mortality for patients with idiopathic pulmonary fibrosis. Am J Respir Crit Care Med 2011; 184: 459–466.
6. Jegal Y, Kim DS, Shim TS, et al. Physiology is a stronger predictor of survival than pathology in fibrotic interstitial pneumonia. Am J Respir Crit Care Med 2005; 171: 639–644.
7. Richeldi L, du Bois RM, Raghu G, et al. Efficacy and safety of nintedanib in idiopathic pulmonary fibrosis. N Engl J Med 2014; 370: 2071–2082.
8. King TE, Bradford WZ, Castro-Bernardini S, et al. A phase 3 trial of pirfenidone in patients with idiopathic pulmonary fibrosis. N Engl J Med 2014; 370: 2083–2092.
9. Martinez FJ, Safrin S, Weycker D, et al. The clinical course of patients with idiopathic pulmonary fibrosis. Ann Intern Med 2005; 142: 963–967.
10. Nathan SD, Albera C, Bradford WZ, et al. Effect of continued treatment with pirfenidone following clinically meaningful declines in forced vital capacity: analysis of data from three phase 3 trials in patients with idiopathic pulmonary fibrosis. Thorax 2016; 71: 429–435.
11. Horimasu Y, Hattori N, Ishikawa N, et al. Different MUC1 gene polymorphisms in German and Japanese ethnicities affect serum KL-6 levels. Respir Med 2012; 106: 1756–1764.
12. Ley B, Brown KK and Collard HR. Molecular biomarkersin idiopathic pulmonary fibrosis. Am J Physiol Cell Mol Physiol 2014; 307: L681–L691.
13. Raghu G, Richeldi L, Jagerschmidt A, et al. Idiopathic pulmonary fibrosis. Chest 2018; 154: 1359–1370.
14. Maher TM, Oballa E, Simpson JK, et al. An epithelial biomarker signature for idiopathic pulmonary fibrosis: an analysis from the multicentre PROFILE cohort study. Lancet Respir Med 2017; 5: 946–955.
15. Del Villano BC, Brennan S, Brock P, et al. Radioimmunometric assay for a monoclonal antibody-defined tumor marker, CA 19-9. Clin Chem 1983; 29: 549–552.
16. Rusanov V, Kramer MR, Raviv Y, et al. The significance of elevated tumor markers among patients with idiopathic pulmonary fibrosis before and after lung transplantation. Chest 2012; 141: 1047–1054.

17. Poruk KE, Gay DZ, Brown K, et al. The clinical utility of CA 19-9 in pancreatic adenocarcinoma: diagnostic and prognostic updates. Curr Mol Med 2013; 13: 340–351.
18. Galli C, Basso D and Plebani M. CA 19-9: handle with care. Clin Chem Lab Med 2013; 51: 1369–1383.
19. Dai H, Liu J, Liang L, et al. Increased lung cancer risk in patients with interstitial lung disease and elevated CEA and CA125 serum tumour markers. Respirology 2014; 19: 707–713.
20. Totani Y, Demura Y, Ameshima S, et al. Serum CA19-9 levels reflect bronchoalveolar lavage fluid neutrophil levels in idiopathic pulmonary fibrosis. Respiration 2001; 68: 438–438.
21. Kodama T, Satoh H, Ishikawa H, et al. Serum levels of CA19-9 in patients with nonmalignant respiratory diseases. J Clin Lab Anal 2007; 21: 103–106.
22. Karampitsakos T, Tzilas V, Tringidou R, et al. Lung cancer in patients with idiopathic pulmonary fibrosis. Pulm Pharmacol Ther 2017; 45: 1–10.
23. Tomassetti S, Gurioli C, Ryu JH, et al. The impact of lung cancer on survival of idiopathic pulmonary fibrosis. Chest 2015; 147: 157–164.
24. Shimizu Y, Hamada T, Tanaka Y, et al. Colocalization of CA19-9 and KL-6 to epithelial cells in dilated bronchioles in a patient with idiopathic pulmonary fibrosis complicated by diffuse alveolar damage. Respirology 2002; 7: 281–284.
25. Mukae H, Hirota M, Kohno S, et al. Elevation of tumor-associated carbohydrate antigens in patients with diffuse panbronchiolitis. Am Rev Respir Dis 1993; 148: 744–751.

Chapter 11

Predictors and protective factors for interstitial lung disease in a multicenter Caucasian cohort of patients affected by idiopathic inflammatory myopathies

Original data not yet published

ABSTRACT

Objectives. Patients with idiopathic inflammatory myopathies (IIMs) have a highly heterogeneous spectrum of serological features and clinical manifestations. They may develop interstitial lung disease (ILD) during the disease course, but it remains unclear which patients are at risk for lung involvement. We aimed: (1) to identify factors associated with ILD in a large multicenter cohort of Caucasian patients with IIMs. (2) To explore whether high-resolution Computed Tomography (HRCT) features differ among patients with different IIMs. (3) To explore clinical and serological characteristics of progressive IIM-ILD patients in a multicentric population.

Methods. Two hundred fifty-three patients affected by IIMs (2017 EULAR/ACR criteria) were retrospectively evaluated. Demographic, serological and clinical features were recorded at time of IIMs diagnosis and during follow-up. When suspected, ILD was detected by chest high-resolution computed tomography (HRCT). Univariate and multivariate analyses were performed to identify predictors of ILD. The prevalent radiological pattern (ground-glass-opacities,GGO; fibrotic changes, FC; consolidation,C) was used to further classified the study population in three groups to assess potential relationship with clinical data. Progression was defined when forced vital capacity (FVC) %pred. decline was ≥ 5% or when a high-resolution CT scan worsens over one-year follow-up.

Results. ILD was detected in 125 out of 253 (49.4%) patients. IIMs-ILD patients compared with IIMs-not ILD had significantly lower creatine phosphokinase (CPK) levels at diagnosis, higher prevalence of anti-Jo-1, anti SSA/Ro, anti-Ro52 and anti-MDA5, mechanic's hands, arthritis and dyspnea. Multivariate analysis identified dyspnea, mechanic's hands, anti-Jo-1, anti-MDA5 and anti-Ro52 as independently associated with ILD.

The prevalent CT pattern was GGO (n=39;50%), characterized by preserved lung volume at presentation compared with other two groups (FVC%pred.=89% GGO vs 74% FC vs 72% C;p=0.003). C group (n=17; 22%) anticipated the diagnosis of IIM (median 0, range[-1-24]GGO vs 0[-5- 13]FC vs 0[-8-0]C years;p=0.03), displayed a significant increase of muscle enzymes (CPK levels 252 GGO vs 121 FC vs 1380 C U/L;p=0.04) and a lower manual muscular test (150 GGO vs 150 FC vs 120 C;p=0.005).

65/79 (82%) were classified as stables (S) and 14(18%) as progressors (P). Compared to S, P displayed a significantly higher prevalence of anti-MDA5 antibodies, heliotropic rash, xerostomia and xerophthalmia. Anti-MDA5 antibodies, heliotropic rash, xerostomia and xerophthalmia were confirmed as progression-associated factors at univariate but not at multivariate analysis.

Conclusion. Besides the specific autoantibodies positivity (anti-Jo1, anti-MDA5 and anti-Ro52), mechanic's hands were the strongest independent clinical predictors of ILD in Caucasian IIMs patients. Ground-glass-opacities is the prevalent HRCT pattern and is associated to normal lung volume and consolidation needs a special attention being associated to muscle injury and anticipating the diagnosis of IIM. Serological and clinical features at diagnosis may predict progression in IIM-ILD patients. Anti-MDA5 antibodies, heliotropic rash, xerostomia and xerophthalmia are prevalent in progressive IIM-ILD population, but their role as independent predictors need to be further investigated.

INTRODUCTION

Interstitial lung disease (ILD) is the most common organ involvement in patients with idiopathic inflammatory myopathies (IIMs), detectable in up to 50% of cases[1]. Although this rate is similar to that observed in Systemic Sclerosis (SSc) – wherein experts agree to perform high resolution computed tomography (HRCT) of the lung at SSc diagnosis and pulmonary function tests (PFTs) at least yearly – there is no shared screening strategy for ILD in IIMs to date[2,3]. Nevertheless, early and timely identification of IIMs-ILD is of the utmost importance, as ILD can potentially change the disease prognosis and, therefore, the follow-up and treatment approach in patients with IIMs.

The disease spectrum of IIMs is highly heterogeneous, with various antibodies and clinical manifestations. Some features, such as the presence of anti-synthetase antibodies, have been generally recognized as risk factors for ILD[4]. On the other hand, antibodies against melanoma differentiation-associated protein 5 (MDA5) has been reported to be associated with ILD in some studies but not confirmed in others, and this discrepancy may be at least partially due to ethnic differences in the presentation and course of IIMs in Asians vs. Caucasians patients[5,6]. In addition, it is worth mentioning that the dosage of some myositis-specific (MSAs) and myositis-associated autoantibodies (MAAs) is not widely available and is often limited to third level referral hospitals[7]. Finally, there is scarce data in literature on clinical characteristics of IIMs which may help to predict the occurrence of ILD.

Another intriguing aspect is the first radiological appearance of interstitial involvement in patients with IIM-ILD with different possible presentations at diagnosis.

The most common radiological presentation is the non-specific interstial pneumonia (NSIP) pattern which is characterized by ground-glass opacities (GGO), intra- and interlobular reticular opacities in a predominantly subpleural and basilar distribution and a subpleural sparing[1,8]. In some patients the radiological findings could be more compatible with organizing pneumonia (OP), with GGO, consolidations and air bronchogram in their context with a predominantly basal distribution[9]. Seldom HRCT pattern shows an irregular reticulation both intralobular and interlobular, with a limited GGO and honeycombing with traction bronchiectasis distinctive for a UIP pattern[10]. In summary, in literature the

correlation between radiologic features and clinical presentation is still unclear and a clear correlation between radiologic features and clinical presentation or disease phenotype is still under investigation.

As evaluated in recent studies, a proportion of patients with IIM-ILD could develop a progressive fibrosing ILD (PF-ILD) despite standard therapy[11,12]. PF-ILD is a self-sustaining process and it is identified by a radiological, clinical and functional decline[13,14]. Nowadays the scientific interest on this topic is deeply increased in fact a recent multicentric trial investigated the efficacy and safety of Nintedanib, a tyrosine-kinase inhibitor already used in patients affected by idiopathic pulmonary fibrosis (IPF), in patients with PF-ILD. This clinical trial revealed that Nintedanib reduces the rate of ILD progression, as measured by FVC decline, in patients affected by PF-ILD[15].

In the wake of raised concern the first aim of our study was to assess clinical and serological predictors of ILD in a large, multicenter and prospectively followed up cohort of Caucasian patients affected by IIMs. Secondly, we aimed to explore the potential association between different HRCT features and the clinical presentation in IIM-ILD patients. Third, we aimed to explore the presence of predictive features associated to progressive fibrosis despite treatment.

METHODS

Study population

All patients affected by IIMs — according to the 2017 EULAR/ACR classification criteria[8]— and prospectively followed up in four third-level referral centers (Padova, Firenze, Udine and Paris) between 2002 and 2020 were retrospectively evaluated (**Figure 1**). Exclusion criteria were: juvenile idiopathic inflammatory myopathies (i.e. IIM diagnosis at <18 years); no available follow-up visits (at least one visit with pulmonary function test (PFT), after the diagnosis of IIMs, was required); patients lost during follow-up; patients with incomplete and/or unavailable clinical and/or serological data; patients with myositis concomitant with other connective tissue diseases.

Demographic variables, and the subsequent clinical data were collected at diagnosis and during follow-up: constitutional signs/symptoms (fever, asthenia and weight loss); articular involvement (arthritis and inflammatory arthralgia); muscular involvement (myalgia, muscular asthenia and dysphagia); skin

manifestations (heliotrope rash, Gottron's papules and signs, mechanic's hands, calcinosis); other manifestations: Raynaud's phenomenon, xerostomia and xerophthalmia.

In addition, all patients underwent manual muscle testing 8 (MMT-8), and serum levels of creatine phosphokinase (CPK), lactate dehydrogenase and myoglobin were obtained at IIMs diagnosis. Further diagnostic investigations i.e. muscle magnetic resonance imaging (MRI) and/or electromyography and/or muscle biopsy were performed according to the physician's judgment. Pulmonary function tests including total lung capacity (TLC), forced vital capacity (FVC) and diffusing capacity for carbon monoxide (DLCO) were collected at diagnosis of IIMs repeated annually during follow-up. At baseline and during follow-up, High Resolution Computed Tomography (HRCT) was performed if ILD was suspected based on signs (e.g. bibasilar crackles), symptoms (cough, dyspnea), X-rays and/or PFTs findings. HRCT features were reviewed by three expert thoracic radiologists (C.G., L.C., F.G.) to confirm interstitial lung involvement which allowed the categorization in IIM associated interstitial lung disease (IIM-ILD) and IIM not associated interstitial lung disease (IIM-non ILD).

Finally, as it pertains to autoantibodies, serum anti-nuclear antibodies (ANA) were analyzed by immunofluorescence (IF) assay on HEp-2 cells, and anti-extractable nuclear antigen (ENA) antibodies by enzyme-linked immunosorbent assay (ELISA) and immunoblot. MSA and MAA were tested in every patient using commercial line blots including recombinant human proteins for Mi-2 alpha, transcription intermediary factor 1-gamma (TIF1γ), small ubiquitin-like modifier-1 activating enzyme (SAE), Ku, PM-Scl75/100, U1RNP, MDA-5, signal recognition particle (SRP), Jo-1, PL-7, PL-12, EJ, and OJ[16].

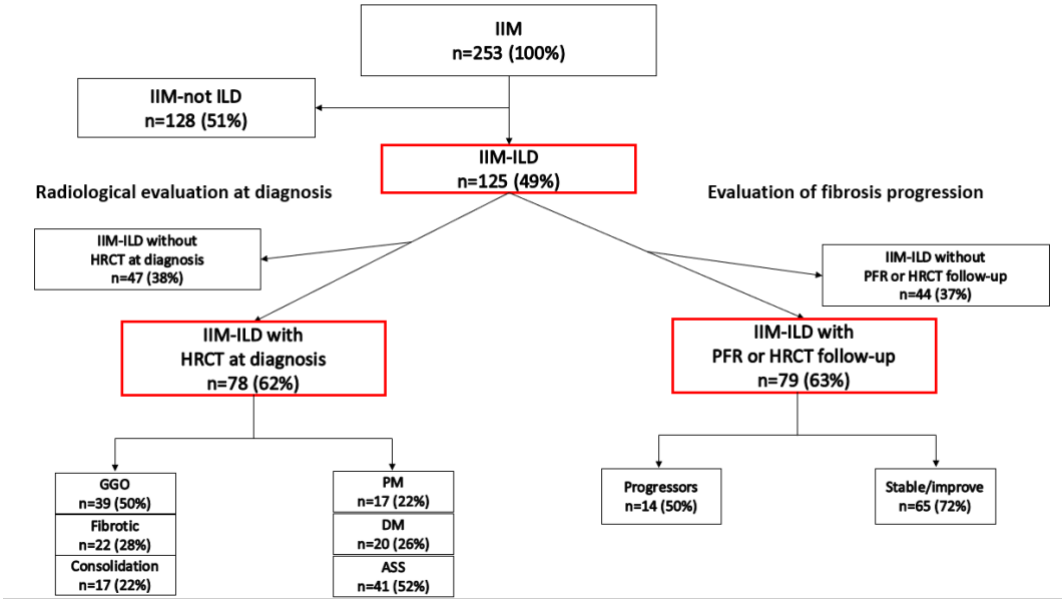

Figure. 1 Flow-chart of the idiopathic inflammatory myopathies (IIM) population. The IIM population has been characterized in two groups according to the presence (IIM-ILD) or absence (IIM-notILD) of interstitial lung involvement on chest CT scan. Moreover, the IIM-ILD population has been categorized according to the main radiological pattern detectable on CT scan at diagnosis and according to the progressive fibrosing criteria[14].

Radiological Evaluation at Diagnosis

Patients with a HRCT at ILD diagnosis available to be reviewed by expert thoracic radiologists were considered and categorized in three groups on the basis of the predominant radiological pattern (**Figure 1**). The first group presented ground glass opacities (GGO), with few or none superimposed consolidations, and was named 'GGO'. The second group presented fibrotic changes, such as reticulation and bronchiectasis, with few or none GGO and consolidations, and was named 'FC. The third group presented a prevalence of consolidations, superimposed to GGO and FC, and was named 'C'. Examples of the three patterns are presented in **Figure 2**. The same IIM-ILD population with available CT scan was also grouped based on the three more frequent IIM diagnosis: i.e. polymyositis (PM), dermatomyositis (DM) and antisynthetase syndrome (ASS) groups and the differences in radiological presentation among the three radiological groups was analyzed.

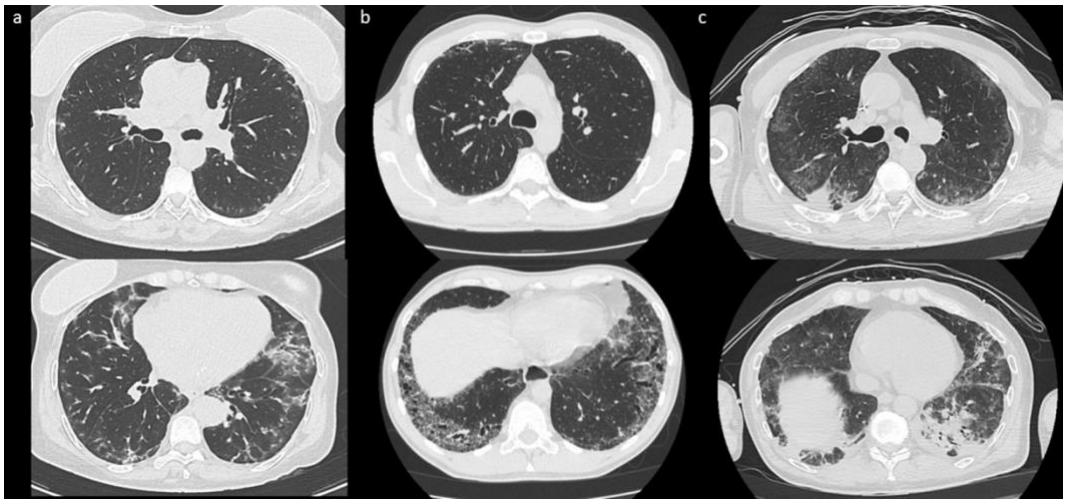

Figure 1. Examples of chest CT patterns in IIM-ILD patients. Axial Chest CT images of: a 60 years old woman with antisynthetase syndrome (aSS) and ground glass opacities (**Panel a**); a 77 years old woman with aSS and fibrotic changes (**Panel b**); a 69 years old man with aSS and a consolidative pattern (**Panel c**).

Identification of progressive fibrosing IIM-ILD patients

To evaluate the progression towards fibrosis in the study population, we subgrouped the patients according to the latest definition of progressive pulmonary fibrosis (PPF)[14]. In particular, patients presenting in the first year after the ILD diagnosis, at least two of the following three characteristics were classified as progressors and compared to stables: (a) the presence of two of the following criteria: a worsening of respiratory symptoms; (b) a functional deterioration [defined by an absolute decline in FVC of more than 5% and in DLCO (corrected for Hb) of more than 10% within 1 year of follow-up], and (c) a radiologic decline (identified as the increase extent of traction bronchiectasis, reticular abnormality, honeycombing, a new ground-glass opacity and increased lobar volume loss) (**Figure 3**). The groups were then compared to evaluate possible clinical, functional or serological data predictive for progression in IIM-ILD. We also evaluated the anti-inflammatory pharmacological treatment during the first year after the ILD diagnosis to search for possible differences in the two groups.

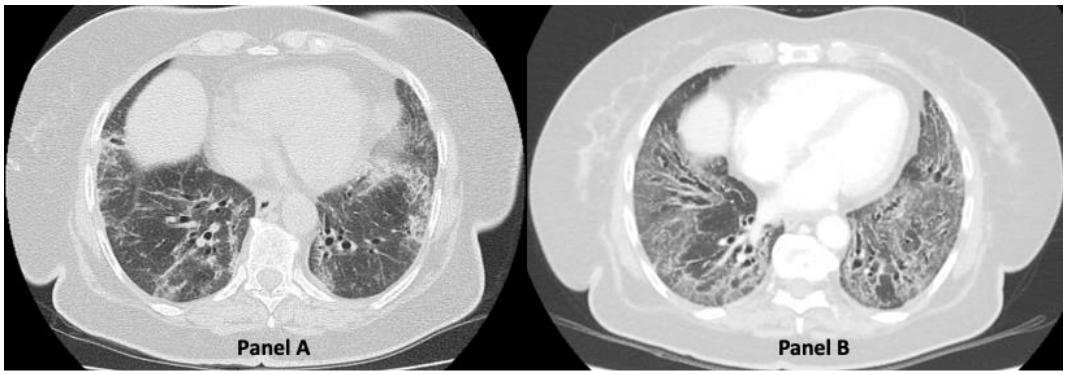

Figure 1. Radiologic progression after one year of treatment. CT images of a 77 years old woman at baseline (**Panel A**) and after the first year of treatment (**Panel B**) showing radiological features consistent with progression.

Ethics Statement

This was a retrospective study on anonymized patient's data collected from medical records. The study protocol complies to the ethical guidelines of the 1975 Declaration of Helsinki and, in agreement with national regulation on retrospective observational studies, it was notified and approved by the local ethics committees, need for patient's informed consent was waived due to the retrospective nature of the study (AOP2093).

Statistical analysis

Continuous variables were expressed as means ± standard deviation (SD) or medians (25th and 75th interquartile range) and categorical variables as frequencies and percentages. Comparison between groups was performed using the Mann–Whitney U-test for continuous variables; and the chi-squared test or Fisher's exact probability test for categorical data, where appropriate. Variables which were found to be different ($p < 0.05$) between patients with and without ILD at univariate analysis, were then included in a multivariate logistic regression model, adjusted for age and sex. Two-sided $p < 0.05$ was considered statistically significant. The statistical analysis was performed using the SPSS statistical package, version 22.0.

RESULTS

Baseline demographic and clinical characteristics

Two hundred fifty-three patients affected by IIMs were included in the study, 183 females (72%), median age at diagnosis 55 (46-66) years. Among the overall population, 125 (49.4%; 89 female) had ILD, of which 91 (36.3%) had ILD

at baseline. Baseline demographic characteristics of the study population are reported in **Table 1**. The median follow-up was 6 (3-10) years, similar in patients with or without ILD (p=0.440).

Considering IIMs subgroups (**Table 1**), most patients were affected with dermatomyositis (DM) (96/253, 38%), followed by anti-synthetase syndrome (77/253, 30%) and polymyositis (PM) (67/253, 27%). IIMs-ILD patients less frequently had a diagnosis of both PM and DM vs. patients without ILD. Diagnosis of necrotizing autoimmune myopathy (NAM) and inclusion body myositis (IBM) were found exclusively in patients without ILD.

Glucocorticoids were prescribed at a higher dose in patients without ILD, albeit with a similar frequency in the two groups. Patients without ILD were more frequently treated with methotrexate and intravenous immunoglobulins, whereas mycophenolate mofetil, azathioprine, cyclophosphamide and Rituximab were more frequently prescribed in IIMs-ILD patients.

Table 1. **Baseline clinical and laboratories features of the overall IIMs population, categorized in NOT associated ILD or IIMs-associated ILD.**

	Overall population (n=253)	**IIMs-NOT ILD (n=128)**	**IIMs-ILD (n=125)**	**p**
Female - *n (%)*	183 (72)	94 (73)	89 (71)	0.69
Age at diagnosis - *yr*	55 (46 - 66)	54 (41 - 67)	57 (49 - 66)	0.056
Follow-up duration - yr	6 (3 - 10)	6 (3 - 10)	5 (3 - 9)	0.44
Muscle biopsy - *n (%)*	108 (43)	70 (55)	38 (30)	<0.0001
Muscle biopsy abnormalities - *n (%)*	95 (38)	62 (48)	33 (26)	<0.0001
Magnetic resonance imaging (MRI) - *n (%)*	109 (43)	65 (51)	44 (35)	0.01
MRI abnormalities - *n (%)*	96 (40)	63 (49)	33 (26)	0.0002
Myositis (biopsy and/or MRI) - *n (%)*	155 (61)	97 (76)	58 (46)	<0.0001
Polymyositis – *n (%)*	67 (27)	41 (32)	26 (21)	0.047
Dermatomyositis – *n (%)*	96 (38)	67 (52)	29 (23)	<0.0001
Inclusion body myositis – *n (%)*	5 (2)	5 (4)	0 (0)	0.06
Necrotizing autoimmune myopathy – *n (%)*	8 (3)	8 (6)	0 (0)	0.007

Anti-synthetase Syndrome – *n (%)*	77 (30)	7 (5)	70 (56)	<0.0001
History of cancer – *n (%)*	37 (15)	20 (16)	17 (14)	0.64
Arthralgia - n (%)	128 (51)	53 (41)	75 (60)	0.003
Arthritis - n (%)	53 (21)	15 (12)	38 (30)	0.0003
Muscular weakness - n (%)	171 (68)	99 (77)	72 (58)	0.001
Fever - n (%)	48 (19)	15 (12)	33 (26)	0.004
Fatigue- n (%)	119 (47)	60 (47)	59 (47)	0.99
Heliotropic rash - n (%)	74 (29)	56 (44)	18 (14)	<0.0001
Gottron's papules - n (%)	40 (16)	23 (18)	17 (14)	0.39
Gottron's sign - n (%)	37 (15)	24 (19)	13 (10)	0.08
Mechanic's hands - n (%)	30 (12)	4 (3)	26 (21)	<0.0001
Raynaud's phenomenon (RP) - n (%)	47 (19)	16 (13)	31 (25)	0.02
Dysphonia - n (%)	9 (4)	3 (2)	6 (5)	0.33
Dysphagia - n (%)	58 (23)	42 (33)	16 (13)	0.0002
Xerostomia - n (%)	23 (9)	9 (7)	14 (11)	0.28
Xerophthalmia - n (%)	21 (8)	8 (6)	13 (10)	0.26
Dyspnea - n (%)	68 (27)	8 (6)	60 (48)	<0.0001
Cough - n (%)	26 (10)	2 (1)	24 (19)	<0.0001
CPK at diagnosis - U/L	674 (128 - 3268)	1264 (173 - 4960)	433 (100 - 2255)	0.001
MMT-8 at diagnosis	140 (120-150)	133.5 (112-148)	148 (130-150)	<0.0001
Myositis-specific antibodies - *n (%)*	138 (55)	51 (40)	87 (70)	<0.0001
Myositis-associated antibodies - *n (%)*	87 (34)	12 (9)	75 (60)	<0.0001
Anti-synthetase - *n (%)*	120 (47)	47 (37)	73 (58)	0.0003
Antinuclear antibodies - *n (%)*	162 (64)	74 (58)	88 (70)	0.049
Anti-Jo-1 - *n (%)*	63 (25)	7 (5)	56 (45)	<0.0001
Anti-PL12 - *n (%)*	13 (5)	4 (3)	9 (7)	0.14
Anti-PL7 - *n (%)*	14 (6)	6 (5)	8 (6)	0.55
Anti - PM/Scl - *n (%)*	29 (11)	12 (9)	17 (14)	0.29
Anti-SSA/Ro - *n (%)*	80 (32)	23 (18)	57 (46)	<0.0001
Anti-SSB/La - *n (%)*	10 (4)	6 (5)	4 (3)	0.54

Anti-U1RNP – *n (%)*	9 (3)	6 (5)	3 (2)	0.33
Anti-Ku - *n (%)*	9 (3)	4 (3)	5 (4)	0.71
Anti-TIF1γ - n (%)	7 (3)	6 (5)	1 (1)	0.12
Anti-Ro52 - n (%)	44 (17)	11 (8)	33 (26)	0.0002
Anti-MDA5 - n (%)	10 (4)	1 (1)	9 (7)	0.01
Anti-EJ - n (%)	4 (1.5)	1 (1)	3 (2)	0.37
Anti-SRP - n (%)	16 (6)	12 (9)	4 (3)	0.07
Anti-Mi2 - n (%)	21 (8)	17 (13)	4 (3)	0.005
Anti-SAE1 - n (%)	3 (1)	3 (2)	0	0.25

Values are expressed as numbers and (%) or median and ranges, as appropriate. Chi squared test and Fisher t test (n < 5) were used for categorical variables. Mann-Whitney U test was used for continuous variables. CPK, Creatine PhosphoKinase; MDA5, anti-melanoma differentiation-associated gene; MMT, manual muscle testing. SAE, small ubiquitin-like modifier-1 activating enzyme; SRP, signal recognition particle TIF1γ, transcription intermediary factor 1-gamma.

Serological and clinical features in patients with and without ILD

Patients affected with ILD more frequently had MSAs and MAAs ($p<0.0001$ for both), and antinuclear and antisynthetase antibodies positivity ($p=0.0003$) (**Table 1**). Considering antibody specificity, anti-Jo1 ($p<0.0001$), anti-SSA/Ro ($p<0.0001$), anti-Ro52 ($p=0.0002$) and anti-MDA5 ($p=0.01$) were more frequently found in IIMs patients with ILD than in those without. By contrast, anti-Mi 2 was more frequently detected in patients without ILD ($p=0.005$). CPK values were higher and MMT-8 score was lower at IIM diagnosis in patients without ILD, with the histological and/or MRI findings specific for myositis in a higher percentage of patients without ILD compared to IIMs with ILD ($p<0.0001$). Patients with ILD more frequently had fever, articular involvement, Raynaud's phenomenon and mechanic's hands. By contrast, dysphagia and heliotrope rash were more frequently reported in patients without ILD (**Table 1**).

Factors associated with ILD at univariate and multivariate analysis

At univariate analysis for the development of ILD (**Table 2**), age at diagnosis, anti-Jo1, anti-Ro52, anti-MDA5, Raynaud's phenomenon and mechanic's hands, as well as articular involvement were associated with ILD. By contrast, anti-Mi 2 positivity, muscular involvement, dysphagia and heliotrope rash were more frequent in patients without ILD.

The multivariate analysis identified higher values of MMT-8, anti-Jo1, anti-MDA5, and anti-Ro52 positivity, Raynaud's phenomenon and mechanic's hands as variables independently associated with ILD in patients with IIMs. Heliotrope rush resulted in an independent protective factor for the occurrence of ILD (**Table 2**).

Table 2. Predictive factors of IIMs-associated ILD in the overall population

	Univariate analysis		**Multivariate analysis**	
	OR (95% IC)	p	OR (95% IC)	p
Sex - (male vs. female)	1.14 (0.66 – 1.98)	0.62	-	-
Age at diagnosis (yr, ≥ 55 vs. < 55)	1.71 (1.04 – 2.80)	0.03	1.62 (0.73 – 3.57)	0.22
CPK at diagnosis – U/L	1.0 (1.0 – 1.0)	0.36	-	-
Antinuclear antibodies (yes vs. no)	1.62 (0.95 – 2.75)	0.07	1.55 (0.68 – 3.51)	0.29
Anti - Jo-1 (yes vs. no)	13.1 (5.64 – 30.2)	**< 0.0001**	4.48 (1.09 – 19.1)	**0.04**
Anti - Ro52 (yes vs. no)	5.64 (2.74 – 11.60)	**< 0.0001**	3.90 (1.42 – 10.7)	**0.008**
Anti-MDA5 (yes vs. no)	9.30 (1.16 – 74.6)	**0.03**	10.9 (1.09 – 107.8)	**0.04**
Anti-Mi 2 (yes vs. no)	0.20 (0.06 – 0.62)	0.005	0.34 (0.06 – 1.98)	0.23
Arthritis (yes vs. no)	3.33 (1.69 – 6.53)	< 0.0001	0.97 (0.30 – 3.07)	0.96
Muscular weakness (yes vs. no)	0.37 (0.21 – 0.66)	0.001	0.68 (0.28 – 1.63)	0.39
Heliotrope rash (yes vs. no)	0.20 (0.11 – 0.37)	**< 0.0001**	0.25 (0.08 – 0.77)	**0.01**
Dysphagia (yes vs. no)	0.28 (0.15 – 0.54)	< 0.0001	0.51 (0.19 – 1.37)	0.18
Mechanic's hands (yes vs. no)	7.67 (2.58 – 22.7)	**< 0.0001**	8.56 (1.95 – 37.6)	**0.004**
Raynaud's phenomenon (yes vs. no)	2.32 (1.18 – 4.57)	**0.01**	3.17 (1.22 – 7.66)	**0.02**
MMT-8	1.02 (1.01 – 1.04)	**< 0.0001**	1.02 (1.00 -1.04)	**0.03**

Values are expressed as OR (95%CI). Logistic regression analysis was used to determine the relationship between clinical data and the occurrence of pulmonary involvement.
CPK, Creatine PhosphoKinase; MDA5, anti-melanoma differentiation-associated gene; MMT, manual muscle testing.

Radiological patterns

In 78 of 125 (62%) of IIM-ILD patients HRCT scan was available at baseline for our radiological evaluation. Based on the predominant radiologic pattern, patients were grouped in GGO (n=39, 50%), FC (n=22, 28%), and C (n=17,

22%) groups. Demographic, clinical, serological and functional data are summarized in **Table 3**.

The three groups did not differ in regards of sex, age, both at IIM and ILD diagnosis, and lag-time from onset of rheumatologic symptoms to IIM diagnosis. The groups did not differ neither for the IIM diagnosis, with a prevalence of patients affected by aSS in all the three groups. The C group anticipated the diagnosis of IIM [0 years, range (-8 – 0)] compared to GGO [0 (-1 – 24), p=0.01], but not to FC [0 (-5 – 13)]. Moreover, the C group displayed a significant increase of creatine phosphokinase (CPK) levels compared to FC (1380 U/L vs. 121; p=0.01), but not to GGO (252 U/L; p=ns). However, the absolute number of patients with CPK elevation did not differ between the groups. C presented a lower manual muscular test (MMT) compared to GGO (120 vs.145; p=0.008) and FC (150; p=0.003) while FC group presented fewer patients with an impaired MMT value compared to GGO (36% vs 59%; p=0.04) and compared to C (82% C, p=0.004).

GGO presented more preserved FVC% pred. value compared to FC [89% pred., (57 – 132) vs 74 (53 – 117); p = 0.007] and C [72 (54 – 109; p = 0.003]. When IIM-ILD population with available CT scan was grouped based on the three more frequent IIM diagnosis (PM, DM and ASS) no difference in clinical and radiological presentation was evident among groups (Table 1 Supplement).

IIM-ILD population, sub-grouped for radiological presentation, did not differ regarding autoantibody positivity, with the exception of anti-SSB antibodies which were present only in 2 (12%) C patients (p=0.04) (Table 2 Supplement). Regarding symptoms at IIM diagnosis, the three groups differed regarding myalgia (p=0.001), and asthenia (p=0.02), in both cases with FC group presenting a significantly minor prevalence of the symptom (Table 3 Supplement). At ILD diagnosis, the groups differed regarding dyspnea (p=0.006), with a lower prevalence in the GGO patient, and arthritis (p=0.006), with GGO patients presenting a significant prevalence of the symptom (Table 4 Supplement).

Table 3. Baseline demographics and functional parameters of IIM-ILD population, categorized among radiological patterns.

	Total population n=78	**GGO n=39**	**Fibrotic n=22**	**Consolidation n=17**	**p value**
Male - *n (%)*	23 (29)	12 (31)	6 (27)	5 (29)	0.96
Female – *n (%)*	55 (71)	27 (69)	16 (73)	12 (71)	

Age at myositis diagnosis - *years*	57 (50-66)	57 (51-64)	58 (48-70)	57 (50-62)	0.90
Age at ILD diagnosis – *years*	57 (50-66)	57 (51-64)	60 (49-69)	57 (50-62)	0.70
Lag time symptoms-diagnosis - *years*	0 (0-1)	0.5 (0-1)	0 (0-1)	0 (0-1)	0.17
Time from myositis diagnosis to ILD - *years*	0 (-8 - 24)	0 (-1-24)	0 (-5-13)	0 (-8-0)	**0.04**
Follow up duration - years	4 (2-6)	5 (3-7)	5.5 (3-7)	3 (2-3)	0.055
PM - *n (%)*	17 (22)	9 (23)	6 (27)	2 (12)	0.34
DM - *n (%)*	20 (26)	13 (33)	3 (14)	4 (24)	
aSS - *n (%)*	41 (53)	17 (44)	13 (59)	11 (65)	
CPK at diagnosis – U/L	567 (100-2117)	525 (139-2005)	121 (80-672)	1380 (157-3339)	**0.04**
CPK increase at diagnosis – *n (%)*	47 (60)	25 (64)	10 (45)	12 (71)	0.22
MMT at diagnosis	145 (122-150)	145 (134-150)	150 (135-150)	120 (105-146)	**0.005**
MMT reduced at diagnosis – *n (%)*	45 (58)	23 (59)	8 (36)	14 (82)	**0.02**
Myositis (biopsy and/or MR) - *n (%)*	42 (54)	19 (49)	11 (50)	12 (71)	0.29
Immunosuppression at ILD diagnosis *n - %*	41 (53)	20 (51)	13 (59)	8 (47)	0.74
FVC at ILD diagnosis - L	2.56 (2.16-3.21)	2.92 (2.44-3.23)	2.56 (1.7-2.83)	2.38 (2.18-2.67)	0.08
FVC at ILD diagnosis - % pred.	84 (70-94)	89 (80-111)	74 (60-92)	72 (58-88)	**0.003**
TLC at ILD diagnosis – L	4.43 (3.56-4.97)	4.58 (3.89-5.55)	4.17 (3.25-4.79)	4.59 (3.54-4.68)	0.45
TLC at ILD diagnosis - % pred.	81 (65-90)	85 (71-99)	75 (61-89)	82 (69-86)	0.13
DLCO at ILD diagnosis - % pred.	58 (42-69)	58 (46-77)	49 (40-66)	58 (45-66)	0.41
KCO at ILD diagnosis - % pred.	81 (64-90)	78 (61-94)	78 (62-85)	86 (74-88)	0.74
Deaths – *n (%)*	1 (1)	0 (0)	1 (5)	0 (0)	na

Values are expressed as numbers and (%) or median and 25^{th} - 75^{th} , as appropriate. Chi square test and Fisher t test (n < 5) for categorical variables and Kruskal-Wallis test for continuous variables were used.

Evaluation of Fibrosis Progression

A functional and radiological one-year follow-up was available in 79 patients. Patients were grouped as progressors (n=14, 18%), when they presented at least two between FVC% reduction equal or major of 5% at 1-year follow-up, progression toward fibrosis at chest CT scans, and worsening of symptoms, characterizing a progressive pulmonary fibrosis. Patients not presenting these

features were categorized as stable/improved (n=65, 82%). Demographic, clinical, serological and functional data are summarized in **Table 4**.

The groups did not differ in regards of sex, age, both at IIM and ILD diagnosis, and lag-time from insurgency of rheumatologic symptoms to IIM diagnosis, or from IIM diagnosis and ILD diagnosis. Progressors and stable/improved patients did not differ either for the IIM diagnosis. Three (3 – 4%) patients died during the follow-up, 1 (7%) in the progressors group, 2 (3%) in the stable/improved, with no statistically significant difference. The two populations presented no significant difference regarding signs of muscle injury, such as CPK increasing or MMT impairment at IIM diagnosis, nor they differed regarding functional values at ILD diagnosis.

Autoantibody positivity, alongside rheumatologic impairment, both at ILD diagnosis, are summarized in the online supplement (Table 5 Supplement). The progressors group presented a higher prevalence of anti-MDA5 antibodies compared to stables (29% vs 6%, p=0.03), with no other significant differences among other autoantibodies. Regarding symptoms at IIM diagnosis, the progressors group presented a higher prevalence of xerophthalmia and xerostomia compared to stables (29% vs. 8%, p=0.047 for both cases). The major prevalence in the progressors group of xerophthalmia (29% vs 5%, p=0.02) and xerostomia (36% vs 6%, p=0.007) was confirmed at ILD diagnosis. Furthermore, at ILD diagnosis the progressors presented a higher prevalence of heliotrope rash (29% vs. 5%, p=0.02). Regarding pharmacological treatment, the two groups did not differ during the first year after ILD diagnosis, as summarized in (Table 6 Supplement). Both groups used steroids in a high percentage of cases (93 vs 86%, p=0.49) with similar initiation dosages, 25 mg die in both groups. The second most used drug was Mycophenolate with similar prevalence both in progressor than in stable/improve groups (36 vs 32%, p=0.81).

Table 4. Baseline demographics and functional parameters of the IIM-ILD population, categorized in progressors and stable/improve.

	Total population n=79	**Progressors n=14**	**Stable/improve n=65**	**p value**
Male – *n (%)*	24 (30)	5 (36)	19 (29)	0.75
Female – *n (%)*	55 (70)	9 (64)	46 (71)	
Age at diagnosis - *years*	57 (18 - 83)	57.5 (44 - 81)	57 (18 - 83)	0.82

Age at ILD diagnosis - *years*	58 (18 - 80)	57 (44 - 80)	58 (18 - 79)	0.99
Lag time symptoms-diagnosis - *years*	0 (0 – 16)	0.25 (0 – 5)	0 (0 – 16)	0.34
Time from diagnosis to ILD - *years*	0 (-8 – 24)	0 (-3 – 1)	0 (-8 – 24)	0.23
Follow up duration - years	4 (0 – 32)	2 (0.25 – 13)	5 (0 – 32)	**0.047**
PM - *n (%)*	16 (20)	3 (21)	13 (20)	0.95
DM - *n (%)*	15 (19)	3 (21)	12 (18)	
ASS - *n (%)*	48 (61)	8 (57)	40 (62)	
CPK at diagnosis – U/L	179 (31 – 7000)	128 (40 – 4500)	400 (31 – 7000)	0.30
CPK increase at diagnosis – *n (%)*	38 (48)	5 (36)	33 (51)	0.38
MMT at diagnosis	150 (70 – 150)	150 (70 - 150)	150 (70 - 150)	0.88
MMT reduced at diagnosis – *n (%)*	38 (48)	6 (43)	32 (49)	0.77
Myositis (biopsy and/or MR) - *n (%)*	34 (43)	3 (21)	31 (48)	0.08
FVC at ILD diagnosis - L	2.58 (1.21 – 4.22)	3.27 (1.56 – 4.08)	2.57 (1.21 – 4.22)	0.29
FVC at ILD diagnosis - % pred.	84 (47 – 146)	89 (53 – 146)	83 (47 – 121)	0.36
TLC at ILD diagnosis - L	4.43 (2.22 – 7.30)	4.27 (3.06 – 5.39)	4.54 (2.22 – 7.30)	0.78
TLC at ILD diagnosis - % pred.	80 (47 – 126)	79 (62 – 126)	80 (47 – 119)	0.94
DLCO at ILD diagnosis - % pred.	58 (28 – 102)	59 (35 – 91)	55 (21 – 102)	0.68
KCO at ILD diagnosis - % pred.	78 (42 – 143)	83 (66 – 99)	77 (42 – 143)	0.51
Immunosuppression at ILD diagnosis - *n (%)*	38 (48)	5 (36)	33 (51)	0.38
Deaths - *n (%)*	3 (4)	1 (7)	2 (3)	0.45

Values are expressed as numbers and (%) or median and Q1-Q3 as appropriate. Chi square test and Fisher t test (n < 5) for categorical variables and Mann-Whitney U test for continuous variables were used. *progression was defined as annual FVC%pred. decline >= 5% or radiological impairment after 12 months of follow up.

Univariate and Multivariate Evaluation of Fibrosis Progression Risk

At univariate analysis for progression towards fibrosis (**Table 5**), anti-MDA5 (OR: 6.10; 95%CI 1.30 – 28.4, p=0.02), heliotrope rash at ILD diagnosis (8.00; 95%CI 1.55 – 41.23, p=0.01), and xerostomia and xerophthalmia at ILD diagnosis (8.19; 95%CI 1.84 – 36.36, p=0.006; and 8.00; 95%CI 1.55 – 41.2, p=0.01, respectively), were associated with progression. However, any of the features statistically significant at the univariate analysis was confirmed as an independent predictor of progression towards fibrosis at the multivariate analysis.

Table 5. Predictive factors of progression in IIM-ILD population.

	Univariate analysis		Multivariate analysis	
	OR (95% IC)	**p**	**OR (95% IC)**	**p**
Sex – (male vs female)	1.34 (0.39 – 4.54)	0.63	-	-
Age at diagnosis ILD (yr, ≥ 58 vs < 58)	0.50 (0.15 – 1.67)	0.26	-	-
Time from diagnosis to ILD - *years*	0.87 (0.65 – 1.17)	0.38	-	-
Anti - MDA5 (yes vs no)	6.10 (1.30 – 28.4)	**0.02**	4.00 (0.53 – 29.8)	0.17
Mechanic hands (yes vs no)	1.09 (0.26 – 4.48)	0.90	-	-
CPK at myositis diagnosis	1.00 (0.99 – 1.00)	0.40	-	-
MMT at diagnosis	0.99 (0.96 – 1.02)	0.75	-	-
Heliotropic rash at ILD diagnosis (yes vs no)	8.00 (1.55 – 41.23)	**0.01**	0.87 (0.13 – 5.65)	0.88
Xerostomia at ILD diagnosis (yes vs no)	8.19 (1.84 – 36.36)	**0.006**	2.61 (0.23 – 28.6)	0.43
Xerophtalmia at ILD diagnosis (yes vs no)	8.00 (1.55 – 41.2)	**0.01**	1.17 (0.08 – 16.1)	0.90
GGO (yes vs no)	0.72 (0.19 – 2.73)	0.63	-	-
Fibrotic (yes vs no)	2.50 (0.68 – 9.08)	0.16	-	-
Consolidation (yes vs no)	0.50 (0.09 – 2.57)	0.40	-	-
FVC (% pred.)	1.02 (0.99 – 1.05)	0.18	-	-
FVC (L)	1.95 (0.67 – 5.70)	0.22	-	-
DLCO (% pred.)	1.07 (0.97 – 1.04)	0.70	-	-

Values are expressed as OR (95%CI). Logistic regression analysis was used to determine the relationship of clinical data and the occurrence of progressive phenotype.

SUPPLEMENTARY MATERIAL

Table S1. Baseline demographics and functional parameters of the IIM-ILD population, categorized among myositis diagnosis.

	Total population n=78	PM n=17	DM n=20	aSS n=41	p value
Male - *n (%)*	23 (29)	6 (35)	7 (35)	10 (24)	0.58
Female - *n (%)*	55 (71)	11 (65)	13 (65)	31 (76)	
Age at myositis diagnosis - *years*	57 (50-66)	62 (53-71)	57 (51-60)	57 (50-65)	0.25
Age at ILD diagnosis - *years*	57 (50-66)	62 (57-69)	57 (53-61)	57 (50-65)	0.22
Lag time symptoms-diagnosis - *years*	0 (0-1)	0.5 (0-1)	0 (0-1)	0 (0-1)	0.51
Time from myositis diagnosis to ILD - *years*	0 (0-0)	0 (-1-1)	0 (0-1)	0 (0-0)	0.14
Follow up duration - years	4 (2-6)	6 (3-6)	4 (3-7)	4 (2-6)	0.55
GGO - *n (%)*	17 (22)	9 (53)	13 (65)	17 (41)	0.33
FC - *n (%)*	20 (26)	6 (35)	3 (15)	13 (32)	
C - *n (%)*	41 (53)	2 (12)	4 (20)	11 (27)	
CPK at diagnosis – U/L	567 (100-2117)	484 (102-1257)	659 (97-1383)	532 (100-3099)	0.67
CPK increase at diagnosis – *n (%)*	47 (60)	9 (53)	13 (65)	25 (61)	0.75
MMT at diagnosis	145 (122-150)	150 (130-150)	143 (129-150)	145 (121-150)	0.90
MMT reduced at diagnosis – *n (%)*	45 (58)	8 (47)	12 (60)	24 (59)	0.68
Myositis (biopsy and/or MR) - *n (%)*	42 (54)	10 (59)	12 (60)	20 (49)	0.64
Immunosuppression at ILD diagnosis - *n (%)*	41 (53)	9 (53)	14 (70)	18 (44)	0.16
FVC at ILD diagnosis - L	2.56 (2.16-3.21)	2.54 (2.11-3.19)	2.83 (2.57-3.2)	2.55 (2.16-3.21)	0.36
FVC at ILD diagnosis - % pred.	84 (70-94)	86 (74-96)	87 (77-95)	83 (57-93)	0.26
TLC at ILD diagnosis - L	4.43 (3.56-4.97)	4.67 (4.06-5.11)	4.62 (3.70-5.53)	4.20 (3.25-4.64)	0.31
TLC at ILD diagnosis - % pred.	81 (65-90)	82 (70-98)	81 (70-92)	79 (63-88)	0.41
DLCO at ILD diagnosis - % pred.	58 (42-69)	68 (52-79)	50 (42-63)	56 (38-65)	0.08
KCO at ILD diagnosis - % pred.	81 (64-90)	87 (84-94)	75 (68-85)	73 (55-88)	0.10
Deaths – *n (%)*	1 (1)	1 (6)	0 (0)	0 (0)	0.22

Values are expressed as numbers and (%) or median and Q1-Q3 as appropriate. Chi square test and Fisher t test (n < 5) for categorical variables and Kruskal-Wallis test for continuous variables were used.

Table S2. Baseline Autoantibody Positivity of the IIM-ILD population, categorized among radiological pattern.

	Total population n=78	GGO n=39	Fibrotic n=22	Consolidation n=17	p value
Myositis-specific antibodies - *n (%)*	54 (69)	27 (69)	14 (63)	13 (76)	0.69
Myositis-associated antibodies - *n (%)*	47 (60)	21 (54)	14 (63)	12 (71)	0.46
Anti-synthetase - *n (%)*	40 (51)	21 (54)	9 (41)	10 (59)	0.49
ENA - *n (%)*	51 (65)	23 (59)	15 (68)	13 (76)	0.43
ANA - *n (%)*	53 (68)	28 (72)	13 (59)	12 (71)	0.57
Anti- Jo1 - *n (%)*	32 (41)	14 (36)	9 (41)	9 (53)	0.49
Anti - PL12 - *n (%)*	6 (8)	2 (5)	4 (18)	0 (0)	0.09
Anti - PL7 - *n (%)*	6 (8)	4 (10)	1 (5)	1 (6)	0.86
Anti - Pm/scl - *n (%)*	12 (15)	6 (15)	4 (18)	2 (12)	0.92
Anti - SSA - *n (%)*	32 (41)	15 (38)	7 (32)	10 (59)	0.21
Anti - SSB - *n (%)*	2 (2)	0 (0)	0 (0)	2 (12)	**0.04**
Anti - U1RNP - *n (%)*	2 (2)	1 (3)	0 (0)	1 (6)	0.46
Anti - Ku - *n (%)*	3 (4)	3 (8)	0 (0)	0 (0)	0.30
Anti - ALP - *n (%)*	0 (0)	0 (0)	0 (0)	0 (0)	na
Anti - TIF1G - *n (%)*	1 (1)	1 (3)	0 (0)	0 (0)	1.00
Anti - Ro52 - *n (%)*	28 (36)	11 (28)	7 (32)	10 (59)	0.08
Anti - MDA5 - *n (%)*	7 (9)	4 (10)	0 (0)	3 (18)	0.13
Anti - EJ - *n (%)*	1 (1)	1 (3)	0 (0)	0 (0)	1.00
Anti - SRP - *n (%)*	2 (2)	1 (3)	1 (5)	0 (0)	1.00
Anti - ASMA - *n (%)*	0 (0)	0 (0)	0 (0)	0 (0)	na
Anti - MI2 - *n (%)*	3 (4)	3 (8)	0 (0)	0 (0)	0.30
Anti - SAE1 - *n (%)*	0 (0)	0 (0)	0 (0)	0 (0)	na
Anti - PM1 - *n (%)*	0 (0)	0 (0)	0 (0)	0 (0)	na

Values are expressed as numbers and (%). Chi square test and Fisher t test ($n < 5$) for categorical variables was used.

Table S3. Baseline Rheumatologic Impairment of the IIM-ILD population at myositis diagnosis, categorized among radiological pattern.

	Total population n=78	GGO n=39	Fibrotic n=22	Consolidation n=17	p value
Myalgia - *n (%)*	40 (51)	24 (62)	4 (18)	12 (71)	**0.001**
Muscular Asthenia - *n (%)*	47 (59)	25 (64)	9 (41)	13 (76)	0.06
Asthenia - *n (%)*	39 (49)	21 (54)	6 (27)	12 (71)	**0.02**
Dyspnea - *n (%)*	36 (46)	17 (44)	9 (41)	10 (59)	0.49
Cough - *n (%)*	19 (24)	8 (21)	6 (27)	5 (29)	0.72
Dysphonia - *n (%)*	4 (5)	2 (5)	2 (9)	0 (0)	0.66
Dysphagia - *n (%)*	12 (15)	4 (10)	5 (23)	3 (18)	0.39
Fever - *n (%)*	21 (27)	10 (26)	5 (23)	6 (35)	0.66
Weight loss - *n (%)*	15 (19)	5 (13)	4 (18)	6 (35)	0.15
Athralgia - *n (%)*	45 (57)	24 (62)	12 (55)	9 (53)	0.79
Arthritis - *n (%)*	26 (33)	18 (46)	4 (18)	4 (24)	0.06
Mechanic hands - *n (%)*	19 (24)	9 (23)	4 (18)	6 (35)	0.45
Heliotropic rash - *n (%)*	15 (19)	7 (18)	4 (18)	4 (24)	0.87
Raynaud's phenomenon - *n (%)*	19 (24)	10 (26)	5 (23)	4 (24)	1.00
Gottron's sign - *n (%)*	10 (13)	5 (13)	2 (9)	3 (18)	0.82
Gottron's papules – *n (%)*	10 (13)	5 (13)	1 (5)	4 (24)	0.22
Calcinosis - *n (%)*	2 (3)	1 (3)	0 (0)	1 (6)	0.47
Neuropaty - *n (%)*	8 (10)	3 (8)	2 (9)	3 (18)	0.55
Xeroftalmia - *n (%)*	12 (15)	6 (15)	2 (9)	4 (24)	0.47
Xerostomia - *n (%)*	9 (11)	5 (13)	1 (5)	3 (18)	0.37
Uveitis - *n (%)*	0 (0)	0 (0)	0 (0)	0 (0)	na
Myocarditis - *n (%)*	2 (3)	2 (5)	0 (0)	0 (0)	0.70

Values are expressed as numbers and (%). Chi square test and Fisher t test (n < 5) for categorical variables was used.

Table S4. Baseline Rheumatologic Impairment of the IIM-ILD population at ILD diagnosis, categorized among radiological pattern.

	Total population n=78	**GGO n=39**	**Fibrotic n=22**	**Consolidation n=17**	**p value**
Myalgia - *n (%)*	36 (46)	18 (46)	7 (32)	11 (65)	0.12
Muscular Asthenia - *n (%)*	35 (44)	15 (38)	9 (41)	11 (65)	0.17
Asthenia - *n (%)*	44 (56)	19 (49)	14 (64)	11 (65)	0.39
Dyspnea - *n (%)*	40 (51)	13 (33)	15 (68)	12 (71)	**0.006**
Cough - *n (%)*	22 (28)	9 (23)	7 (32)	6 (35)	0.59
Dysphagia - *n (%)*	10 (13)	6 (15)	1 (5)	3 (18)	0.44
Fever - *n (%)*	17 (22)	7 (18)	5 (23)	5 (29)	0.63
Athralgia - *n (%)*	50 (63)	25 (64)	15 (68)	10 (59)	0.83
Arthritis - *n (%)*	20 (25)	16 (41)	3 (14)	1 (6)	**0.006**
Mechanic hands - *n (%)*	16 (20)	9 (23)	3 (14)	4 (24)	0.71
Heliotropic rash - *n (%)*	11 (14)	5 (13)	3 (14)	3 (18)	0.91
Raynaud's phenomenon - *n (%)*	19 (24)	10 (26)	6 (27)	3 (18)	0.76
Gottron's sign - *n (%)*	8 (10)	4 (10)	2 (9)	2 (12)	1.00
Gottron's papules – *n (%)*	11 (14)	6 (15)	1 (5)	4 (24)	0.24
Neuropaty - *n (%)*	6 (8)	2 (5)	3 (14)	1 (6)	0.54
Xeroftalmia - *n (%)*	7 (9)	5 (13)	0 (0)	2 (12)	0.19
Xerostomia - *n (%)*	9 (11)	6 (15)	2 (9)	1 (6)	0.65
Myocarditis - *n (%)*	1 (1)	1 (3)	0 (0)	0 (0)	1.00

Values are expressed as numbers and (%). Chi square test and Fisher t test (n < 5) for categorical variables was used.

Table S5. Baseline rheumatological blood samples at symptoms at ILD diagnosis of the IIM-ILD population, categorized in progressors and stable/improve.

	Total population n=79	Progressors n=14	Stable/improve n=65	p value
Myositis-specific antibodies - *n (%)*	59 (75)	11 (79)	48 (74)	0.38
Myositis-associated antibodies - *n (%)*	44 (56)	5 (36)	39 (60)	0.14
Anti-synthetase - *n (%)*	51 (65)	8 (57)	43 (66)	0.55
ENA - *n (%)*	60 (76)	11 (79)	49 (75)	0.99
ANA - *n (%)*	56 (71)	8 (57)	48 (74)	0.33
Anti- Jo1 - *n (%)*	36 (46)	5 (36)	31 (48)	0.56
Anti - PL12 - *n (%)*	7 (9)	2 (14)	5 (8)	0.60
Anti - PL7 - *n (%)*	7 (9)	1 (7)	6 (9)	0.99
Anti - Pm/scl - *n (%)*	13 (16)	0 (0)	13 (20)	0.11
Anti - SSA - *n (%)*	37 (47)	6 (43)	31 (48)	0.78
Anti - SSB - *n (%)*	4 (5)	0 (0)	4 (6)	1.00
Anti - U1RNP - *n (%)*	3 (4)	1 (7)	2 (3)	0.45
Anti - Ku - *n (%)*	3 (4)	1 (7)	2 (3)	0.45
Anti - ALP - *n (%)*	0 (0)	0 (0)	0 (0)	na
Anti - TIF1G - *n (%)*	0 (0)	0 (0)	0 (0)	na
Anti - Ro52 - *n (%)*	28 (35)	4 (29)	24 (37)	0.76
Anti - MDA5 - *n (%)*	8 (10)	4 (29)	4 (6)	**0.03**
Anti - EJ - *n (%)*	1 (1)	0 (0)	1 (2)	0.99
Anti - SRP - *n (%)*	4 (5)	1 (7)	3 (5)	0.55
Anti - ASMA - *n (%)*	0 (0)	0 (0)	0 (0)	na
Anti - MI2 - *n (%)*	3 (4)	0 (0)	3 (5)	1.00
Anti - SAE1 - *n (%)*	0 (0)	0 (0)	0 (0)	na
Anti - PM1 - *n (%)*	1 (1)	0 (0)	1 (2)	0.99
Myalgia - *n (%)*	30 (34)	5 (36)	25 (38)	0.85
Muscular Asthenia - *n (%)*	35 (44)	6 (43)	29 (45)	0.90
Asthenia - *n (%)*	40 (51)	7 (50)	33 (51)	0.96
Dyspnea - *n (%)*	46 (58)	8 (47)	38 (54)	0.93
Cough - *n (%)*	27 (34)	4 (29)	23 (35)	0.76
Dysphagia - *n (%)*	6 (8)	2 (14)	4 (6)	0.28
Fever - *n (%)*	20 (25)	3 (21)	17 (26)	0.71
Athralgia - *n (%)*	52 (66)	9 (64)	43 (66)	0.89
Arthritis - *n (%)*	19 (24)	5 (36)	14 (22)	0.31
Mechanic hands - *n (%)*	18 (23)	4 (29)	14 (22)	0.73
Heliotropic rash - *n (%)*	7 (9)	4 (29)	3 (5)	**0.02**
Raynaud's phenomenon - *n (%)*	18 (23)	2 (14)	16 (25)	0.63
Gottron's sign - *n (%)*	6 (8)	1 (7)	5 (8)	0.94
Gottron's papules – *n (%)*	8 (10)	2 (14)	6 (9)	0.63
Neuropathy - *n (%)*	4 (5)	0 (0)	4 (6)	1.00
Xerophthalmia - *n (%)*	7 (9)	4 (29)	3 (5)	**0.02**
Xerostomia - *n (%)*	9 (11)	5 (36)	4 (6)	**0.007**
Myocarditis - *n (%)*	1 (1)	0 (0)	1 (2)	0.99
Xerophthalmia - *n (%)*	9 (11)	4 (29)	5 (8)	**0.047**
Xerostomia - *n (%)*	9 (11)	4 (29)	5 (8)	**0.047**
Uveitis - *n (%)*	0 (0)	0 (0)	0 (0)	na
Myocarditis - *n (%)*	2 (3)	0 (0)	2 (3)	0.51

Values are expressed as numbers and (%). Chi square test and Fisher t test (n < 5) for categorical variables was used.

Table 6S. TREATMENT of the IIM-ILD population during the first year after ILD diagnosis, categorized in progressors and stable/improve.

	Total population n=79	Progressors n=14	Stable/improve n=65	p value
Systemic steroids – *n (%)*	69 (87)	13 (93)	56 (86)	0.49
• **Dose at treatment initiation - *mg***	25 (12.5 – 37.5)	25 (10 – 37.5)	25 (12.5 – 46.5)	0.61
Cyclophosphamide – *n (%)*	9 (11)	1 (7)	8 (12)	0.58
Methotrexate - *n (%)*	15 (19)	1 (7)	14 (21)	0.21
Mycophenolate Mofetil – *n (%)*	26 (33)	5 (36)	21 (32)	0.81
Azathioprine - *n (%)*	11 (14)	1 (7)	10 (15)	0.42
Cyclosporine – *n (%)*	5 (6)	0	5 (8)	0.28
Rituximab – *n (%)*	9 (11)	1 (7)	8 (12)	0.58
Intravenous immunoglobulin – *n (%)*	6 (8)	1 (7)	5 (8)	0.94

Values are expressed as numbers and (%) or median and ranges as appropriate. Chi square test and Fisher t test ($n < 5$) for categorical variables and Kruskal-Wallis test for continuous variables were used.

DISCUSSION

IIMs are an umbrella of clinical conditions characterized by an extremely high heterogeneity[4,15].

Although lung disease is the most frequent organ involvement, the risk of developing ILD can vary considerably among patients and shared screening strategies are lacking.

ILD occurred in about half (49.4%) of our cohort of patients with IIMs, with a slight higher frequency than that reported in a recent monocentric study (31.5%)[17]. This discrepancy may be attributable to the different definition of ILD adopted, as the latter study only considered patients with restrictive values (i.e. FVC <80%) on PFTs, likely excluding milder forms of ILD.

Our data suggest older patients at onset of IIMs and those with milder myositis and without dysphagia carry a particularly high risk of developing ILD. Anti-Jo1 positivity, the most frequent anti-synthetase antibody, was confirmed as strongly associated with ILD, as well as anti-Ro52 antibody. The latter has been linked to ILD in several connective tissue disorders, not only IIMs, though data on its prognostic value are conflicting[17,18]. It has been debated whether the association between anti-Ro52 and ILD could be driven by the frequent concomitant positive anti-synthetase antibodies (in particular anti-Jo1)[19,20]; however, it should be emphasized that in our study anti-Ro52 was independently associated with ILD on multivariate analysis. There are also conflicting reports on the association between ILD and positive anti-MDA5, which has been hypothesized to differ among ethnicities (e.g. present in Asians and absent/less strong in Caucasians). In our study anti-MDA5 was found to be associated with ILD, highlighting that Caucasian patients with anti-MDA5 ought to be to be carefully and promptly screened for ILD, also considering the high frequency of rapidly progressive disease course as previously reported[21].

Although specific autoantibodies are partially able to identify some subsets of IIMs and may therefore guide clinicians in daily practice, it bears noting that the detection of several MSAs and MAAs is not yet widely available, especially in non-referral centers. This underlines the importance for clinicians to identify clinical predictors of lung involvement. With this regard, of note, we found that patients with mechanic's hands have a ~15-fold higher risk of developing ILD than those without. This association was also recently reported in Asian patients by Huang et

al.[22,23]. Considering the established ethnic differences in the disease phenotype of IIMs, it was paramount to further investigate this finding in Caucasian patients. Furthermore, although the presence of mechanic's hands is one of the hallmarks of anti-synthetase syndrome[24], it is not present in all patients and it may be found in other types of IIMs as well. Mechanic's hands are easily detectable and their presence may drive clinicians to thoroughly screen patients for ILD at baseline (e.g. by performing HRCT in all IIMs patients presenting this feature) and during follow-up. Interestingly, our multivariate analysis also revealed that patients with higher values of MMT-8 carry a higher ILD risk and another clinical features – i.e. the presence of dysphagia – as the only independent protective factor for ILD, further supporting that clinical evaluation is a cornerstone in the ILD-risk stratification of IIMs patients.

The first presentation of pulmonary involvement at high-resolution Computed Tomography (HRCT) may vary among patients. However, the correlation between radiologic features and clinical presentation is a matter of great interest. Of interest in our subgroup of patients we observed that half of the population presented GGO as the prevalent radiologic pattern, those patients displayed preserved lung function, as compared to patients with predominant consolidative and fibrotic pattern. Patients with consolidation at presentation need a special attention being associated to muscle injury (higher CPK and lower MMT) compared to the other groups and anticipating the diagnosis of IIM. The distribution of the three different CT patterns did not differ among polymyositis (PM), dermatomyositis (DM) and aSS groups.

When we explored disease progression after one year of treatment, we found that almost a fifth of the whole IIM-ILD patients developed a progressive phenotype. Comparing clinical and serological characteristics, at diagnosis, of the two groups (progressors and stable/improved IIM-ILD patients), we observed that both were similar regarding demographic, functional data and treatment while Anti-MDA5 antibodies, heliotropic rash, xerostomia and xerophthalmia are prevalent in the progressive phenotype. These findings were confirmed as progression-associated factors at univariate analysis however, none were confirmed as independent risk factors at multivariate analysis. These first evidences suggested that clinicians have to consider also clinical parameters as potential variables associated to progression.

The main strength of our work lies in the large number of patients included, given that idiopathic inflammatory myopathies are recognized as rare diseases. Furthermore, to the best of our knowledge this is the first large multicenter international study evaluating clinical and serological predictors of ILD in Caucasian patients affected with IIMs, followed-up for a long observational period. We would be remiss not to mention some of the limitations of our study. First, although ours are third level reference centers for connective tissue diseases, there may have been slight differences in patient management and follow-up among centers and in different time periods. Second, given that the study was conducted retrospectively on prospectively collected data, a limited percentage of incomplete data was tolerated.

In conclusion, our study confirms the close association between specific autoantibodies (anti-Jo1, anti-MDA5 and anti-Ro52) and IIMs-ILD, and of note highlighted mechanic's hands as a strong independent clinical predictor of ILD in Caucasian patients affected with IIMs, whereas dysphagia was the strongest protective factors. Besides the specific autoantibodies positivity (anti-Jo1, anti-MDA5 and anti-Ro52), mechanic's hands were the strongest independent clinical predictors of ILD in Caucasian IIMs patients. Ground-glass-opacities is the prevalent HRCT pattern and is associated to normal lung volume and consolidation needs a special attention being associated to muscle injury and anticipating the diagnosis of IIM. Serological and clinical features at diagnosis may predict progression in IIM-ILD patients. Anti-MDA5 antibodies, heliotropic rash, xerostomia and xerophthalmia are prevalent in progressive IIM-ILD population, but their role as independent predictors need to be further investigated.

In IIMs patients with such serological and clinical features a complete ILD screening through PFTs and HRCT is highly recommended at IIMs diagnosis and a close monitoring for the occurrence of lung involvement and progression should be considered during follow-up.

REFERENCES

1. De Zorzi E, Spagnolo P, Cocconcelli E, et al (2022) Thoracic Involvement in Systemic Autoimmune Rheumatic Diseases: Pathogenesis and Management. Clin Rev Allergy Immunol. https://doi.org/10.1007/s12016-022-08926-0
2. Zanatta E, Codullo V, Avouac J, Allanore Y (2020) Systemic sclerosis: Recent insight in clinical management. Jt Bone Spine 87:293–299. https://doi.org/10.1016/j.jbspin.2019.09.015
3. Hoffmann-Vold AM, Distler O, Murray B, et al (2019) Setting the international standard for longitudinal follow-up of patients with systemic sclerosis: A Delphi-based expert consensus on core clinical features. RMD Open 5:1–7. https://doi.org/10.1136/rmdopen-2018-000826
4. Lundberg IE, Fujimoto M, Vencovsky J, et al (2021) Idiopathic inflammatory myopathies. Nat Rev Dis Prim 7:1–22. https://doi.org/10.1038/s41572-021-00321-x
5. Cavagna L, Meloni F, Meyer A, et al (2022) Clinical spectrum time course in non-Asian patients positive for anti-MDA5 antibodies. Clin Exp Rheumatol 40:274–283. https://doi.org/10.55563/clinexprheumatol/di1083
6. Nombel A, Fabien N, Coutant F (2021) Dermatomyositis With Anti-MDA5 Antibodies: Bioclinical Features, Pathogenesis and Emerging Therapies. Front Immunol 12:1–18. https://doi.org/10.3389/fimmu.2021.773352
7. Ghirardello A, Doria A (2018) New insights in myositis-specific autoantibodies. Curr Opin Rheumatol 30:614–622. https://doi.org/10.1097/BOR.0000000000000548
8. Gutsche M, Rosen GD, Swigris JJ (2012) Connective tissue disease-associated interstitial lung disease: a review. Curr Respir Care Rep 1:224–232. https://doi.org/10.1007/s13665-012-0028-7
9. Zuo Y, Ye L, Liu M, et al (2020) Clinical significance of radiological patterns of HRCT and their association with macrophage activation in dermatomyositis. Rheumatology 59:2829–2837. https://doi.org/10.1093/rheumatology/keaa034
10. Egashira R (2021) High-Resolution CT Findings of Myositis-Related Interstitial Lung Disease. Medicina (B Aires) 57:692. https://doi.org/10.3390/medicina57070692
11. Cottin V (2019) Treatment of progressive fibrosing interstitial lung diseases: A milestone in the management of interstitial lung diseases. Eur Respir Rev 28:. https://doi.org/10.1183/16000617.0109-2019
12. Kolb M, Vašáková M (2019) The natural history of progressive fibrosing interstitial lung diseases. Respir Res 20:57. https://doi.org/10.1186/s12931-019-1022-1
13. Lundberg IE, Tjärnlund A, Bottai M, et al (2017) 2017 European League Against Rheumatism/American College of Rheumatology classification criteria for adult and juvenile idiopathic inflammatory myopathies and their major subgroups. Ann Rheum Dis 76:1955–1964. https://doi.org/10.1136/annrheumdis-2017-211468
14. Raghu G, Remy-Jardin M, Richeldi L, et al (2022) Idiopathic Pulmonary Fibrosis (an Update) and Progressive Pulmonary Fibrosis in Adults: An Official

ATS/ERS/JRS/ALAT Clinical Practice Guideline. Am J Respir Crit Care Med 205:E18–E47. https://doi.org/10.1164/rccm.202202-0399ST

15. Iaccarino L, Ghirardello A, Bettio S, et al (2014) The clinical features, diagnosis and classification of dermatomyositis. J Autoimmun 48–49:122–127. https://doi.org/10.1016/j.jaut.2013.11.005
16. Ghirardello A, Bettio S, Bassi N, et al (2017) Autoantibody testing in patients with myositis: clinical accuracy of a multiparametric line immunoassay. Clin Exp Rheumatol 35:176–177
17. Vojinovic T, Cavazzana I, Ceruti P, et al (2021) Predictive Features and Clinical Presentation of Interstitial Lung Disease in Inflammatory Myositis. Clin Rev Allergy Immunol 60:87–94. https://doi.org/10.1007/s12016-020-08814-5
18. Ferreira JP, Almeida I, Marinho A, et al (2012) Anti-Ro52 Antibodies and Interstitial Lung Disease in Connective Tissue Diseases Excluding Scleroderma. ISRN Rheumatol 2012:1–4. https://doi.org/10.5402/2012/415272
19. Marie I, Hatron PY, Dominique S, et al (2012) Short-Term and Long-Term Outcome of Anti-Jo1-Positive Patients with Anti-Ro52 Antibody. Semin Arthritis Rheum 41:890–899. https://doi.org/10.1016/j.semarthrit.2011.09.008
20. Sclafani A, D'Silva KM, Little BP, et al (2019) Presentations and outcomes of interstitial lung disease and the anti-Ro52 autoantibody. Respir Res 20:1–9. https://doi.org/10.1186/s12931-019-1231-7
21. Moghadam-Kia S, Oddis C V., Sato S, et al (2016) Anti-Melanoma Differentiation-Associated Gene 5 Is Associated with Rapidly Progressive Lung Disease and Poor Survival in US Patients with Amyopathic and Myopathic Dermatomyositis. Arthritis Care Res 68:689–694. https://doi.org/10.1002/acr.22728
22. Xing X, Li A, Li C (2020) Anti-Ro52 antibody is an independent risk factor for interstitial lung disease in dermatomyositis. Respir Med 172:106134. https://doi.org/10.1016/j.rmed.2020.106134
23. Huang HL, Lin WC, Lin PY, et al (2021) The significance of myositis autoantibodies in idiopathic inflammatory myopathy concomitant with interstitial lung disease. Neurol Sci 42:2855–2864. https://doi.org/10.1007/s10072-020-04911-7
24. Gasparotto M, Gatto M, Saccon F, et al (2019) Pulmonary involvement in antisynthetase syndrome. Curr Opin Rheumatol 31:603–610. https://doi.org/10.1097/BOR.0000000000000663

Chapter 12

Clinical features and chest imaging as predictors of intensity of care in patients with COVID-19.

Elisabetta Cocconcelli, Davide Biondini, Chiara Giraudo, Sara Lococo, Nicol Bernardinello, Giulia Fichera, Giulio Barbiero, Gioele Castelli, Silvia Cavinato, Anna Ferrari, Marina Saetta, Annamaria Cattelan, Paolo Spagnolo and Elisabetta Balestro.

J Clin Med. 2020 Sep 16;9(9):2990. doi: 10.3390/jcm9092990. PMID: 32947904; PMCID: PMC7565657.

ABSTRACT

Coronavirus disease 2019 (COVID-19) has rapidly become a global pandemic with lung disease representing the main cause of morbidity and mortality. Conventional chest-X ray (CXR) and ultrasound (US) are valuable instruments to assess the extent of lung involvement. We investigated the relationship between CXR scores on admission and the level of medical care required in patients with COVID-19. Further, we assessed the CXR-US correlation to explore the role of ultrasound in monitoring the course of COVID -19 pneumonia. Clinical features and CXR scores were obtained at admission and correlated with the level of intensity of care required (high- [HIMC] vs. low-intensity medical care [LIMC]). In a subgroup of patients, US findings were correlated with clinical and radiographic parameters. On hospital admission, CXR global score was higher in HIMCs compared to LIMC. Smoking history, pO2 on admission, cardiovascular and oncologic diseases were independent predictors of HIMC. The US score was positively correlated with FiO2 while the correlation with CXR global score only trended towards significance. Our study identifies clinical and radiographic features that strongly correlate with higher levels of medical care. The role of lung ultrasound in this setting remains undetermined and needs to be explored in larger prospective studies.

INTRODUCTION

Since December 2019, when the first cases of coronavirus disease 2019 (COVID-19) were reported, the diffusion of the Severe acute respiratory syndrome coronavirus type 2 (SARS-CoV-2) has rapidly spread from the Hubei Province in China to involve up to 213 states and territories to date, reaching pandemic proportions[1]. Despite epidemiological reports showing that approximately half of the infected people are asymptomatic[1], the spectrum of respiratory manifestations may range from mild symptoms such as dry cough, fever and fatigue to acute respiratory distress syndrome (ARDS), requiring admission to intensive care unit (ICU) and mechanical ventilation (MV). In this scenario, thoracic radiology plays a key role in early detection of lung involvement from COVID-19. Chest computed tomography (CT) is the technique with the highest sensitivity, but the risk of contamination and the need for a dedicated hospital organization makes CT hardly available in an emergency setting. Portable chest X-ray (CXR) and ultrasonography (US) are quicker, safer and less expensive alternatives[2]. CXR is recommended as first level assessment by several scientific societies (ACR, STR, SIRM) in the context of the SARS-CoV-2 pandemic[3]. Predominant CXR features in patients with COVID-19 include lower lobe, peripheral, bilateral ground glass opacities (GGO) or consolidations[2], similar to other forms of viral pneumonias, such as the H1N1 strain[4]. Yet, CXR could be normal in as many as 31% cases, peaking its sensibility in patients with advanced disease[5-7].

In the last three decades, lung US (LUS) has become increasingly important in clinical practice, particularly in the assessment of patients with pneumonia, with sensitivity and specificity of 92% and 93%, respectively, especially when performed by experienced operators[8]. In the COVID-19 pandemic, LUS has been used in multiple centers as first radiological approach in patients with suspected pneumonia. The main ultrasound findings include multiple B-lines (separated or coalescent), peripheral consolidations and thickened pleural lines[9], which however are nonspecific and found in a number of infectious and non-infectious diseases[10]. The use of LUS and CXR in combination has the potential to facilitate the identifications of ARDS[11].

With this background, we investigated the relationship between CXR severity score on admission and the level of medical care required in patients with COVID-19. Further, we assessed the radiographic – ultrasound correlation with the

aim to explore the value of ultrasound in monitoring the course of COVID -19 pneumonia.

MATERIALS AND METHODS

Study population and study design

In this longitudinal retrospective study, we identified a cohort of clinically well-characterized patients with SARS-CoV-2 infection referred to the University Hospital of Padova (Division of Infectious and Tropical Diseases, Respiratory Disease Unit and Intensive Care Unit) between March and May 2020. One hundred and two patients were included in the study (**Table 1**) and were followed clinically and radiologically (CXR and LUS) from admission to discharge. The diagnosis of SARS-CoV-2 infection was made based on nasopharyngeal swab positivity as well as clinical and radiological data.

Table 1 - Baseline demographics and clinical features of the overall population hospitalized for SARS-CoV-2 related infection, and of the two subgroups categorized in low (LIMC) and high (HIMC) intensity medical care.

	Overall Population (n =102)	Low-intensity medical care (LIMC) (n = 71)	High-intensity medical care (HIMC) (n = 31)	*p* Value
Male – *n (%)*	75 (73)	48 (67)	27 (87)	**0.05**
Age at admission – *years*	68 (22 - 94)	63 (22 - 94)	74 (28 - 85)	**0.03**
Smoking history – *pack years*	0 (0 - 60)	0 (0 - 60)	10 (0 - 60)	**0.01**
• **Current – *n (%)***	9 (9)	8 (11)	1 (3)	0.18
• **Former – *n (%)***	43 (42)	24 (34)	19 (61)	**0.009**
• **Non smokers – *n (%)***	50 (49)	41 (57)	9 (29)	**0.007**
BMI (kg/m^2)	25 (16 - 43)	24 (16 - 31)	31 (21 - 43)	**0.02**
Lag time symptoms - diagnosis – *days*	4 (-4 - 23)	3 (-4 - 23)	6 (-2 - 22)	0.07
FiO2 at admission (room air) - %	21 (21 - 100)	21 (21 - 51)	39 (21 - 100)	**<0.0001**
pO2 at admission (room air) – mmHg	90 (21.2 - 119)	90 (54 - 119)	60 (21 - 90)	**<0.0001**
P/F at admission - value	429 (33 - 567)	429 (106 - 567)	158 (33- 429)	**<0.0001**
Hospitalization - *days*	10.5 (2 - 119)	8 (2 - 50)	26 (7 - 119)	**<0.0001**
Bacterial co-infections - *n (%)*	24 (23)	11 (15)	13 (42)	**0.002**
Comorbidities				
• **CVD - *n (%)***	60 (59)	35 (49)	25 (80)	**0.002**
• **Respiratory diseases - *n (%)***	18 (18)	11 (15)	7 (22)	0.39
• **Autoimmune diseases - *n (%)***	12 (12)	10 (14)	2 (6)	0.34
• **Metabolic diseases - *n (%)***	45 (44)	26 (37)	19 (61)	**0.002**
• **Oncologic diseases - *n (%)***	13 (13)	6 (8)	7 (22)	**0.05**
Death - *n (%)*	6 (6)	1 (1)	4 (13)	**0.01**

Values are expressed as numbers and (%) or median and range, as appropriate. Negative values refer to patients with symptoms occurring after admission to the hospital. To compare demographic between LIMC and HIMC, Chi square test and Fisher t test (n < 5) for categorical variables and Mann-Whitney t test for continuous variables were used.

Level of care definition

The need for invasive/non-invasive ventilation or high-flow nasal cannula (HFNC), which required admission to ICU or to the Respiratory ICU, was considered as high-intensity medical care (HIMC), while the need for low flow oxygen supplementation through nasal cannula or face mask, which required the setting of a general ward, was considered as low-intensity medical care (LIMC). The level of care could change over time based on patient's clinical conditions. For all patients, clinical data (demographics and comorbidities), gas exchange values (FiO2, pO2 and pO2/FiO2) were collected on admission (**Table 1**).

Ethics statement

This was a retrospective study on anonymized patient's data collected from electronic medical records. The study protocol complies to the ethical guidelines of the 1975 Declaration of Helsinki and, in agreement with national regulation on retrospective observational studies, it was notified to the local ethics committee and the need for patient's informed consent was waived.

Data collection

We retrieved data on patients hospitalized for COVID-19 between March and May 2020 at the University Hospital of Padova, one of the most affected areas in North-East of Italy. We screened records of all patients admitted to our Hospital with a diagnosis of SARS-CoV2 infection.

Radiological evaluation

For each patient, a CXR was available on hospital admission. Two expert thoracic radiologists (C.G., G.B.), who were blind to clinical data, scored the images independently using a semi-quantitative scale. This represented a modification of previously reported scoring systems that allowed to evaluate the extension of ground glass opacities (GGO) and consolidation (CO)[6,12,13]. For each lung lobe, the two radiologists assessed the extent of GGO and CO using the following scale: 0 (normal), 1 (up to 30% of the lobe involved), 2 (30% to 60% of the lobe involved), and 3 (more than 60% of the lobe involved). The sum of the scores for each lung lobe and a final value of GGO and CO score for each patient

was then calculated (**Table 2**). The CXR "global" score was calculated as the sum of the GGO and CO scores of each patient, with a maximum score of 36. Finally, each patient was classified as "normal", "GGO prevalent", "CO prevalent", or "mixed" based on the prevalent CXR pattern.

Table 2 - Baseline radiological scores of the overall population hospitalized for SARS-CoV-2 related infection, and of the two subgroups categorized in low (LIMC) and high (HIMC) intensity medical care.

	Overall Population (n =102)	Low-intensity medical care (LIMC) (n = 71)	High-intensity medical care (HIMC) (n = 31)	*p* Value
X-ray global score (GGO + consolidations)	3 (0 – 35)	3 (0 – 22)	8 (0 – 35)	**< 0.0001**
GGO – score	2 (0 – 18)	1 (0 – 18)	5 (0 – 15)	**<0.0001**
Consolidation – score	0 (0 – 35)	0 (0 – 10)	0 (0 – 35)	**0.02**
Normal – n (%)	15 (15)	14 (20)	1 (3)	**0.003**
GGO prevalent – n (%)	66 (65)	44 (62)	22 (71)	0.38
Consolidation prevalent – n (%)	15 (15)	11 (16)	4 (13)	0.73
Mixed – n (%)	6 (6)	2 (3)	4 (13)	**0.04**

Values are expressed as numbers and (%) or median and range as appropriate. To compare demographic data and baseline clinical characteristic between LIMC and HIMC, Chi square test and Fisher t test (n < 5) for categorical variables and Mann-Whitney t test for continuous variables were used.

Ultrasound evaluation

A subset of 25 patients underwent bed-side LUS. The LUS score was calculated across 12 chest zones (six on each hemithorax) using a scale from 0 (normal pattern, A-lines or non-significant B-lines), 1 (significant B-lines ≥3 per rib space), 2 (coalescent B-lines with or without small consolidations) to 3 (consolidation), as previously reported[14]. A final "US global score" was calculated for each patient with a maximum score of 36.

Statistical analysis

Categorical variables were described as absolute (n) and relative values (%) whereas continuous variables were described as median and range. To compare demographic data and baseline clinical characteristics between LIMC and HIMC groups, Chi square test and Fisher's exact test for categorical variables and Mann-Whitney U test for continuous variables were used, as appropriate. The correlation between CXR global score and pO2, FiO2, P/F on admission was assessed for the entire study population and in the LIMC and HIMC groups using the nonparametric Spearman's rank method. Univariate logistic regression analysis, followed by a

multivariate logistic regression, was performed to detect the strongest predictors of level of care. The covariates included in the final model were those that were significant in the univariate regression analyses.

RESULTS

Patient demographics and clinical characteristics at baseline

Demographic and clinical characteristics at baseline (i.e., on hospital admission) are summarized in **Table 1.**

Most patients were male (73%) with a median age on admission of 68 years. Seventy-one patients required LIMC during hospitalization and thirty-one HIMC. Patients requiring HIMC (HIMCs) were mainly male (87 vs. 67%; p=0.05) and older [74 (28 - 85) vs. 63 (22 - 94) years; p=0.03], with a higher body mass index (BMI) [31 (21 - 43) vs. 24 (16 - 31) kg/m2; p=0.02]. Moreover, they had a heavier smoking history [10 (0 - 60) vs. 0 (0 - 60) pack/year (py); p=0.01] and were mainly former smokers (61%). The most common presenting symptoms were fever (92%), cough (61%) and shortness of breath (34%), and with 5% of patients complaining of impaired sensory. The frequency of these symptoms did not differ between HIMCs and LIMCs. Interestingly, although the time interval between onset of respiratory symptoms and admission to the emergency unit was similar, HIMCs showed a greater impairment of respiratory gas exchange with a lower pO2 on room air on admission [60 (21 - 90) vs. 90 (54 - 119) mmHg; p<0.0001], greater FiO2 requirement at the time of admission [39 (21 - 100) vs. 21 (21 - 51) %; p<0.001] and worse P/F [158 (33 - 429) vs. 429 (106 - 567); p<0.0001] compared to LIMCs. HIMCs reported more comorbidities, in particular cardiovascular diseases (CVDs) (80 vs. 49% of cases; p=002), metabolic diseases (61 vs. 37%; p=002) and oncologic diseases (22 vs. 8%; p=0.05). Furthermore, this patient group showed a higher frequency of bacterial co-infections (42 vs. 15%; p=0.002) during hospitalization. Finally, the hospitalization time was significantly longer for HIMCs compared to LIMCs [26 (7 -119) vs. 8 (2 - 50) days; p<0.001), with 4 patients dying among HIMCs and only one among LIMCs (p = 0.01).

Radiological features on admission

On admission, HIMCs showed a more severe radiological impairment compared to LIMCs, with higher x-ray global score [8 (0 - 35) vs. 3 (0 - 22);

p<0.001), GGO score [5 (0 - 15) vs. 1 (0 - 18); p<0.001] and CO score [0 (0 - 35) vs. 0 (0 - 10); p=0.02], respectively. When considering the prevalent CXR pattern, only one patient among HIMCs had a normal CXR on admission compared to LIMCs (14; p=0.003), with similar proportion of patients with "GGO prevalent" and "CO prevalent" patterns in the HIMC and LIMC groups.

Radiological correlations

In the overall study population, a positive correlation was observed between CXR global score and FiO2 on admission (r = 0.6, p<0.001). When stratified by level of care, the correlation between CXR global score and FiO2 on admission was confirmed in LIMCs (r=0.51, p<0.0001) but not in HIMC (**Figure 1a).** In the overall study population, we observed a negative correlation between CXR global score and pO2 on admission (r = - 0.6, p<0.001). When stratified by level of care, the correlation between CXR global score and pO2 on admission was confirmed in LIMCs (r= - 0.37; p= 0.02) but not in HIMCs (**Figure 1b**). Finally, in the overall study population, we observed a negative correlation between CXR global score and P/F on admission (r = - 0.6, p<0.001). When stratified by level of care, the correlation between CXR global score and P/F at admission was confirmed in both LIMCs (r= - 0.40; p= 0.0003) and HIMCs (r = - 0.37; p = 0.04) (**Figure 1c**).

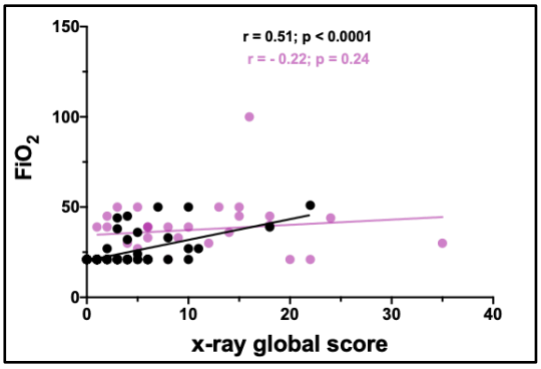

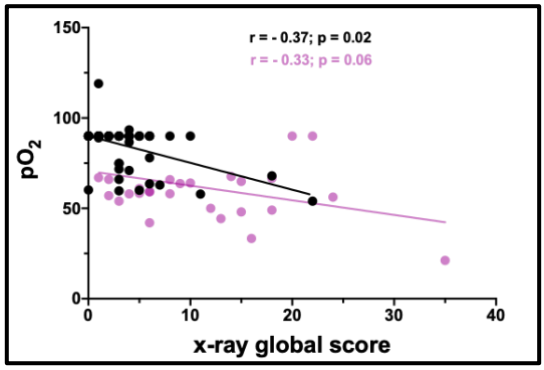

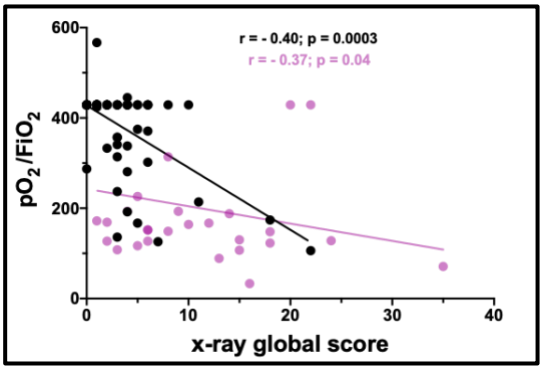

Figure 1. Correlation between chest x-ray global score and (a) FiO2 at admission, (b) pO2 at admission in room air, (c) pO2/FiO2 at admission in room air in the study population categorized in LIMC and HIMC groups. Black points indicate LIMC patients and purple points indicate HIMC patients.

Predictors of level of care requirement

Univariate logistic regression analysis of factors associated with level of care revealed that sex, age, smoking history, FiO2, pO2 in room air at admission, bacterial co-infections developed during hospitalization, CVDs, metabolic and oncologic diseases and chest x-ray global score had significant positive association with a higher level of care in the entire study population (**Table 3**). Multivariate analysis performed using variables with statistical significance in univariate analysis revealed that smoking history (OR: 6.55; 95%CI: 1.15 - 52.09; p = 0.04), pO2 (36.7, 3.64 - 681.4; p = 0.005), CVDs (10.89, 1.44 - 112; p = 0.02) and oncologic diseases (17.13, 1.76 - 242.6; p = 0.02) were independent predictors of higher level of care in patients with SARS-CoV-2 infection.

Table 3. Predictive factors of higher level of care in the overall population of patients hospitalized for COVID related infection.

	Univariate analysis		Multivariate analysis	
	OR (95% IC)	P	OR (95% IC)	p
Sex (male vs. female)	3.23 (1.01 – 11.89)	**0.04**	0.54 (0.06 – 4.22)	0.55
Age (yr, ≥ 68 vs. < 68)	3.34 (1.38 – 8.61)	**0.009**	0.51 (0.06 – 3.03)	0.49
Smoking history (p/y, > 0 vs. ≤ 0)	2.72 (1.08 – 7.27)	**0.03**	6.55 (1.15 – 52.09)	**0.04**
FiO2 at admission (%, > 21 vs ≤ 21)	13.1 (4.92 – 39.2)	**< 0.0001**	4.17 (0.60 – 29.89)	0.14
pO2 at admission (room air) (mmHg, <90, ≥ 90)	13 (4.78 – 40.4)	**< 0.0001**	36.7 (3.64 – 681.4)	**0.005**
Lag time symptoms - diagnosis – (days, ≥4 vs. <4)	2.18 (0.90 – 5.50)	0.08	-	-
P/F at admission (≥429 vs. < 429)	9.60 (3.59 – 29.26)	**< 0.0001**	16.61 (3.34 – 128.3)	**0.002**
Bacterial co-infections (yes vs. no)	4.64 (1.75 – 12.72)	**0.002**	2.48 (0.38 – 17.78)	0.34
CVDs - (yes vs. no)	5.14 (1.89 – 16.6)	**0.002**	10.89 (1.44 – 112.0)	**0.02**
Respiratory diseases – (yes vs. no)	5.14 (1.89 – 16.6)	0.34	-	-
Autoimmune diseases - (yes vs. no)	0.43 (0.06 – 1.79)	0.30	-	-
Metabolic diseases - (yes vs. no)	2.99 (1.25 – 7.44)	**0.01**	2.63 (0.54 – 14.76)	0.24
Oncologic diseases - (yes vs. no)	3.29 (1.00 – 11.25)	**0.04**	17.13 (1.76 – 242.6)	**0.02**
X-ray global score (> 3 vs. < 3)	3.33 (1.32 – 9.29)	**0.01**	0.40 (0.02 – 3.63)	0.43

Values are expressed as OR (95% IC). Logistic regression analysis in relation to level of care was used to determine the relationship of clinical and radiological characteristics with higher level of care needed during hospitalization.

Ultrasound evaluation

A subset of 25 patients underwent a bed-side LUS after a median time of 11 days from admission. In parallel, CXRs were performed in the same patients at the same time point. The median LUS global score was 7 (2 - 22) whereas the median CXR global score was 9 (3-13). The LUS global score positively correlated with the FiO2 requirement at the time of the US examination (r = 0.36; p = 0.03) (**Figure 2**). Conversely, the correlation between LUS global score and CXR global score only trended towards statistical significance (r = 0.36, p = 0.07) (**Figure 3**). Finally, the LUS global score positively correlated with the CXR CO score (r = 0.38; p = 0.05) (**Figure 4**) but not with the GGO score.

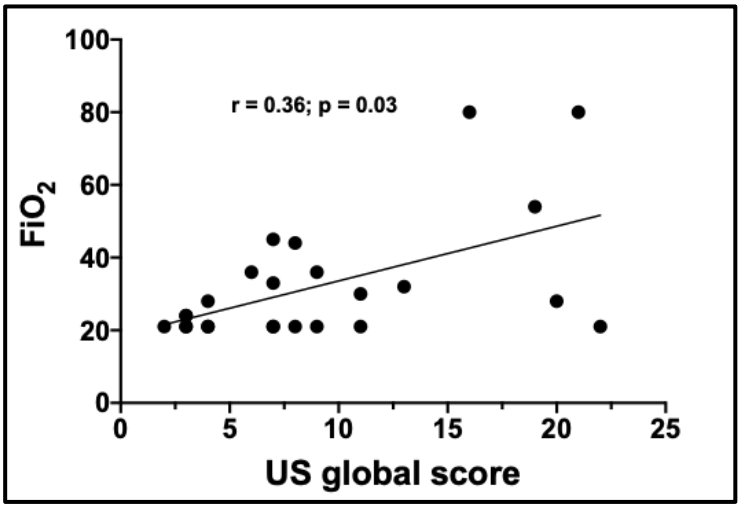

Figure 2. Correlation between lung US global score and FiO2 in the subgroup of patients undergoing US examination.

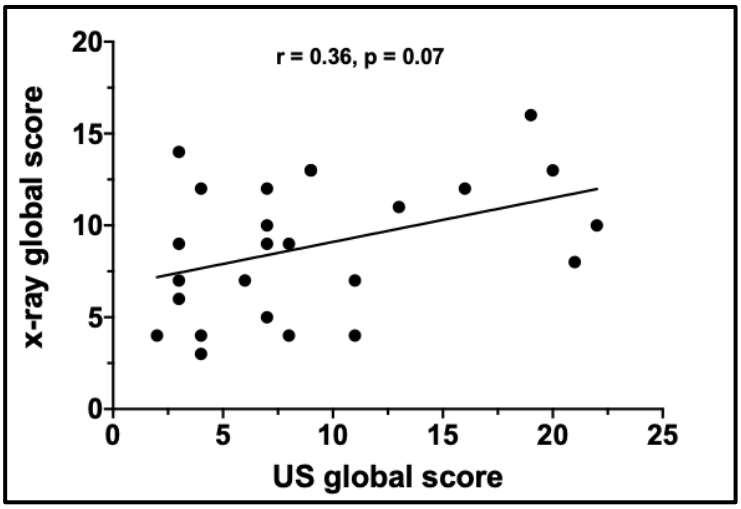

Figure 3. Correlation between lung US global score and x-ray global score in the overall study population.

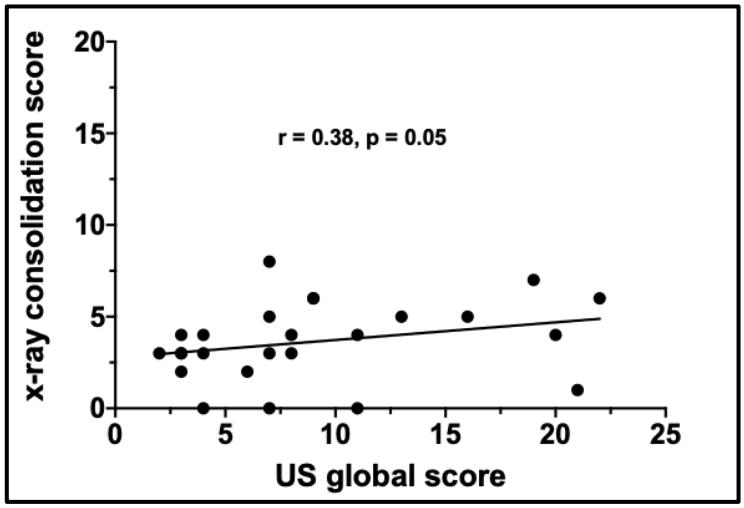

Figure 4. Correlation between chest x-ray consolidation score and US global score in the overall study population.

DISCUSSION

This is a retrospective analysis of clinical features and radiographic severity scores in patients with COVID-19 and how these parameters on hospital admission correlate with different levels of medical care (i.e., HIMC vs. LIMC). A subgroup of patients also underwent LUS, which was correlated with chest radiographs. Our study revealed that patients with COVID-19 who required a HIMC are mainly men, former smokers with a higher pack/year of smoking history, older and with a higher BMI compared to patients requiring LIMC. Furthermore, the majority of them reported at least one comorbidity (i.e., cardiovascular, metabolic, or oncologic) and required on emergency room oxygen supplementation due to low alveolar oxygen partial pressure (PaO2). Moreover, using a multivariate analysis, we found that a heavier smoking history, PO2 level on room air and presence of cardiovascular or oncological disease on admission were independent predictors of the need of HIMC. Our findings mirror those from previous studies indicating that older male patients with comorbidities are at higher risk of pulmonary infection and fatal consequences from Covid-19[15,16]. In our study, we show that the number of pack-years was significantly higher in former smokers who required intensive care compared to those requiring LIMC. Moreover, the proportion of former smokers was markedly increased among severe patients whereas nonsmokers with COVID-19 experienced a milder illness, which required low-flow oxygen supplementation. This is in line with other reports that explored the association between smoking and progression of COVID-19 pneumonia[17]. Notably, in our study, multivariate

analysis revealed that smoking history was an independent risk factor for HIMC. We speculate that cigarette smoke upregulates the expression of ACE2 receptors, which in turn facilitate SARS-CoV-2 entry in the respiratory epithelium; this implies that that smoking habit may represent a risk factor for developing severe illness even among former smokers. In other words, having quit smoking does not seem to prevent the risk of severe COVID-19 pneumonia[18]. Chronic respiratory disease, including, among others, Chronic Obstructive Pulmonary Disease (COPD), carry a worse prognosis when associated with chronic conditions such as cardiovascular diseases[19-21]. Interestingly, in our cohort, concomitant CVDs and neoplasms were independent risk factors for hospitalization in HIMC, with up to 80% of patients who required HIMC reporting an history of CVD (mainly arterial hypertension). A recent meta-analysis of 1,576 patients concluded that hypertension, chronic respiratory disease and CVD are risk factors for severe Covid-19 disease[22]. These findings emphasize the importance of past medical history and comorbidities in the disease course of Covid-19 patients, as they may predispose to worse outcome and higher intensity of care. PO2 level <90 mmHg on admission to emergency room was an additional independent predictor of HIMC requirement. This is interesting, as the duration of symptoms (i.e., median of 4 days) did not differ between patients requiring HIMC and patients requiring LIMC. Thirty-one subjects required subsequent admission to ICU due to worsening of pneumonia and gas exchange. On admission, these patients displayed extensive radiological impairment in terms of both GGO score and consolidation. Radiological score correlated negatively with PO2 levels and positively with FiO2, although only in the group requiring LIMC. Conversely, among patients who required HIMC, CXR at baseline showed a variety of severity scores, ranging from normal to high. These findings are particularly important, as they suggest that even patients with mild radiologic abnormalities may rapidly progress to HIMC requirement. Previous reports on CXR findings in COVID-19 patients focused on the distribution and type of lung abnormalities. Wong and coauthors demonstrated that CXR at baseline has a sensitivity of 69% for a diagnosis of COVID-19 pneumonia, corroborating the utility of CXR in the initial evaluation of subjects with suspected COVID-19 pneumonia, thus obviating the need for CT [6]. Toussie and colleagues have recently reported that initial CXR severity score is also an independent predictor of outcome in COVID-19 patients[3]. We could not replicate

this finding, but our study population was older than that studied by Toussie et al. The prognostic role of CXR in Covid-19 pneumonia therefore needs to be clarified in larger studies.

Lung ultrasound has been suggested as a potential diagnostic tool for COVID-19 pneumonia given the predominant involvement of the lung periphery[7]; lung ultrasound is a relatively simple technique that can be easily applied at patient bedside[23]. In our study, we investigated its role in the late phase of Covid-19 pneumonia and its relation with CXR in a subgroup of patients hospitalized in a low-intensity care setting. We found a significant correlation between LUS features and FiO2 level, suggesting these two parameters can be integrated into the evaluation of patients with COVID-19 pneumonia. LUS global score positively correlated with CXR consolidation score while the correlation with CXR global score only trended towards statistical significance. Although only exploratory, these data support the utility of LUS as a monitoring tool, possibly limiting the use of serial CXR, at least in the advanced phase of covid-19 pneumonia. In this regard, LUS has been suggested as a potential substitute for CXR in the follow-up of various lung diseases in ICU[24], reducing the number of CXRs performed and relative medical costs without affecting patient outcome. Soldati and colleagues have also suggested that LUS can be useful in Covid-19 pneumonia by identifying disease extension and specific patterns as well as their evolution toward the consolidation phase[25], thus providing further support to the role of LUS in the follow-up of patients with Covid-19 pneumonia. At present, however, the majority of studies performed during the Covid-19 pandemic focused on ultrasonographic signs and disease patterns at presentation rather than overtime[26-30]. Accordingly, the role of LUS in monitoring the evolution of Covid-19 pneumonia needs to be confirmed in larger studies. The results of our study should be interpreted in the light of important limitations. First, this was a retrospective cohort study, therefore the accuracy of the data depends on medical records, which may introduce inaccuracies. However, every effort was made to limit this risk. Second, the study population was relatively small, particularly the subset of patients for whom LUS data were available, although this was an exploratory analysis and its findings should be viewed as such. Clearly, these data need to be validated in larger, independent, prospectively collected populations of patients. In summary, our study identified clinical features that strongly predict the level of medical setting required

by patients with Covid-19 pneumonia (HIMC or LIMC). These findings allow the identification of patients at risk for severe disease and worse outcome already on hospital admission. The correlation of LUS with clinical parameters and radiological score provides the basis for future studies on the utility of LUS in the follow-up of patients with Covid-19 pneumonia.

REFERENCES

1. Lavezzo, E.; Franchin, E.; Ciavarella, C.; Cuomo-Dannenburg, G.; Barzon, L.; Del Vecchio, C.; Rossi, L.; Manganelli, R.; Loregian, A.; Navarin, N.; et al. Suppression of a SARS-CoV-2 Outbreak in the Italian Municipality of Vo'. Nature, 2020.
2. Litmanovich, D. E.; Chung, M.; R. Kirkbride, R.; Kicska, G.; P. Kanne, J. Review of Chest Radiograph Findings of COVID-19 Pneumonia and Suggested Reporting Language. J. Thorac. Imaging, 2020, 00 (00), 1–7.
3. Toussie, D.; Voutsinas, N.; Finkelstein, M.; Cedillo, M. A.; Manna, S.; Maron, S. Z.; Jacobi, A.; Chung, M.; Bernheim, A.; Eber, C.; et al. Clinical and Chest Radiography Features Determine Patient Outcomes In Young and Middle Age Adults with COVID-19. Radiology, 2020, 201754.
4. Minns, F. C.; Mhuineachain, A. N.; Van Beek, E. J. R.; Ritchie, G.; Hill, A.; Murchison, J. T. "Presenting CXR Phenotype of H1N1" Flu Compared with Contemporaneous Non-H1N1, Community Acquired Pneumonia, during Pandemic and Post-Pandemic Outbreaks'. Eur. J. Radiol., 2015, 84 (9), 1810–1815.
5. Cozzi, D.; Albanesi, M.; Cavigli, E.; Moroni, C.; Bindi, A.; Luvarà, S.; Lucarini, S.; Busoni, S.; Mazzoni, L. N.; Miele, V. Chest X-Ray in New Coronavirus Disease 2019 (COVID-19) Infection: Findings and Correlation with Clinical Outcome. Radiol. Medica, 2020, 125 (8), 730–737.
6. Yuen Frank Wong, H.; Yin Sonia Lam, H.; Ho-Tung Fong, A.; Ting Leung, S.; Wing-Yan Chin, T.; Shing Yen Lo, C.; Mei-Sze Lui, M.; Chun Yin Lee, J.; Wan-Hang Chiu, K.; Chung, T.; et al. Frequency and Distribution of Chest Radiographic Findings in COVID-19 Positive Patients Authors. Radiology, 2020
7. Rubin, G. D.; Ryerson, C. J.; Haramati, L. B.; Sverzellati, N.; Kanne, J. P.; Raoof, S.; Schluger, N. W.; Volpi, A.; Yim, J.-J.; Martin, I. B. K.; et al. The Role of Chest Imaging in Patient Management During the COVID-19 Pandemic. Chest, 2020, 158 (1), 106–116.
8. Orso, D.; Guglielmo, N.; Copetti, R. Lung Ultrasound in Diagnosing Pneumonia in the Emergency Department: A Systematic Review and Meta-Analysis. Eur. J. Emerg. Med., 2018, 25 (5), 312–321.
9. Gargani, L.; Soliman-Aboumarie, H.; Volpicelli, G.; Corradi, F.; Pastore, M. C.; Cameli, M. Why, When, and How to Use Lung Ultrasound during the COVID-19 Pandemic: Enthusiasm and Caution. Eur. Hear. J. - Cardiovasc. Imaging, 2020, 1–8.
10. Pierce, C. W. Clarifying the Role of Lung Ultrasonography in COVID-19 Respiratory Disease. Cmaj, 2020, 192 (16), E436.
11. See, K. C.; Ong, V.; Tan, Y. L.; Sahagun, J.; Taculod, J. Chest Radiography versus Lung Ultrasound for Identification of Acute Respiratory Distress Syndrome: A Retrospective Observational Study. Crit. Care, 2018, 22 (1), 1–9.

12. Borghesi, A.; Maroldi, R. COVID-19 Outbreak in Italy: Experimental Chest X-Ray Scoring System for Quantifying and Monitoring Disease Progression. Radiol. Medica, 2020, 125 (5), 509–513.
13. Nicolini, A.; Ferrera, L.; Rao, F.; Senarega, R.; Ferrari-Bravo, M. Achados Radiológicos Do Tórax Da Pneumonia Da Gripe A H1N1. Rev. Port. Pneumol., 2012, 18 (3), 120–127.
14. Smith, M. J.; Hayward, S. A.; Innes, S. M.; Miller, A. Point-of-Care Lung Ultrasound in Patients with COVID-19 – a Narrative Review. Anaesthesia, 2020.
15. Chen, N.; Zhou, M.; Dong, X.; Qu, J.; Gong, F.; Han, Y.; Qiu, Y.; Wang, J.; Liu, Y.; Wei, Y.; et al. Epidemiological and Clinical Characteristics of 99 Cases of 2019 Novel Coronavirus Pneumonia in Wuhan, China: A Descriptive Study. Lancet, 2020, 395 (10223), 507–513.
16. Yang, X.; Yu, Y.; Xu, J.; Shu, H.; Xia, J.; Liu, H.; Wu, Y.; Zhang, L.; Yu, Z.; Fang, M.; et al. Clinical Course and Outcomes of Critically Ill Patients with SARS-CoV-2 Pneumonia in Wuhan, China: A Single-Centered, Retrospective, Observational Study. Lancet Respir. Med., 2020, 8 (5), 475–481.
17. Vardavas, C. I.; Nikitara, K. COVID-19 and Smoking: A Systematic Review of the Evidence. Tob. Induc. Dis., 2020, 18 (March), 1–4.
18. Smith, J. C.; Sausville, E. L.; Girish, V.; Yuan, M. Lou; Vasudevan, A.; John, K. M.; Sheltzer Correspondence, J. M. Cigarette Smoke Exposure and Inflammatory Signaling Increase the Expression of the SARS-CoV-2 Receptor ACE2 in the Respiratory Tract. Dev. Cell, 2020, 53, 514-529.e3.
19. Huiart, L.; Ernst, P.; Suissa, S. Cardiovascular Morbidity and Mortality in COPD. Chest, 2005, 128 (4), 2640–2646.
20. Curkendall, S. M.; Lanes, S.; De Luise, C.; Stang, M. R.; Jones, J. K.; She, D.; Goehring, E. Chronic Obstructive Pulmonary Disease Severity and Cardiovascular Outcomes. Eur. J. Epidemiol., 2006, 21 (11), 803–813.
21. Gan, W. Q.; Man, S. F. P.; Senthilselvan, A.; Sin, D. D. Association between Chronic Obstructive Pulmonary Disease and Systemic Inflammation: A Systematic Review and a Meta-Analysis. Thorax, 2004, 59 (7), 574–580.
22. Yang, J.; Zheng, Y.; Gou, X.; Pu, K.; Chen, Z.; Guo, Q.; Ji, R.; Wang, H.; Wang, Y.; Zhou, Y. Prevalence of Comorbidities and Its Effects in Coronavirus Disease 2019 Patients: A Systematic Review and Meta-Analysis. Int. J. Infect. Dis., 2020, 94, 91–95.
23. Soldati, G.; Demi, M. The Use of Lung Ultrasound Images for the Differential Diagnosis of Pulmonary and Cardiac Interstitial Pathology. J. Ultrasound, 2017, 20 (2), 91–96.
24. Brogi, E.; Bignami, E.; Sidoti, A.; Shawar, M.; Gargani, L.; Vetrugno, L.; Volpicelli, G.; Forfori, F. Could the Use of Bedside Lung Ultrasound Reduce the Number of Chest X-Rays in the Intensive Care Unit? Cardiovasc. Ultrasound, 2017, 15 (1), 1–5.

25. Soldati, G.; Smargiassi, A.; Inchingolo, R.; Buonsenso, D.; Perrone, T.; Briganti, D. F.; Perlini, S.; Torri, E.; Mariani, A.; Mossolani, E. E.; et al. Is There a Role for Lung Ultrasound During the COVID-19 Pandemic? J. Ultrasound Med., 2020.
26. Volpicelli, G.; Gargani, L. Sonographic Signs and Patterns of COVID-19 Pneumonia. Ultrasound J., 2020, 12 (1), 20–22.
27. Huang, Y.; Wang, S.; Liu, Y.; Zhang, Y.; Zheng, C.; Zheng, Y.; Zhang, C.; Min, W.; Zhou, H.; Yu, M.; et al. A Preliminary Study on the Ultrasonic Manifestations of Peripulmonary Lesions of Non-Critical Novel Coronavirus Pneumonia (COVID-19). SSRN Electron. J., 2020.
28. Nazerian, P.; Cerini, G.; Vanni, S.; Gigli, C.; Zanobetti, M.; Bartolucci, M.; Grifoni, S.; Volpicelli, G. Diagnostic Accuracy of Lung Ultrasonography Combined with Procalcitonin for the Diagnosis of Pneumonia: A Pilot Study. Crit. Ultrasound J., 2016, 8 (1).
29. Poggiali, E.; Dacrema, A.; Bastoni, D.; Tinelli, V.; Demichele, E.; Ramos, P. M.; Marcianò, T.; Silva, M.; Vercelli, A.; Magnacavallo, A. Can Lung US Help Critical Care Clinicians in the Early Diagnosis of Novel Coronavirus (COVID-19) Pneumonia? Radiology. 2020.
30. Peng, Q. Y.; Wang, X. T.; Zhang, L. N. Findings of Lung Ultrasonography of Novel Corona Virus Pneumonia during the 2019–2020 Epidemic. Intensive Care Med., 2020, 46 (5), 849–850.

Chapter 13

Disease Severity and prognosis of SARS-CoV2 infection in hospitalized patients is not associated with viral load in nasopharyngeal swab.

Elisabetta Cocconcelli, Gioele Castelli, Francesco Onelia , Enrico Lavezzo, Chiara Giraudo, Nicol Bernardinello, Giulia Fichera, Davide Leoni, , Marco Trevenzoli, Marina Saetta, Annamaria Cattelan, Andrea Crisanti, Paolo Spagnolo and Elisabetta Balestro

Front Med (Lausanne). 2021 Sep 10;8:714221. doi: 10.3389/fmed.2021.714221. PMID: 34568371; PMCID: PMC8460755.

ABSTRACT

Background. The impact of viral burden on severity and prognosis of patients hospitalized for Coronavirus Disease 2019 (COVID-19) is still a matter of debate due to controversial results. Herein, we sought to assess viral load in the nasopharyngeal swab and its association with severity score indexes and prognostic parameters. **Methods**. We included 127 symptomatic patients and 21 asymptomatic subjects with a diagnosis of SARS-CoV-2 infection obtained by reverse transcription polymerase chain reaction and presence of cycle threshold. According to the level of care needed during hospitalization, the population was categorized as high-intensity (HIMC, n=76) or low intensity medical care setting (LIMC, n=51). **Results**. Viral load did not differ among asymptomatic, LIMC, and HIMC SARS-CoV-2 positive patients [4.4 (2.9–5.3) vs 4.8 (3.6–6.1) vs 4.6 (3.9–5.7) log10copies/ml respectively; p=0.31]. Similar results were observed when asymptomatic individuals were compared to hospitalized patients [4.4 (2.9-5.3) vs 4.68 (3.8-5.9) log10copies/ml; p=0.13]. When the study population was divided in High (HVL, n=64) and Low Viral Load (LVL, n=63) group no differences were observed in disease severity at diagnosis. Furthermore, LVL and HVL groups did not differ with regard to duration of hospital stay, number of bacterial co-infections, need for high-intensity medical care and number of deaths. The viral load was not an independent risk factor for HIMC in an adjusted multivariate regression model (OR: 1.59; 95%CI: 0.46–5.55, p=0.46). **Conclusions**. Viral load at diagnosis is similar in asymptomatic and hospitalized patients and is not associated with either worse outcomes during hospitalization. SARS CoV-2 viral load might not be the right tool to assist clinicians in risk-stratifying hospitalized patients.

INTRODUCTION

Severe acute respiratory syndrome-Coronavirus-2 (SARS-CoV-2) is the etiological agent of the second pandemic infection of the 3rd millennium, following the H1N1 influenza outbreak in 2009. This new virus, which causes Coronavirus-Disease-19 (COVID-19), rapidly spread from China, where the first cases were discovered in late December 2019. As of February 2021, COVID-19 has infected more than 6.000.000 people worldwide.

Epidemiological studies found that a large fraction of individuals infected with SARS-CoV-2 are asymptomatic[1,2]. Yet, the greatest health care burden is accounted for by symptomatic patients. In this regard, COVID-19 may cause a wide range of clinical manifestations, ranging from mild flu-like symptoms with cough and fatigue to severe respiratory failure, leading to non-invasive/invasive mechanical ventilation (NIV/IMV) in the high-intensity (HIMC) or intensive medical care units (ICUs)[3].

Several studies tried to identify prognostic tools. Of these, chest X-rays (CXRs) at admission[4,5], laboratory findings[6], and clinical composed scores[7] have been proposed as predictors of worst clinical outcomes.

The importance of COVID-19 viral load detectable in the nasopharyngeal swab has been addressed in a number of studies, yet with controversial results[8-11]. In particular, it has been reported that the viral load reaches a peak during the first week from symptoms onset, followed by a decrease in the next one or three weeks. Others have described an independent association between the viral load and mortality or ICU admission[12-15]. Conversely, Argyropoulos et al. did not find any associations between viral load and predictors of worst prognosis (i.e. admission to ICU, duration of oxygen supplementation and overall survival)[16]. Similarly, other authors did not find any differences in the viral load between asymptomatic and symptomatic patients[1,17]. Finally, in France, patients from the summer outbreak displayed higher viral load with lower severity markers compared with patients from the spring outbreak[18].

With this background, we sought to assess the role of viral load, obtained from SARS-CoV-2 positive patients hospitalized in a tertiary care center in Padova, as a predictor of the need of High Intensity Medical Care (HIMC), and its relation with other established prognostic parameters.

MATERIALS AND METHODS

Study Population and Study Design

Among subjects who were hospitalized for SARS-CoV-2 infection in the Division of Infectious and Tropical Diseases of the University Hospital of Padova between February and April 2020, we retrospectively collected 127 patients diagnosed by RT-PCR at nasopharyngeal swab (NP) and with the presence of Gene E cycle threshold (Ct) in the diagnostic RT-PCR. Were excluded patients whose sample was analyzed on a different diagnostic platform or at a different institution or with a different Gene Ct.

In our study population, demographical and clinical data, gas exchange values (PaO2/FiO2), blood samples, SARS-CoV-2 Gene E Ct, and chest X-rays (CXRs) were collected at hospital admission. Comorbidities were categorized as: cardiovascular diseases (CVDs), respiratory diseases, metabolic diseases (including diabetes mellitus, obesity and dyslipidemia), autoimmune diseases and oncologic diseases (including lung, prostate, pancreatic, breast, and colon cancers). Twenty-one asymptomatic or mildly symptomatic SARS-CoV-2 positive patients treated at home, from the cohort previously reported by Lavezzo et al.[1] were included as controls.

Based on patient's clinical conditions during hospitalization, the study population was categorized according to the level of care needed. The use of high-flow nasal cannula (HFNC) or NIV/IMV which required admission either to the ICU or to the Respiratory ICU, was considered as a high-intensity medical care setting (HIMC, n = 76), while the need for oxygen supplementation through low-flow nasal cannula or face mask was considered as a low-intensity medical care setting (LIMC, n = 51), as previously described[5].

Moreover, in order to compare the clinical data according to the viral load, the overall study population was further categorized in two groups, namely High (HVL, n = 64) and Low Viral Load (LVL, n = 63).

Radiological Evaluation

For each patient, a single image plane CXR was available at hospital admission. Two radiologists (C.G., G.B.) with more than ten-year experience in thoracic imaging, who were blind to clinical data, scored the images independently using a composite semi-quantitative scale, as previously described[4]. Thus, a

radiological global score (CARE) including ground-glass opacities and consolidations was assessed for each patient.

SARS-CoV-2 detection and assessment of genome equivalents

Upper respiratory tract samples were collected by healthcare professionals with a flocked swab and immediately put into transport medium (eSwab, Copan Italia Spa). Sampling was performed either at the day of hospitalization or, at most, the day before for all patients. Detection of SARS-CoV-2 RNA was performed with an in-house reverse transcription polymerase chain reaction (RT–PCR) protocol, developed according to the diagnostic methodology by Corman et al.[19] with primers and probes targeting the gene encoding the envelope (E). Additionally, to assess the correct execution of the sampling, each sample was tested using primers designed to amplify the human housekeeping gene encoding RNase P, serving as an internal control. Reactions that failed to show the internal positive control were repeated. Ct data from real-time RT–PCR assays was collected for E gene. Genome equivalent copies per ml were inferred according to linear regression performed on calibration standard curves. The interpolated Ct values were further multiplied by 100, according to the final dilution factor (1:100). Linear regression was calculated in Python3.7.3 using modules scipy 1.4.1, numpy 1.18.1 and matplotlib 3.2.1.

Ethics Statement

This was a retrospective study on anonymized patient's data collected from electronic medical records. The study protocol complies to the ethical guidelines of the 1975 Declaration of Helsinki and, in agreement with national regulation on retrospective observational studies, it was notified and approved by the local ethics committee (nr.: 46430/03.08.2020) and the need for patient's informed consent was waived.

Statistical Analysis

Categorical variables were described as absolute (n) and relative values (%), whereas continuous variables were described as median and interquartile range. To compare demographic data and baseline clinical characteristics between asymptomatic, LIMC and HIMC groups or between LVL and HVL groups, Chi square test and Fisher's exact test for categorical variables and Kruskal-Wallis tests

or Mann–Whitney U test for continuous variables were used, as appropriate. The correlation was assessed using the nonparametric Spearman's rank method. In a univariate logistic regression analysis, followed by a regression model adjusted for gender, age, BMI, pack years, lag time symptoms – diagnosis, cardiovascular diseases, metabolic diseases, autoimmune diseases, oncologic diseases, respiratory diseases, we analyzed the role of viral load as predictor of the different level of care. All data were analyzed using SPSS Software version 25.0 (US: IBM Corp., New York, NY, USA). p-values <0.05 were considered statistically significant.

RESULTS

Viral Load Differences in Asymptomatic and Hospitalized Patients

Baseline demographic and viral load data of asymptomatic, LIMC, and HIMC SARS-CoV-2 positive patients included in the study are summarized in **Table 1**.

No differences in sex were observed across the study groups, although individuals were mostly males in each cohort (62 vs 55 vs 71%; respectively). Age and BMI were significantly different between both asymptomatic and LIMC patients as compared with HIMC patients [65 (58–73) vs 64 (52-75) vs 77 (63-82) years; p=0.001 for age and 24.9 (22.2–29.8) vs 26.1 (21.2–29.2) vs 30 (25-31) kg/m2; p=0.007, for BMI respectively]. However, viral load did not differ across the three groups [4.4 (2.9–5.3) vs 4.8 (3.6–6.1) vs 4.6 (3.9–5.7) log10copies/ml; p=0.31] even when comparing asymptomatic individuals with all hospitalized patients [4.4 (2.9-5.3) vs 4.68 (3.8-5.9) log10copies/ml; p=0.13].

Table 1 - Baseline demographics and viral load of SARS-CoV-2 positive asymptomatic patients and hospitalized patients for SARS-CoV-2 related infection *categorized in low* (LIMC) and *high* (HIMC) intensity medical care.

	Asymptomatic patients (n = 21)	**Low-intensity medical care (LIMC) (n = 51)**	**High-intensity medical care (HIMC) (n = 76)**	***p* Value**
Male – *n (%)*	13 (62)	28 (55)	54 (71)	0.17
Age at diagnosis – *years*	65 (58 – 73)*	64 (52 - 75)**	77 (63 - 82)	**0.001**
BMI - *kg/m²*	24.9 (22.2 – 29.8)*	26.1 (21.2 – 29.2)**	30 (25 - 31)	**0.007**
Viral load (Gene E) – *log_{10} copies/ml*	4.4 (2.9 – 5.3)	4.8 (3.6 – 6.1)	4.6 (3.9 – 5.7)	0.31

Values are expressed as numbers and (%) or median and interquartile range, as appropriate. To compare demographic Chi square test for categorical variables and Kruskal-Wallis for continuous variables were used. As compared to HIMC patients, (*) (**) indicates the presence of statistically significant differences.

Patient Demographics and Clinical Characteristics at Baseline and During Hospitalization

Demographic and clinical characteristics of LIMC and HIMC group at admission and during hospitalization are summarized in **Table 2**.

In the entire study population, most patients were males (65%) and the median age was 72 years. Half of them were nonsmokers (53%) and the most prevalent comorbidities were CVDs (64%), followed by metabolic disease (49%).

According to the level of care required during hospitalization, 76 patients were classified as HIMC (when HFNC, or NIV or IVM were used) and 51 as LIMC (when low-flow nasal cannula or mask were used).

Compared to LIMC patients, HIMC patients were mainly males [71 (54%) vs 28 (55%); p=0.06], older [77 (63-82) vs 64 (52-75) years; p=0.001] and with a higher BMI [30 (25-31) vs 26.1 (21.2–29.2) kg/m2; p=0.003]. The HIMC and LIMC groups were similar with regard to smoking history. Regarding comorbidities, patients requiring HIMC had more frequently CVDs [58 (76%) vs 23 (45%); p<0.0001], metabolic diseases [40 (53%) vs 14 (27%); p=0.0003] and chronic respiratory diseases [18 (24% vs 5 (10%); p=0.04), conversely, they did not differ for autoimmune and oncologic diseases.

The duration of symptoms before hospital admission did not differ between patients requiring

HIMC and LIMC [5 (2-7) vs 4 (0-7) days; p=0.20]. At hospital admission, patients requiring HIMC displayed a higher impairment of respiratory gas exchange with a worse P/F ratio [125 (66–191) vs 429 (364-429); p<0.0001] and a higher CARE score [13 (5–20) vs 3 (1–5); p<0.0001]. HIMC patients presented also a longer duration of hospitalization [18 (8-29) vs 7 (3-13) days; p<0.0001], a higher number of bacterial co-infections [33 (34%) vs. 7 (14%); < 0.0001] and a worse outcome [26 (34%) of deaths vs. 0 (0%); p < 0.0001] compared to LIMC patients.

As previously mentioned, no differences were found in the viral load at the first positive nasopharyngeal swab between HIMC and LIMC patients [4.8 (3.6–6.1) vs 4.6 (3.9–5.7) log10copies/ml; p=0.31].

Table 2 - Baseline demographics and clinical features of the overall hospitalized study population for SARS-CoV-2 related infection, and of the two subgroups categorized in *low* (LIMC) and *high* (HIMC) intensity medical care**.**

	Overall Hospitalized Study Population (n =127)	**Low-intensity medical care (LIMC) (n = 51)**	**High-intensity medical care (HIMC) (n = 76)**	***p* Value**
Male – *n (%)*	82 (65)	28 (55)	54 (71)	0.06
Age at admission – *years*	72 (58 – 81)	64 (52 - 75)	77 (63 - 82)	**0.001**
Smoking history – *pack years*	0 (0 – 16)	0 (0 – 10)	0 (0 - 25)	0.29
• **Current – *n (%)***	6 (5)	3 (6)	3 (4)	0.61
• **Former – *n (%)***	54 (42)	19 (37)	35 (46)	0.32
• **Nonsmokers – *n (%)***	67 (53)	29 (57)	38 (50)	0.52
BMI - kg/m²	27.1 (23.5 – 30.5)	26.1 (21.2 – 29.2)	30 (25 - 31)	**0.003**
Comorbidities – n (%)				
• **Cardiovascular diseases (CVD)**	81 (64)	23 (45)	58 (76)	**<0.0001**
• **Chronic respiratory diseases**	23 (18)	5 (10)	18 (24)	**0.04**
• **Autoimmune diseases**	15 (12)	6 (12)	9 (12)	0.99
• **Metabolic diseases**	54 (43)	14 (27)	40 (53)	**0.0003**
• **Oncologic diseases**	20 (16)	8 (16)	12 (16)	0.98
Viral load (Gene E) – *log_{10} copies/ml*	4.68 (3.8 – 5.9)	4.8 (3.6 – 6.1)	4.6 (3.9 – 5.7)	0.96
Lag time symptoms - diagnosis – *days*	5 (1 - 7)	4 (0 - 7)	5 (2 - 7)	0.20
P/F at admission - *ratio*	225 (108 - 429)	429 (364 - 429)	125 (66 – 191)	**<0.0001**
CARE score at admission	7 (2 – 15)	3 (1 – 5)	13 (5 – 20)	**<0.0001**
Hospitalization - *days*	13 (5 - 24)	7 (3 - 13)	18 (8 - 29)	**<0.0001**
Bacterial co-infections - *n (%)*	40 (32)	7 (14)	33 (34)	**<0.0001**
Dead – *n (%)*	26 (20)	0 (0)	26 (34)	**<0.0001**

Values are expressed as numbers and (%) or median and interquartile range, as appropriate. To compare demographic between LIMC and HIMC, Chi square test and Fisher t test (n < 5) for categorical variables and Mann-Whitney t test for continuous variables were used, as appropriate.

Comparison between Patients with High and Low Viral Load

In further analysis, the study population was divided in two groups, namely High (HVL, n=64) and Low Viral Load (LVL, n=63), according to the median value of the viral load (i.e. 4.68 log10copies/ml). Demographic and clinical characteristics at admission and during the hospitalization are summarized in **Table 3.**

No differences in sex, age, smoking history, chronic respiratory diseases and oncologic diseases were found between LVL and HVL. Compared to patients with LVLs, those with HVL included a higher percentage of nonsmokers (50% vs 30%;

p=0.03), and had a lower BMI [26.1 (22.1-30) vs 29 (24.8–31.2) kg/m2; p=0.04], more frequently autoimmune diseases [12 (19%) vs. 3 (5%); p=0.02] and less frequently CVDs [34 (53%) vs. 47 (75%); p=0.01] and metabolic disease [20 (31%) vs 34 (54%); p=0.01].

Interestingly, disease severity at the emergency department was similar in the two groups regardless of viral load. In particular, patients with LVL and HVL showed the same CARE score, gas exchange impairment and symptom duration before diagnosis. **Figure 1** displays the CXR of two patients with high CARE score requiring high intensity medical care but with different viral load at hospital admission (under 25th and over 75th interquartile, respectively). Blood samples at hospital admission revealed that neutrophils [3.7 (2.2–5.7)x109 vs. 4.8 (2.9–7.7)x109/L; p=0.04], C-reactive protein [61.5 (19–130) mg/dL vs. 109 (50-170) mg/dL; p=0.03] and LDH [282 (204–402) U/L vs. 341 (265-464) U/L; p=0.03] were lower in HVL compared to LVL. Of interest, LVL and HVL did not differ when considering other outcome measures such as duration of the hospital stay, number of bacterial co-infections, need for high-intensity medical care and number of deaths.

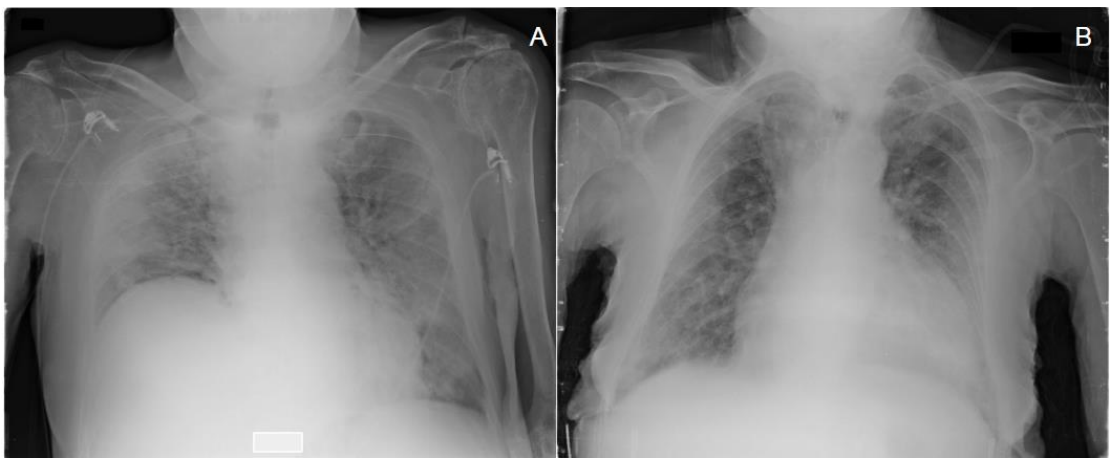

Figure 1. Chest X-ray with a high CARE score at admission of two patients treated with high intensity medical care (HIMC) during hospitalization and with different values of viral load (Gene E) at diagnosis: A) a 81 years old patient presenting a CARE score of 22 points and a viral load of 2.43 log10 copies/ml, (< 25th percentile); B) a 92 years old patient presenting a CARE score of 18 points and a viral load of 6.72 log10 copies/ml, (>75th percentile).

Table 3 - Baseline demographics and clinical features of the population hospitalized for SARS-CoV-2 related infection categorized in *low* (LVL) and *high* (HVL) viral load.

	Low viral load (LVL) (n = 63)	High viral load (HVL) (n = 64)	*p* Value
Male – *n (%)*	40 (63)	42 (66)	0.80
Age at admission – *years*	74 (62 - 81)	70 (56 - 80)	0.19
Smoking history – *pack years*	1 (0 – 23)	0 (0 - 10)	0.17
• **Current – *n (%)***	2 (3)	4 (6)	0.41
• **Former – *n (%)***	28 (44)	20 (31)	0.12
• **Nonsmokers – *n (%)***	20 (30)	32 (50)	**0.03**
BMI - *kg/m²*	29 (24.8 – 31.2)	26.1 (22.1 - 30)	**0.04**
Comorbidities - *n (%)*			
• **Cardiovascular diseases**	47 (75)	34 (53)	**0.01**
• **Respiratory diseases**	11 (17)	12 (19)	0.85
• **Autoimmune diseases**	3 (5)	12 (19)	**0.02**
• **Metabolic diseases**	34 (54)	20 (31)	**0.01**
• **Oncologic diseases**	10 (16)	10 (16)	0.96
Lag time symptoms - diagnosis – *days*	5 (2 - 7)	4 (1 - 7)	0.12
PaO2/FiO2 - ratio	209 (101 - 429)	283 (0 – 429)	0.52
CARE score at admission	9 (3 – 16)	5 (2 – 14)	0.20
High-intensity medical care – *n(%)*	39 (62)	37 (58)	0.64
Hospitalization - *days*	10 (6 - 24)	13 (4 - 22)	0.91
Bacterial co-infections - *n (%)*	19 (30)	21 (33)	0.65
Dead – *n (%)*	13 (21)	13 (20)	0.96
White cells count – *10^9/L*	6.2 (4.1 – 8.7)	5.1 (3.6 – 6.4)	0.07
Hemoglobin – *g/L*	132 (118 - 143)	129 (116 - 142)	0.71
Neutrophils - *10^9/L*	4.8 (2.9 – 7.7)	3.7 (2.2 – 5.7)	**0.04**
Lymphocytes - *10^9/L*	0.8 (0.6 – 1.2)	0.9 (0.5 – 1.2)	0.94
Monocytes - *10^9/L*	0.4 (0.2 – 0.7)	0.4 (0.3 – 0.6)	0.71
Eosinophils - *10^9/L*	0 (0 – 0.02)	0 (0 – 0.01)	0.69
C-reactive protein - *mg/dL*	109 (50 - 170)	61.5 (19 – 130)	**0.03**
D-Dimer – *µg/L*	299 (158 - 908)	217 (179 – 350)	0.06
Albumin – *g/L*	30 (26 - 33)	30.5 (27 - 36)	0.27
Ferritin- *µg/L*	876 (505 -1481)	849 (404 - 1258)	0.64
LDH – *U/L*	341 (265 - 464)	282 (204 – 402)	**0.03**

Values are expressed as numbers and (%) or median and interquartile range, as appropriate. To compare demographic between LVL and HVL, Chi square test and Fisher t test (n < 5) for categorical variables and Mann-Whitney t test for continuous variables were used. LDH = Lactate Dehydrogenase; BMI = body mass index; CARE = radiological global score.

Viral Load Correlations and its prognostic role

A negative correlation between viral load at hospital admission and BMI was observed in the whole population (r = - 0.26; p=0.01). The viral load was also negatively correlated with the lag time (days) between symptoms initiation and diagnosis of SARS-CoV-2 infection by nasopharyngeal swab (r = - 0.24; p=0.007). The viral load was not an independent risk factor for HIMC in a univariate regression model (OR: 0.84; 95%CI 0.41–1.72, p=0.64). This finding was confirmed when the regression model was adjusted for gender, age, BMI, pack

years, lag time symptoms – diagnosis, and cardiovascular, metabolic, autoimmune, oncologic and respiratory diseases (OR: 1.59; 95%CI: 0.46–5.55, p=0.46).

DISCUSSION

In this study, we explored the association between viral load detectable in the first positive nasopharyngeal swab and clinical outcomes of SARS-CoV-2 infected patients. Notably, the viral load did not differ between asymptomatic patients managed at home and patients who needed hospitalization. Moreover, when considering only hospitalized patients, viral load at first presentation was similar in patients requiring low intensity medical care (LIMC) and those requiring high-intensity (HIMC) setting. Moreover, viral load was not associated with either worse outcome measures during hospitalization or with mortality.

A large body of studies have addressed the issue of the viral load both in terms of change over time, from early detection of SARS-CoV-2 infection to recovery, and quantitative changes across the different respiratory samples (upper or lower respiratory tract) simultaneously collected. In particular, in a systematic review of 113 studies, Walsh KA et al. reported that the highest viral load from upper respiratory tract samples was observed at the time of symptoms onset and for a few days thereafter, with levels progressively slowing down over the following one to three weeks[8]. Hence, in order to investigate the prognostic role of the viral load, we considered the first available nasopharyngeal swab positive for SARS-CoV-2 performed at admission and correlated it with clinical outcomes and prognosis. We observed that the viral load was similar across all study subsets of hospitalized (both LIMC and HIMC groups) and asymptomatic patients.

The association between viral load and disease severity remains controversial and debated. Previous studies have reported an association with severity of outcome. A retrospective cohort study of 875 patients hospitalized with COVID-19 in Brazil observed that SARS-CoV-2 viral load at admission was independently associated with mortality. However, the authors did not include comorbidities, clinical symptoms, and duration of symptoms before testing, which are clinically important variables and might have influenced the interpretation of their results[15]. Similarly, Magleby Reed and colleagues demonstrated that SARS-CoV-2 viral load at admission among hospitalized patients with COVID-19 (n=678) independently correlates with the risk of intubation and in-hospital

mortality. However, they reported a different symptom duration prior to admission between high and low viral load group[13]. Pujadas et al. reported that the mean log10 viral load in patients who were alive (n = 807; mean log10 viral load 5.2 copies per mL [SD 3]) significantly differed from that of patients who died (n = 338; 6.4 copies per mL [2.7]). They also demonstrated an independent relationship between high viral load and mortality after adjusting for demographics and comorbidities (hazard ratio 1.07 [95% CI 1·03–1·11], p=0.0014)[12].

In line with our findings, in a cohort of 205 patients from New York City, Argyropoulos and coworkers did not find any associations between viral load and clinical outcomes, including length of stay, oxygen support requirement, or survival[16], suggesting that severe symptoms and outcomes are unlikely to be related to high viral titers. However, this study evaluated mainly non-hospitalized patients with the exception of a small subset of patients with severe COVID-19 infection. In this regard, our study that conducted mild vs. severe hospitalized patients (i.e. LIMC and HIMC group) reinforces the lack of association between outcomes and viral load values. Notably, despite their similar viral load, these two populations differ in terms of age and BMI. Specifically, HIMC patients were older and had a significantly higher BMI compared to both asymptomatic and LIMC patients, in keeping with previous data from our group[5]. If further confirmed, this finding is important, as predictors of worse outcome in individuals infected by SARS-CoV-2 are lacking.

In further analysis, we stratified patients requiring hospitalization based on their median viral load value (lower versus higher). Age, sex, smoking history and symptom duration before the diagnosis of COVID-19 were similar in patients with high (HVL) and low viral load (LVL). Viral load of SARS-CoV-2 peaks around the time of symptom onset (or a few days after) and decreases over time, and symptom duration negatively correlates with viral load. Of note, both the high and low viral load groups exhibited similar disease severity at diagnosis/admission, as assessed by PaO2/FiO2 ratio and radiographic CARE score, need for HIMC, number of bacterial co-infections, duration of hospitalization, and number of deaths. Similarly, the viral load was not associated with the need for high-intensity medical care both on univariate regression model and after adjusting for age, sex, BMI, pack years, symptoms duration, and cardiovascular, metabolic, autoimmune, oncologic and respiratory comorbidities.

Our findings are in contrast with previous data[12,13] suggesting that viral load is associated with mortality after adjustment for other concurrent clinical confounding factors. However, we analyzed not only the association of viral load with mortality, but also with the need for high-intensity medical care, which is associated with poor outcomes even long term. The lack of association between viral load and clinical outcomes and prognosis might suggest that the viral load in nasopharyngeal swab does not reflect the viral load in the lung and thus the severity of lung involvement and/or the degree of cytokine storm in the lung. In this regard, the level of a number of inflammatory markers (i.e., neutrophils, LDH, C-reactive-protein) is significantly increased in patients with a lower viral load.

The results of our study should be interpreted in light of some limitations, mainly the relatively small sample size, which implies that our findings need further validation in larger, independent, prospectively collected populations of patients. However, in contrast with previous studies, our patient population included a wide range of disease severity. Secondly, we retrospectively collected all clinical data from our electronic medical records; however, every effort was made to limit inaccuracy and missing data to a minimum.

In conclusion, this study shows that SARS-CoV-2 viral load at diagnosis is similar across asymptomatic patients, and patients hospitalized in a low and high intensity medical care. Moreover, viral load is not associated with either worse outcomes during hospitalization or with mortality, but appears to decrease with longer history of symptoms. Therefore, SARS CoV-2 viral load assessed by RT-PCR might not be the most useful tool for patient risk stratification.

REFERENCES

1. Lavezzo E., Franchin E., Ciavarella C. et al. Suppression of a SARS-CoV-2 outbreak in the Italian municipality of Vo'. Nature. 2020 Aug;584(7821):425—429.
2. Yanes-Lane M., Winters N., Fregonese F. Proportion of asymptomatic infection among COVID-19 positive persons and their transmission potential: A systematic review and meta-analysis. PLoS One. 2020 Nov 3;15(11):e0241536.
3. Grant MC., Geoghegan L., Arbyn M. et al. The prevalence of symptoms in 24,410 adults infected by the novel coronavirus (SARS-CoV-2; COVID-19): A systematic review and metaanalysis of 148 studies from 9 countries. PLoS One. 2020 Jun 23;15(6):e0234765.
4. Giraudo C., Cavaliere A., Fichera G. et al. Validation of a composed COVID-19 chest radiography score: the CARE project. ERJ Open Res. 2020 Oct 26;6(4):00359-2020.
5. Cocconcelli E., Biondini D., Giraudo C. et al. Clinical features and chest imaging as predictors of intensity of care in patients with COVID-19. J Clin Med. 2020 Sep 16;9(9):2990.
6. Pourbagheri-Sigaroodi A., Bashasha D., Fatehb F. et al. Laboratory findings in COVID-19 diagnosis and prognosis. Clin Chim Acta. 2020 Nov;510:475-482.
7. Liang W., Jianhua Y., Ailan C. et al. Early triage of critically ill COVID-19 patients using deep learning. Nature Communications. (2020) 11:3543.
8. Walsh K.A., Jordan K., Clyne B. et al. SARS-CoV-2 detection, viral load and infectivity over the course of an infection. Journal of Infection 81 (2020) 357–371.
9. To K.K., Tsang OT., Leung W. et al. Temporal profiles of viral load in posterior oropharyngeal saliva samples and serum antibody responses during infection by SARS-CoV-2: an observational cohort study. Lancet Infect Dis 2020; 20: 565–74.
10. Salvatore PP., Dawson P., Wadhwa A.: Epidemiological Correlates of PCR Cycle Threshold Values in the Detection of SARS-CoV-2. Clin Infect Dis 2020 Sep 28;ciaa1469.
11. Zou L., Feng Ruan F., Huang M. et al. SARS-CoV-2 Viral Load in Upper Respiratory Specimens of Infected Patients N Engl J Med 382;12 2020.
12. Pujadas E., Chaudhry F., McBride R., SARS-CoV-2 viral load predicts COVID-19 mortality Lancet Respir Med 2020 Sep;8(9):e70.
13. Magleby R., Westblade L.F., Trzebucki A. et al. Impact of Severe Acute Respiratory Syndrome Coronavirus 2 Viral Load on Risk of Intubation and Mortality Among Hospitalized Patients With Coronavirus Disease 2019. Clinical Infectious Disease 2020.
14. Westblade L.F., Brar G., Pinheiro L.C. et al. SARS-CoV-2 Viral Load Predicts Mortality in Patients with and without Cancer Who Are Hospitalized with COVID-19. Cancer Cell 2020 Nov 9;38(5):661-671.e2.
15. Faíco-Filho K.S. Passarelli V.C., Bellei N. et al. Is Higher Viral Load in SARS-CoV-2 Associated with Death? Am. J. Trop. Med. Hyg., 00(0), 2020, pp. 1–3.

16. Argyropoulos K.V., Serrano A., Hu J. et al. Association of Initial Viral Load in Severe Acute Respiratory Syndrome Coronavirus 2 (SARS-CoV-2) Patients with Outcome and Symptoms 2020. The American Journal of Pathology, Vol. 190, No. 9, September 2020.
17. Ra S.H., Lim J.S., Gwang-un Kim G. et al. Upper respiratory viral load in asymptomatic individuals and mildly symptomatic patients with SARS-CoV- 2 infection. Thorax 2020;0:1–4.
18. Gautret P., Colson P., Lagier J.C. et al. Different pattern of the second outbreak of COVID-19 in Marseille, France. Int J Infect Dis 2021 Jan;102:17-19.
19. Corman V.M., Landt O., Kaiser M. et al. Detection of 2019 novel coronavirus (2019-nCoV) by real-time RT-PCR. Euro Surveill. 2020 Jan;25(3):2000045.

Chapter 14

Characteristics and Prognostic Factors of Pulmonary Fibrosis After COVID-19 Pneumonia

Elisabetta Cocconcelli, Nicol Bernardinello, Chiara Giraudo, Gioele Castelli, Adelaide Giorgino, Davide Leoni, Simone Petrarulo, Anna Ferrari, Marina Saetta, Annamaria Cattelan, Paolo Spagnolo, and Elisabetta Balestro.

Front Med (Lausanne). 2022 Jan 31;8:823600. doi: 10.3389/fmed.2021.823600. PMID: 35174188; PMCID: PMC8841677.

ABSTRACT

Background. Little is known about the long-term pulmonary sequelae after COVID-19 infection.

Hence, the aim of this study is to characterize patients with persisting pulmonary sequelae at follow-up after hospitalization. We also aimed to explore clinical and radiological predictors of pulmonary fibrosis following COVID-19.

Methods. Two hundred-twenty consecutive patients were evaluated at 3–6 months after discharge with high-resolution computed tomography (HRCT) and categorized as recovered (REC) or not recovered (NOT-REC). Both HRCTs at hospitalization (HRCT0), when available, and HRCT1 during follow-up were analyzed semi-quantitatively as: ground glass opacities (Alveolar Score,AS), consolidations (CONS) and reticulations (Interstitial Score, IS).

Results. 175/220 (80%) patients showed disease resolution at their initial radiological evaluation following discharge. NOT-REC patients (45/220; 20%) were mostly older males [66 (35-85) years vs. 56 (19 - 87); p=0.03] with a longer in-hospital stay [16 (0 - 75) vs. 8 (1 - 52) days; p<0.0001], and lower P/F at admission [233 (40-424) vs. 318 (33-543); p=0.04]. Moreover, NOT-REC patients presented, at hospital admission, higher ALV [14(0.0–62.0) vs. 4.4(0.0–44.0);p=0.0005], CONS [1.9(0.0–26.0 vs. 0.4(0.0–18.0);p=0.0064], and IS [11.5(0.0– 29.0) vs. 0.0(0.0–22.0);p<0.0001] compared to REC patients. On multivariate analysis, the presence of CONS and IS at HRCT0 were independent predictors of radiological sequelae at follow-up [OR 14.87(95%CI: 1.25–175.8; p=0.03) and 28.9 (95%CI: 2.17–386.6; p=0.01, respectively).

Conclusions. In our population, only twenty percent of patients showed persistent lung abnormalities at six-months after hospitalization for COVID-19 pneumonia. These patients are predominantly older males with longer hospital stay. The presence of reticulations and consolidation on HRCT at hospital admission predict the persistence of radiological abnormalities during follow-up.

BACKGROUND

Coronavirus disease 2019 (COVID-19), which is caused by the severe acute respiratory syndrome coronavirus 2 (SARS-CoV-2), has infected more than 130 million people worldwide. COVID-19 leads to respiratory manifestations that can range from mild flu-like symptoms like fever, cough, and fatigue to severe respiratory failure requiring intensive care[1,2].

Data from previous pandemics caused by coronaviruses suggested that there may be pulmonary sequelae in one third of patients at twelve weeks after discharge[3,4].

Some recent studies tried to characterize radiological sequelae after COVID-19 pneumonia[5,6]. This condition, which is referred to as 'post-COVID syndrome' still lacks a universally agreed definition[7]. On May 2020, a document of the British Thoracic Society (BTS) proposed an algorithm on post-discharge management of COVID-19 patients and distinguished two groups of interest: patients with severe pneumonia and patients with mild to moderate pneumonia[8]. Following up on this document, George and colleagues suggested a structured respiratory follow-up for patients with clinico-radiological confirmation of Covid-19 pneumonia[9]. Importantly, they proposed patients with severe pneumonia undergo a full clinical assessment at 12 weeks with a chest X-ray while patients with persisting radiological abnormalities should undergo a high-resolution CT (HRCT) scan. In this regard, the role of chest X-ray and HRCT in disease management both during hospitalization and follow-up is well established[10,11]. Han and co-authors recently reported that fibrotic-like changes on CT performed at six months during follow-up persist in approximately one-third of Covid-19 patients[12], but the data on long-term pulmonary sequelae in this patient population remains scarce. The aim of the present study is to characterize, among patients hospitalized for COVID-19 pneumonia, those presenting persisting pulmonary sequelae during follow-up, and to define which clinical and radiological features are predictive of persistent radiological abnormalities.

MATERIALS AND METHODS

Study Population and Study Design

We prospectively collected patients evaluated at the post-COVID Clinic of the University Hospital of Padova between June and December 2020. The patients evaluated at the post-COVID Clinic were initially admitted to the Division of Infectious and Tropical Diseases of the University Hospital of Padova between February and September 2020 for SARS-CoV-2 infection confirmed by the real time-polymerase chain reaction (RT-PCR) at nasopharyngeal swab.

Among all patients evaluated, we specifically followed-up every 3 months those presenting a COVID-19 related severe disease according to the WHO criteria (n=220)[13]. Demographics and clinical data at hospital admission [symptoms, gas exchange values (paO2/FiO2)] and during hospitalization [days of hospital stay, maximal FiO2 (FiO2 max) needed, level of care, treatment] were collected. Comorbidities were categorized as cardiovascular diseases (CVDs), respiratory diseases, metabolic diseases (including diabetes mellitus, obesity and dyslipidemia), autoimmune diseases and oncologic diseases (including lung, prostate, pancreatic, breast, colon cancer). Based on patient's clinical conditions during hospitalization, we distinguished those requiring a low- (LIMC) and high-intensity medical care (HIMC), as previously described[14].

Radiological Evaluation

At follow-up, HRCT was available for the entire study population (HRCT1) whereas at hospital admission, it was available in only a subgroup of patients (HRCT0) (n=79, 36%). The HRCTs were performed by a 64 slice Siemens Somatom Sensation (Siemens Healthcare, Erlangen, Germany) applying a slice thickness ≤ .5 mm.

According to the presence or absence of radiological abnormalities on HCRT1, the study population was categorized as recovered patients (REC, n = 175) or not recovered patients (NOT-REC, n = 45).

Two expert thoracic radiologists (C.G., A.G.), who were blinded to clinical data and timing of HRCTs, scored the images independently using a composite semi-quantitative scale. This represented a modification of the previously reported scoring systems standardized by our group[13]. Specifically, ground glass opacities

(GGO) (alveolar score, AS), consolidations (CONS) and reticulations (interstitial score, IS) were analyzed. For each lung lobe, the two radiologists assessed the extent of AS, CONS and IS using a scale from 0-100 and estimated extent to the nearest 2%. The result was expressed as the mean value of the five lobes in AS, CONS and IS. The level of interobserver agreement was obtained for each patient as a mean of 5 lobes and for each radiological abnormality (AS, CONS and IS) and expressed as Cohen's k value. Disagreement between radiologists was resolved by consensus.

Statistical Analysis

Categorical variables were described as absolute (n) and relative values (%), whereas continuous variables were described as median and range. To compare demographic and clinical data between REC and NOT-REC patients, Chi square test and Fisher's exact test ($n < 5$) for categorical variables and Mann–Whitney U tests for continuous variables were used, as appropriate.

To compare radiological scores at HRCT1 in NOT-REC patients, Mann–Whitney U test for continuous variables was used, whereas while Wilcoxon signed rank test was used to compare radiological scores between HRCT0 and HRCT1. A univariate logistic regression analysis, followed by a regression model adjusted for gender, pack years, paO2/FiO2 at admission, degree of medical care (high or low) and FiO2 max, was performed to detect the predictive factors of radiologic sequelae (NOT-REC) at follow up. All data was analyzed using SPSS Software version 25.0 (US: IBM Corp., New York, NY, USA). p-values <0.05 were considered statistically significant. The graphs were obtained using the statistical package GraphPad Prism 7.0 (GraphPad Software, Inc., La Jolla, CA, USA).

Ethics Statement

The study protocol complies to the ethical guidelines of the 1975 Declaration of Helsinki and, in agreement with national regulation on observational studies, it was notified and approved by the local ethics committee (nr.: 46430/03.08.2020) and the need for patient's informed consent was waived.

RESULTS

Clinical evaluation at hospital admission and during hospitalization.

Two hundred and twenty patients with COVID-19 pneumonia evaluated at the post-COVID Clinic were included in the study (**Table 1**). 115 patients (52%) were males, with a median age of 59 years (range 19 - 84) and body mass index (BMI) 26 (18-39). The most prevalent comorbidities were cardiovascular diseases (CVDs) (n=98, 45%), followed by the chronic respiratory diseases (18%). Based on the presence of radiological sequelae on HRCT performed at follow-up (HRCT1), 175 (80%) patients were categorized as REC and 45 (20%) as NOT-REC (**Figure 1**). Baseline demographic and clinical data of REC and NOT-REC patients are summarized in **Table 1.**

No differences in sex, smoking history, or BMI were observed between the two groups, with a prevalence of males in NOT-REC compared to REC (64 vs. 49%; respectively). NOT-REC patients were significantly older compared to REC [66 (35 - 85) vs. 56 (19 - 87) years; $p < 0.0001$]. CVDs were significantly more frequent in NOT-REC compared to REC [26 (58%) vs 72 (41%); p=0.04] whereas autoimmune, metabolic and oncologic diseases did not differ between the two groups. Symptoms before hospital admission were also similar, except for a higher proportion of patients presenting with dyspnea in NOT-REC compared to REC group [33 (73%) vs. 64 (37%); $p < 0.0001$] (online supplement, Table 1).

At hospital admission, NOT-REC had a worse gas exchange with a lower PiO2/FiO2 ratio than REC [233 (40 – 424) vs.318 (33 - 543); $p = 0.04$]. In addition, compared to REC, during hospitalization NOT-REC required more frequently high-intensity medical care (HIMC) (20, 44% vs. 37, 21%; $p = 0.002$), higher FiO2 max [45 (21 – 100) vs. 27 (21 – 100); $p < 0.0001$], and longer in-hospital stay [16 (0 - 75) vs. 8 (1 - 52) days; $p<0.0001$].

The majority of patients were admitted during the first SARS-CoV-2 wave when no standardized protocols existed for treatment of hospitalized patients. NOT-REC patients were more frequently treated with hydroxychloroquine (n=37, 82% vs. 111, 63%; $p = 0.01$), antibiotics other than ceftriaxone and azithromycin (n=25, 56% vs. 44, 25%; $p < 0.0001$), remdesevir (n=7, 16% vs. 10, 6%, $p = 0.02$), tocilizumab (n=8, 18% vs. 12, 7%; $p = 0.02$), steroids (n=27, 60% vs. 74, 42%; $p = 0.03$) compared to REC. Conversely, the two groups did not differ with regard to use of ceftriaxone, azithromycin, lopinovir/ritonavir, and hyperimmune plasma

(online supplement, Table 2). At discharge, a similar proportion of patients in both groups was prescribed steroids.

Table 1. Baseline demographics and clinical features of the overall population evaluated at post-COVID Clinic, and of the two subgroups categorized according to the presence of radiological recovery during the follow up period.

	Overall population (n =220)	**REC (n = 175; 80%)**	**NOT - REC (n = 45; 20%)**	***p* Value**
Male – *n (%)*	115 (52)	86 (49)	29 (64)	0.06
Age at admission – *years*	59 (19 - 87)	56 (19 - 87)	66 (35 - 85)	**< 0.0001**
Smoking history – *pack years*	0 (0 - 67)	0 (0 - 67)	0 (0 - 60)	0.07
· **Current – *n (%)***	15 (7)	10 (6)	5 (11)	0.20
· **Former – *n (%)***	70 (32)	54 (31)	16 (36)	0.54
· **Non smokers – *n (%)***	135 (61)	111 (63)	24 (53)	0.21
BMI - (kg/m^2)	26 (18 - 39)	27 (18 - 39)	26 (21 - 35)	0.35
Cardiovascular diseases - n (%)	98 (45)	72 (41)	26 (58)	**0.04**
Respiratory diseases - n (%)	39 (18)	30 (17)	9 (20)	0.65
Autoimmune diseases - n (%)	36 (16)	25 (14)	11 (24)	0.10
Metabolic diseases - n (%)	102 (4)	78 (45)	24 (53)	0.29
Oncologic diseases - n (%)	25 (11)	17 (8)	8 (18)	0.12
PaO_2 / FiO_2 at admission	314 (33 - 543)	318 (33 - 543)	233 (40 - 424)	**0.04**

FiO_2max during hospitalization - %	28 (21 - 100)	27 (21 - 100)	45 (21 - 100)	**< 0.0001**
Hospitalization - days	9 (0 - 75)	8 (1 - 52)	16 (0 - 75)	**< 0.0001**
Low degree of care – n (%)	163 (74)	138 (79)	25 (56)	**0.002**
High degree of care – n (%)	57 (26)	37 (21)	20 (44)	

Values are expressed as numbers and (%) or median and range, as appropriate. To compare demographic between recovery (REC) and not recovery (NOT-REC), Chi square test and Fisher t test (n < 5) for categorical variables and Mann-Whitney t test for continuous variables were used.

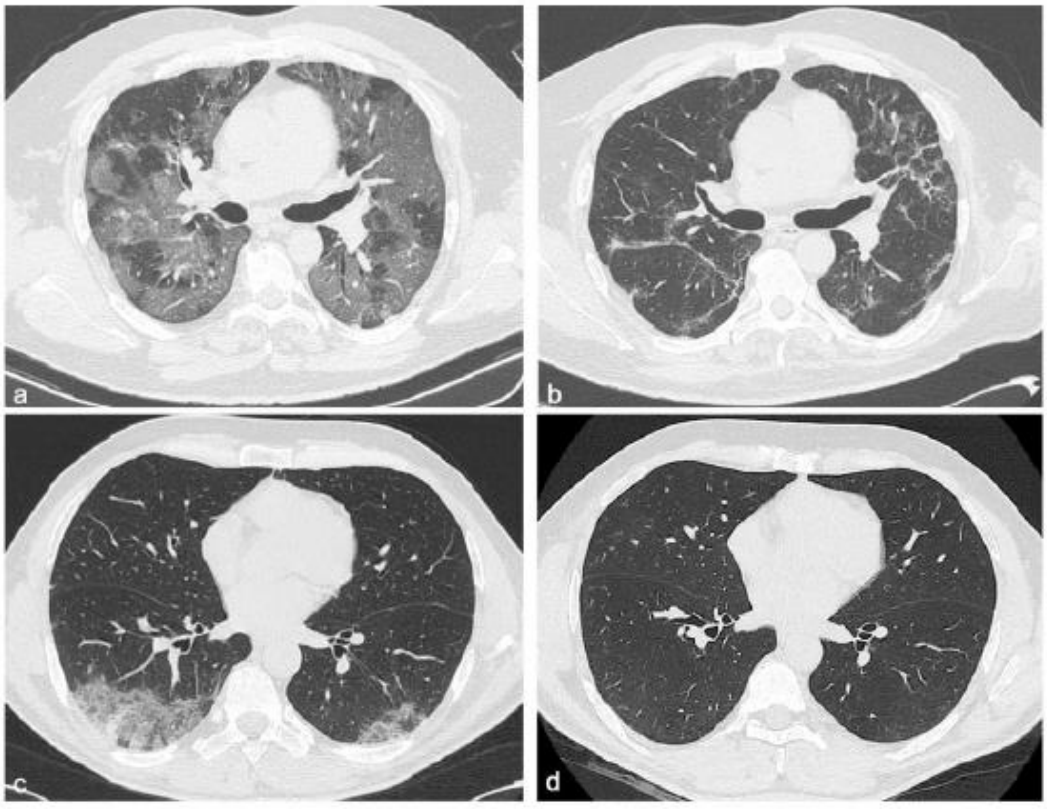

Figure 1. Chest CT features of two patients with COVID-19 pneumonia at different time points: hospitalization and 6 months after discharge. CT images of a 58-year-old male patient with COVID-19, not recovery patient (a,b). The first CT performed at admission shows bilateral areas of ground-glass opacities in a peripheral distribution (a) and after 6 months from discharge, CT shows persistent of interlobular septal thickening with peripheral distribution (b). Chest CT images of a 51-year-old male patient with COVID-19, recovery patient (c,d). The first CT shows, at admission, a small consolidation at the right lower lobe accompanied by ground glass opacities in both lower lobes (c) and after 6 months from discharge, no residual abnormalities were observed (d).

Clinical, functional and radiologic evaluation at follow-up

Patients were evaluated at post-COVID Clinic at regular three-month intervals after discharge. At first evaluation, NOT-REC patients presented more frequently a modified Medical Research Council (mMRC) score of 1 and 2 compared to REC [15 (33%) vs. 22 (13%), p = 0.0009 and 7 (16%) vs. 3 (2%), p < 0.0001, respectively]. In the overall population, pulmonary function tests (PFTs) revealed a median forced vital capacity (FVC) of 3.40 liters (L) (range 1.40 – 7.96), 96%pred. and a median total lung capacity (TLC) of 5.36 L (3.63 – 8.09), 89% pred. within the normal range. Likewise, NOT-REC patients showed preserved lung volumes within normal range (online supplement, Table 3). 32 patients out of 220 (14.5%) had an abnormal diffusing capacity of the lung for carbon monoxide (DLco) at the 6-month follow up, which occurred in those with persistent interstitial lung abnormalities (NOT-REC patients). At follow up CT (HRCT1), NOT-REC patients presented higher ALV [2.8 (0.0 – 40.0)] compared to CONS [0.0 (0.0 – 2.0); p < 0.0001] and IS [0.6 (0.0 – 24.0); p < 0.0001] (online supplement, Figure 1). Overall, the inter-observer agreement between the two radiologists with regard to change in AS, CONS and IS was good (Cohen's kappa = 0.79 for AS, k = 0.88 for CONS and k = 0.81 for IS).

Longitudinal evaluation of radiologic manifestation: from hospitalization to follow-up.

At hospital admission, HRCT (HRCT0) was available for 79/220 (36%) patients. ALV [5.0 (0.0 – 62-0)] was significantly more prevalent compared to CONS [0.8 (0.0 – 26.0); p < 0.0001] and IS [0.8 (0.0 – 29.0); p < 0.0001]. When this patient subgroup was stratified in NOT-REC and REC, NOT-REC patients (n = 20) had at hospital admission higher ALV [14.0 (0.0 – 62.0) vs. 4.4 (0.0 – 44.0); p = 0.0005] (**Figure 2 Panel A**), CONS [1.9 (0.0 – 26.0 vs. 0.4 (0.0 – 18.0); p = 0.0064] (**Figure 2 Panel B**), and IS [11.5 (0.0– 29.0) vs. 0.0 (0.0 – 22.0); p < 0.0001] (**Figure 2 Panel C**) compared to REC patients (n = 59) (**Table 2).** Finally, when comparing HRCT0 with HRCT1, we observed that in NOT-REC patients ALV [from 14 (0.0 – 62.0) to 2.6 (0.0 – 40.0); p < 0.0001], CONS [from 1.9 (0.0 –

26.0) to 0.0 (0.0 – 2.2); p = 0.0001] and IS [1.5 (0.0 – 29.0) to 1.4 (0.0 – 24.0)] decreased significantly (**Figure 3**).

Table 2. HRCT scores during hospitalization ($HRCT_0$) of the overall population evaluated at post-COVID Clinic, and of the two subgroups categorized according to the presence of radiological recovery during the follow up period.

	Overall population (n =220)	REC (n = 175; 80%)	NOT - REC (n = 45; 20%)	*p* Value
Alveolar score - %	5.0 (0.0 – 62)	4.4 (0.0 – 44.0)	14.0 (0.0 – 62.0)	**0.0005**
Consolidations - %	0.8 (0.0 – 26.0)	0.4 (0.0 – 18.0)	1.9 (0.0 – 26.0)	**0.006**
Interstitial score - %	0.8 (0.0 – 29.0)	0.0 (0.0 – 22.0)	11.5 (0.0 – 29.0)	< **0.0001**

Values are expressed as median and range, as appropriate. To compare HRCT scores at hospitalization ($HRCT_0$) between recovery (REC) and not recovery (NOT-REC), Mann-Whitney t test for continuous variables was used.

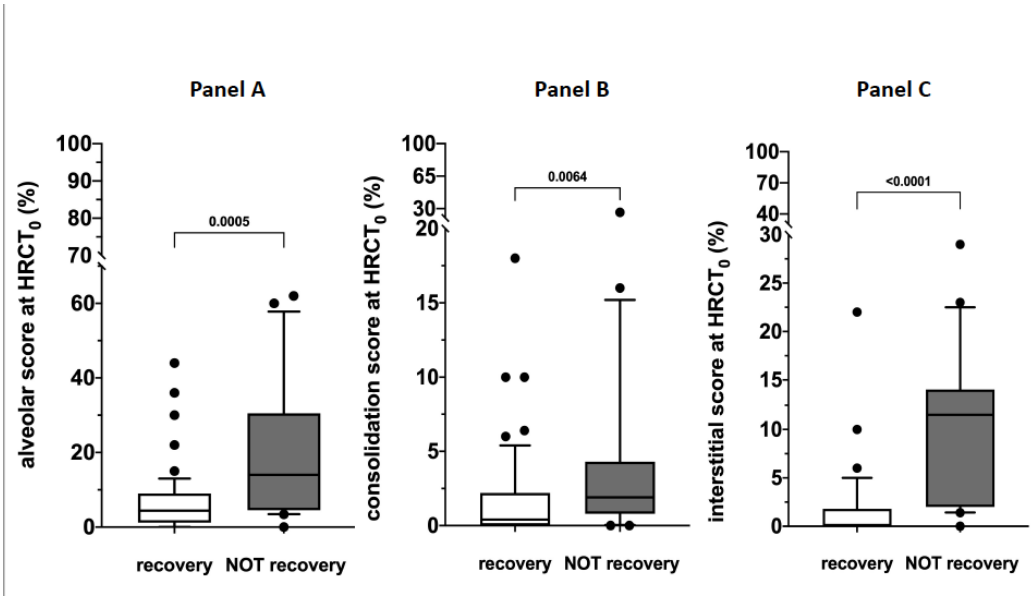

Figure 2. HRCT scores during hospitalization (HRCT0) of the two subgroups categorized according to the presence of radiological recovery [recovery (REC) or NOT-recovery (NOT-REC)] at follow up period. Horizontal bars represent median values; bottom and top of each box plot 25th and 75th; brackets show 10th and 90th percentiles; and circles represent outliers. White boxes indicate values

for recovery group and grey boxes not recovery group. Panel A: ALV [14.0 (0.0 – 62.0) vs. 4.4 (0.0 – 44.0); p = 0.0005]; Panel B: CONS [1.9 (0.0 – 26.0 vs. 0.4 (0.0 – 18.0); p = 0.0064]; Panel C: INT [11.5 (0.0– 29.0) vs. 0.0 (0.0 – 22.0); p < 0.0001].

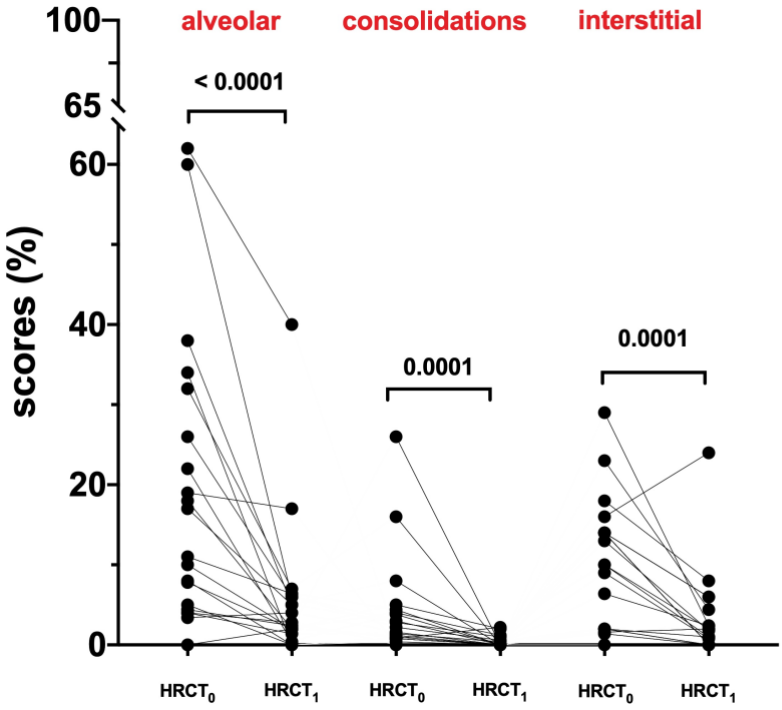

Figure 3. HRCT scores of the not recovery population (NOT-REC) from HRCT0 to HRCT1: ALV [from 14 (0.0 – 62.0) to 2.6 (0.0 – 40.0); p < 0.0001], CONS [from 1.9 (0.0 – 26.0) to 0.0 (0.0 – 2.2); p = 0.0001] and INT [1.5 (0.0 – 29.0) to 1.4 (0.0 – 24.0)].

Prognostic Factors for radiological sequelae at follow-up

Univariate analysis showed that older age, a prolonged in-hospital stay, a lower PiO2/FiO2 at hospital admission, cardiovascular comorbidities, a higher degree of medical care, a higher FiO2 max, and higher ALV, CONS and INT scores at HRCT0, not use of hydroxychloroquine, antibiotics other than azithromycin and ceftriaxone, tocilizumab, remdesevir and systemic steroids are associated with persistent radiological abnormalities at follow-up. Multivariate analysis revealed that CONS [OR: 20.6 (95%CI: 1.4 – 301.2); p = 0.02] and IS score [23.0 (1.4 – 377.2); p = 0.02] are independent predictors of radiological sequelae at follow up (**Table 3**).

Table 3. Predictive factors of radiological sequelae at follow-up in patients hospitalized for SARS-COV-2 related pneumonia.

	Univariate analysis		Multivariate analysis	
	OR (95% IC)	**p**	**OR (95% IC)**	**p**
Sex				
• **female**	Ref.	-	-	-
• **male**	1.87 (0.95 – 3.69)	0.07	-	-
Age – years				
• **< 59**	Ref.	-	Ref.	-
• **≥ 59**	2.99 (1.47 – 6.08)	**0.002**	0.81 (0.10 – 6.39)	0.84
BMI - (kg/m^2)				
• **< 26**	Ref.	-	-	-
• **≥ 26**	0.80 (0.41 – 1.58)	0.52	-	-
Smoking history – *pack years*				
• **= 0**	Ref.	-	-	-
• **> 0**	1.56 (0.79 – 3.10)	0.19	-	-
Hospitalization – *days*				
• **< 9**	Ref.	-	Ref.	-
• **≥ 9**	4.77 (2.15 – 10.5)	**< 0.0001**	12.77 (0.65 – 248.8)	0.09
PiO_2/FiO_2 at admission				
• **< 314**	Ref.	-	Ref.	-
• **≥ 314**	0.33 (0.13 – 0.80)	**0.01**	1.24 (0.13 – 11.46)	0.84
CVD				
• **No**	Ref.	-	Ref.	-
• **Yes**	1.95 (1.00 – 3.80)	**0.04**	1.40 (0.15 – 12.48)	0.76
Respiratory diseases				
• **No**	Ref.	-	-	-
• **Yes**	1.20 (0.52 – 2.77)	0.65	-	-
Autoimmune diseases				
• **No**	Ref.	-	-	-
• **Yes**	1.94 (0.87 – 4.32)	0.11	-	-
Metabolic diseases				
• **No**	Ref.	-	-	-
• **Yes**	1.42 (0.73 – 2.74)	0.29	-	-
Oncologic diseases				
• **No**	Ref.	-	-	-
• **Yes**	2.01 (0.80 – 5.01)	0.13	-	-
Degree of care				
• **Low**	Ref.	-	Ref.	-
• **High**	2.98 (1.49 – 5.95)	**0.002**	1.35 (0.13 – 13.12)	0.79
FiO2 max - %				
• **< 28**	Ref.	-	Ref.	-
• **≥ 28**	3.25 (1.54 – 6.80)	**0.002**	1.01 (0.07 – 16.2)	0.99

Alveolar score HRCT0 - % • **< 7** • **≥ 7**	Ref. 4.0 (1.33 – 11.98)	- **0.01**	Ref. 0.74 (0.09 – 5.99)	- 0.78
Consolidations HRCT0 - % • **< 0.8** • **≥ 0.8**	Ref. 6.29 (1.66 – 23.87)	- **0.007**	Ref. 20.6 (1.40 – 301.2)	- **0.02**
Interstitial score HRCT0 - % • **< 1.4** • **≥ 1.4**	Ref. 41.2 (5.1 – 331.8)	- **< 0.0001**	Ref. 23.0 (1.40 – 377.2)	- **0.02**
Hidroxicloroquina • **Yes** • **No**	Ref 2.66 (1.17 – 6.07)	**0.02**	Ref 1.26 (0.18 – 8.82)	**0.80**
Azithromycin • **Yes** • **No**	Ref. 0.76 (0.39 – 1.47)	- 0.41	- -	- -
Ceftriaxone • **Yes** • **No**	Ref. 1.74 (0.89 – 3.40)	- 0.10	- -	- -
Other antibiotics • **Yes** • **No**	Ref. 3.72 (1.88 – 7.34)	- **< 0.0001**	Ref. 4.87 (0.52 – 45.7)	- 0.16
Lopinovir/Ritonavir • **Yes** • **No**	Ref. 1.49 (0.75 – 2.94)	- 0.24	- -	- -
Remdesevir • **Yes** • **No**	Ref. 3.03 (1.08 – 8.49)	- **0.03**	Ref. 12.5 (0.41 – 3.85)	- 0.14
Glutathione • **Yes** • **No**	Ref. 0.22 (0.09 – 1.75)	- 0.15	- -	- -
Tocilizumab • **Yes** • **No**	Ref. 2.93 (1.12 – 7.69)	- **0.02**	Ref. 0.6 (0.03 – 11.1)	- 0.73
Plasma • **Yes** • **No**	Ref. 1.49 (0.37 – 5.86)	- 0.56	- -	- -
Steroids during hospitalization • **Yes** • **No**	Ref. 2.04 (1.05 – 3.99)	- **0.03**	Ref. 1.04 (0.09 – 11.6)	- 0.97

Values are expressed as OR (95%CI). Logistic regression analysis was used to determine the relationship of clinical data with radiological sequelae at follow-up.

Finally, on multivariate analysis adjusted for gender, pack years, PiO2/FiO2 ratio at admission, degree of care (high or low) and FiO2 max, both CONS and IS at HRCT0 are independent predictors of radiological sequelae at follow-up with an OR of 14.87 (95%CI: 1.25 – 175.8; p = 0.03) and 28.9 (95%CI: 2.17 – 386.6; p = 0.01), respectively (**Table 4**).

Table 4. Multivariate analysis for factors independently associated with radiological sequelae at follow-up in patients hospitalized for SARS-COV-2 related pneumonia.

	Multivariate analysis*	
	OR (95% IC)	**p**
Alveolar score HRCT0 - %		
• **< 7**	Ref.	-
• **≥ 7**	1.80 (0.39 – 8.20)	0.44
Consolidations HRCT0 - %		
• **< 0.8**	Ref.	-
• **≥ 0.8**	14.87 (1.25 – 175.8)	**0.03**
Interstitial score HRCT0 - %		
• **< 1.4**	Ref.	-
• **≥ 1.4**	28.9 (2.17 – 386.6)	**0.01**

Values are expressed as OR (95%CI). Univariate and multivariate-adjusted odds ratio for radiological NOT recovery according to radiological patterns during hospitalization ($HRCT_0$). *Adjusted for gender, pack years, PiO_2/FiO_2 ratio at admission, degree of care (high or low), FiO_2 max.

DISCUSSION

In our study, we demonstrated that only a significant minority of patients hospitalized for COVID-19 pneumonia has persistent radiological abnormalities at follow-up. Patients who did not recover are mainly elderly males, with a more severe gas exchange impairment at hospital admission and a more severe clinical course during hospitalization. Interestingly, the presence of reticulation and consolidation at admission was predictive of persistent interstitial changes at follow-up.

To date, few studies have reported on the follow-up of patients hospitalized for Covid-19 pneumonia[5,6]. Different approaches based on disease severity have been proposed with the aim to standardize patients' follow-up. Specifically, the British Thoracic Society guidelines for management of post COVID-19 syndrome distinguished patients with severe pneumonia requiring intensive care from patients with mild to moderate pneumonia treated in a medical ward or at home[4]. However, it is becoming increasingly clear that radiological changes following COVID-19 pneumonia do not resolve completely in a large minority of patients[5,16]. Some studies have started to use CT to assess the presence of long-term lung abnormalities. A recent work from the Chongqing University Three Gorges Hospital evaluated 41 patients and showed that in most patients the chest CT lesions were no longer present at 7 months after discharge, whereas older patients with severe comorbidities were more prone to develop fibrosis[17]. From the Wuhan cohort, Han and colleagues investigated 114 patients with severe pneumonia according to the WHO criteria[12] and observed fibrotic changes in one-third of them at the 6-month follow-up. Of note, on multivariate analysis, they found that a higher baseline/initial CT lung involvement score (>18 in a score of 25) was independently associated with fibrotic-like changes in the lung[12]. Huang and colleagues conducted a cohort study that included 353 patients enrolled between January and May 2020 who underwent HRCT at follow-up after discharge. They found that more than 50% of the patients had residual lung abnormalities. Moreover, they found that disease severity in the acute phase was independently associated with the percentage change of CT score in a multivariable analysis[18].

In our hospital, the first patients with Covid-19 pneumonia were admitted in February 2020 and were evaluated in the post-COVID Clinic in June 2020. We enrolled prospectively patients diagnosed with COVID-19 pneumonia according to the WHO criteria. Two-hundred and twenty patients were evaluated at three months after discharge and every three months thereafter, according to the current guidelines[8]. We found that as many as 20% of our entire patient population had radiological pulmonary sequelae at follow-up. This percentage is lower than that observed in previous studies [12,18], but our patients' population has been followed-up for a longer period of time, thus allowing non-fibrotic pulmonary abnormalities to clear. Patients who did not recover (NOT-REC) were older, mostly males and with worse disease impairment both at admission and during hospitalization

compared to patients without radiological sequelae at follow-up. Specifically, NOT-REC patients had a lower PiO2/FiO2 ratio at admission and a more severe clinical course. Moreover, NOT-REC patients required higher maximal FiO2 during hospital stay, were more often treated in a high-intensive care setting and required a longer in-hospital stay, consistent with the findings from the Wuhan cohort[18]. Furthermore, we have shown that, in NOT-REC patients, the HRCT performed at hospital admission is more likely to display ground glass opacities, consolidations and reticulation. These data suggest that the risk of pulmonary sequelae may be related to the severity of the acute illness and to the intensity of care needed. This is in line with the hypothesis that a cytokine storm might contribute to the pathogenesis of COVID-19 while its severity is associated with poor outcomes[19]. However, mechanical ventilation and ventilator-induced lung injury, and high-flow oxygen therapy might also have contributed to the development of fibrotic-like changes[20,21].

The primary aim of our study was to identify predictors of radiological sequelae following Covid-19 pneumonia. While on univariate analysis age, prolonged in-hospital stay, lower PiO2/FiO2 at hospital admission, cardiovascular comorbidities, higher intensity of medical care, and higher FiO2 max, not using hydroxychloroquine, antibiotics other than azithromycin and ceftriaxone, tocilizumab, remdesevir or systemic steroids were significantly associated with the presence of interstitial changes during follow-up, we found that higher CONS [OR: 20.6 (95%CI: 1.4 – 301.2); p = 0.02] and IS [23.0 (1.4 – 377.2); p = 0.02] at hospitalization were the only variables independently associated with the persistence of fibrotic changes at follow-up in multivariate analysis. In particular, this latter observation is consistent with that of Han and colleagues who found that a more extensive baseline/initial CT lung involvement was independently associated with permanent fibrotic-like changes in the lung[12]. Additionally, the higher amount of consolidation and reticulation at admission remained significantly associated with persistent radiological abnormalities when adjusted for gender, pack years of smoking, and PiO2/FiO2 ratio. However, it remains uncertain whether the fibrotic-like changes we observed represent irreversible pulmonary fibrosis and further monitoring is warranted to answer this question.

The findings of our study should be interpreted in the light of some limitations. Firstly, this is a single center study; however, it is among the first to

analyze HRCT changes over time in a large population of patients hospitalized for COVID-19 pneumonia. In addition, we included a large proportion of patients with severe COVID-19, who are at higher risk of developing persistent lung disease. Secondly, the CT scan at hospital admission was available for only a subset of patients; however, the aim of our study was to characterize the radiological changes occurring over time and to identify predictors of persistent radiological abnormalities.

In conclusion, in our study about 20% of patients with COVID-19 pneumonia had radiological sequelae at follow-up. Patients who did not fully recover showed a more severe impairment at hospital admission and during hospitalization. Moreover, the presence of reticulation and consolidation on the initial chest CT is predictive of persistent radiological interstitial changes at follow-up.

REFERENCES

1. Ranard BL, Megjhani M, Terilli K, Doyle K, Claassen J, Pinsky MR, et al. Identification of Endotypes of Hospitalized COVID-19 Patients. Front Med (Lausanne). 2021 Nov 11;8:770343. doi: 10.3389/fmed.2021.770343. PMID: 34859018; PMCID: PMC8632028.
2. Baratella E, Bussani R, Zanconati F, Marrocchio C, Fabiola G, Braga L, et al. Radiological-pathological signatures of patients with COVID-19-related pneumomediastinum: is there a role for the Sonic hedgehog and Wnt5a pathways? ERJ Open Res. 2021 Aug 23;7(3):00346-2021. doi: 10.1183/23120541.00346-2021. PMID: 34435038; PMCID: PMC8381265.
3. Antonio GE, Wong KT, Hui DS, Wu A, Lee N, Yuen EH, et al. Thin-section CT in patients with severe acute respiratory syndrome following hospital discharge: preliminary experience. Radiology. 2003 Sep;228(3):810-5.
4. Das KM, Lee EY, Singh R, Enani MA, Al Dossari K, Van Gorkom K, et al. Follow-up chest radiographic findings in patients with MERS-CoV after recovery. Indian J Radiol Imaging. 2017 Jul-Sep;27(3):342-349.
5. Baratella E, Ruaro B, Marrocchio C, Starvaggi N, Salton F, Giudici F, Quaia E, Confalonieri M, Cova MA. Interstitial Lung Disease at High Resolution CT after SARS-CoV-2-Related Acute Respiratory Distress Syndrome According to Pulmonary Segmental Anatomy. J Clin Med. 2021 Sep 2;10(17):3985. doi: 10.3390/jcm10173985. PMID: 34501430; PMCID: PMC8432464.
6. Korkmaz İ, Keleş F. COVID-19-Related Lung Involvement at Different Time Intervals: Evaluation of Computed Tomography Images With Semiquantitative Scoring System and COVID-19 Reporting and Data System Scoring. Cureus. 2021 Oct 6;13(10):e18554. doi: 10.7759/cureus.18554. PMID: 34765340; PMCID: PMC8575326.
7. Greenhalgh T, Knight M, A'Court C, Buxton M, Husain L. Management of post-acute covid-19 in primary care. BMJ. 2020 Aug 11;370:m3026.
8. British Thoracic Society Guidance on Respiratory Follow Up of Patients with a Clinico-Radiological Diagnosis of COVID-19 Pneumonia. https://brit thoracic.org. uk/ about- us/ covid- 19- information- for the-respiratory- community/. Date last updated: May 6 2020. Date last accessed: May 7 2021.
9. George PM, Barratt SL, Condliffe R, Desai SR, Devaraj A, Forrest I, et al. Respiratory follow-up of patients with COVID-19 pneumonia. Thorax. 2020 Nov;75(11):1009-1016.
10. Fichera G, Stramare R, De Conti G, Motta R, Giraudo C. It's not over until it's over: the chameleonic behavior of COVID-19 over a six-day period. Radiol Med. 2020 May;125(5):514-516.
11. Kwee TC, Kwee RM. Chest CT in COVID-19: What the Radiologist Needs to Know. Radiographics. 2020 Nov-Dec;40(7):1848-1865.
12. Han X, Fan Y, Alwalid O, Li N, Jia X, Yuan M, et al. Six-month Follow-up Chest CT Findings after Severe COVID-19 Pneumonia. Radiology. 2021 Apr;299(1):E177-E186.

13. WHO. Clinical management of severe acute respiratory infection when novel coronavirus (nCoV) infection is suspected: interim guidance. https://www.who.int/docs/default-source/coronaviruse/clinical-management-of-novel-cov.pdf Published March 13, 2020).
14. Cocconcelli E, Biondini D, Giraudo C, Lococo S, Bernardinello N, Fichera G, et al. Clinical Features and Chest Imaging as Predictors of Intensity of Care in Patients with COVID-19. J Clin Med. 2020 Sep 16;9(9):2990.
15. Balestro E, Cocconcelli E, Giraudo C, Polverosi R, Biondini D, Lacedonia D, et al. High-Resolution CT Change over Time in Patients with Idiopathic Pulmonary Fibrosis on Antifibrotic Treatment. J Clin Med. 2019 Sep 15;8(9):1469.
16. Spagnolo P, Balestro E, Aliberti S, Cocconcelli E, Biondini D, Casa GD, et al. Pulmonary fibrosis secondary to COVID-19: a call to arms? Lancet Respir Med. 2020 Aug;8(8):750-752.
17. Liu M, Lv F, Huang Y, Xiao K. Follow-Up Study of the Chest CT Characteristics of COVID-19 Survivors Seven Months After Recovery. Front Med (Lausanne). 2021 Mar 1;8:636298.
18. Huang C, Huang L, Wang Y, Li X, Ren L, Gu X, et al. 6-month consequences of COVID-19 in patients discharged from hospital: a cohort study. Lancet. 2021 Jan 16;397(10270):220-232.
19. Fajgenbaum DC, June CH. Cytokine Storm. N Engl J Med. 2020 Dec 3;383(23):2255-2273.
20. Beitler JR, Malhotra A, Thompson BT. Ventilator-induced Lung Injury. Clin Chest Med. 2016 Dec;37(4):633-646.
21. Bates JH, Smith BJ, Allen GB. Computational Models of Ventilator Induced Lung Injury and Surfactant Dysfunction. Drug Discov Today Dis Models. 2015 Spring;15:17-22.

Chapter 15

Conclusions

Elisabetta Cocconcelli

CONCLUSIONS

In this thesis I focused on identifying potential useful tools which may predict the clinical course of patients with idiopathic pulmonary fibrosis (IPF).

IPF is a chronic and progressive lung disease, associated with a highly heterogeneous and unpredictable clinical course, alternating periods of stability to periods of rapid deterioration. To date, the main challenge of each pneumologist is to understand which could be the clinical course of patients, when the diagnosis of IPF is postulated.

In this thesis I decided to analyze both clinical, radiological and biological potential predictors. I think that the results I explained could offer some useful and easy to apply strategies for the clinical practice of each of us.

Specifically, the first main result is that ground glass opacities on CT scan are associated with patients presenting a rapid functional decline even despite antifibrotic treatment. In my first work, I considered a cohort of IPF population not treated with antifibrotics. Patients were categorized according to the functional decline in the first year of follow up either in rapid (decline in FVC % pred. > 10%) or slow decliners (FVC%pred. decline < 10%). Our results showed that, in the HRCT performed at diagnosis, patients who had experienced a rapid functional decline, ground glass extension was higher than in slow decliners, while the extent of fibrosis (Interstitial Score, IS) was similar in the two groups. In this context, the ground glass opacity should be regarded as part of the fibrotic process, as indicated by the recent ATS/ERS/ALAT/JRS guidelines and, as such, we believe it needed to be assessed. We postulated that HRCT finding, showing that at baseline rapid progressors had significantly higher extension of ground glass than slow progressors, is of high interest since it might help to identify, early in the course of the disease, the more aggressive phenotype with worse prognosis.

In a second work on radiological score, we observed that, despite a similar treatment efficacy on lung function after 1 year of treatment, patients who progresses both ground glass and honeycombing increased significantly after 1 year of treatment**.** On the other hand, in stable patients, only honeycombing increased significantly, while ground glass did not. This is an interesting finding, although the significance of alveolar opacity or ground glass attenuation remains debated. Ground-glass opacities refers to the presence of a hazy and diffuse homogeneous increase in lung density and, when located akin dense fibrotic areas, may represent

mild/initial fibrosis. However, ground glass attenuation may also be associated with the presence of inflammatory cells in the alveolar or interstitial space, which is often more evident in cases with more aggressive disease. This finding coupled with the observation that rapid progressors despite treatment also exhibit an increased extension in alveolar score suggests that the alveolar score may help to identify, even early in the disease course, the more aggressive IPF phenotype and supports the routine use of CT and its visual characterization in clinical practice both in treated and untreated patients with IPF.

The intriguing role of ground glass opacities is confirmed in the other works on genotyping. Firstly, we confirmed previous evidence of the protective role of MUC5B polymorphs (which is the most frequent polymorphism among IPF patients) in a cohort of patients under antifibrotic treatment. A previous study by Peljto AL. demonstrated that carriers of the mutant allele present a better survival compared to wild type patients, in a cohort of patients not treated with antifibrotics. We confirmed the same protective role of MUC5B T allele in a cohort of patients despite being under antifibrotic treatment. To corroborate this evidence, we observed that the wild type population presents also an increase over time in ground glass opacities, when compared to carriers of the mutant T allele. Ground glass opacities are once again associated to worse clinical course.

In my pathological work, for the first time I demonstrate the presence of lymphoid follicles in IPF patients, both at diagnosis and in the end stage phase of disease. Specifically, lymphoid follicles are more numerous at diagnosis and become larger and more activated at the end stage phase. These evidences confirm what previously observed and that an extensive cellular immune infiltrate, both innate and adaptive, is more prominent among IPF patients presenting a rapid functional decline. The role of immune cells in driving the IPF disease is still under debate, but we think that our work could be a perfect starting point for future perspectives.

Another intriguing chapter is the novelty of the progressive interstitial lung diseases. In the last three or four years some evidence suggested that almost the forty per cent of non-IPF interstitial lung disease patients, currently treated with specific treatment, may present a clinical course similar to IPF. In my research project, I identified the progressive phenotype among the idiopathic inflammatory myopathies (IIMs) patients and I described patients presenting a progressive

phenotype. Anti-MDA5 antibodies, heliotropic rash, xerostomia and xerophthalmia are prevalent in progressive IIM-ILD population.

Finally, my Coronavirus Disease 19 (COVID-19) research was conducted together my research on IPF and extremely closed to my clinical daily activity. We assessed that chest ultrasound is a useful tool in clinical practice because it correlates with clinical and radiographic parameters. Viral load on nasopharyngeal swab at diagnosis of COVID-19 is similar in asymptomatic and hospitalized patients and is not associated with either worse outcome during hospitalization. Finally, maybe the most interesting among the three studies, is the evidence that only a minority of patients hospitalized for COVID-19 pneumonia showed persisting lung abnormalities at the 6-month follow-up. These patients are predominantly older males with longer hospital stay.

In my near future, I hope to continue my research projects on prognostic predictors maybe by using other ‘easy to collect’ samples like blood or bronchoalveolar lavage and to deepen the ‘genetic predisposition’ of some patients for developing IPF.